Influence of design requirements on the spur gear pair parameters selection

Miler, Daniel

Doctoral thesis / Disertacija

2019

Sveučilište u Zagrebu

Faculty of Mechanical Engineering and Naval Architecture

Daniel Miler

INFLUENCE OF DESIGN REQUIREMENTS ON THE SPUR GEAR PAIR PARAMETERS SELECTION

DOCTORAL THESIS

Zagreb, 2019.

Sveučilište u Zagrebu

Fakultet strojarstva i brodogradnje

Daniel Miler

UTJECAJ KONSTRUKCIJSKIH ZAHTJEVA NA IZBOR PARAME- TARA PAROVA ZUPČANIKA

DOKTORSKI RAD

Zagreb, 2019.

Sveučilište u Zagrebu

Faculty of Mechanical Engineering and Naval Architecture

Daniel Miler

INFLUENCE OF DESIGN REQUIREMENTS ON THE SPUR GEAR PAIR PARAMETERS SELECTION

DOCTORAL THESIS

Supervisor:
Dragan Žeželj, Associate professor

Zagreb, 2019.

Sveučilište u Zagrebu

Faculty of Mechanical Engineering and Naval Architecture

Daniel Miler

UTJECAJ KONSTRUKCIJSKIH ZAHTJEVA NA IZBOR PARAMETARA PAROVA ZUPČANIKA

DOCTORAL THESIS

Mentor:
Izv. prof. dr. sc. Dragan Žeželj

Zagreb, 2019.

Bibliography data

Table of Contents

I

Acknowledgement

Summary

The gear pair design is well-defined within the technical literature, resulting in a straightforward design process. However, transmission performance largely depends on the designer's skill and experience. Thus, including the optimisation phase in the design process increases the transmission value. Besides the necessary strength requirements, additional characteristics can be ensured. The research was divided into six phases: literature review, the single-objective optimisation, formulation of power loss calculation, the multi-objective optimisation (steel gears), the multi-objective optimisation (polymer gears), and the experimental validation.

The single-objective optimisation was carried out to determine the necessary number of variables. No consensus between the authors was found during the literature review. The resulting design variable vector consisted of a gear module, face width, pinion number of teeth, and profile shift coefficients of both the pinion and the wheel. The power loss expression was found by combining the models for friction coefficient, load distribution, and power losses formulated by other authors. The multi-objective optimisation of steel gear pairs was carried out next, showing the influences of volume and power losses on the selection of optimal design variable values.

Besides the guidelines for steel gears, the novelty is polymer gear optimisation. By replacing the steel gear calculations with their polymer gear counterparts, optimisation of polymer gear pairs was carried out. The objective functions remained the same: volume and power loss. However, it was not possible to calculate power losses as no applicable expression for the prediction of friction coefficient was found. The experimental study was carried out to mitigate the problem; results were used to devise the required mathematical expression. The results of polymer gear optimisation have shown that differences in design variable behaviour exist, implying the need for separate design guidelines. Lastly, the optimal gear pairs were manufactured, allowing for the experimental validation of the proposed procedure.

Keywords:

Gears, design, gear optimisation, guidelines, polymer gear, polyoxymethylene.

Prošireni sažetak

U modernoj tehnici nesmetano funkcioniranje proizvoda u skladu sa specifikacijom se podrazumijeva. Drugim riječima, optimiranje radnih karakteristika je ključno kako bi se proizvod isticao na tržištu. Proces dimenzioniranja i konstruiranja zupčaničkih prijenosnika je, kako bi se osigurali nužni uvjeti čvrstoće, dobro definiran tehničkom literaturom. S druge strane, osiguravanje boljih radnih karakteristika zahtijeva specifična znanja i uvelike ovisi o vještini i iskustvu konstruktora.

U okviru rada promatran je utjecaj posebnih konstrukcijskih zahtjeva na način izbora vrijednosti geometrijskih parametara parova zupčanika. Posebni zahtjevi naručitelja odnose se na osiguravanje radnih karakteristika prijenosnika u skladu s njegovom budućom primjenom. Oni najčešće uključuju smanjenu masu, viši stupanj djelovanja ili nižu razinu buke.

Ciljevi i hipoteze

Cilj istraživanja je razviti postupak za više-kriterijsku optimizaciju zupčanika s ravnim zubima primjenjiv za oblikovanje prijenosa s posebnim konstrukcijskim zahtjevima. Prvi korak je formalizacija postupka optimizacije zupčaničkih parova izrađenih od čelika i polimera. U sklopu formalizacije podrazumijeva se određivanje potrebnog broja konstrukcijskih varijabli, detektiranje nužnih ograničenja i formulacija funkcija cilja. Rezultati optimizacije polimernih zupčanika bit će provjereni eksperimentalno. U skladu s navedenim ciljevima, izvedene su dvije hipoteze:

(I) Korištenjem više-kriterijskog postupka optimizacije moguće je raspoznati utjecaj posebnih konstrukcijskih zahtjeva na vrijednosti parametara parova zupčanika.

(II) Predloženim postupkom moguće je usporediti zakonitosti prilikom oblikovanja polimernih u odnosu na čelične zupčanike.

Očekivani znanstveni doprinos rada očituje se u razvoju postupka za više-kriterijsku optimizaciju čeličnih i polimernih parova zupčanika s ravnim zubima. Ovakav postupak omogućit će brže i učinkovitije dimenzioniranje ozubljenih prijenosnika. Primjenom razvijenog postupka bit će moguće utvrđivati utjecaj posebnih konstrukcijskih zahtjeva na parametre zupčaničkog para, prvenstveno modul, širinu, brojeve zubi i pomake profila.

Struktura rada

Sam doktorski rad je formalno oblikovan prema skandinavskom modelu i sastoji se od četiri znanstvena članka. Članci su povezani pregledom literature, diskusijom i kritičkim osvrtom te zajedno tvore cjelinu. Budući da tijekom pregleda literature nije pronađen konsenzus između autora, broj konstrukcijskih varijabli određen je pomoću jedno-kriterijskog postupka (Članak I). Jedno-kriterijski postupak primjenjiv na čelične zupčanike je unaprijeđen uključivanjem gubitaka trenja kao dodatnu funkciju cilja (Članak II). Primjena takvog postupka na polimerne zupčanike nije bila moguća zbog razlika u ograničenjima i funkciji cilja. Stoga je novi postupak primjenjiv isključivo na polimerne zupčanike prikazan u Članku III. Rezultati su validirani eksperimentalno. Tijekom određivanja funkcije cilja koja je opisivala gubitke kod polimernih zupčanika, nije pronađena primjenjiva formulacija faktora trenja. Izrazi za određivanje faktora trenja između zupčanika izrađenih od polioksimetilena (POM) stoga su dobiveni eksperimentalno (Članak IV).

Metode

Najveći broj istraživanja na području optimizacije zupčaničkih parova koristi tri varijable - modul, širinu i broj zubi zupčanika. Dio autora tomu je pridodao i pomake profila, pritom omogućavajući promjenu debljine zuba i promjenu nagiba zahvatne crte. S druge strane, veći broj varijabli povećava potrebno računalno vrijeme, zbog čega je potrebno odrediti utjecaj dodatnih varijabli na konačni rezultat.

Broj varijabli određen je provedbom optimizacijskog postupka s jednim kriterijem, gdje je volumen korišten kao funkcija cilja (Članak I). Rezultati dobiveni korištenjem tri varijable (modul, širina i broj zubi) uspoređeni su s onima dobivenim uz uporabu pet varijabli (modul, širina, broj zubi, te pomaci profila pogonskog i gonjenog zupčanika). Ograničenja geometrije i čvrstoće preuzeta su iz tehničkog standarda ISO 6336:2006 te je svaki postupak optimizacije proveden s istim ulaznim podacima. Ulazni podaci su se sastojali od tri seta podataka, svaki od kojih je sadržavao ulazni moment, brzinu vrtnje, faktor primjene, vrijeme potrebno za ubrzavanje, traženi prijenosni omjer, te materijal i kvalitetu ozubljenja. Za rješavanje problema korišten je genetski algoritam, kao najčešće korišten algoritam unutar područja. Svaki od postupaka proveden je koristeći populaciju od 500 jedinki uz 500 generacija te repliciran 10 puta kako bismo potvrdili da je globalni optimum pronađen. Rezultati su uspoređeni s rezultatima dobivenim koristeći komercijalno dostupan softver.

U sljedećem koraku formuliran je više-kriterijski postupak primjenjiv na čelične zupčanike (Članak II). Kao kriteriji optimizacije odabrani su volumen i gubici snage. Funkcija cilja koja opisuje gubitke u obzir uzima promjenu opterećenja, brzine klizanja te faktora trenja duž zahvata. Ograničenja čvrstoće i geometrije istovjetna su onima iz prethodnog koraka. NSGA-II (*eng. non-dominated sorting genetic algorithm II*) je korišten za rješavanje optimizacijskog problema te su rješenja prikazana u obliku Pareto fronte. Dovršetak ovog koraka omogućio je provjeru ispravnosti prve hipoteze.

Drugi više-kriterijski postupak optimizacije je razvijen s ciljem primjene na polimerne zupčanike (Članak III). Korišteni su isti kriteriji (volumen i gubici snage), algoritam i brojevi generacija, ali uz promijenjena ograničenja. Kontrola nosivosti zupčanika provedena je prema smjernicama VDI 2736, odnosno uz čvrstoću korijena i boka kontrolirani su i temperatura, trošenje i elastična deformacija. Također, potrebna je bila promjena funkcije cilja koja opisuje gubitke snage, zbog različitosti u mehaničkim svojstvima polimera (odabran je polioksimetilen) i čelika. Tijekom pregleda literature nije pronađena formulacija faktora trenja (više u sljedećem paragrafu). Rezultati su validirani eksperimentalno; optimalni parovi zupčanika su proizvedeni i ispitani. Eksperimentalni postav se sastoji od dva elektromotora, dva vratila, četiri ležajna mjesta te dva senzora za mjerenje okretnog momenta. Dovršavanje ove faze omogućilo je provjeru ispravnosti druge hipoteze.

Faktor trenja između zupčanika izrađenih od polioksimetilena određen je modelskim eksperimentom (Članak IV). Budući da se tijekom zahvata para zubi duž zahvatne crte mijenjaju radijusi zakrivljenosti, normalna sila i brzina klizanja, isti su odabrani kao varijable. Eksperiment je oblikovan kao puni faktorski, uz tri razine normalne sile, četiri razine brzine klizanja i pet razina radijusa zakrivljenosti. Razine su dobivene koristeći umjetno stvorenu populaciju zupčanika, pomoću koje su dobivene moguće vrijednosti parametara i gustoće njihovih vrijednosti. Svako od mjerenja replicirano je tri puta, odnosno provedeno je ukupno 180 mjerenja. Na svakom od parova uzoraka napravljeno 12 mjerenja (redoslijed je bio nasumičan), svako u trajanju od 10 sekundi s pauzom od 60 s između dva mjerenja. Budući da su se uzorci bez maziva izrazito brzo trošili, bilo je nužno koristiti teflon (PTFE) kao mazivo. Funkcija za izračun faktora trenja dobivena je linearnom regresijom.

Rezultati i diskusija

Jedno-kriterijski postupak optimizacije korišten s ciljem određivanja potrebnog broja varijabli je proveden (rezultati su prikazani u Članku I, tablica 4). Usporedbom rješenja dobivenih na-

kon 500 (potrebno vrijeme proračuna 0,81 s) i 30.000 generacija (36,9 s) pronađena je razlika u vrijednosti funkcije cilja od 0,066% (set 1), 1.84% (set 2) i 0.0048% (set 3) kod parova s pomakom profila. Na osnovu toga zaključeno je da je korištenje 500 generacija opravdano te da postupak konvergira.

Iz rezultata je vidljivo da svi promatrani setovi teže izboru manje širine i većeg broja zubi zupčanika, te se isti trend nastavio nakon snižavanja donjeg ograničenja širine s 6 na 2 modula. Kontaktni pritisak je bio aktivno ograničenje kod svih promatranih setova. Utjecaj pomaka profila kao varijable pokazao se kao izrazito značajan – pronađene razlike u vrijednosti funkcije cilja (volumen) bile su redom 34,6%, 32.3% i 34.7%. To znači da optimizacijski proces koji zanemaruje njihov utjecaj gubi praktički smisao. Varijable odabrane za nastavak istraživanja prikazane su vektorom $x_{var} = [m, b, z_1, x_1, x_2]$.

Rješenja više-kriterijskog postupka prikazana su grafički u obliku Pareto fronti (Članak II, slike 2, 3 i 4). Kod sva tri seta čeličnih zupčanika uočena je potreba za kompromisom između kriterija; smanjivanjem gubitaka volumen raste i obrnuto. Ekstremi, odnosno izbor para s najmanjom volumenom ili najvišim stupnjem djelovanja, prema jednom kriteriju su izrazito nepovoljni s obzirom na drugi. Kod sva tri promatrana seta uočeni su slijedeći trendovi:

- niži gubici dobiveni su izborom većih modula,
- povećavanjem pomaka profila na gonjenom zupčaniku u kombinaciji s pozitivnim pomakom na pogonskom zupčaniku moguće je značajno smanjiti gubitke,
- veća širina para uzrokuje smanjenje gubitaka, ali i povećanje volumena,
- svi setovi su konvergirali prema zupčanicima s većim brojem zubi.

Više-kriterijska optimizacija provedena je i za zupčanike izrađene od polioksimetilena (rezultati prikazani u Članku III, slika 3). Za razliku od čeličnih zupčanika, aktivni kriterij je bilo trošenje. Eksperiment je potvrdio dobivene rezultate. Na osnovu rezultata, uočeni su slijedeći trendovi:

- niži gubici dobiveni su izborom većih modula,
- kod promatranih parova bolja rješenja su u pravilu imala pozitivne pomake profila; kod setova 2 i 3 pomaci su bili značajni,
- veća širina para bila je povezana s većim gubicima, ali i manjim volumenom,
- svi setovi konvergirali su prema zupčanicima s većim brojem zubi.

Formulacija faktora trenja potrebna za provedbu optimizacije prikazana je u Članku IV – dobivena vrijednost prikazana je u jednadžbi (9), dok se rezultati mjerenja nalaze u tablici 3 istog članka. Promatrajući reziduale, moguće je reći da predložena krivulja dobro opisuje rezultate dobivene mjerenjima. Normalna sila imala je najveći utjecaj na promjenu faktora trenja; faktor trenja se smanjivao s povećanjem sile. Povećanje brzine klizanja također je negativno utjecalo na faktor trenja. Naposljetku, radijus relativne zakrivljenosti pokazao je zanemariv utjecaj na faktor trenja.

Zaključak

Na osnovu rezultata moguće je ustanoviti da su obje hipoteze potvrđene. Vezano za prvu hipotezu, promatrana su dva posebna zahtjeva – volumen i gubici (iskoristivost). U slučaju da je cilj smanjiti volumen prijenosnika, potrebno je težiti manjim vrijednostima modula, pozitivnim pomacima profila te većim brojevima zubi. Širina para treba težiti nižim vrijednostima u slučaju da će par biti izrađen od čelika, ili širim vrijednostima u slučaju da par izrađujemo od polimera (polioksimetilen). Ako je isključivi cilj smanjiti gubitke, potrebno je odabirati veće module. Brojevi zubi i pomaci profila ostaju nepromijenjeni u odnosu na konstruiranje s ciljem smanjenja volumena. Također, kod čeličnih zupčanika u tom slučaju je potrebno odabrati veću, a kod polimernih (polioksimetilen) manju širinu.

Druga hipoteza je također potvrđena – prilikom oblikovanja čeličnih i polimernih zupčanika će se, unatoč velikom stupnju sličnosti, koristiti različiti principi. Kao što je prikazano u prethodnim paragrafima, kod oba materijala potrebno je težiti manjim modulima i većim brojevima zubi, no postoje velike razlike prilikom odabira širine para.

Naposljetku, provedeno istraživanje pruža bazu za nastavak daljnjih istraživanja. Područje optimizacije sve češće korištenih polimernih zupčanika je relativno nerazvijeno i pruža mnogo prostora za rad. Potrebno je proširiti istraživanje i na ostale često korištene polimere, poput poliamida, te na uobičajene korištene kombinacije (npr. poliamid – polioksimetilen).

Ključne riječi

Zupčanici, konstruiranje, optimiranje zupčanika, smjernice, optimiranje polimernih zupčanika, polioksimetilen.

Nomenclature

Symbol	Unit	Description
A_G	mm^2	outer gearbox housing surface
b	mm	face width
d_{a1}	mm	tip diameter (pinion)
d_{a2}	mm	tip diameter (wheel)
ED	%	load spectre
F_n	N	normal load
$F_{bnHertz}$	N	allowed normal load in polymer gears (Hertzian stress)
F_{bnTemp}	N	allowed normal load in polymer gears (temperature)
i	-	transmission ratio
K_A	-	application factor
$K_{F\alpha}$	-	transverse load factor (root stress)
$K_{F\beta}$	-	face load factor (root stress)
$K_{H\alpha}$	-	transverse load factor (contact stress)
$K_{H\beta}$	-	face load factor (contact stress)
k_{9Flank}	K(m/s)$^{0.75}$mm$^{1.75}$/W	effective gear flank heat conductivity
K_v	-	dynamic factor
M	mm	gear module
n_1	min^{-1}	rotational velocity (pinion)
P	W	transmitted power
P_{loss}	W	power loss
p_{et}	mm	transverse base pitch
Ra	μm	arithmetic mean roughness
R_M	-	load sharing ratio along the line of action
$R_{\lambda G}$	Km^2/W	calculation factor accounting for the housing design
T_1	Nm	input torque
T_m	Nm	measured torque
t_{st}	s	starting time
V	mm^3	gear pair volume
V	m/s	pitch line velocity
v_d	mPa·s	dynamic oil viscosity

v_s	m/s	sliding velocity
$V_{\Sigma C}$	m/s	sum velocity
w	N/mm	specific load (Fn /b)
x_1	-	profile shift coefficient (pinion)
x_{maxT}	-	maximal allowable profile shift coefficient (in relation to the tooth tip thickness)
x_2	-	profile shift coefficient (wheel)
Y_F	-	tooth form factor
Y_{NT}	-	life factor for tooth root stress for reference test conditions
Y_S	-	stress correction factor
Z_B	-	single pair tooth contact factor (pinion)
Z_D	-	single pair tooth contact factor (wheel)
Z_E	-	elasticity factor
Z_H	-	zone factor
Z_L	-	lubricant factor
Z_{NT}	-	life factor for contact stress for reference test conditions
Z_ε	-	contact ratio factor
z_1	-	number of teeth (pinion)
z_2	-	number of teeth (wheel)
A	rad	pressure angle
α_w	rad	operating pressure angle
B	rad	helix angle
ε_α	-	transverse contact ratio
H	-	efficiency
μ	-	friction coefficient
μ_m	-	mean friction coefficient (along the line of action)
Ξ	-	involute parameter
P	mm	flank curvature radius
ρ_{redC}	mm	radius of relative curvature at pitch point C
ρ_{rel}	mm	radius of relative curvature
ρ_{rot}	mm	radius of a rotating specimen

ρ_{stat}	mm	radius of a static specimen
σ_{Flim}	N/mm^2	nominal stress number (bending)
σ_{FP}	N/mm^2	permissible stress (bending)
σ_{Hlim}	N/mm^2	allowable stress number (contact)
σ_{HP}	N/mm^2	permissible stress (contact)
Θ	°C	larger of the tooth root and flank temperatures
ϑ_{Flank}	°C	tooth flank temperature
ϑ_{Root}	°C	tooth root temperature
Θ	rad	rotation angle
ψ_i	mm	curvature radius at point i on the line of action

List of figures

List of tables

1. INTRODUCTION

An overview of the research field is presented in this section. The aim of doctoral research is shown, along with its expected scientific contribution. Two hypotheses are formulated, and the research required to determine whether they are correct is divided into six phases. Lastly, the list of appended papers is attached.

The transmission of power from the site of generation to the place of consumption is one of the prerequisites for the development of modern industry. The long-distance power transmission is solely achieved by means of electricity, while the short-distance transmissions are dominantly conducted mechanically, mostly due to the inherent ability of mechanical transmissions to easily modify the operational torque and rotational velocity. Gears are most frequently used among the mechanical transmission elements, which is the reason enough for strict safety, durability, and effectiveness demands. The gearbox design process is well-known, mostly due to abundant technical literature.

Gear geometry can be divided into two groups – gear macro-geometry and gear micro-geometry. The former includes the gear module, face width, number of teeth, profile shift coefficient, tooth symmetry, and type of flank curve. It is primarily affected by the tool geometry. The latter requires additional machining operations and includes the tooth tip relief, root relief, profile angle and crowning, flank end relief, crowning, and helix modification [1]. It is possible to satisfy strength criteria using different combinations of geometric parameters. However, variations in gear geometry also affect the transmission properties, such as efficiency and noise level.

Unfortunately, values of geometric parameters are most often determined using approximate calculations and practical guidelines, combined with the designer's experience. By utilising the existing design guidelines, it is possible to coarsely determine the required gear module, number of teeth, and face width, meaning that using such guidelines will often yield a sub-optimal design. Even though the resulting combinations of parameters will satisfy the necessary strength requirements such as the tooth root bending stress or flank durability, the product market value will be limited.

In modern time, it is fully expected that the product will execute its original function without error, as contrary would have numerous negative implications for the manufacturer. For this reason, to gain a head start ahead of the competition, a product design must contain additional desirable features (i.e. the low volume, high efficiency, straightforward design, or low noise). Additional design features enhance the product performances, and indirectly, increase its market value.

Traditionally, the design process includes the recognition of need, an act of design creation, and a selection of alternatives [2], meaning that the desire to select the best design is self-imposed. After including the additional features along with the necessary strength requirements, the problem at hand becomes more complex, often requiring the use of computational algorithms. The optimisation algorithms are used to mitigate the problem; the strength requirements and geometrical limitations are implemented as constraints, while the objective function is defined by choosing one or more desired additional features, such as the transmission volume and power losses.

However, downsides of gear design by means of optimisation processes must be mentioned. To start off, the process itself is time-consuming – even though modern computers solve complex optimisation problems in a matter of seconds, proper formulation of a problem may take weeks or months. Besides the time, the knowledge of problem, its constraints, and evaluation criteria is essential. When observing gears, the complexity is additionally increased by variations in the material; gears are often made of the grey iron, steel, or polymer materials. Constraints, which are necessary to ensure gear pair feasibility, vary accordingly. Steel and grey iron gears are limited by tooth root strength and flank surface durability [3], while polymer gears require additional restrictions, such as the tooth temperature, flank wear, and tip deformation. The calculation procedure to determine the load capacity of the former is ISO 6336:2006 [3], while the latter are evaluated using the VDI 2736 [4].

Thus, more detailed guidelines devised with respect to additional criteria (i.e. volume, power losses) could increase the quality of geared transmissions while avoiding the time-consuming optimisation methods. The research study at hand is conducted in lines with the previous statement.

1.1. Research aim and motivation

The research aim is to develop a procedure for multi-objective optimisation of spur gear pairs applicable to design of gearboxes with additional requirements. Within the study, the impacts of different types of additional requirements on the optimal selection of macro-geometric parameters were assessed. The research study is focused on reducing the gear pair volume and power losses.

Not including the micro-geometric modifications such as the gear crowning, the standard involute gear pair geometry is determined by six variables: gear module, face width, pinion and gear teeth numbers, and pinion and teeth profile shift coefficients. Within the study, the required number of optimisation variables is to be determined, as lowering their number would reduce the task complexity, and subsequently, the computational cost.

Additionally, besides devising the guidelines for the design of steel gears with additional requirements, polymer gear pairs will also be studied. No guidelines for the design of polymer gears were found during the literature review even though they are quickly rising in numbers. The results of polymer and steel gear pairs will be compared aiming to further explore the material influence. Lastly, results will be validated experimentally; the experiment will be used to confirm the results of the polymer gear pair optimisation.

1.2. Hypotheses

Two hypotheses were formulated to fulfil the research aims:

> *By using a multi-objective optimisation procedure it is possible to detect the influence of additional criteria, caused by the special design requirements, on the values of gear pair parameters.*

> *Proposed procedure will enable the comparison of parameter influences on the final design for gear pairs made of polymer and steel.*

The multi-objective optimisation procedure will be formulated and used as a tool for testing the first hypothesis. By carrying out such procedure using multiple sets of input data, the influence of the special design requirements such as low gear pair volume or high efficiency on the gear pair parameters will be identified. Finally, the robustness of solutions will be tested in order to determine whether the first hypothesis is valid.

The scientific and technical literature on steel gear pairs is numerous, easing the verification of results. Thus, guidelines for steel gear pairs are derived first, followed by those for gear pairs made of polymer materials. The literature on polymer gear optimisation is non-existent and is one of the key topics of the research study at hand. Due to lacking literature, the experimental validation of results is essential.

1.3. Expected scientific contribution

The expected scientific contribution will be manifested in the development of the multi-objective optimisation procedure for steel and polymer spur gear pairs with objectives being their volume and power loss. Such a procedure will enable faster and more efficient gearbox design.

By using a developed procedure, it will be possible to observe the influence of special design requirements on the gear pair parameters, primarily the gear module, face width, teeth numbers and profile shift coefficients.

1.4. Research structure

In order to prove the hypotheses, the research study is conducted. For better traceability, the research is divided into the six phases. The former five are theoretical, while the sixth, serving to validate the results, is experimental. The phases are:

1. The preliminary phase includes a thorough review of literature and calculation standards. Through discussion with experts, users and consultation of the literature, often requested additional design requirements will be identified. Limited exterior dimensions, weight and power loss are good examples of additional requirements. After the essential requirements are identified, optimisation results from the earlier studies will be collected to enable procedure verification in the latter phases. Lastly, it is necessary to gain insight into the architecture of optimisation algorithms used in related studies.

2. The second phase of the research refers to the integration of strength calculation methods into the single-objective optimisation algorithm. It is necessary to evaluate the existing algorithms and select the most applicable ones. Optimisation objective will be volume, primarily because of the abundant technical literature and simple calculations. In addition to the primary objective, there will be additional requirements, such as sufficient tooth root strength and surface durability. Furthermore, in order for the gear

pair to be industrially viable, values of optimization variables must be limited; the modules will be standard, the width factor will be an integer, while the profile shift coefficients will be selected depending on the number of teeth in order to avoid the undercutting and pointing of the gear tooth.

3. The third research phase is focused on the power loss calculations. Gear losses consist of frictional, lubrication and bearing losses. At high speeds (above 8,000 revolutions per minute) windage losses [5] become noticeable, but they will not be included in this study. The efficiency of gearing is high, often above 99%, meaning that the optimisation algorithm will require a precise calculation procedure, which will be sensitive to small variations in the parameter value. It is, therefore, necessary to conduct a review of existing loss calculation procedures. If the appropriate procedure is not found, a new one will be proposed. The procedure must include the influence of normal load, sliding speed, change of friction coefficient concerning the working conditions and the impact of load distribution across the meshing gear pairs.

4. By selecting the method for calculation of power losses in gear pairs, conditions for forming a multi-criteria optimisation process are created. Said process would take the volume and power loss into account. No such research has been found in the literature. The algorithm will be selected and written following the guidelines outlined in [6]. NSGA-II is an example of a frequently used algorithm for multi-objective optimisation [7]. Optimisation results presented as a set of Pareto optimal solutions will, together with the parameter values each set consists of, enable us to provide design guidelines.

5. Optimisation of polymer gears is relatively unexplored; during the literature review no research that deals with automated solving of volume or power loss optimisation has been found. Significant differences compared to the previous step, designed to solve the steel gear optimisation, are the polymer gear sensitivity to the temperature and low Young's modulus value. In this phase VDI 2736 [4] guidelines will be used, as the ISO 6336: 2006 [3] standard is limited to gears made of steel and cast iron. The resulting procedure will enable the comparison of polymer and steel gear behaviour, as well as the formulation of guidelines for the polymer gear parameter selection.

6. After developing a multi-objective procedure for optimisation of polymer gear pairs, conditions for the last phase consisting of experimental procedure verification are

achieved. The experiment will compare theoretically obtained power losses with the regular ones. For this reason, it is necessary to use an open-circuit device. A device consisting of two servomotors, four bearings, two measuring shafts and a linear guide with a brake and spindle will be designed and manufactured. The first motor serves as a drive and the second one as a brake, enabling precise measurement of gearing power loss. The linear guide serves to adjust the centre distance, which will be non-standard; as the standard value would significantly reduce the optimisation space.

Thus, this thesis is structured in six sections as follows: within Section 2, a short review of the gear design fundamentals is shown, including the annotation and manufacturing. The requirements each pair must meet in order to be viable are divided into two groups: geometric and strength requirements. The optimisation criteria are covered next. Each of the criteria provides a design with an additional feature (for example, low weight or low power losses). The existing design guidelines are shown along with the experimental studies needed for model validation. Lastly, the optimisation algorithms used within the research field are presented.

The design optimisation model is shown in the third section and is formulated using the five-step model [8]. The first step, the problem formulation, is covered during the literature review in Section 2. Design variables are defined and selected next. Optimisation criteria are selected and presented in Section 3.3 and the constraints in Section 3.4, completing the problem formulation. Finally, the selection of the algorithm used for solving the problem is shown.

The results of each phase are further explained in Section 4, while the appended papers are included in the Appendix. In Paper I, the number of variables required for spur gear pair optimisation is determined using the single-objective process. After devising the second optimisation criterion, the multi-objective optimisation process was conducted. The gear pair volume and power losses were used as the criteria. A similar process was carried out for the polyoxymethylene (POM) gears in Paper III. The suitable friction coefficient formulation for POM gears was not found during the literature review; thus, an additional study was conducted to obtain them, presented in Paper IV.

The results of the four papers are consolidated and discussed in Section 5. The presented six phases enabled the formulation of guidelines for dimensioning of spur gear pairs. Robustness was tested to verify that the procedure applies to a general case. The guidelines for the selection of geometric parameters of steel and POM spur gear pairs are presented, after which the

guidelines for the two types of gears are compared. The critical review of the conducted research study is also shown.

After summarising the findings of a presented research study within Section 6, both hypotheses are tested. Lastly, the possible directions for future work are shown.

1.5. Appended papers

Paper I

Miler D, Lončar A, Žeželj D, Domitran Z. *Influence of profile shift on the spur gear pair optimization*. Mechanism and Machine Theory, 2017;117:189–197.

doi:10.1016/j.mechmachtheory.2017.07.001.

> Daniel Miler has written the article and formulated the design problem (selection of design variables, formulation of constraints and objective functions, algorithm selection). Antonio Lončar has implemented the calculations into the computational algorithm. Dragan Žeželj helped devise the constraints. Dragan Žeželj and Zoran Domitran have reviewed the article.

Paper II

Miler D, Žeželj D, Lončar A, Vučković K. *Multi-objective spur gear pair optimization focused on volume and efficiency*. Mechanism and Machine Theory, 2018;125:185–195.

doi:10.1016/j.mechmachtheory.2018.03.012.

> Daniel Miler has written the article, formulated the design problem (selection of design variables, formulation of constraints and objective functions, algorithm selection), and devised the expression for power loss calculation. Antonio Lončar has implemented the calculations into the computational algorithm. Dragan Žeželj has checked the calculation method. Dragan Žeželj and Krešimir Vučković have reviewed the article.

Paper III

Miler D, Hoić M, Škec S, Žeželj D. *Optimisation of polymer spur gear pairs with experimental validation*. Submitted to: Mechanism and Machine Theory, 2019 (under review).

> Daniel Miler has written the article and designed the experimental rig. Dragan Žeželj and Daniel Miler carried out the experimental measurements. Matija Hoić has provid-

ed valuable insight into the experiment planning and experimental rig design. Matija Hoić, Stanko Škec, and Dragan Žeželj have reviewed the article.

Paper IV

<u>Miler D</u>, Hoić M, Domitran Z, Žeželj D. *Prediction of friction coefficient in dry-lubricated polyoxymethylene spur gear pairs*. Mechanism and Machine Theory, 2019;138:205-222.

doi:10.1016/j.mechmachtheory.2019.03.040

> Daniel Miler has written the article and carried out the experiment. He and Matija Hoić have determined the experiment design and measuring points. Matija Hoić, Dragan Žeželj and Zoran Domitran have reviewed the article.

2. LITERATURE REVIEW

The literature review consists of four segments. First includes the gear design fundamentals and method used for rating of gear pairs were reviewed (Sections 2.1 to 2.4). An overview of computational algorithms used within the field is provided in second (Section 2.5), followed by the studies on gear pair optimisation (Section 2.6). The studies on polymer gear pairs are reviewed in the fourth segment (Section 2.7).

2.1. Gear design fundamentals

The fundamentals of gear pair design are covered before further investigation to ease the following problem formulation (Section 3.1). In the following considerations, it is assumed that gear profiles are involute, meaning that Fundamental law of gearing is applicable [9].

The macro-geometry of a standard involute spur gear is defined by a gear module, pressure angle, teeth number, profile shift coefficient, and face width b. The gear module m is a standard measure of tooth size [10], while the pressure angle α is the angle of the tooth rack cutting tool. The number of teeth z influences the tooth profile; low teeth numbers can lead to undercutting of tooth root (further explanations in Section 2.2.1). It directly influences the tooth thickness and line of action angle. The displacement of the rack cutting tool from the workpiece axis is calculated by multiplying the gear module and profile shift coefficient x (also shown in Figure 1). Lastly, the face width b shows the axial width of the gear.

Further modifications of the gear tooth geometry, known as the micro-geometry profile modifications can be made. The micro-geometry modifications are often used to decrease the transmission error, aiming to reduce the ensuing noise. Such modifications require additional machining, which is conducted once the gear macro-geometry is formed. Linke et al. [11] divided them into three groups:

1. <u>Profile modifications</u> (profile crowning), including the tip and root relief of a pinion and a tip relief of wheel.
2. <u>Flank line modifications</u>, consisting of either end relief or lead crowning.
3. <u>General 3D modification</u> (topography), including the combined profile and line modifications.

As the gears are used in pairs, variable indexing must be explained. The pair consists of the drive and driven gears; drive gear being the one that transmits the torque to the driven gear. Within this dissertation, term pinion will be used for the drive gear and wheel for the driven gear, as the focus is on the reducers. Indexes determining the gear within the pair are written in subscript; index 1 is used for the parameters belonging to the pinion and 2 to the wheel. For example, z_1 indicates the number of teeth of a pinion. When observing the multi-stage problem, the number in the superscript determines the number of the pair observed from the motor (i.e. $m^{(1)}$ indicates the module of the first pair, while $x^{(2)}_2$ denotes the profile shift coefficient of second gear pair wheel).

The gear manufacturing process (Figure 1) is explained to illustrate the importance of geometric requirements. During the gear manufacturing, the workpiece is rotating around the future gear axis, while the cutting tool moves tangentially. The gear tooth thickness can be altered by adjusting the distance between the cutting tool and the gear axis. A proper selection of the profile shift coefficient has beneficial effects on the gear pair load capacity and eases the use of standardised centre distances.
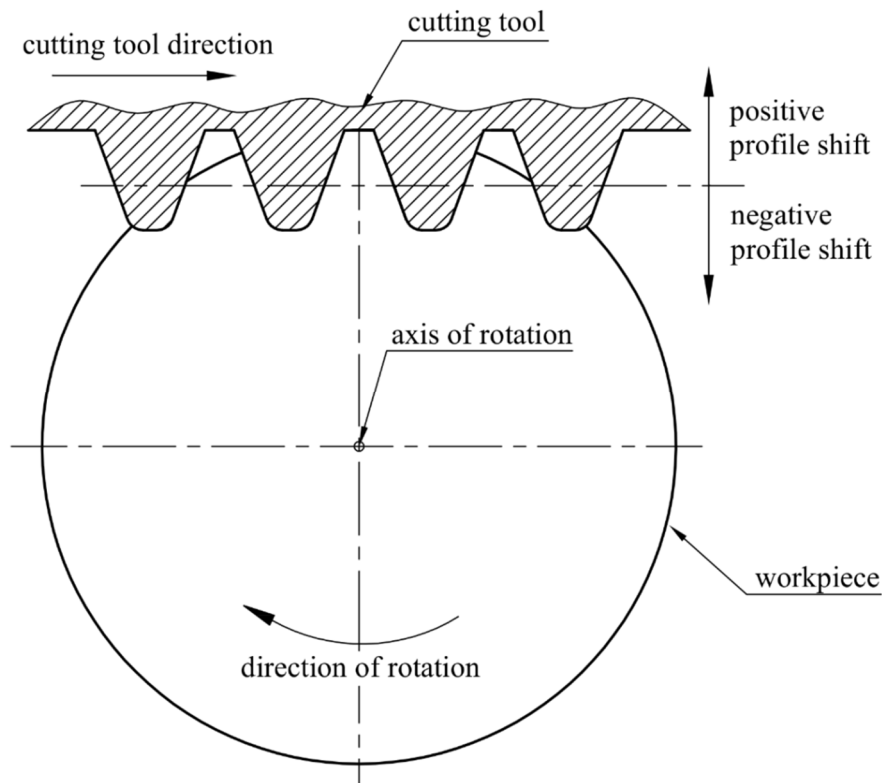
Figure 1 – Gear manufacturing process

Standard basic rack tooth profile used in gear manufacturing is defined in ISO 53:1998 [12] standard, while the hob accuracy requirements are specified in ISO 4468:2009 [13].

2.2. Design requirements in spur gear pairs

The geometric and strength requirements must be met in order to design an operational spur gear pair. Once the pair geometry is fully defined, the design is analysed to verify whether it satisfies the necessary geometric and strength requirements. By satisfying the geometric requirements (constraints), it is warranted that selected pair geometry, centre distance, and the corresponding tolerances are mutually compatible [9]. On the other hand, the strength requirements make sure that the analysed pair will be able to transmit the load within the previously defined working conditions.

2.2.1. Geometric requirements

In order to be feasible, gear pair parameters must satisfy geometric conditions. They can be divided into two groups; the first group is concerned with the geometry of the individual gear, while the second is focused on the gear pair as an assembly and aimed at enabling gears to mesh. The geometric conditions that must be satisfied are listed next.

Gears must not be undercut

Gear tooth is undercut when excessive material is removed from its root. It is caused in one of two ways; by designing a gear with too few teeth or by excessive negative profile shift. The lower number of gear teeth causes the root to be undercut by the tip of the cutting tool. The profile shift coefficient (addendum modification) is negative when the cutting tool is moved closer to the workpiece axis of rotation. If the profile shift coefficient x is too small, the tooth root is undercut, significantly lowering the load capacity. Furthermore, if both paired gears are undercut, jamming is possible. Undercut gear teeth are shown in Figure 2.a.

The profile shift coefficient required to prevent gear undercutting of the tooth root can be calculated [11]:

$$x \geq h_{\text{Fa}} - \frac{z}{2} \cdot \sin^2 \alpha \tag{1}$$

where hFa [] is

Gear tip sharpness must be avoided

The gear tooth thickness and working angle α_w increase with an increase in profile shift coefficient. Increased thickness has a beneficial effect on tooth load capacity as it increases both the tooth root thickness and tooth flank curvature radius. Thicker tooth root has a larger moment of inertia, lowering the bending stress, while the increased flank curvature reduces the

contact (Hertzian) stress. However, excessive positive profile shift causes the gear tip to become too narrow, ultimately sharp (Figure 2.b), increasing the possibility of damaging its counterpart. The sharp teeth also have a rather low moment of inertia at the tip, enabling the particles to break off. For this reason, the upper bound of profile shift coefficient is limited to prevent it:

$$s_a = d_a \left(\frac{s}{d} + \text{inv } \alpha - \text{inv } \alpha_a \right) \le s_{a-min};$$

$$\text{where: } s = m \left(\frac{\pi}{2} + 2x \tan \alpha \right); \quad \alpha_a = \arccos \frac{d_b}{d_a} \tag{2}$$

Expression (2) is found using the necessary geometric relations presented in [11]. The required tooth tip thickness s_{a-min} is chosen depending on the material and manufacturing technology; minimally required tooth tip thickness of $0.2\ m$ is chosen for the regular steel gears and $0.4\ m$ for the quenched ones.

a)

b)

$z = 12$
$x = 0$

$z = 12$
$x = 0.7$
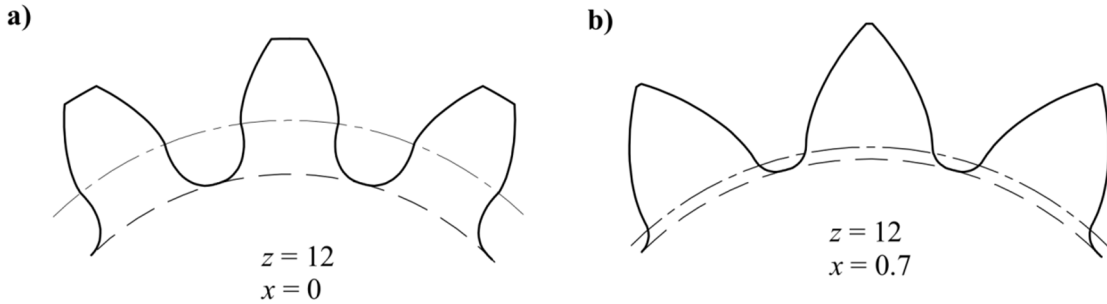
Figure 2 – a) undercut gear teeth; b) sharpened gear teeth

Gear face width must be in the acceptable range

The gear face width b is the axial dimension of a gear, defined as a product of gear module m and width factor λ. The gear width factor value can be found in the guidelines and is chosen depending on the bearing arrangement, shaft and housing stiffness, position of gear on the shaft, and the manufacturing technology [14]. When attempting to find an optimal design solution for a given problem, it is recommended to choose the width factor from the interval:

$$\lambda = [6 \dots 30] \cdot m. \tag{3}$$

The lower boundary is set to prevent the bending of the gear and tooth in the axial dimension due to axial load component in helical gears, or due to the irregularities in work for spur gears. The upper boundary restricts overdesigned solutions as in wide gears the manufacturing error and axis misalignment have a significant, but adverse, role.

For general engineering applications, face width factor is selected depending on the bearing type and arrangement.

Both gears must have the same module size

Both gears must have the same profile in order to mesh correctly. Even though this condition is often tacitly assumed, when generating the mathematical model all the limitations must be stated explicitly.

Centre distance must be appropriate

The centre distance is a distance between axes of meshing gears. It is a function of pinion and wheel teeth numbers, their modules, and profile shift coefficients. In practice, standard centre distance values are often used to increase the part exchangeability. Standard centre distance is achieved through the selection of the teeth numbers, modules, and profile shift coefficients. Expression (4) is used to determine the required profile shift coefficients [11,14]:

$$x_1 + x_2 = \frac{\text{inv } \alpha_w - \text{inv } \alpha}{2 \tan \alpha} \cdot (z_1 + z_2) \tag{4}$$

Moreover, gear pairs are capable of transmitting the torque when the small increases in the centre distance exist. Thus makes them less susceptible to manufacturing and assembly errors [14]. The robustness regarding the centre distance is, however, limited with the transverse contact ratio; further explanation is offered in the next paragraph. On the other side, the centre distance decrease is limited by the manufacturing tolerances. By further reducing it, interference between tooth tips and root fillets will occur, rendering the gear pair unfeasible.

Transverse contact ratio is above the recommended value

The transverse contact ratio ε_α states the average simultaneously meshing gear teeth pairs. At every point along the line of action at least one pair must be in mesh, setting its lowest theoretical value at 1. In practice, its lowest recommended value is 1.2 [10]. For the gears with standard tooth profiles ($\alpha = 20°$), the largest attainable ε_α is 1.98 [11,14]. Generally, higher values of transverse contact ratio result in lower noise levels [15].

2.2.2. Steel gear strength requirements

The load capacity of steel spur and helical gears is calculated using ISO 6336:2006 standard [3]. The formulae within are applicable when the above-listed geometrical constraints are satisfied. Two criteria limit the load capacity; tooth root bending strength and flank durability.

An overview of ISO 6336:2006 calculation procedure required to form the design constraints is shown in this section.

Tooth root bending strength

As noted in the standard [3], tooth root breakage will most likely end the transmission service life. The broken tooth particles may enter the mesh, causing critical damage to other transmission components. According to the Method B of the ISO 6336 the local tooth root stress is calculated as a product of nominal stress (in parentheses) and correction factor (1):

$$\sigma_F = \left(\frac{F_t}{b \cdot m_n} \cdot Y_F \cdot Y_S \cdot Y_\beta \cdot Y_B \cdot Y_{DT} \right) \cdot K_A \cdot K_v \cdot K_{F\beta} \cdot K_{F\alpha} \leq \sigma_{FP} \tag{5}$$

The nominal tooth root stress σ_{F0} is calculated for static torque at the root of the error-free gear pair. The *Y* members denominate the calculation factors required to calculate it, while the *K* members include the dynamic effects such as the load irregularity and transmission errors. The detailed calculation procedures of *Y* members are covered in the part 3 of the standard:

- Form factor Y_F accounts for the influence of the tooth geometry on tooth root stress; it mainly depends on the moment arm of the normal load h_{Fe}, the critical tooth normal chord s_F, radius of the root fillet ρ_F, and the load direction angle α_{Fe}. It can be determined analytically, numerically, or experimentally [16]. According to standard, for spur gears it is determined as (6):

$$Y_F = \frac{\dfrac{6 h_{Fe}}{m} \cdot \cos \alpha_{Fe}}{\left(\dfrac{s_F}{m} \right)^2 \cdot \cos \alpha} \tag{6}$$

- Stress correction factor Y_S converts the nominal into local tooth root stress. It includes the influences of section change in the tooth root fillet.

$$Y_S = \left(1.2 + 1.3 \cdot \frac{s_F}{h_{Fe}} \right) \cdot \left(\frac{s_F}{2 \rho_F} \right)^{\frac{1}{1.21 + \frac{2.3 h_{Fe}}{s_F}}} \tag{7}$$

- Helix angle factor Y_β is used to include the influence of the mesh line orientation in helical gears. As the standard is derived for the spur gears, Y_β is used to convert the values to the helical gears. Within this thesis, the helix angle factor was not considered ($Y_\beta = 1$) as the study is focused on the spur gear pairs.

- Rim thickness factor Y_B is used to account for the influence of rim thickness. It is possible that the crack initiation will start on the gear rim instead of the tooth root fillet due to its low thickness. In this thesis the thin rim gears were not considered, meaning that rim thickness factor value was $Y_B = 1$.

- Deep tooth factor Y_{DT} is used in high accuracy gearing (accuracy grades bellow or equal to 4) with large contact ratios (above 2). As the maximum contact ratio for the standard spur gears with pressure angle $\alpha = 20°$ is 1.98, deep tooth factor is taken as $Y_{DT} = 1$.

It is evident that only form and stress correction factors will be included when observing the spur gear pairs. In the other hand, the dynamic factors K will be included for all the cases. Their detailed calculation procedures are shown in part 1 of the standard [3]. It must be noted that lowest plausible values of dynamic factors are 1. In short:

- Application factor K_A compensates for the occasional increase in the nominal load. Within the standard, it is defined as a ratio between the equivalent and nominal torque. During the gearbox design, it is often provided by the client, or agreed upon between the client and the designer. If K_A value is not provided, it can either be calculated or taken according to the empirical guidelines in dependence on the driven and driving machine (as found in [3] part 6, annex B).

- Internal dynamic factor K_v accounts for the undesirable dynamic effects caused by the manufacturing tolerances. As such, it is largely dependent on the accuracy grade, tangential velocity, specific load, and the transmission ratio. In this study, it is calculated using the Method C of ISO 6336:2006. Regarding the optimization process, it should be noted that K_v is not a smooth function as factor K_3 required for its calculation is not derivable due to a break in function:

$$
K_3 = \begin{cases} 2; & \dfrac{vz_1}{100}\sqrt{\dfrac{u^2}{1+u^2}} \leq 0.2 \\[4mm] -0.357 \cdot \dfrac{vz_1}{100}\sqrt{\dfrac{u^2}{1+u^2}} + 2.071; & \dfrac{vz_1}{100}\sqrt{\dfrac{u^2}{1+u^2}} > 0.2 \end{cases} \tag{8}
$$

- Face load factor (for tooth root stress) $K_{F\beta}$ includes the influence of uneven load distribution across the gear face width. It is affected by overall stiffness and accuracy of the system. The latter includes the accuracy grade, geometrical tolerances of gears, shafts and housing, assembly error, microgeometry modifications of the gear profile,

15

and bearing clearances [3]. It is calculated using the Method C, as system elements required to use other listed methods, such as bearings, were not considered in this study:

$$
K_{F\beta} =
\begin{cases}
\left(\sqrt{\dfrac{2F_{\beta y} \cdot c_{y\beta} \cdot b}{F_m}} \right)^{\frac{1}{1 + \frac{h}{b} + \left(\frac{h}{b}\right)^2}}; & \dfrac{F_{\beta y} \cdot c_{y\beta} \cdot b}{2F_m} \geq 1 \\[3ex]
\left(1 + \dfrac{F_{\beta y} \cdot c_{y\beta} \cdot b}{2F_m} \right)^{\frac{1}{1 + \frac{h}{b} + \left(\frac{h}{b}\right)^2}}; & \dfrac{F_{\beta y} \cdot c_{y\beta} \cdot b}{2F_m} < 1
\end{cases}
\tag{9}
$$

- Transverse load factor $K_{F\alpha}$ is used to include the influence of load distribution along the meshing teeth pairs. It is affected by the gear geometry, modifications, accuracy grade, and overall stiffness. For spur gears, it is calculated using expression (10):

$$
K_{F\alpha} =
\begin{cases}
1; & K_{F\alpha} < 1 \\[2ex]
\dfrac{\varepsilon_\alpha}{2}\left[0.9 + 0.4 \dfrac{b \cdot c_{y\alpha}(f_{pb} - y_\alpha)}{F_{tH}} \right]; & 1 \leq K_{F\alpha} \leq \dfrac{\varepsilon_\alpha}{0.25 \cdot \varepsilon_\alpha + 0.75} \\[2ex]
\dfrac{\varepsilon_\alpha}{0.25 \cdot \varepsilon_\alpha + 0.75}; & \dfrac{\varepsilon_\alpha}{0.25 \cdot \varepsilon_\alpha + 0.75} < K_{F\alpha}
\end{cases}
\tag{10}
$$

After calculating the existing stress, it is compared to the permissible value. The permissible tooth root stress is found using the expression (11):

$$
\sigma_{FP} = \frac{\sigma_{Flim} \cdot Y_{ST} \cdot Y_{NT}}{S_{Fmin}} \cdot Y_{\delta relT} \cdot Y_{RrelT} \cdot Y_X
\tag{11}
$$

The permissible stress is influenced by a number of factors. The allowable stress number σ_{Flim} is used as a basis, further divided by safety factor for tooth breakage S_{Fmin}. The influences of load cycle number, notch sensitivity, surface properties, and size are introduced through calculation factors:

- Stress correction factor Y_{ST} is used to relate the dimensions to the standard reference test gears. As recommended in standard [3], $Y_{ST} = 2$ is used.
- Life factor Y_{NT} is used to assess the influence of number of load cycles. The number of load cycles gear can endure is mostly limited by the mechanical properties of the material and heat treatment applied to it. Accordingly, value of Y_{NT} can be found in standard [3].
- Relative notch sensitivity factor $Y_{\delta relT}$ accounts for the notch sensitivity of the material, and is a function of stress correction factor and material properties:

$$Y_{\delta\text{relT}} = \frac{1 + 0.82(Y_S - 1) \cdot \sqrt[4]{\dfrac{300}{\sigma_{0.2}}}}{1 + 0.82 \sqrt[4]{\dfrac{300}{\sigma_{0.2}}}} \tag{12}$$

- Relative surface factor Y_{RrelT} is used to include the influence of surface properties on the allowable tooth root stress. It depends on the material and the surface roughness:

$$Y_{\text{RrelT}} = 5.306 - 4.203(Rz + 1)^{0.01} \tag{13}$$

- Size factor Y_X accounts for the influence of size on material properties and its homogeneity. For steel gears it is determined as a function of gear module m:

$$Y_X = \begin{cases} 1; & m \le 5 \\ 1.03 - 0.006\,m; & 5 < m < 30 \\ 0.85; & 30 \le m \end{cases} \tag{14}$$

Flank surface durability

Alongside the tooth root stress, the surface durability of the flanks is one of the limiting factors when designing the geared transmission. As the curvature radii of the gear flanks are varying, calculation is conducted using the pitch point data, while the load capacity in points B and D is verified additionally. The critical stress is usually found in the inner point of single tooth contact B [3]. Furthermore, due to the less critical form of damage, safety factors are usually lower than ones used for tooth root bending strength calculation. To calculate the Hertzian (contact) stress of the gear pair, expression (15) is used:

$$\sigma_H = \left(Z_H \cdot Z_E \cdot Z_\varepsilon \cdot Z_\beta \cdot \sqrt{\frac{F_t}{d_1 \cdot b} \cdot \frac{u + 1}{u}} \right) \cdot Z_B \cdot Z_D \sqrt{K_A \cdot K_v \cdot K_{H\beta} \cdot K_{H\alpha}} \tag{15}$$

The part of the equation inside the parentheses represents the nominal contact stress σ_{H0}; the stress in a flawless gear loaded with a static torque. The Z members denominate the calculation factors required to calculate it, while the K members, correspondingly to the tooth root stress, include the dynamic effects. The calculation procedures of all the Z members are covered in the part 2 of standard. An overview of the calculation members is shown next:

- Zone factor Z_H is introduced to describe the geometry of tooth flanks. Since the flanks are involute, curvature radii are different for each point on the line of action, directly influencing the contact area. It is tied to the pitch point; to check other points, single

tooth contact factors Z_B and Z_D are used along. It is strongly influenced by the number of teeth, profile shift coefficients, and the centre distance:

$$Z_H = \sqrt{\frac{2 \cos \beta_b \cdot \cos \alpha_{wt}}{\cos^2 \alpha_t \cdot \sin \alpha_{wt}}} \tag{16}$$

- Elasticity factor Z_E accounts for the influence of material elasticity by including the Young moduli of elasticity and Poisson's ratios [3]. Materials with lower Young moduli values have a significantly lower Z_E, resulting in lower Hertzian stress. If materials of meshing gears differ, it is calculated as:

$$Z_E = \sqrt{\frac{1}{\pi \left(\dfrac{1 - v_1^2}{E_1} + \dfrac{1 - v_2^2}{E_2} \right)}} \tag{17}$$

- Contact ratio factor Z_ε includes the influence of contact ratio. In spur gear pairs, it depends only on the transversal component ε_α as the helix angle is 0°:

$$Z_\varepsilon = \sqrt{\frac{4 - \varepsilon_\alpha}{3}} \tag{18}$$

- Helix angle factor Z_β introduces the influence of the helix angle on the load distribution and depends only on helix angle β. Since only the spur gear pairs are considered, its value is 1.

- Single tooth contact factors Z_B and Z_D are required to calculate contact stresses in critical points of contact. In inner and outer point of single tooth contact B and D, curvature radii and thus a relative curvature radius are different due to involute geometry of a gear pair. Factors Z_B and Z_D account for this change:

$$Z_B = \begin{cases} 1; & \sqrt{\dfrac{\rho_{C1}\rho_{C2}}{\rho_{B1}\rho_{B2}}} \leq 1 \\ \sqrt{\dfrac{\rho_{C1}\rho_{C2}}{\rho_{B1}\rho_{B2}}}; & \sqrt{\dfrac{\rho_{C1}\rho_{C2}}{\rho_{B1}\rho_{B2}}} > 1 \end{cases} ; \quad Z_D = \begin{cases} 1; & \sqrt{\dfrac{\rho_{C1}\rho_{C2}}{\rho_{D1}\rho_{D2}}} \leq 1 \\ \sqrt{\dfrac{\rho_{C1}\rho_{C2}}{\rho_{D1}\rho_{D2}}}; & \sqrt{\dfrac{\rho_{C1}\rho_{C2}}{\rho_{D1}\rho_{D2}}} > 1 \end{cases} \tag{19}$$

When observing the dynamic factors, only $K_{H\beta}$ has to be calculated. The values of application K_A and internal dynamic factor K_v are calculated while determining the tooth root load capaci-

ty. Furthermore, when observing the spur gear pairs, values of transverse contact factors for tooth root $K_{F\alpha}$ and flank $K_{H\alpha}$ load calculation are equal [3]; $K_{F\alpha} = K_{H\alpha}$. Only remaining dynamic calculation factor is:

- Face load factor $K_{H\beta}$ is calculated using the Method C of the ISO 6336:2006. As the above mentioned $K_{F\beta}$ factor, it also accounts for the irregularities in load distribution across the gear face and is dependent on manufacturing and assembly errors andmeshing stiffness:

$$K_{H\beta} = \begin{cases} \left(\sqrt{\dfrac{2F_{\beta y} \cdot c_{y\beta} \cdot b}{F_m}} \right); & \dfrac{F_{\beta y} \cdot c_{y\beta} \cdot b}{2F_m} \geq 1 \\ \left(1 + \dfrac{F_{\beta y} \cdot c_{y\beta} \cdot b}{2F_m} \right); & \dfrac{F_{\beta y} \cdot c_{y\beta} \cdot b}{2F_m} < 1 \end{cases} \tag{20}$$

Permissible contact stress is, similarly to the permissible tooth root bending stress, determined using the allowable stress number σ_{Hlim} and S_{Hmin} adjusted by the calculation factors:

$$\sigma_{HP} = \frac{\sigma_{Hlim} \cdot Z_{NT}}{S_{Hmin}} \cdot Z_L \cdot Z_v \cdot Z_R \cdot Z_W \cdot Z_X \tag{21}$$

Through said calculation factors, influences of the required number of cycles, lubricant film properties, work hardening, and size are included:

- Life factor Z_{NT} accounts for the variations in stress during the gear working life. Life factor value largely depends on the number of load cycles, gear material, its mechanical properties and applied heat treatment, lubrication, and pitchline velocity. It is determined empirically; for up to 10^9 load cycles, $Z_{NT} = 1$.

- Lubricant film factor (lubricant viscosity) Z_L is first of the three lubricant film factors that further include the influence of lubrication which is necessary in steel gear pairs. Factor Z_L is focused on the lubricant viscosity and is calculated as:

$$Z_L = C_{ZL} + 4(1 - C_{ZL}) \cdot v_f \tag{22}$$

- Lubricant film factor (sliding velocity) Z_v is focused on the influence of the sliding velocity on the lubrication regime. It is calculated using expression (23):

$$Z_v = C_{Zv} + \frac{2 \cdot (1 - C_{Zv})}{\sqrt{0.8 + \dfrac{32}{v_{visc}}}} \tag{23}$$

- Lubricant film factor (surface roughness) Z_R is the last lubricant film factor, focused on influence of surface roughness. It is a function of gear pair accuracy grade, mean surface roughness, relative curvature radius, and mechanical properties of the material:

$$Z_R = \left(\frac{3}{Rz \sqrt[3]{\frac{10}{\rho_{red}}}} \right)^{C_{ZR}} \tag{24}$$

- Work hardening factor Z_W introduces the beneficial effects of meshing a surface hardened gears:

$$Z_W = \begin{cases} 1.2 \left(\dfrac{3}{Rz_H} \right)^{0.15}; & \text{HB} < 130 \\[2mm] \left(1.2 - \dfrac{\text{HB} - 130}{1700} \right) \left(\dfrac{3}{Rz_H} \right)^{0.15}; & 130 \leq \text{HB} \leq 470 \\[2mm] \left(\dfrac{3}{Rz_H} \right)^{0.15}; & 470 < \text{HB} \end{cases} \tag{25}$$

- Size factor Z_X similarly to Y_X accounts for the influence of gear size and material homogeneity. Its recommended value is $Z_X = 1$.

2.2.3. Thermoplastic gear strength requirements

The load capacity of thermoplastic gears is determined via the VDI 2736 guidelines [4]. While the calculation process is based on ISO 6336:2006, additional requirements exist; the root and flank temperatures, wear rate, and elastic deformation of the tip must be checked.

__Tooth temperature__

The tooth root and flank temperatures mainly affect the mechanical properties of the material. The effect is more prominent as the thermoplastics are thermal insulants, resulting in temperature spikes near the contact of point caused by low heat transfer coefficient. The root temperature is calculated as:

$$\vartheta_{Root} = \vartheta_0 + P \cdot \mu \cdot H_v \cdot \left[\frac{k_{\vartheta,Root}}{b \cdot z \cdot (v \cdot m)^{0.75}} + \frac{R_{\lambda,G}}{A_G} \right] \cdot ED^{0.64}, \tag{26}$$

where the ϑ_0 [°C] is ambient temperature, P [W] is total transmitted power, H_v [-] tooth loss degree, $k_{\vartheta,Root}$ [K(m/s)$^{0.75}$mm$^{1.75}$/W] heat transfer coefficient of the plastic wheel, $R_{\lambda,G}$

[Km^2/W] heat transfer resistance of the gearbox housing, A_G [m^2] heat dissipating surface of the housing, and relative duty based on ten minute cycle ED [-].

Tooth flank temperature is calculated in a same manner:

$$\vartheta_{\text{Flank}} = \vartheta_0 + P \cdot \mu \cdot H_v \cdot \left[\frac{k_{\vartheta,\text{Flank}}}{b \cdot z \cdot (v \cdot m)^{0.75}} + \frac{R_{\lambda,G}}{A_G} \right] \cdot ED^{0.64} \tag{27}$$

As seen in expressions (26) and (27), the friction coefficient has a significant influence on tooth temperature. Since VDI 2736 offers coarse friction coefficient values (i.e. value $\mu = 0.09$ is to be used in lubricated thermoplastic gears, regardless of the operating conditions), it was necessary to devise a more precise friction coefficient formulation (presented in Paper IV).

Tooth root bending strength

The calculation procedure is based on the ISO 6336:2006 presented in Section 2.2.2. However, in VDI 2736 it is recommended to use the tooth root stress factor K_F equal to:

$$K_F = K_A \cdot K_v \cdot K_{F\beta} \cdot K_{F\alpha} \tag{28}$$

There are two explanations for such simplifications. First, the low Young elasticity factors of thermoplastic gears result in lower sensitivity to manufacturing errors and tolerances as gear teeth have lower mesh stiffness, and thus, larger deflections. Low E values influence the factors $K_{F\beta}$ and $K_{F\alpha}$. Second reason are the good vibration damping properties of thermoplastic materials, directly reducing the vibrations covered by factor K_v.

The permissible tooth root stress is calculated as a ratio of nominal root strength number (bending) σ_{Flim} and minimum required safety S_{FminN}. It is influenced by the temperature and a number of load cycles [17].

Surface durability

The tooth flank load capacity is found using methods analogous to ones used in steel gear pairs. Similarly to tooth root bending strength calculation, factor K_H is used:

$$K_H = K_A \cdot K_v \cdot K_{H\beta} \cdot K_{H\alpha} \tag{29}$$

The permissible contact stress is affected by the number of cycles and expected working temperature. It is calculated as a function of allowable contact stress number, a minimum required safety, and a surface roughness factor (for thermoplastic gears $Z_R \approx 1$):

$$\sigma_{HP} = \sigma_{HlimN} \cdot \frac{Z_R}{S_{Hmin}}.$$

(30)

Wear resistance

When compared to steel gears, the wear resistance is a novel calculation criterion. It accounts for the abrasion wear prominent in dry running gear pairs. Mean wear is calculated as:

$$W_m = \frac{T \cdot 2 \cdot \pi \cdot N_L \cdot H_v \cdot k_w}{b \cdot z \cdot l_{Fl}}$$

(31)

In expression (31), T [Nm] is a rated torque, N_L [-] is desired number of load cycles, k_w [10^{-6} mm^3/(Nm)] wear coefficient, H_v [-] tooth loss degree, and l_{Fl} [mm] length of the active flank. Two ways of calculating the active flank length are advised; first being $l_{Fl} = 2\ m$. Within this study the second, more precise expression is used:

$$l_{Fl} = \frac{d_b}{4} \cdot \left\{ \tan^2\left[\arccos\left(\frac{d_b}{d_{Na}}\right)\right] - \tan^2\left[\arccos\left(\frac{d_b}{d_{Nf}}\right)\right] \right\}$$

(32)

Lastly, the mean wear value W_m is compared to the permissible wear:

$$W_m \leq W_P = (0.1 \dots 0.2) \cdot m$$

(33)

Tooth tip deformation

The tooth tip deformation calculation is required in thermoplastic gears due to low values of Young moduli, which result in high tooth deflections. Even though the tooth deflection can be beneficial by increasing the number of simultaneously meshing gear teeth pairs, it is limited to prevent the noise caused by the impact of such deviations and material creeping. The tooth addendum deformation λ is calculated as:

$$\lambda = \frac{7.5 \cdot F_t}{b \cdot \cos\beta} \cdot \left(\frac{1}{E_1} + \frac{1}{E_2}\right)$$

(34)

The permissible deformation is limited to $0.07\ m$. However, VDI 2736 notes that by further increasing it, the permissible tooth root stresses can be exceeded.

2.3. Power losses in gear pairs

Ever increasing environmental concerns and contemporary sustainable engineering mantra have emphasised the design of energy efficient mechanical systems. Since geared transmissions are necessary elements of such systems, low power losses are often one of the desired optimisation criteria. As put by Michaelis et al. [18] while observing personal vehicles, saving

a fraction of energy in gearbox results in multiple savings in fuel energy due to the inherent inefficiencies of the internal combustion engines. In this chapter, types of gearbox power losses and the factors that influence them are reviewed.

The gearbox power losses include losses of all system components: gears, bearings, seals, and auxiliary parts [18]. The power losses are divided into two main categories, the load dependent (load losses) and load independent (no-load) losses. Under constant load, the former are generally linearly dependant on the increase in sliding velocity, while the latter increase exponentially [15]. The overall gearbox losses are calculated using the following equation [18]:

$$P_{\text{loss}} = P_{\text{gi}} + P_{\text{gd}} + P_{\text{bi}} + P_{\text{bd}} + P_{\text{si}} + P_{\text{ai}} \qquad (35)$$

The first indices in equation (X) denote the component; gears (g), bearings (b), seals (s), and auxiliary parts (a), while the second denote whether the losses are load dependent (d) or load independent (i). The gear and bearing losses have both components, while the seal and auxiliary losses are exclusively load independent.

The load independent power losses are not affected by load changes and occur when the elements are moving, independently of the load. An experimental study on power losses in spur gear pairs was conducted by Petry-Johnson et al. [5], in which the authors assessed the influence of gear module size, surface roughness, and lubricant on both the load dependent and independent losses. According to [5], examples of load independent losses include the oil churning losses, rotating bearings and seals, inertial power losses, and air windage losses in gears. It was found that lubricant viscosity has a significant influence on load independent power losses, followed by the gear module. The load independent losses were significantly lower at 2000 revolutions per minute.

In this research study, the focus was on transmissions used in general engineering applications, operating at rotational velocities of up to 1500 to 2000 revolutions per minute. Consequently, the emphasis is on load dependent losses. As implied by their name, load dependent power losses occur in elements that transmit the load [19] and therefore are affected by its variations. Examples include the friction in gear pairs when transmitting torque and bearings working under the radial and axial loads.

Many theoretical studies on the subject were carried out [20–28], most of which were focused on load dependent (frictional) gear losses. Diez-Ibarbia et al. studied power losses in gear pairs, including the gears with tip relief [20,21] by using the method described in their earlier

work [23]. They have shown that load distribution along the line of action affects the losses in gears with tip relief. For this reason, it is important to point out that approximate equations for the load distribution calculation are developed by Sanchez et al. [29], who studied the stiffness of meshing gear teeth pairs.

Experimental study on the influence of profile shift and gear module on the power losses was carried out by Naruse et al. [30], who discovered that the losses increase with the module. Petry-Johnson et al. expanded this experiment by observing the influence of rotational speeds on the mechanical losses [5]. The experimental studies are more often conducted using the polymer gear pairs due to their sensitivity on variations in temperature. Polymer gears and related specifics are discussed in Section 2.7.

In the following subsections, theoretical approximations of power losses in gear pairs are reviewed. The influential factors were identified and discussed. The friction coefficient and load distribution were selected as such and are discussed in detail.

2.3.1. Theoretical approximations (formulations)

Based on the review shown in previous section, it can be concluded that gear pair power losses are affected by operational conditions (load, rotational velocity), gear geometry, and mechanical properties of both the material and lubricant. However, several formulations for calculation of gear pair power losses were used by researchers. In this subsection, existing models are reviewed aiming to find one applicable as the objective function. For a mathematical expressions of discussed power loss formulations, see Table 1.

When observing the power loss calculation in the context of objective function, additional criteria must be considered - the formulation should be analytic and straightforward. By utilising complex power loss formulation in combination with complex friction coefficient formulation, calculation and integration of objective function will a tedious task. On the other hand, even though some studies on gear pair power losses utilise the numerical finite element models, they are not suitable for optimisation for two main reasons. First, the numerical solutions lack generality [31] meaning that the implementation of such calculation would significantly increase the computational cost of the optimisation process. Secondly, the computational cost would be enormous as the numerical simulations would have to be repeated until the solution converges.

24

Xu et al. [32] have proposed a model for prediction of frictional power losses in gear pairs, which included load distribution and friction coefficient models. Influences of operational conditions, surface roughness, and lubrication regime were also accounted for. Results were validated using experimental data, demonstrating good overlapping with existing literature. Lastly, the parametric study was carried out by varying the operational conditions, geometric parameters, and modifications of tooth micro-geometry.

Velex and Ville [33] have suggested a displacement-based formulation to predict frictional power losses in gear pairs. Since displacements were used instead of the normal loads, no previous assumptions of load distribution model are required. The friction coefficient is assumed to be constant along the line of action. The deviations were found when observing spur gear pairs, while the agreement is satisfactory in helical gears.

Li and Kahraman [22] presented a theoretical model to predict losses in spur gear pairs based on transient elastohydrodynamic lubrication (EHL) model. A presented model accounted for rolling and sliding velocities, tooth curvatures, and normal load, and both the sliding and rolling

Table 1 – An overview of different power loss formulations

Authors	Formulation
Xu et al. [32], 2007.	$$P_{\text{loss}} = \sum_{q=1}^{Q} [\lvert F_s(\omega_1\rho_1 - \omega_2\rho_2)\rvert + \lvert F_r(\omega_1\rho_1 - \omega_2\rho_2)\rvert]_q$$ where: $$F_s = \mu(z, \theta, \phi_{\text{m}})F_{\text{n}}(z, \theta, \phi_{\text{m}})$$ $$F_r = \varphi_{\text{T}}(4.318)\left[\frac{\alpha E' v_0(u_1 + u_2)}{E'\rho_{\text{rel}}}\right]^{0.658}\left(\frac{F_{\text{n}}}{E'\rho_{\text{rel}}}\right)^{0.0126}\frac{\rho_{\text{rel}}}{\alpha}$$
Velex and Ville [33], 2009.	$$E_{\text{loss}} = -\mu_{\text{m}}k_{\text{m}}(1+u)r_{\text{b1}}\omega_1\Delta_{\text{m}} \times \int_0^1 [\tan\alpha_{\text{p}} J_2(\tau) - \frac{2\pi J_3(\tau)}{z_1} d\tau]$$ where: $$J_2(\tau) = \frac{1}{\varepsilon_\alpha b}\int_{L(\tau)}\left(1 - \delta E(M)\right)S_\delta(M)dM$$ $$J_3(\tau) = \frac{1}{\varepsilon_\alpha b}\int_{L(\tau)}\left(1 - \delta E(M)\right)S_\delta(M)\hat{x}(M)dM$$

Höhn [15], 2010.	$$P_{\text{loss}} = T_1 \omega_1 \mu_{\text{m}} \frac{\pi(i+1)}{z_1 i} (1 - \varepsilon_\alpha + \varepsilon_1^2 + \varepsilon_2^2)$$

Li and Kahraman [22], 2010.

$$P_{\text{mesh}} = \frac{1}{N} \sum_{n=1}^{N} P_{\text{mesh}}(n, \Delta\psi)$$

where:

$$P_{\text{mesh}}(\psi) = \begin{cases} = P_{\text{m}}(\psi); & \psi \in [A, B]; [D, E] \\ = P_{\text{m1}}(\psi) + P_{\text{m2}}(\psi); & \psi \in [B, D] \end{cases}$$

$$P_{\text{m}}(t) = \sum_{i=1}^{M} P(x_i, t)$$

$$P(x, t) = A \left[C_{\text{r}} \frac{h^3}{12\eta^*} \left(\frac{\partial p}{\partial x} \right)^2 + C_{\text{s}} \eta^* \frac{u_{\text{s}}^2}{h} \right]$$

Diez-Ibarbia et al. [23], 2016.

$$P_{\text{loss}} = \frac{F_{\text{tmax}} v}{\theta_N \cos\varphi} \int_{\theta_A}^{\theta_E} \frac{\mu(\theta) F_N(\theta) v_s(\theta)}{F_{\text{Nmax}} v} d\theta$$

power losses are considered. Finally, it is concluded that the contribution of rolling power losses is noted, and as such should be included when calculating pair efficiency.

Diez-Ibarbia et al. [34] also proposed a model to determine the efficiency of spur gear pairs, in which power losses depended on friction coefficient, sliding velocity, and load sharing (distribution) ratio. Even though friction coefficient is taken as constant and calculated using Schlenk's formulation [35], the model is compatible with formulations assuming that friction coefficient varies along the line of action (as presented in further studies [20]).

2.3.2. Friction coefficient in gear pairs

As seen in the previous subsection, the friction coefficient is one of the key factors when assessing the gear pair efficiency. Although many analytical and experimental studies have carried out on the subject, it remains an appealing and fruitful topic. The friction coefficient is a function of many variables, with a specific load, surface roughness, sliding velocity, flank curvature, and temperature being among them. Furthermore, since most gear pairs are lubricated using oil or grease, lubrication regime and lubricant viscosity have a significant effect. Three lubricating conditions are encountered depending on the oil film thickness: elastohydrodynamic (EHD) lubrication, mixed wear lubrication, and boundary lubrication [36]. Thus, due to the complexity of problem at hand, there are several different formulations. In this section, the general studies on the friction coefficient in the spur gear pairs are reviewed, along with the proposed formulations.

Influential variables

Xu [37] noted that a large part of the formulae was obtained by carrying out the experiment and subsequently curve fitting the measured data. The author suggested that expression (36) is often used as a general form:

$$\mu = f(\eta_\mathrm{k}, \eta_\mathrm{d}, v_\mathrm{s}, v_\mathrm{r}, \rho_\mathrm{red}, w, p_\mathrm{max}, Ra, \ldots) \tag{36}$$

In his review study Martin [38] observed that, when using EHD lubrication, the sliding velocity and load influence the friction coefficient. It was found to increase with the load, and decrease as the sliding velocity increases, up to a certain limit. Same results were acquired by Marjanović et al. in an experimental study [39]. The curvature radius was, however, not found to influence the friction coefficient [38].

When considering lubricant properties, Höglund observed that an increase in oil viscosity causes an increase in shear stress, while the lubricant shearing is one of the notable factors contributing to the friction coefficient [40]. Britton et al. [41] have carried out an experiment to investigate the effect of surface finish on the frictional losses in spur gear pairs. After comparing the specimens with a mean surface roughness of 0.05 μm and 0.5 μm, the authors have concluded that superfinishing decreased the friction for up to 30%.

Friction coefficient formulations

Over time, many empirical formulae for estimation of friction coefficient were devised. In a detailed overview written by Hai Xu in [37], the formulations by Drozdov and Gavrikov [42], O'donoghue and Cameron [43], and Benedict and Kelley [44] were explained. Said studies are not covered within this work, as the focus is on the more recent formulations. A thorough review of studies on the friction coefficient estimation was conducted by Martin [38].

Most of the recent studies are conducted by using either Niemann's equation derived by Schlenk [35], or a formulation based on non-Newtonian thermal elastohydrodynamic lubrication theory suggested by Hai Xu [37]. Two formulations were compared by Diez-Ibarbia et al. who assessed their influence on the efficiency of gears with tip relief [20]. It was observed that hybrid friction coefficient formulation by Xu was generally more conservative. An overview of formulations found during the literature review is shown in Table 2.

While studies are exclusively conducted on steel gears, there is no data for polymer gears. No friction coefficient formulations for polymer gears that include the influences of normal load, sliding velocity, and flank curvature were found during the literature review. For this reason,

an experimental study was conducted within the scope of this thesis. It is further described in Section 4.4 and can be seen in Paper IV.

Table 2 – An overview of different friction coefficient formulations

Authors	Formulation and observations
	$$\mu_{\mathrm{m}} = 0.048 \cdot \left(\frac{\frac{F_{\mathrm{b}}}{b}}{v_{\Sigma\mathrm{C}} \cdot \rho_{\mathrm{C}}} \right)^{0.2} \eta_{\mathrm{oil}}^{-0.05} \cdot R_{\mathrm{a}}^{0.25} \cdot X_{\mathrm{L}}$$
Schlenk [35], 1995.	As written in [15], Schlenk [35] assumed that the friction coefficient is constant along the line of action. The mean friction coefficient is calculated using the specific load F_{b}/b, sum speed at operating pitch circle $v_{\Sigma\mathrm{C}}$, relative curvature radii (reduced) ρ_{C}, dynamic oil viscosity η_{oil}, mean surface roughness Ra, and oil type factor X_{L}. Most of the studies are conducted using this formulation, mostly due to its simple integration. The coefficient is the same for all the points along the line of action so it can be separated from the integral.
	$$\mu = \frac{f(\xi)}{w(\xi)} = \frac{\int_{x_{\min}}^{x_{\max}} \tau_1(x,\xi)\,dx}{\int_{x_{\min}}^{x_{\max}} p(x,\xi)\,dx}$$
Larsson [45], 1997.	Larsson [45] has found the film thickness, pressure, and friction in the contact of two meshing involute spur gears by solving the transient Reynolds equation. The equation was discretised into 256 elements, and contact pressure was solved in 200 time steps. Such a calculation procedure could require significant computational resources when used as an objective function within the optimisation algorithm.
	$$\mu = e^{f(SR,P_{\mathrm{h}},v_0,R_{\mathrm{a}})} \cdot P_{\mathrm{h}}^{b_2} \cdot |SR|^{b_3} \cdot V_{\mathrm{e}}^{b_6} \cdot \eta_{\mathrm{oil}}^{b_7} \cdot \rho_{\mathrm{rel}}^{b_8};$$ $$f(SR,P_{\mathrm{h}},v_0,R_{\mathrm{a}}) = b_1 + b_4|SR| \cdot P_{\mathrm{h}} \log_{10}(\eta_{\mathrm{oil}}) + b_5 e^{-|SR| \cdot P_{\mathrm{h}} \log_{10}(\eta_{\mathrm{oil}})} + b_9 e^{R_{\mathrm{a}}}$$
Hai Xu [37], 2005.	The proposed friction coefficient expression is based on a non-Newtonian thermal elastohydrodynamic lubrication (EHL) model. The ball-on-disc type machine was designed to carry out the initial experiment. The entrainment velocity, slide-to-roll ratio, and maximum Hertzian pressure were selected as experimental variables. The expression is obtained by multiple linear regression analysis and shown to agree with experimental data. The adjusted R^2 is used to measure the goodness of fit. The suggested expression is applicable for calculation of power losses. The coefficients b_1 to b_9 are constant, while the determination of Hertzian pressure P_{h}, slide-to-roll ratio SR, entrainment velocity V_{e}, oil viscosity η_{oil}, and radius of relative curvature ρ_{rel} is trivial. The downside is the dependence of $\mu = f(\rho_{\mathrm{rel}})$, which

adds to the complexity of integration when calculating power losses.

$$\mu = c \cdot \frac{\sigma_{\mathrm{H}}^{\alpha}}{v_{\mathrm{s}}^{\beta}}$$

Marjanović et al. [39], 2010.	The authors conducted an experimental study to determine the most suitable form of the friction coefficient formulation. Three forms were assessed and using the empirical results, the coefficients can be calculated. However, as the constants are dependent on the experiment, no general solution was given, rendering the formulation not suitable for use as objective function in spur gear optimization.

$$\mu_{\mathrm{t}} = \frac{1}{W} \int_{x_{\mathrm{s}}}^{x_{\mathrm{e}}} q(x,t)\, dx$$

Li and Kahraman [46], 2011.	The authors suggested a method enabling the calculation of sliding and rolling power losses in mixed EHD lubrication. The friction coefficient formula was obtained by using linear regression. The model is robust, including the normal load, rolling and sliding velocities, radius of curvature, lubricant parameters, and surface roughness. The high R^2 value is reported, with authors characterising model as *"reasonably accurate under various contact conditions"*.

2.3.3. Load distribution

The distribution of load across the simultaneously meshing gear teeth pairs is not uniform along the line of action. It mostly depends on the mesh stiffness, which is primarily affected by a number of teeth pairs in contact and geometry of gear pair. Load distribution is shown in Figure 3, illustrating the load division. A pair of teeth enters the mesh at point A; by moving along the line of action, it reaches the lowest point of single tooth contact B. Upon reaching point A, the preceding pair of teeth is located in the highest point of single tooth contact D, meaning that two pairs are meshing simultaneously. When one of the pairs is located in point B, the preceding one is located at the end of the mesh (point E).
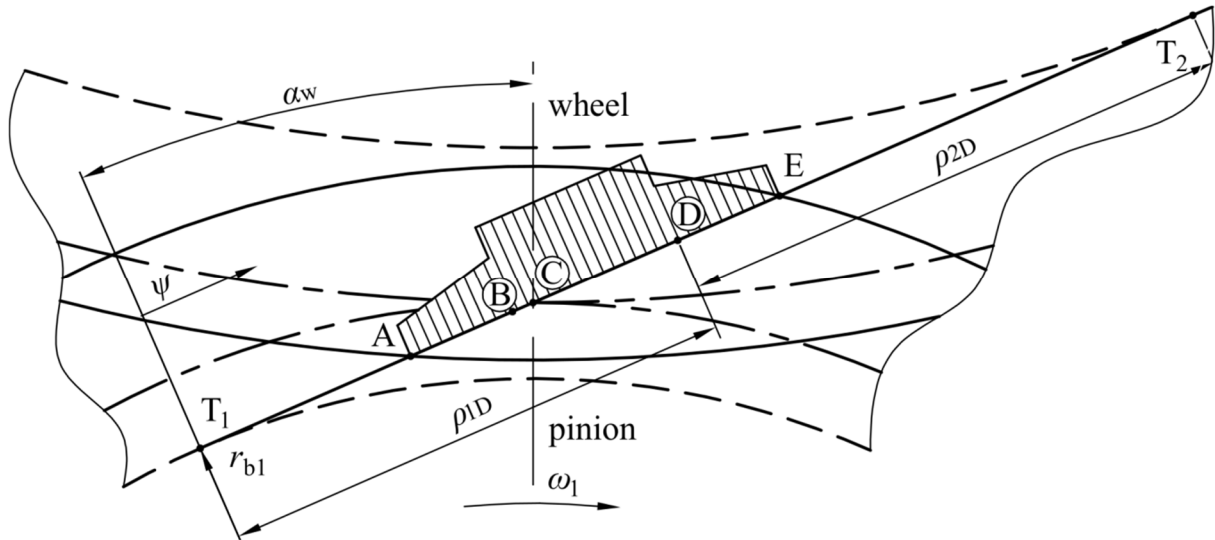
Figure 3 – Load distribution along the path of action (Paper II)

The exact load distribution across the meshing teeth can be calculated by utilising minimum elastic potential energy (MEPE) method, as shown by Sánchez et al. [29,31]. The approximate equations for calculation of load distribution ratio R_M [29] are straightforward and easy to embed into power loss expression:

$$R_M(\xi) \begin{cases} 0.36 + \dfrac{0.28}{\varepsilon_\alpha - 1}(\xi - \xi_A); & [\xi_A, \xi_B] \\ 1; & [\xi_B, \xi_D] \\ 0.36 - \dfrac{0.28}{\varepsilon_\alpha - 1}(\xi - \xi_A - \varepsilon_\alpha); & [\xi_D, \xi_E] \end{cases} \qquad (37)$$

2.4. Gear pair noise

The perceived quality of a machine or mechanism is highly dependent on the noise [47]. For example, blind tests have shown that loudness in axial piston pumps has a strong positive correlation with "dislike" and "unpleasantness" [48]. In gear pairs, it is widely accepted that noise is caused by vibrations stemming from tooth deformation along the mesh and transmission error [49,50].

Transmission error is defined as *"the difference between the actual position of the output gear and the position it would occupy if the gear drive were perfectly conjugate"* [51,52]. Many studies aiming to reduce gear noise were conducted. When compared to volume or power losses, determining the objective function which will accurately describe gear pair noise is a more complex task. Among the factors adding to the complexity are manufacturing errors

altering the gear pitch and flank profile, and variable tooth pair stiffness along the pitch line [29,31,53] causing variations in load distribution.

2.5. Optimisation algorithms in transmission design

A transmission design optimisation problem is complex, meaning that the use of computational algorithms is needed. Optimisation algorithms enable automated solving of such tasks with reasonable computational cost, avoiding the use of costly brute force approach. A general overview of algorithms applied by other researchers and accompanying guidelines are shown in this section. The algorithm selection process and related requirements applied to research at hand are presented in Section 3.4.

As seen in Table 2, evolutionary algorithms are used in the vast majority of the gear pair optimisation problems [76], with genetic algorithm being the most frequently used among them. In addition to the genetic algorithm, other evolutionary optimisation algorithms, such as the particle swarm optimisation or simulated annealing, can be used. A necessary condition for the use of evolutionary algorithms is the ability to evaluate the value of fitness function in each point within the design space.

Due to their dependence on the random number generation, algorithms mentioned above belong to the group of stochastic optimisation methods, meaning that it is possible to obtain different results in two consecutive runs of the same optimisation process. Stochastic methods have an inherent set of advantages and shortcomings. Arora [8] noted two: computational cost caused by a large number of required evaluations, and no guarantees that the global optimum was reached. The latter can be mitigated by rerunning the optimisation process several times. Savsani et al. [60] compared the performance of these algorithms by solving the gearbox volume minimisation problem [54].

If more objectives exist, the procedure is designed as multi-objective, since conducting the optimisation according to one of the objectives can negatively affect others [57]. An excellent example of the multi-objective optimisation algorithm is a non-dominated sorting genetic algorithm, NSGA-II [7], which has so far been applied to various technical problems. The algorithm output consists of Pareto optimal solutions, each of which offers a different weighting between the objectives, leaving the final decision to the operator. Alternatively, the weighted sum method can be used to carry out the multi-objective optimisation (see Section 3.2).

Currently, the design is often carried out by using simulation-based tools, while the scientific studies on optimisation are conducted using the evolutionary algorithms. As pointed out by Artoni [76], design optimisation of geared transmissions is a necessity as the design goals are often conflicting. Unfortunately, the two are not compatible as the computational costs would be astronomical. Thus, the author presented a methodology for simulation-based gear pair design optimisation when multiple objectives exist [76].

2.5.1. Genetic algorithm

The genetic algorithm is a nature-inspired search and optimisation method. Contrary to the linear (or quadratic) programming methods where the solution is found using the mathematical methods (for example, gradients), in the genetic algorithm, initial solutions are randomly generated. A set of initial solutions approaches the global optimum by utilising a set of genetic operators.

The randomly generated solutions are called the population, with first population being called the initial population. For each of the solutions within the initial population the fitness value is assigned, which is directly related or equal to the objective function value [77]. The solutions not satisfying the boundary conditions are given penalty to the fitness function value, or removed from the population. Each of the variable sets forming a solution is represented by a chromosome, which can be coded binary or floating point [78]. It was shown in [79] that a floating point representation is more consistent, and thus superior.

The solutions with the higher fitness are then submitted to a set of genetic operators (as presented by Deb in [77]):

1. *Selection (reproduction)* – the solutions with an above average fitness are selected as parents for the next generation (expression *mating pool* can be used instead). The strings are selected from the chromosome, similarly to the process in nature, and combined into a new unit. Solutions with higher fitness are often assigned a higher chance to be selected from a mating pool.

2. *Crossover* – after the selection, two strings are selected from the mating pool and their parts are exchanged. The length of the exchanged string fractions is random.

3. *Mutation* – a random part of the string is randomly changed (*"mutated"*), aiming to prevent the loss of genetic material. In the case of binary representation, 0 is changed to 1, or vice versa.

After the genetic operations are carried out, the new population is assembled. Its size is equal to size of the initial population. Additionally, elite chromosomes can be included in the genetic algorithm. The specimen with the highest fitness function value in a generation is an elite chromosome and is included in the next generation without being modified by genetic operators. The schema of a genetic algorithm is shown in Figure 4.
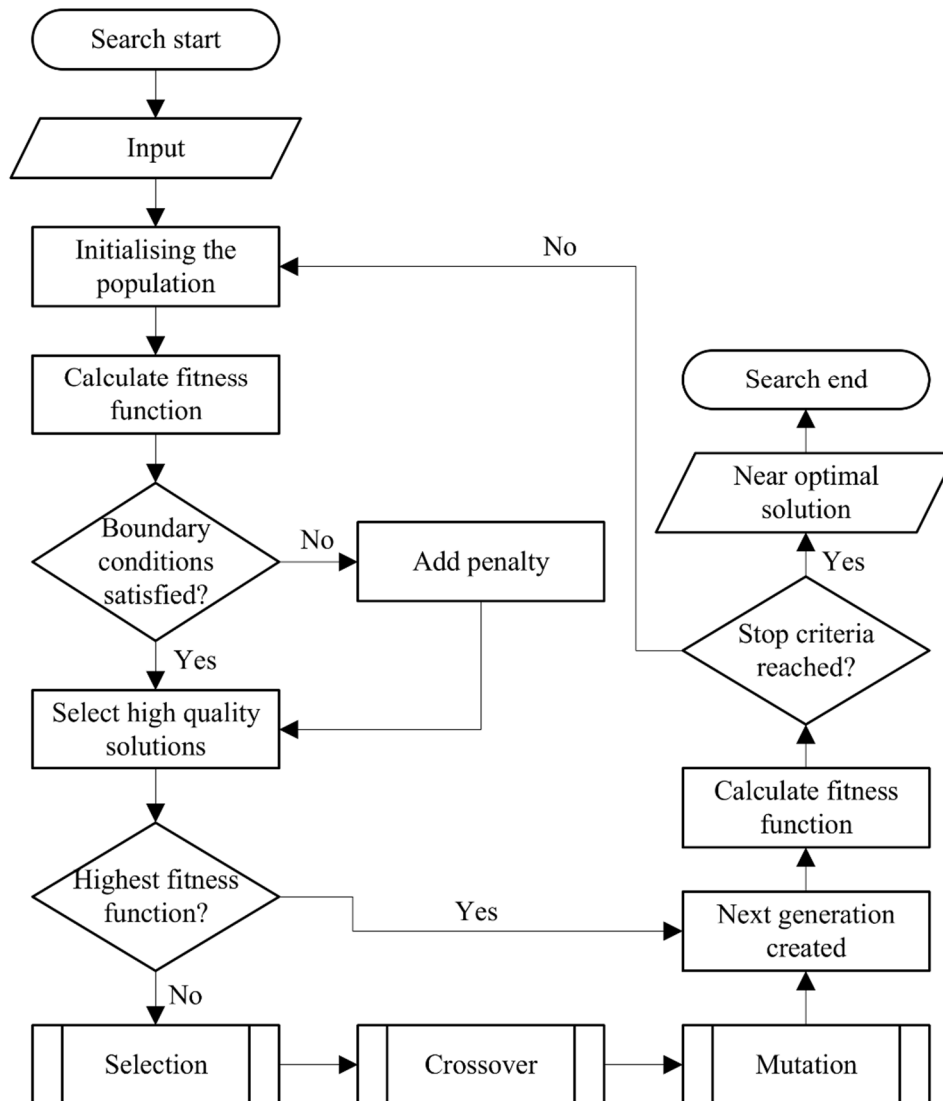
Figure 4 – Genetic algorithm flowchart (including the elite chromosome)

The genetic algorithm moves towards the optimal solution in each generation, meaning that the convergence is assured [55]. As such, genetic algorithms are suitable for solving complex technical problems. However, if there are continuous variables used, it will be almost impossible to find the optimal solution using the genetic algorithm. It is not an exact optimisation method, meaning that the final result will not be mathematically optimal, but heuristic (near-

optical) and good enough for the use in engineering. For this reason, the stop criteria are required.

The algorithm also relies on the randomly generated population to find the optimal solution, meaning that population size [80] and unit distribution across the population affect the convergence rate. Maaranen et al. state that uniform distribution is more important than the randomness of units in a population [81,82]. The authors compared using the pseudorandom and quasi-random sequences during the creation of the initial population. Using the quasi-random sequences improved the objective function value of the final solution.

2.5.2. Particle swarm optimisation

Particle swarm optimisation (PSO) is a type of evolutionary computational technique based on the behaviour of fish schools and bird flocks [8]. An individual (particle) behaves according to both its own and collective intelligence, for example, by adjusting its movements to the movements of the collective. The flowchart of particle swarm optimisation algorithm is shown in Figure 5.

Similarly to genetic algorithms, it requires an initial population [83], which is often randomly selected. In addition to initial values of design variables, each particle is assigned a velocity and potential solutions. Coordinates of each particle are tracked while advancing through the generations. With each new step, the velocity of each particle is altered towards the best solution so far (*pbest*) and global best value (*gbest*) [83].

In addition to the inherent advantages of evolutionary algorithms, particle swarm optimisation has two advantages when compared to genetic algorithms. First, there is no need for design representation (in genetic algorithms designs are represented as sets of binary numbers), and second, complex genetic operators are not required [8].
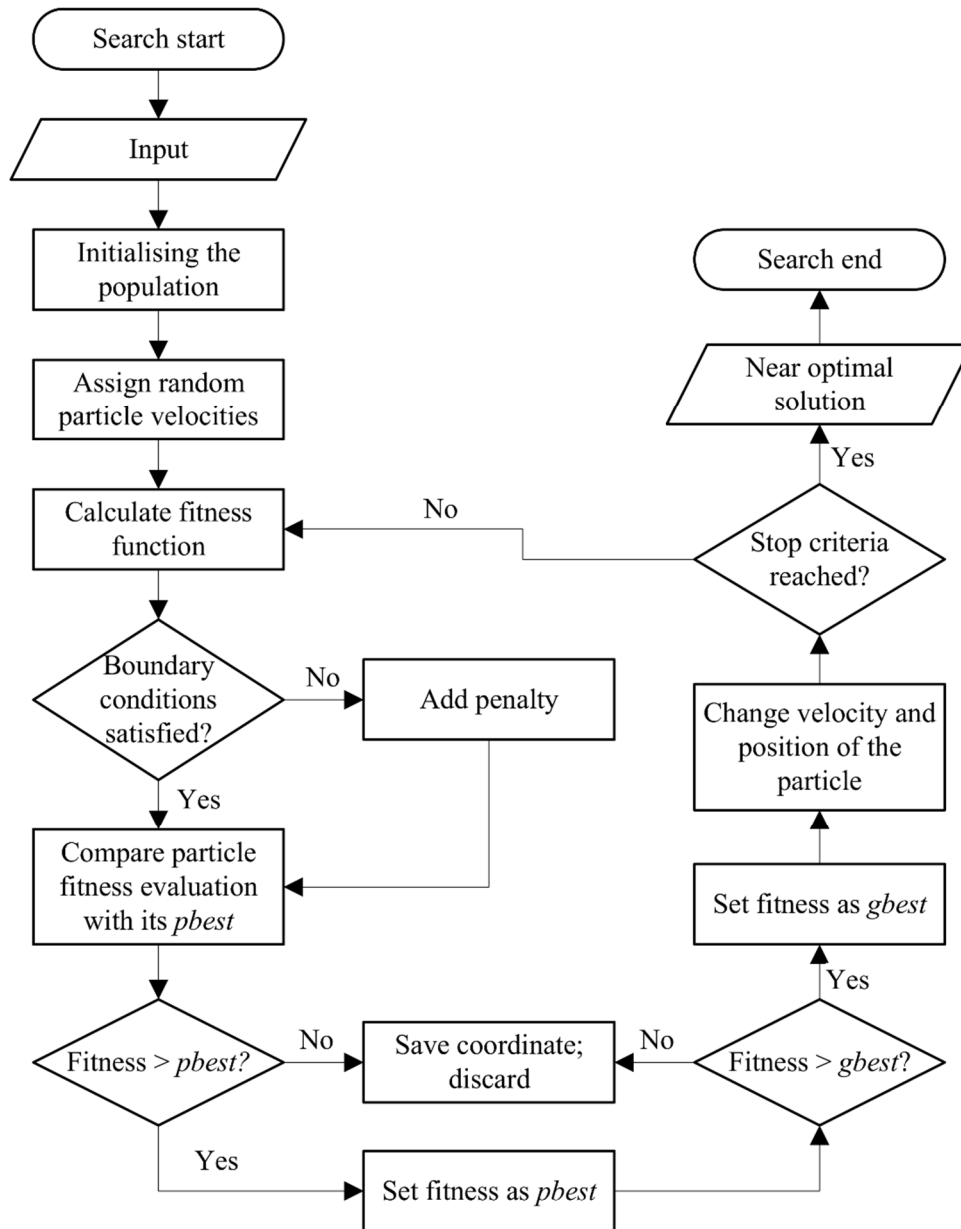
Figure 5 – Particle swarm optimisation flowchart (as presented in [83]*)*

2.5.3. Simulated annealing

Simulated annealing is a type of evolutionary algorithm based on the simulation of annealing of solid materials. The optimisation algorithm is inspired by, as Gelatt et al. [84] put it, *"a deep and useful connection between statistical mechanics and multivariate or combinatorial optimisation"*. In the metallurgical process of annealing, material is heated until it reaches liquid phase. The particles rearrange themselves in the low energy state during the slow cooling [85]. Descriptions within the following paragraph are based on the explanations by Arora [8]. The flowchart of simulated annealing optimisation process is shown in Figure 6.
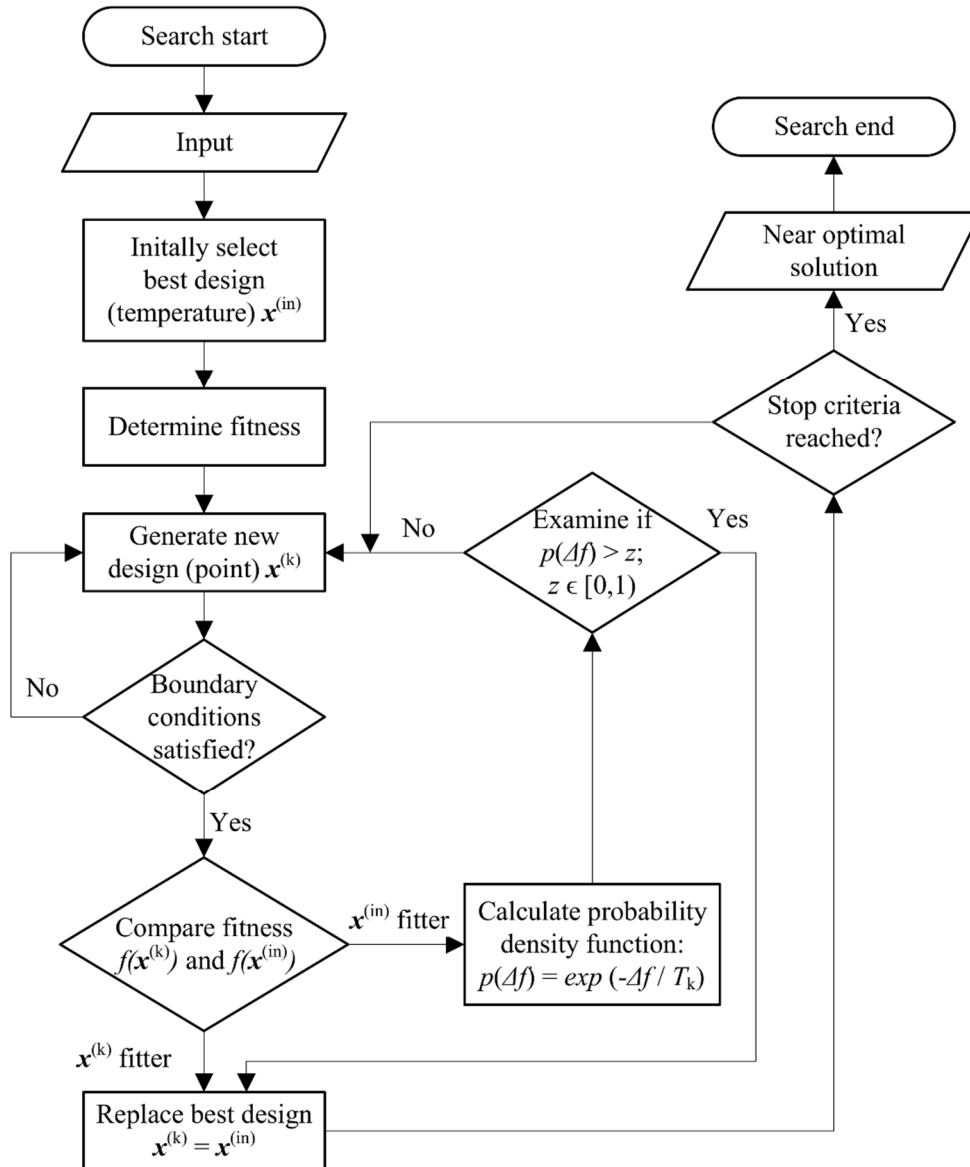
35

Figure 6 – Simulated annealing algorithm flowchart

The initialisation is the first step of the simulated annealing optimisation algorithm. In the initial step, the temperature reduction factor and stop criterion are set. The initial temperature and design are selected, and the value of fitness function is calculated for selected design. The random point is generated, and fitness function is calculated providing that suggested design satisfies pre-set constraints. If new design has a better value of the fitness function, it is accepted as new best design. If new design is found to be worse, Boltzman-Gibbs probability density function value is calculated:

$$p(\Delta f) = \exp\left(-\frac{\Delta f}{T_k}\right); \quad \Delta f = f\left(x^{(k)}\right) - f\left(x^{(in)}\right) \tag{38}$$

36

Value of probability density function is compared to the random variable $z \in [0, 1)$. If $p(\Delta f)$ value is greater than z, design $x^{(k)}$ is accepted as the best one, even though its fitness function value is not the lowest. This operation enables the algorithm to keep searching the design space for the global minimum. As the number of iterations increases, T_k value is reduced by temperature reduction factor r, meaning that it becomes harder to select an inferior design as the best one due to the lower value of $p(\Delta f)$.

2.6. Optimisation of steel spur gear pairs

Gear pairs are used in a wide array of machines, ranging from pharmaceutical to automotive industry, each having specific demands. Thus, the term optimal has different connotations for different systems [8] – transmission weight is an essential criterion in a design of racing vehicles, whereas it is irrelevant in the railroad industry and naval architecture. Other criteria, such the efficiency, noise level, durability, or cost can also be used. In this section, a literature review of the studies on gear pair optimisation is shown.

During the literature review, the gear pair volume (sometimes replaced with weight) was found to be used in a vast majority of studies, followed by the gear pair power losses and the noise level. Observed studies are split into sections according to the criterion (objective function) used. After each of the sub-sections, an overview is given in the form of a table for better visibility. In the fourth sub-section, the variables used in the reviewed studies are shown.

2.6.1. Gear pair volume/weight

Lower gear pair volume (and consequently, weight) results in a handier and more compact design. As such it is an important feature and remains the most sought-after requirement; a majority of studies have been conducted with volume as an optimisation objective. Nowadays, the minimum weight optimisation problem is often solved using computational algorithms. In the field of geared transmissions, use of genetic algorithm was first suggested by Yokota et al. [54]. The authors formulated and solved the optimal weight design problem consisting of one gear pair. The gear geometry was defined using three variables: gear module, face width, and the number of teeth. Each of the gears had a bore to fit the shafts. The pinion bending strength determined using the Lewis formula, surface durability, shaft strength, and the centre distance served as constraints.

The possibility of gear optimisation using the genetic algorithm was also studied by Marcelin [55]. In an attempt to reduce the gear pair volume, balance the sliding speeds, and balance the

transmissible power regarding the contact pressure and tooth root strength, an optimisation problem was formulated. Even though the multiple criteria were used, there was only one objective function. It included all three criteria adjusted using the weighting coefficients, enabling the use of single-objective optimisation methods. The teeth numbers, gear module, profile shift coefficients, and the helix angle were used as design variables. In his later work [56], Marcelin also examined the performance of the genetic algorithm on other mechanisms.

Complexity increases when solving multi-stage optimisation problems. The optimal multi-stage transmission will most likely not be the sum of optimal solutions for each of the pairs, thus requiring the objective function to include the total volume [57]. Gologlu and Zeyveli [58] used a genetic algorithm to automate the design of two-stage gearboxes. Contrary to the study by Marcelin [55], the profile shift coefficient was not used as a design variable as authors focused on the preliminary design. The design variable vector included the gear module, face width, and teeth numbers. It was shown that the results converged after 50 generations, resulting in a low computational cost.

Tudose et al. [59] attempted to solve the two-stage helical gear transmission design problem. The two-phase genetic algorithm was used. The six design variables were used; variables used by Gologlu and Zeyveli [58] were supplemented with standard centre distances, profile shift coefficients, and helix angles. The authors focused on algorithm performance; no design guidelines were presented.

Savsani et al. [60] examined the performance of different optimisation algorithms using the minimum weight problem presented by Yokota et al. [54]. Besides the genetic algorithm, the authors used the particle swarm optimisation and simulated annealing algorithms. The results have shown that both the particle swarm and simulated annealing algorithms performed better when compared to the genetic algorithm.

Mendi et al. [61] extended the multi-stage gearbox optimisation by including shafts and bearings into the objective function, thus ensuring the optimised final design. The objective function was simple and was equal to the total volume of the gearbox. Marjanović et al. [62] attempted to determine the optimal concept of a gearbox design. The novelty of a presented study is that the authors provided an algorithm that, besides the optimisation of geometric parameters, selects the optimal gear train concept. The authors have not stated which algorithm was used, only that the study was conducted using the "original software". Even though more studies are focused on the spur gears, some including helical gears also exist [63].

Golabi et al. [63] intended to provide guidelines for gearbox design. After conducting an optimisation process, the authors presented diagrams aiming to help designers to select a number of stages, and gear pair modules and face widths.

Table 3 – The optimization processes using the volume/weight as objective function

Authors	Algorithm	Aim	Algorithm properties (G – weight, V – volume)
Yokota et al. [54], 1998.	Genetic	To determine whether the GA is suitable for solving the optimal gear weight design problem (one-stage).	$f(x) = G$ $x = [m, z_i, b]$
Marcelin [55], 2001.	Genetic	To examine the possibility of using the genetic algorithm for solving a one-stage gear design problem.	$f(x) = V$ $x = [m, z_i, x_i, \beta]$
Gologlu and Zeyveli [58], 2009.	Genetic	To automate the preliminary design of a two-stage helical gear train.	$f(x) = V$ $x = [m^{(i)}, z^{(i)}, b^{(i)}]$
Tudose et al. [59], 2010.	Genetic	To optimise two-stage helical gear transmission design problem, including shafts, bearings, and housing.	$f(x) = G$ $x = [m^{(i)}, z^{(i)}, x^{(i)}, \beta^{(i)}]$
Savsani et al. [60], 2010.	Genetic, particle swarm, simulated annealing	To compare the performances of different algorithms when solving the minimum weight problem in spur gear design.	$f(x) = G$ $x = [m, z_i, b]$
Mendi et al. [61], 2010.	Genetic	To obtain the optimal dimensions of the gearbox shafts, gears, and the rolling bearing.	$f(x) = V$ $x = [m, z_i, b]$
Marjanović et al. [62]. 2012.	Not stated	To select the optimal gearbox concept and reduce its weight.	$f(x) = G$
Golabi et al. [63], 2014.	*fmincon* function (Matlab)	To derive diagrams for a selection of a number of stages, and gear pair modules and face widths.	$f(x) = V$

2.6.2. Power losses

Aiming to decrease the power losses in gear pairs, Baglioni et al. [25] studied the influence of addendum modification on the pair efficiency. Two friction coefficient formulations were used; formulation by Schlenk [35], in which the friction coefficient is considered constant along the mesh, and by Hai Xu [37], in which the friction coefficient is variable and depends on local stresses (For additional details on friction coefficient formulations see Section 2.3.2).

The resulting procedure was used to assess the impact of profile shift on the gearing effectiveness. The authors have made the following conclusions:

- An increase in the sum of profile shift coefficients increases efficiency; increasing the pinion profile shift coefficient is more beneficial.

- Efficiency decreases as the torque and normal load increase, while the contrary is observed as the rotational velocity.

Höhn et al. [19] attempted to reduce power losses in gear pairs by evaluating the influences of each geometric parameter individually. The power loss was calculated by integration of sliding velocity, friction coefficient (formulation by Schlenk [35] was used), and normal load along the line of action. The transverse contact ratio and gear module were identified as the most influential geometric parameters. In order to reduce the power losses, the authors suggested reducing the gear module and transverse contact ratio, and increasing the root fillet radius, pressure angle, and face width.

2.6.3. Noise level

Bonori et al. [64] used a genetic algorithm to find the optimal values of the micro-geometric modifications of gear profile. The static transmission error (STE) was calculated using the finite element calculations and served as objective function. Bozca [65] carried out a research study aiming to reduce gear-rattle noise in automotive transmission gearbox by utilising optimisation algorithms. The transmission error was used as an objective function, while the ensuing noise (rattle and clatter) was calculated as suggested by Dogan et al. [66]:

$$L_{\text{pComp}} = 10 \log \sum_{i=1}^{n} \left(10^{0.1} L_{\text{p}i} \right). \tag{39}$$

A 95% reduction in transmission error resulted in 12% decrease in noise. Based on the results, the author concluded that:

- It is possible to reduce the ensuing gearbox noise through a careful selection of geometric parameters.

- An increase in gear module results in the increased gear-rattle noise. Same was found for the number of teeth.

- An increase in profile shift coefficient resulted in reduced gear-rattle noise.

2.7. Design of polymer gears

The use of polymers as materials for gears manufacturing is on the rise. They are frequently used in household appliances or hobby tools due to their distinct advantages: the inexpensive serial production, ability to work without lubrication (dry running), low material density, and recyclability. However, in hand also come the disadvantages – their sensitivity to variations in temperature and humidity, lower permissible stresses, and Young modulus values. The calculation method is defined in VDI 2736 [4] guidelines. For more details on the load capacity calculation, see Section 2.2.3.

Most of the current studies on polymer gear pairs are concerned with the power losses and ensuing temperature. Thermoplastics, as the most frequently used polymer subtype in gear manufacture, are thermal insulants. Walton et al. experimentally evaluated the influence of material [67] and teeth geometry on the gear efficiency [68]. An open-circuit device was used to conduct the experiment, enabling a more precise measurement of power losses. The higher values of the friction coefficient were observed in gears with a lower gear module and at larger sliding velocities. In comparison, Mao [69] used a closed-circuit device to observe the influence of heating on the wear of polymer composite gear.

The efficiency of polyamide gear pairs was assessed by Kirupasankar et al. [70] through the use of numerical methods. The authors noted that torque has a significant effect on power losses. Even though the results were verified experimentally, it should be pointed out that the friction coefficient formulation for steel gear pairs [35] was used, as no comprehensive friction coefficient formulation for polymer gears was found. For this reason, a novel formulation is proposed in Paper IV.

Temperature generation and dissipation is another frequently studied subject within the field. In a study aimed at identifying the applicability of different polymers as gear materials, Singh et al. [71] assessed the thermal and wear behaviour of said materials. The operational torque was found to have seven to eight times larger influence on the flank temperature when compared to sliding velocity. Fernandes et al. [72] used a finite element method to predict a thermal model which could be used to predict temperatures in polymer gears. Roda-Casanova and Sanchez-Marin [73] proposed a universal analytical approach to determine the thermal field in spur gears, regardless of the material.

In addition to the temperature, polymer gears are highly sensitive to the number of load cycles, as confirmed by Kalin and Kupec in [74]. They found S-N curves at different tempera-

tures and loads. To mitigate the resulting diminishing of mechanical properties, Bravo et al. proposed a modelling strategy to predict the damage mode depending on the number of load cycles [75].

3. DESIGN OPTIMIZATION MODEL

Within this section, the design optimisation model used to conduct the study is explained. The typical design optimisation model is presented, after which the model is built using the five-step formulation, as advised in [8]. Since steps one and two are covered within the introduction and the literature review, this section is focused on: defining the variables, determining the optimisation criteria to evaluate the design and the constraints formulation.

Once modelled, the optimal design problems are easily and quickly solved through the use of modern computers in a matter of seconds. However, analytical modelling and accompanying research may take days, weeks, or even months, depending on the problem. Besides, outputs are only as good as the inputs, meaning that overlooking one of the problem aspects can lead to unfeasible design. For this reason, in order to solve the design optimisation problem, it is imperative to formulate it accurately [8]; thus, the process of problem formulation is formalised. Within this study, the five-step formulation procedure presented by Arora [8] was used:

1. Project/problem description
2. Data and information collection
3. Definition of design variables
4. Optimisation criteria
5. Formulation of constraints

The first step aims to describe the problem at hand accurately. In this thesis, the problem is defined in Sections 1.1 to 1.3. Moreover, as indicated in the Hypotheses section, general guidelines for the design of both the steel and polymer spur gear pairs can be derived from the optimisation procedure.

The data and information collection step is required to gather all components of the future optimisation model. Here, the mathematical and physical expressions required for the accurate description of the model are investigated. This step is completed within Section 2, where the existing design guidelines were reviewed, along with the design space boundaries and constraints used within the field.

The steps three to five, concerned with the design variables, optimisation criteria, and design constraints are not yet completed and are covered in detail in the following subsections.

3.1. Definition of design variables

To start, relevant design variables must be detected; they should be as independent of each other as possible [8]. Based on the literature review shown in Section 2, the following variables are often selected as design variables:

1. **Gear pair module** is a standard value that determines the gearing size; it is a crucial factor when determining the gear tooth height, tooth thickness, and the gear pitch. As such, the module is detrimental when dimensioning the gearing.

2. **Gear pair face width** is a dimension of a gear pair along the shaft axis. It affects its load capacity and is necessary for the calculation of pair volume and friction coefficient between the meshing teeth.

3. **A number of teeth** influences the tooth geometry and curvature of its flanks, in addition to the gear diameter.

4. **Profile shift coefficients** alter the gear tooth geometry, affecting the pair load capacity accordingly.

Unfortunately, consensus regarding the selection of optimisation variables was not found during the literature review; one group of researchers uses three variables – gear module, face width and a number of teeth, while the other group uses five variables, also including profile shift coefficients of both gears. Additional research (see Appendix – Paper I) was necessary to determine the influence of profile shift coefficients. Results have shown that profile shift coefficients have a significant impact when minimising the volume.

Gears with asymmetric teeth, albeit exceptional in specific operating conditions [86,87], were not considered in this thesis. The manufacturing of gears with asymmetric tooth geometry requires asymmetric tools or use of more expensive manufacturing technologies such as the electrical discharge machining (EDM). On the other hand, the principal aim of this thesis was to achieve higher quality gear pairs through the integration of knowledge, while retaining the same, simple manufacturing techniques.

Lastly, the micro-geometry modifications were not considered. The motive for such decision is simplicity; additional machining operations are required to modify the gear tooth microgeometry. In this thesis, it was meant to increase the gear pair value while retaining the same level of complexity. The additional value is achieved by introducing knowledge stored within the optimisation process.

3.2. Optimization criteria

A quote by Arora is used to stress the importance of optimisation criteria: *"There can be many feasible designs for a system, and some are better than others"* [8]. The optimisation criteria enable a comparison of all the feasible designs and to determine which one is best aligned with the requirements. The optimisation criteria are mathematically expressed in forms of objective functions.

The objective function assigns a numerical value to the specific design, enabling us to rank feasible solutions. It should be added that objective functions must be affected by design variables [8]. The optimisation processes can be divided by a number of criteria; when there is only one criterion, the process is single-objective as there is only one objective function. When there are two or more criteria, it is multi-objective, requiring multiple objective functions.

The multi-objective optimisation cannot be carried out as a series of single-objective processes, each having a different criterion. The solution optimal concerning one of the criteria (objectives) will often result in a mediocre solution according to the remaining criteria [6]. In the context of gear pair optimisation, a literature review has shown that most of the conducted studies are using a single objective – gear pair volume. Solutions resulting from such process are most likely sub-par when observing other important criteria, such as power losses or noise levels. The multi-objective optimisation will result in a set of more comprehensive solutions displayed as Pareto optimal front.

Pareto optimal front consists of solutions that are not dominated by any other solutions. A solution is dominated if a better solution considering the set criterion exists within the feasible set. For the multi-objective optimisation, that means that no solution that has the same score according to one or more criteria, and better according to one other criterion exists. Such dominant solutions constitute the Pareto optimal front [88].

Besides using multiple objective functions resulting in Pareto optimal set, there are additional ways to conduct the multi-objective optimisation. The weighted sum method is a simple and commonly used approach to such problems. The value of the objective function is determined by assigning weights to partial objective functions, which ought to be normalised [8]:

$$f_{\text{obj}}(x) = \sum_{i=1}^{k} w_i f_i(x), \tag{40}$$

where f_i are partial objective functions, w_i weights assigned to each objective, and k is a number of objectives. The selected weights generally mirror the importance of each objective and significantly affect the solution [89]. Lastly, each solution obtained using the weighted sum method is a point on Pareto optimal front.

Based on the literature review, two optimization criteria are selected; gear pair volume (weight) and power losses (efficiency). Thus, two objective functions were required. The first objective function aims to rate the design solutions according to the volume. It is derived to include all the design variables, including the profile shift coefficient:

$$f_1(m, z_1, z_2, x_1, x_2, b) = \frac{\pi b}{4} \cdot m^2 \cdot [(z_1 + 2 + x_1)^2 + (z_2 + 2 + x_2)^2] \qquad (41)$$

The second objective function, used to rate design solutions by power losses was derived in Paper II:

$$f_2(m, z_1, z_2, x_1, x_2, b) =$$

$$= \frac{\mu_m F_{Nmax}}{m\pi \cos \alpha_w} \left[\begin{array}{l} \int_{\psi_A}^{\psi_B} v_s(\psi) R_{AB}(\psi) d\psi + \int_{\psi_B}^{\psi_C} v_s(\psi) R_{BD}(\psi) d\psi + \\ \int_{\psi_C}^{\psi_D} |v_s(\psi)| R_{BD}(\psi) d\psi + \int_{\psi_D}^{\psi_E} |v_s(\psi)| R_{AB}(\psi) d\psi \end{array} \right] \qquad (42)$$

The absolute values are inserted inside the integral to point out that the sliding velocity is always positive, since in case of negative value power losses also become negative. Negative frictional power losses would imply that the friction is producing additional energy, which is not in agreement with physical laws.

In the standard design optimization model, objective functions are always minimized. As the aim is to reduce both the volume and power losses, expressions (41) and (42) do not have to be altered. On the other hand, if the task would be a maximization of an objective, objective function would have to be reworked using the equation (43). The new objective function $F(x)$ would be minimized.

$$F(x) = -f(x) \qquad (43)$$

3.3. Formulation of constraints

The design space includes all combinations of design variables, not all of which adhere to the requirements set by clients or technical standards. Additional mathematical expressions called constraints are included to ensure that the optimal solution is feasible (i.e. meets all the requirements), limiting the design space to a set of feasible solutions. Identical to objective functions, constraints depend on the design variables [8]. A simple example of constraints are the design variable boundaries.

There are two types of constraints – equality and inequality constraints. In equality constraints, the relationship between the design variables and requirements are expressed by using the equals sign, wherein inequality constraints the less-than and greater-than signs are used. The former type is much more restrictive to the design space. However, when optimising gear pairs, only the latter is used.

The constraints in steel and grey iron gear pairs are governed by the ISO 6336:2006 standard [3]. Following constraints ensuing the necessary load capacity and transverse contact ratio must be satisfied to confirm that pair is feasible (for detailed explanations see Section 2.2.2):

$$\frac{F_t}{b \cdot m_n} Y_F Y_S Y_\beta Y_B Y_{DT} K_A K_v K_{F\beta} K_{F\alpha} - \frac{\sigma_{Flim} Y_{ST} Y_{NT}}{S_{Fmin}} Y_{\delta relT} Y_{RrelT} Y_X \leq 0 \tag{44}$$

$$Z_H Z_E Z_\varepsilon Z_\beta Z_B Z_D \sqrt{\frac{F_t(u+1)}{d_1 bu} K_A K_v K_{H\beta} K_{H\alpha}} - \frac{\sigma_{Hlim} Z_{NT}}{S_{Hmin}} Z_L Z_v Z_R Z_W Z_X \leq 0 \tag{45}$$

$$1.2 - \varepsilon_\alpha \leq 0 \tag{46}$$

Generally, calculation parameters found in equations (44), (45), and (46) are calculated for each observed design separately. However, parameters dependent only on the input data such as the stress correction factor Y_{ST}, life factors Y_{NT} and Z_{NT}, lubricant factor Z_L, material factor Z_E, and safety factors S_{Hmin} and S_{Fmin} can be calculated once and used for each unit in a population to reduce computational cost.

Expressions governing the load capacity of polymer gear pairs (thermoplastic are most widely used) are found in VDI 2736 [4]. Thermoplastic gears are more delicate than their steel counterparts, mainly due to extensive influence of temperature on their mechanical properties [17,90]. Besides the additional constraints (root and flank temperature, flank wear, and tip deformation), the tooth root and surface durability expressions are simplified when compared to equations (5) and (15). The values of factors $K_{F\alpha}$, $K_{F\beta}$, $K_{H\alpha}$, $K_{H\beta}$, and K_v are neglected (see

Equation 28 and Equation 29) as thermoplastic materials are elastic and capable vibration dampers [REF]. The necessary constraints for designing feasible thermoplastic gear pairs are:

$$\frac{F_t}{b \cdot m_n} Y_{Fa} Y_{Sa} Y_\varepsilon Y_\beta K_F - \frac{\sigma_{Flim}}{S_{Fmin}} \leq 0 \tag{47}$$

$$Z_H Z_E Z_\varepsilon Z_\beta Z_B Z_D \sqrt{\frac{F_t(u+1)}{d_1 bu} K_H} - \frac{\sigma_{Hlim} Z_R}{S_{Hmin}} \leq 0 \tag{48}$$

$$\frac{T \cdot 2 \cdot \pi \cdot N_L \cdot H_v \cdot k_w}{b \cdot z \cdot l_{Fl}} - (0.1 \ldots 0.2)m \leq 0 \tag{49}$$

$$\frac{7.5 \cdot F_t}{b \cos\beta}\left(\frac{1}{E_1} + \frac{1}{E_2}\right) - 0.07m \leq 0 \tag{50}$$

$$\vartheta_0 + P\mu H_v \left[\frac{k_{\vartheta,Root}}{bz(v \cdot m)^{0.75}} + \frac{R_{\lambda,G}}{A_G}\right] ED^{0.64} - \vartheta_{max} \leq 0 \tag{51}$$

$$\vartheta_0 + P\mu H_v \left[\frac{k_{\vartheta,Flank}}{bz(v \cdot m)^{0.75}} + \frac{R_{\lambda,G}}{A_G}\right] ED^{0.64} - \vartheta_{max} \leq 0 \tag{52}$$

$$1.2 - \varepsilon_\alpha \leq 0 \tag{53}$$

3.3.1. Design variable boundaries

A trivial example follows – a gear module of 0 yields a lowest gear pair volume, although such a solution has no practical value. For this reason, the intervals from which the design variables may be selected are limited, aiming to ensure the feasibility of solutions. Those simple constraints are called implicit constraints. Intervals from which the design variables were selected are shown in Table X.

Table 4 – Design variable boundary conditions

Design variable	Data type	Boundary
Gear module	Discrete	Standard value (ISO 54:1996 [91])
Face width	Continuous	$6 \ldots 30 \cdot m$
Number of teeth (pinion)	Integer	$14 \ldots 24$
Profile shift coefficient (pinion)	Continuous	$0 \ldots x_{1max}$
Profile shift coefficient (wheel)	Continuous	$-0.7 \ldots 0.7$

The gear pair modules were limited to standard values, as they are determined by cutting tool geometry. Thus, using a non-standard gear module would require a non-standard cutting tool, resulting in an increased cost. The optimisation can be carried out in two steps to determine the upper and lower interval boundary. In the first step, the process is carried out using a broad gear module boundaries, while in the second, the interval is reduced around the initial optimal solution.

The face width is also limited; the lower boundary prevents the selection of near-zero width gears. In helical gears, it is possible that such teeth lack the stability in the axial direction. The upper boundary ensures better load distribution across the face width since uniform distribution is rather hard to achieve at high widths, and requires narrow geometrical tolerances of both the shafts and housing.

Values of numbers of teeth and profile shift coefficients are restricted to ensure that gear tooth geometry is viable. Furthermore, selecting a large pinion number of teeth results in an uncondensed design due to a large centre distance. For more details on geometric requirements in gear teeth, see Section 2.2.1.

3.4. Algorithm selection

The algorithm that will be used for solving the design optimization problem is selected based on the literature review and presented design constraints. Several constraints on algorithm selection were recognized:

1. *Mixed variable problem* – the design optimization model consists of both the discrete (including the discrete variables) and continuous variables. The examples of discrete variables include teeth numbers of both the pinion and wheel, gear module, while the profile shift coefficients and face width are continuous variables.

2. *Non-smooth functions* – the functions are not smooth, rendering the gradient methods unusable. The discontinuities are found in some of calculation factors required to formulate the boundary conditions. Examples include the factors K_3 (8), $K_{F\beta}$ (9), $K_{F\alpha}$ (10), Y_X (14), Z_B (19), Z_D (19), and Z_W (25).

3. *Ensured convergence* – the convergence of the solution must be assured, and the global minimum must be found. While the modern computational algorithms have assured convergence, finding the global minimum is often problematic. As there are five mixed variables, it is unlikely that there are no local minima which algorithms often recognize as the global minimum.

According to Arora [8], the mixed variable optimisation problems (MV-OPT) can be divided into five categories. When assigning the category to a specific problem, following properties must be considered (also shown in Table 5): which variable types are encountered, are the functions differentiable, are the functions defined at non-discrete points, if the non-discrete variables are allowed for discrete ones, and whether the variables are linked.

Table 5 – Characteristics of different MV-OPT problems (as presented by Arora in [8])

MV-OPT	Variable types	Functions differentiable?	Functions defined at non-discrete points?	Non-discrete variables allowed for discrete ones?	Variables linked?
1	Mixed	Yes	Yes	Yes	No
2	Mixed	No	Yes	Yes	No
3	Mixed	Yes/No	No	No	No
4	Mixed	Yes/No	No	No	Yes
5	Discrete	No	No	No	Yes/No

The problem observed in this research study is classified as MV-OPT 3. Even though objective functions are well-defined when using the non-discrete values for gear modules or numbers of teeth, non-discrete solutions for discrete variables are not satisfactory. By subsequent rounding up or down of discrete variables, solution accuracy would be compromised.

The genetic algorithm was selected as it satisfies all the above-listed requirements. Firstly, it can solve the mixed variable problems without the use of relaxation, which could reduce the solution accuracy. Furthermore, as it uses the population upon which the function values are calculated, it requires neither the continuity nor differentiability of functions. Lastly, the convergence is assured as only the units with the highest objective function value progress into the next generation. In addition to satisfying all requirements, the genetic algorithm is the most often used algorithm within the field, as shown in Table 3. It was successfully used in previous studies [54–56,58–61].

The fast and elitist multi-objective genetic algorithm called NSGA-II *(non-dominated sorting genetic algorithm II)* proposed by Deb et al. [7] was used to conduct a multi-objective optimisation within this study. In NSGA-II, a crowded-comparison approach was used instead of the sharing function. The algorithm is effective and frequently used in numerous scientific fields, as witnessed by over 20,000 citations.

4. OVERVIEW OF CONDUCTED RESEARCH

The research was divided into six phases, which are then published in four research articles. The first two phases are published within the Paper I (Section 4.1.), third and fourth are contained in the Paper II (Section 4.2.), while the fifth and sixth phase are presented in the Paper III (Section 4.3.). Paper IV (Section 4.4.) includes the necessary friction coefficient data, which had to be found experimentally. Within each of the following sections, a summary, method, results, and conclusion subsections are shown.

The overview of the conducted research is divided into four papers. A brief summary containing the paper title, aim in the context of doctoral thesis, and research phases it completes (Table 6). The phases necessary to conduct a study are outlined in sections 4.1 to 4.4, each covering one of the appended papers. For each paper, the abstract is shown, after which the method is outlined. The method is supplemented with additional commentary and limitations observed in later phases. After outlining the main findings of the study, findings are discussed in the context of the thesis as a whole.

Table 6 – Appended papers in context of doctoral thesis

No.	Title	Aim in the context of thesis	Related to:
Paper I	*Influence of profile shift on the spur gear pair optimization*	- To review the existing literature and generate new ideas. - To examine whether the field of research is interesting to the scientific community. - To determine the number of required design variables for the optimization of spur gear pair macro-geometry.	Phase 1 Phase 2
Paper II	*Multi-objective spur gear pair optimization focused on volume and efficiency*	- To obtain a power loss formulation suitable for implementation in optimization algorithm. - To find the algorithm applicable to design optimization problem. - To determine how the geometric variables affect Pareto optimal fronts.	Phase 3 Phase 4
Paper III	*Optimization of polyox-*	- To develop objective functions and	Phase 5

51

ymethylene spur gear pairs with experimental validation	boundary conditions for thermoplastic gears. - To carry out the multi-objective optimization using volume and power losses as criteria. - To validate the obtained results by carrying out an experimental study.	Phase 6
Paper IV[1] *Prediction of friction coefficient in dry-lubricated polyoxymethylene spur gear pairs*	- To detect variables that significantly affect the friction coefficient. - To design an experiment accordingly. - To develop a friction coefficient prediction formula applicable to polyoxymethylene (POM) spur gear pairs.	Phase 5

4.1. Determining the number of design variables

The number of variables was determined in paper entitled *"Influence of profile shift on the spur gear pair optimization"* (Paper I).

Abstract

Due to the established load capacity calculations and extensive literature, gearbox design process is rather simple. In order to gain a competitive edge, transmission designers and manufacturers are forced to constantly improve the design process and the product quality. The gearbox design process can be improved by using genetic algorithm to determine the optimal values of gear pair parameters. In this paper, besides the frequently used gear optimization variables, i.e. the module, the face width, and the number of teeth, profile shift coefficients of both gears are included to create a five-variable process. Since the pro- file shift influences the form, zone and stress factors, as well as the transversal and face load factors, it affects the optimization results significantly. The gear pair volume served as a fitness function, while the tooth root bending strength and the contact pressure calculations were used as constraints. Optimization results of the pair without profile shift and the arbitrary profile shifted pair were compared. The genetic algorithm solution is found for three data sets; the solution is verified using commercial gear optimization software.

Method

---

[1] Note: the study was not planned at the beginning; it was conducted due to a lack of relevant literature discovered in the latter phases.

During a literature review, no consensus regarding the number of variables to be used in spur gear pair optimization was found (as shown in Table 2). The point of debate was the profile shift coefficient (addendum modification). In studies [54,58,60,61] the profile shift coefficient was not used in addition to the gear module, teeth numbers, and face width, meaning that algorithms always gave null-shift gears as the optimal solution. On the other hand, in [55,59] the profile shift was used as one of the design variables. The downside of including the profile shift coefficients as variables are increased algorithm complexity and computational cost.

To determine whether the profile shift coefficient has a notable influence on the spur gear pair optimization, the optimization process was conducted. The optimization process was carried out for the null-shift gears, and then repeated using the gear pairs with profile shift. For both cases, the gear pair volume was used as an objective function. It was calculated using the addendum circles instead of the pitch circles to account for the profile shift influence on the volume:

$$V(m, z_1, z_2, x_1, x_2, b) = \frac{\pi b}{4} \cdot (d_{a1}^2 + d_{a2}^2) \tag{54}$$

The values of design variables were limited to provide viable solutions. The variables were both discrete (gear module, numbers of teeth) and continuous (profile shift coefficients, face width). Standard values defined by ISO 54:1996 [91] were used for gear modules. Furthermore, pinion teeth number was limited to [14, 24] to prevent both the undercutting and excessive radial dimensions. The pair face width and profile shift coefficients were limited according to geometric requirements shown in Section 2.1; with width ranging from $6m$ to $30\ m$ and profile shift from 0 to $x_{1\max}$ for the pinion and -0.7 to 0.7 for the wheel.

Additional boundaries were included so the solution satisfies the strength requirements. The calculation of gear pair load capacity is conducted according to methods provided in ISO 6336:2006 [3] outlined in Section 2.1.

The genetic algorithm is selected to solve the optimization problem as it can solve both the non-smooth and mixed variable problems. In addition, it is prevalently used within the scientific field, as can be seen in Table 2. The number of generations was 500 to reduce the computational cost. To validate that the results will converge, optimization was repeated using the 30.000 generations. Optimization process was repeated 10 times for each of the sets to ensure that the global minimum is found.

There were two key findings:

1. The profile shift coefficients should be included as the design variables. The differences in volume between the optimal solutions for null-shift pairs and pairs with profile shift was ranging from 32% to 35%.

2. When the only objective is reduced gear pair volume, the pairs with lower face width tend to provide better results. The optimal results were regularly on the lower boundary ($b = 6m$). After further reducing the lower boundary to $2m$, optimal solutions followed.

Limitations

During the publishing process and in the period after, limitations of a conducted study were found. The limitations that can be improved in the future work are:

1. To ensure faster convergence, discrete face width and profile shift coefficient values should be used instead of the continuous ones. By replacing the continuous variables with discrete ones in steps of 0.001, solution accuracy would remain the same as the gears are manufactured with tolerances, while the initial population required for the algorithm would be more uniform.

2. All the pairs converged towards the larger pinion teeth number. By increasing the upper boundary, further tooth number implications could be studied.

3. Dynamic transmission error (DTE) was not considered within the study; dynamic effects are included through the dynamic factors K_A, K_v, $K_{F\alpha}$, $K_{F\beta}$, $K_{H\alpha}$, and $K_{H\beta}$.

4.2. Multi-objective optimization of steel gear pairs

Abstract

Besides satisfying the essential strength requirements, gearbox design should ensure additional desirable properties in order to be competitive. For example, a gearbox should be efficient, durable, quiet, compact, and light. Nowadays, as a consequence of rising environmental concerns, high efficiency is a rather desirable feature. In this article, a genetic algorithm was used for conducting a multi-objective optimization of gear pair parameters with a goal of reducing the transmission volume and power losses. Gearing efficiency primarily depends on the normal load, sliding velocities, and the friction coefficient. Gearing efficiency was calculated analytically, using the approximate load distribution formulae and efficiency formulation developed by Schlenk. The resulting formula was included in the genetic algorithm as an objec-

tive. To verify it, results were compared to the ones obtained by other authors. Optimization variables consisted of the gear module, the face width, the pinion and wheel profile shift coefficients and the number of teeth of the pinion. Solutions have shown that the trade-off between volume and efficiency is obligatory and a combination of the lower gear module, the lower face width, the higher profile shift coefficients and the higher number of teeth of the pinion yield good results regarding both objectives.

Method

The design variables were selected in accord with the findings of Paper I; gear module, pinion number of teeth, gear pair face width, and profile shift coefficients of both the pinion and the wheel were used. The intervals from which design variables were chosen and data sets used for testing the algorithm also remained the same. Additional constraints used were identical to the previously used ones.

To conduct a comprehensive optimization of spur gear pairs, power losses were included as an additional objective function. By combining volume and power losses as design criteria, a compact and efficient transmission can be made. As a first objective function, the gear pair volume calculated using the addendum circles was used. A power loss expression that can be easily integrated into the optimization algorithm as an objective function was derived.

To derive a gear pair power loss formulation, the formula provided by Diez-Ibarbia et al. in [23] was used as a basis. To account for the change in friction coefficient depending on the working conditions and gear geometry, friction coefficient formulation presented by Schlenk [35] was used. Lastly, to include the variations in load distribution due to the variations in mesh stiffness, approximate load distribution expressions by Sanchez et al. [29] were used. Variations in sliding velocity were calculated using the technical literature [11,14].

In contrast to the single-objective optimization process presented in Paper I, multiple objectives are present. By using multiple objectives, the algorithm output changes; optimization results are shown in form of Pareto optimal front, which enables the transmission designer to select the most suitable trade-off.

Key findings

The conducted study resulted in following key findings:

1. Power loss formulation suitable for use as an objective function was derived. When compared to the studies conducted by other authors, it provided more accurate results than previously used expression [15].

2. Increase in gear module resulted in lower power losses, while increasing the volume.

3. Increase in the gear wheel profile shift coefficient had a beneficial impact on the power losses, when combined with the pinion having a positive profile shift coefficient. The downside is increased working pressure angle α_w.

4. Increase in gear pair face width slightly decreases the power losses, while significantly increasing the gear pair volume.

5. All the sets converged towards the larger number of teeth in pinion.

Limitations

There was one main limitation to the presented study:

1. Dynamic transmission error was not considered in detail; dynamic effects are included through the use of dynamic factors K provided in ISO 6336:2006 standard.

4.3. Optimization of thermoplastic spur gear pairs

Abstract

This research study aimed to compare the trends for optimal design of steel and polyoxymethylene gears. For this reason, a multi-objective optimisation of spur gears made of polyoxymethylene was conducted. The results were compared to similar studies concerned with the gears made of steel. The gear pair module, face width, pinion number of teeth, and both the pinion and wheel profile shift coefficients were used as design variables. Two objective functions were used, gear pair volume and frictional power losses. Compared to steel gear pairs, additional boundary conditions were necessary: tooth flank and root temperatures, abrasion wear, and tooth addendum displacement. Three arbitrary datasets were used as examples. For each of the sets, one Pareto optimal solution was manufactured, and results were validated experimentally, using an open-circuit experimental rig. The results have shown that there are distinct differences in trends; lower volume pairs made of polyoxymethylene had greater widths, while the opposite was observed in steel gears.

Method

The optimisation of polymer gear pairs was conducted to determine whether the steel gear guidelines found in Paper II are applicable. Even though the design variables and algorithm used for solving the optimisation problem (NSGA-II) remained the same, differences in optimisation process were notable. The essential differences were in the objective function used to rate power losses and boundary conditions.

The first objective function (volume) remained the same, while the second (power losses) was altered. The same power loss formulation was used, but the friction coefficient formulation was different. The change in friction coefficient formulation was required as one proposed by Schlenk (used in Paper II) is to be used for steel gear pairs with liquid lubrication. For this reason, a new formulation, applicable to polyoxymethlene (POM) gears lubricated using dry lubricant was proposed in Paper IV.

When considering the boundary conditions, additional limitations were necessary. In the guidelines for load capacity calculation of thermoplastic gears VDI 2736 [4], tooth temperature (flank and root), flank wear, and tooth tip deflection are to be checked complementary to the tooth root stress and surface durability.

The analytical results were experimentally validated. An open-circuit rig (see Figure 7) was designed to measure the power losses.
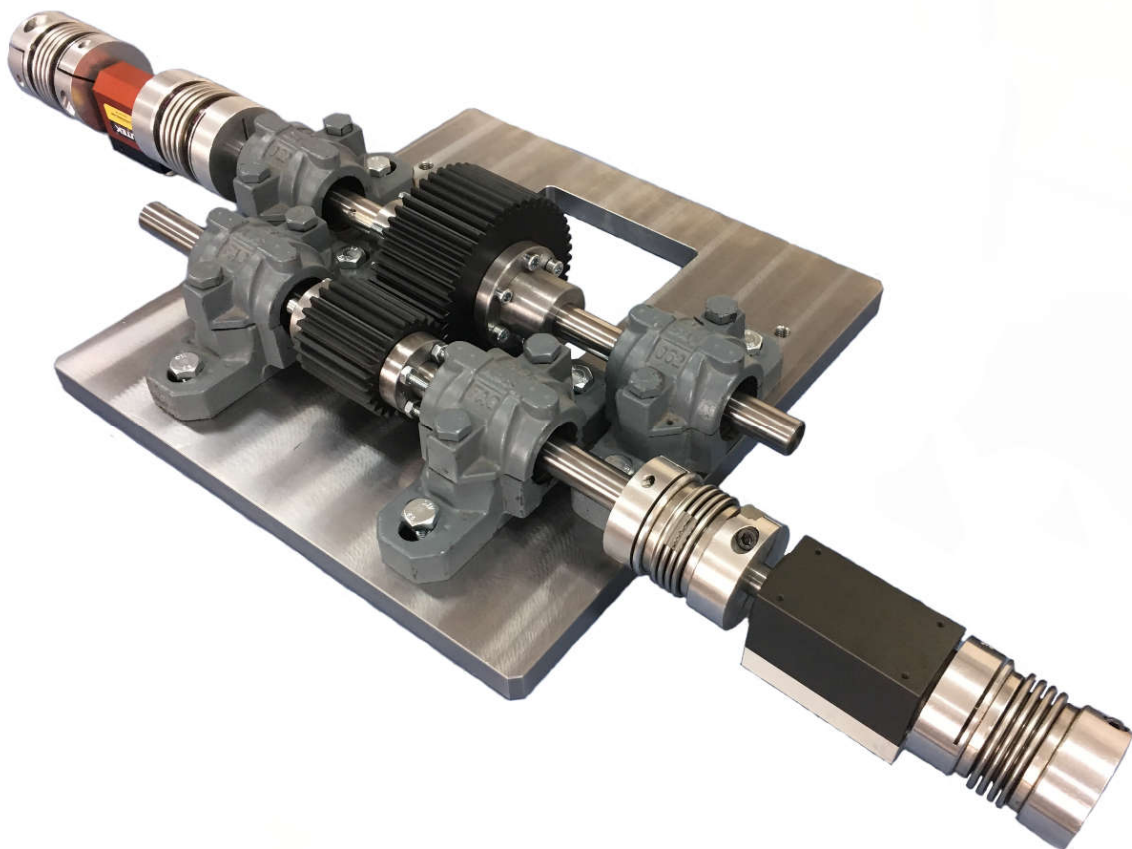
Figure 7 – Open-circuit experimental rig

Key findings

The conducted study resulted in following findings:

1. Thermoplastic gear pairs require different design guidelines when compared to gear pairs made of steel. Even though there are considerable similarities, face width selection process varies.

2. Similarly to steel gear pairs, both sets converged to solutions with large numbers of teeth and high profile shift coefficient values (0.53 for the pinion and 0.7 for wheel).

3. The efficiency of thermoplastic gear pairs was found to be slightly below the values found in steel gear pairs. The efficiencies in polymer gear pairs ranged from 0.980 to 0.986.

4. The analytical and experimental results are in agreement, with differences ranging from -19.6% to 21%.

__Limitations__

The following limitations of the study presented in Paper III should be addressed:

1. The quality of results obtained using the open-circuit experimental rig heavily depends on the torque transducer accuracy grade.

2. The friction coefficient formulation suggested in Paper IV does not account for the slide-to-roll ratio, adding to the error in efficiency prediction.

3. The friction coefficient value provided in VDI 2736 [4] was used to carry out the load capacity calculations. Using the expression proposed in Paper IV, the friction coefficient ranged between 0.06 and 0.2, while the value of 0.28 is suggested by VDI 2736. Using higher friction coefficient resulted in a more conservative temperature prediction, leading up to underestimation of material properties; the properties of thermoplastic materials degrade with the increase in temperature.

4.4. Prediction of friction coefficient in polyoxymethylene gear pairs

__Abstract__

In this article, the authors have experimentally determined the friction coefficient in the polyoxymethylene gear pairs lubricated by a dry lubricant. The obtained expression increases the precision of the frictional power loss calculation, which is essential when the frictional power loss is used as the optimization criterion. The friction coefficient was characterized for three influencing parameters: radius of relative curvature, sliding velocity, and normal load. The full factorial organization was used for the experiment design; five curvature radii levels, four sliding velocity levels, and three load levels were used. Each of the runs was recorded three times, which resulted in a total of 180 experimental runs. The resulting expression for the friction coefficient is valid for the gear modules between 1 and 4.5 mm and sliding speeds of up

to 2.7 m/s. The normal load was found to have the greatest influence on the friction coefficient, while the sliding velocity influenced only the specimens running under lower load levels. A further increase in the values of radii of relative curvature above 5 mm had no effect on the friction coefficient. The experimental data is provided in full.

Method

An expression for prediction of friction coefficient in polyoxymethylene (POM) gear pairs was found experimentally. The experiment was designed as full factorial, aiming to capture all the interactions between the parameters. Based on the literature review, the normal load, sliding velocity, and radius of relative curvature were selected as experimental variables. Variable levels were selected based on the sample gear pair population.

The sample gear pair population was generated to select more representative variable levels. The permissible normal load, the sliding velocity, and radii of relative curvature were calculated for each of the pairs, allowing the increase in grid density in more populous areas. Following geometrical parameters were used to generate the sample population:

- Standard gear modules ranging from 1.5 mm to 4.5 mm,
- Pinions with tooth numbers of 14, 19, and 24,
- Transmission ratios of 1, 2, 3, and 4,
- Profile shift coefficients of 0, 0.35, and 0.7 of both the pinion and the wheel. In pairs where a profile shift coefficient of 0.7 resulted in gears with a sharp tip (tooth tip thickness $s_a < 0.2 \; m$), levels of 0, 0.5 x_{maxT}, and x_{maxT} were used.

The sample population resulted in 1404 gear pairs. Variable values were calculated at five specific points along the line of action (points A, B, C, D, and E) for each of the pairs. Three levels of normal load, four levels of sliding velocity, and five levels of radius of relative curvature were selected based on the results.

The experimental rig consisting of an electric motor, a shaft, a housing, two load cells, and a load application mechanism was used (shown in Figure 8). Two specimens were required, a rotating one, mounted to the shaft connected to a torque load cell, and a static one, installed onto the normal load cell. For more details on the experimental rig, see Paper IV.
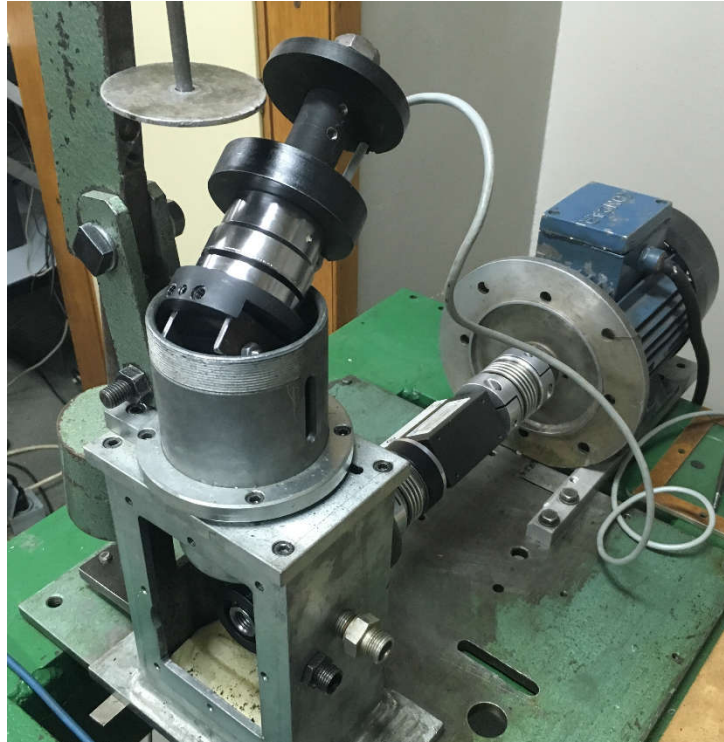
Figure 8 – Experimental rig (Paper IV)

Key findings

The following conclusions were drawn:

1. The function fitted to experimental data was assessed; by observing the residuals, it was determined that the fitted function properly describes the observed data.

2. The results are in agreement with studies conducted by other researchers who used both gears and simplified models. The most notable examples include the studies done by Mao et al. [92] and Walton et al. [67,68].

3. When compared to other gear pair friction coefficient models, a difference in trends along the intervals with higher sliding velocities notably the AB and DE intervals, is found. The most likely reason is the lack of an oil film; most of the studies on friction in gear pairs were conducted using lubricated steel gears, where an increase in the sliding velocity has a beneficial effect on the hydrodynamic lubrication. In the presented study, the contact is dry, which means that an increase in the sliding velocity also increases the friction coefficient.

4. The normal load has dominant influence on the friction coefficient between the specimens of POM pairs. With the increase in load, the friction coefficient decreases; the change is more marked at lower load levels.

5. The sliding velocity also affected the friction coefficient; its value increased as the sliding velocity increased. Variations were more prominent in specimens running under lighter loads.

6. The radius of relative curvature had a rather small amount of influence on the results.

Limitations

The research presented in Paper IV has a number of limitations inherent for experimental studies, caused primarily by a limited number of measurements and available equipment. The limitations are:

1. The full factorial experiment design was used as influences of individual parameters were not known. Thus, covering the entire range of investigated parameters was decided. Carrying out the full factorial experiment, despite the sort experimental runes, reduced the number of possible variables. For this reason, only three variables were used to conduct the experiment; normal load, sliding velocity, and radius of relative curvature.

2. In line with limitation 1, the slide-to-roll ratio was not considered, even though it affects the friction coefficient values [93].

3. An increase in temperature adversely affects the mechanical properties of thermoplastics. In this article, the influence of temperature was not considered. There are three reasons:

   a. Home appliances in which the polymer gears are generally used have short working intervals, meaning that steep increase in temperature is not expected

   b. To mitigate the influence of temperature, experimental runs were rather short (10 s); no significant variations in friction coefficient were found during the experimental run

   c. Heating the test specimens to the necessary temperature would significantly increase the experiment complexity

4. When determining the sample population, Hertzian pressure, temperature, and bending strength were used as a failure criterion. In the continuation of the doctoral study (Paper III), it was found that wear was generally the active constraint.

5. DISCUSSION

In this section, the design guidelines for steel and polymer gear pairs are discussed. Based on the results, guidelines for the design of low volume and low power loss gear pairs are suggested. This section also includes a critical review of the conducted research.

The quality of a transmission design regarding the selected criteria can be increased by including the optimisation phase within the gear pair design process (Papers I, II, and III). However, when aiming to include the optimisation, it must be noted that problem formulation is time-consuming and overlooking a constraint or limiting the design variable range too conservatively yields obsolete results. Depending on the application, different criteria can be used to evaluate the quality of a gear pair.

The differences were found while comparing steel and polymer gear pairs, implying the need for separate design guidelines. Despite the same geometry and rather similar calculation procedure (polymer gear calculation procedure VDI 2736 is based on ISO 6336:2006), differences in mechanical properties are too great. In the context of gear optimisation and needed calculations, differences are manifested in additional constraints and changes in one of the objective functions. The active constraints are also different; steel gear pairs were mostly limited by the Hertzian (contact) pressure, while the polymer (POM) gears were susceptible to wear.

5.1. Steel gear pair design

The steel gear pair design was examined in the single-objective and multi-objective study. In the former, volume was used as the objective function, while in the latter both the gear pair volume and power losses were used. The objectives were selected in line with the literature review. Based on the results of the single-objective optimisation (Paper I) using the volume as a criterion, the following was concluded:

- The lower face width constraint was selected as optimal face width *b* for all the observed sets of input data. The trend continued after the lower constraint value was lowered from 6*m* to 2*m*.
- The selected number of teeth was equal to the upper number of teeth boundary for all the observed sets.

- Large profile shift coefficients were selected for pinion in all the three cases (0.699, 0.638, and 0.691), while the wheel profile shift was generally more conservative (0.136, 0.559, and 0.291). The most likely reason for such behaviour is Hertzian pressure; in reducers, wheel flanks have larger curvature radii then pinions due to the larger number of teeth. For the same reason, increasing the wheel profile shift yields a more significant increase in volume.

- It should be mentioned that gear modules were not studied in detail, as it was expected that lower volume would require a lower gear module.

By including the power losses as the additional criterion, changes in parameter values are prominent. In a vast majority of cases, multiple objectives are opposed, meaning that compromise is necessary. The trivial cases, in which the objective functions are similar or erroneously defined, are the exception. A most suitable compromise is selected from the Pareto optimal front by the transmission designer. The influences of variations in design variables on the values of objective functions are shown in Figure 8 (the figure is based on results for sets 1 to 3 described in Paper II). The values of power losses and volumes are normalised for each set.
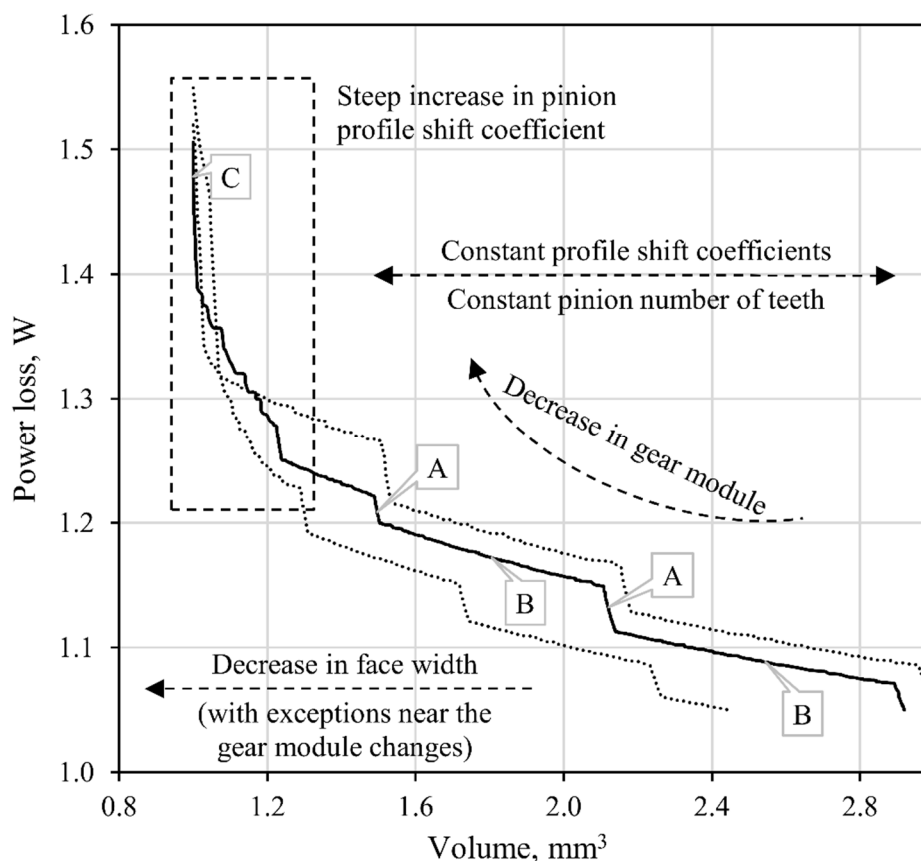
Figure 9 – Influences rating criteria on the design variables in steel gear pairs

Based on the figure, three different regions are identified on Pareto fronts of each set (set 1 data is shown as a continuous line and used as an example):

- *Region A* is characterised by a steep increase in power losses as the volume decreases. It is found at the changes of gear module – by lowering the module, face width must be increased to compensate for the loss of load capacity. Lower face widths are found in the left part of the region A. Decreases in wheel profile shift coefficient are found in the right parts of the region, slowly increasing when moving left.

- *Region B* is marked by a lower change in power losses as the volume changes. Along each B region, the module remains the same, while the face width decreases. Profile shift coefficients and numbers of teeth are constant.

- *Region C* is characterised by an increase in pinion profile shift, enabling the use of lower face width to reduce the volume at the expense of power losses.

In the studies by other authors, the consensus is that the lower values of gear module are to be used in combination with higher numbers of teeth. The upper constraint of pinion number of teeth is often selected as optimal. Results of Paper II support this statement and in a study by Savsani et al. [60], where only gear pair volume was used as an objective function. When including volumes of the shafts into the objective function, a higher number of teeth remains desirable [61].

The influence of power losses on gear geometry was compared to findings by Höhn et al. [19], Baglioni et al. [25], and Petry-Johnson et al. [5]. The former group concluded that power losses in bearings are subordinate to the ones found in gear pairs and that load-dependent power losses are dominant to load-independent power losses. To reduce power losses in gear pairs, Höhn et al. [19] suggested reducing the gear module and transverse contact ratio while increasing the pressure angle and face width. Baglioni et al. [25] found that gearing efficiency can be increased by increasing the sum of profile shift coefficients. Furthermore, the authors stated that the friction coefficient decreases as the number of teeth increases. The last group, Petry-Johnson et al. [5] have studied gear pair operating at rotational velocities above 6000 rpm. In addition to variations in lubricant viscosity and surface roughness, pairs with a larger module and lower number of teeth were compared to pairs with the lower module and higher number of teeth. The authors have found that the former is more efficient in all the observed cases, agreeing to the experimental results by Naruse et al. [30].

When comparing the results presented in Paper II to the above-referenced studies, it should be stressed that multiple objectives were used to find them, meaning that direct comparison is not possible. Following comparisons were made:

1. The optimal gear pairs in the low-volume side of the Pareto front (see the left-hand side of the diagram in Figure 8; for example, region C) have low gear modules. Even though the low-volume side is linked to the increased power losses, the low gear module is not the cause. The increase in power losses should be attributed to the nature of solutions located on the Pareto front instead; each is a result of different combinations of weights assigned to objective functions. Furthermore, as concluded by Baglioni et al. [25], a decrease in normal load causes a decrease in power losses. In gears with lower module power losses are expected since an increase in normal load is caused by a decrease of the module while keeping the torque constant. Generally, since the gear module affects both the design variables and calculation factors, it is hard to draw general conclusions regarding its influence.

2. Hőhn et al. [19] suggested increasing the face width to decrease power losses. Such results are in agreement with the ones presented in Paper II and Figure 8. By increasing the face width, power losses also increase.

3. Baglioni et al. [25] concluded that an increase in the sum of profile shift coefficients has a positive effect on gear pair efficiency. Similar behaviour was observed in Paper II (for more details see Figure 6 of the paper), where the increase of profile shift coefficients positively affected power losses in most of the cases. The lowest power losses were found with pinion and wheel profile shifts of 0.3 and 0.7, respectively. Further increase in pinion profile shift caused an increase in power losses.

4. The increase in a number of teeth is recommended by all authors [5,19,25,30], which is in agreement with the findings of Paper II. Additionally, a larger number of teeth results in larger radii of curvature and transverse contact ratio.

Lastly, the constraints should be discussed. The surface durability was an active criterion in all the observed sets, despite the lower value of safety factor (1, 1.175, and 1.2 compared to 1.5 used in tooth root stress). Such behaviour is favourable since pitting resulting from increased flank stress is preferred to tooth root failure, as tooth root failure is often catastrophic and damages the remaining elements of the power train.

5.2. Polymer gear pair design

No general guidelines associating the desired transmission criteria and the corresponding macro-geometry of polymer gear pairs were found during the literature review. As a starting point and due to the geometric similarities, the design variables were selected based on studies on steel gear pairs. In addition to the design variable values and ranges, possible over-constraining in polymer gear pairs should be addressed. Furthermore, guidelines for selection of macro-geometric parameters are outlined in this section, along with the active boundary conditions.

Besides the constraints used in steel gear pair design – tooth root strength, Hertzian (contact) stress, and transmission ratio, four additional constraints are bestowed upon their polymer counterparts. Those include tooth root and flank temperatures, flank wear, and tooth tip deformation. A total of 7 constraints severely limits the design space, as seen in Figure 10. Much larger variations of designs are possible for steel gears. The ratio between the lowest values of objective functions for steel gears is up to 2.9 (volume) and 1.6 (power losses). In polymer gears, values of the same ratio are up to 1.34 (volume) and 1.10, consequently leaving fewer possibilities to the designers.
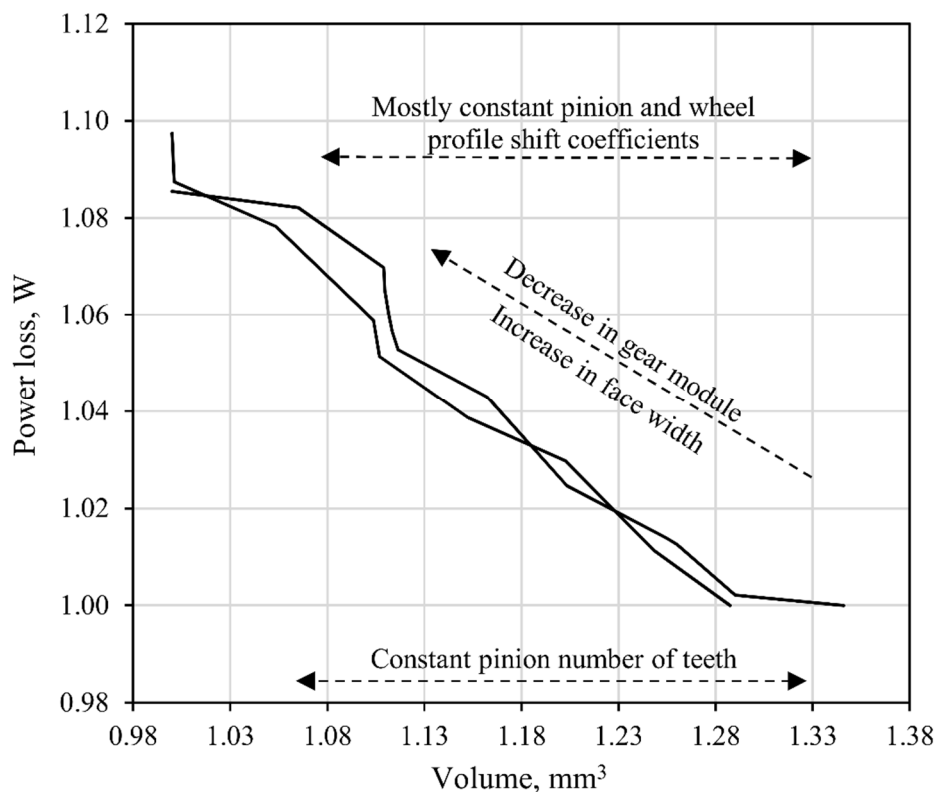
Figure 10 – Influences rating criteria on the design variables in polymer gear pairs

When compared to steel gears (see Figure 9), no distinct regions can be recognised in Figure 10 due to a low number of solutions in the Pareto optimal front. However, the following was concluded based on two observed sets:

1. The solutions with lower volume and higher power losses had lower gear modules. On the other hand, based on the experimental study, Walton et al. [67,68] concluded that lower power losses occur in gear pairs with a lower gear module. However, direct comparison is not possible. Besides altering the gear pair module, Walton et al. have increased the number of teeth in pairs with a lower module to preserve the equal working diameter.

2. Each of the optimal pairs converged towards the larger number of teeth. Using the point by Walton et al. in [68] regarding the gear module influence, it can be argued that higher efficiency is achieved by increasing the number of teeth, which is in agreement with the presented data.

3. Positive profile shift coefficient values are selected for all the optimal pairs. Based on the pairs studied in Paper III, it can be concluded that profile shift values of +0.5 should be used for the pinion.

Sliding velocity is also found to affect the power losses in polymer gear pairs. In addition to direct influence, according to Equation (42), an increase in sliding velocity also increases the friction coefficient (Paper IV). The same effect was observed by Walton et al. [68]; the efficiency lowered as the rotational velocity increased. Thus, power losses can be reduced by lowering the working diameter. Additionally, assuming that the transmitted torque is constant, lowering the working diameter increases the normal load. An increase in normal load has a positive effect on the friction coefficient, further lowering the power losses.

When compared to their steel counterparts [5,23,25], calculated power losses for polymer gears are of the same order of magnitude (for more details see Paper III). Both the measured and calculated values are slightly higher than the corresponding values for steel gear pairs. The polymer gear pair efficiency ranged between 0.98 and 0.986, while for steel gear pairs Petry-Johnson et al. [29] reported the efficiency of 0.9979 [5], Baglioni et al. 0.985 (Method I) and 0.981 (Method 2) [25], and Diez-Ibarbia et al. 0.994 [23].

Another difference was found within the active constraints. In steel gears, gear pair load capacity was mainly limited by Hertzian pressure, regardless of whether the steel was heat treated or not. In polymer gears, load capacity was limited by wear criterion, which was an active constraint in all three observed sets. Such results were expected, as wear is one of the most

common failure types in polymer gears (other being the tooth root failure). The wear failure is most often encountered in dry running gear pairs.

Lastly, in addition to the lacking guidelines, the polymer gear design is severely limited by a limited number of available materials. Polyamide (PA) and polyoxymethylene (POM) remain the most frequently used materials despite many available polymers. The problem is caused by lengthy experimental research needed to determine the mechanical properties required to carry out the load capacity calculations. The number of combinations additionally rises when polymer materials are used as matrix and reinforced with additional material (polymer matrix composites). Some of the mechanical properties are hard to find even for the widely used gear materials; for example, finding the wear rate for POM-POM gear pair. Luckily, studies aiming to provide the methodology to fasten the said process were carried out recently [90,94].

5.3. A critical review of the conducted work

Several simplifications were required in order to conduct the proposed research. To start, in studies on gear optimisation, the procedure proposed within is usually validated using one case study/example case [54,58,61]. Such approach prohibits any conclusions on the general behaviour of gear pairs. In this thesis, the problem is only partially solved; the conclusions are based on three diverse sets of input data. The further increase in the number of sets is required to ensure the guideline robustness.

The presented work was also limited to spur gears for the sake of simplicity, even though it could be applied to helical gears by introducing the helix angle. The helix angle could be introduced as user-defined or as an additional design variable. In the former case, changes to the algorithm would be minor, meaning that the computational cost would practically remain the same; this remains the most frequently used approach [58,95]. The latter approach requires a rework of the optimisation process. To preserve the same level of accuracy, an increase in a number of design variables requires a larger initial population. Consequently, more generations are necessary to ensure convergence, causing the computational cost to increase exponentially. Tudose et al. [59] and Marjanović et al. [62] have solved the helical gear optimisation problem by increasing the number of design variables. In both papers, the helix angle influence was not discussed in detail.

Besides including more design variables, the constraints and objective functions could be tailored to adapt the solutions to the desired design outcomes further. For example, the centre

distance could be limited to standard values, and the transmission ratio tolerances could be set, since a ratio of two integer's causes deviations from sought after values. Furthermore, the objective functions could be extended; some studies are carried out using volumes of shafts and bearings as the objective function, in addition to the gear pair volume.

The experimental study has confirmed the analytical results, with an error of 20%. The open-circuit rig was used in an attempt to isolate the frictional power losses. The drawback of the open-circuit device is the significant expenditure of energy if the regenerative braking is not possible. For this reason, the closed-circuit device should be used when studying pairs with higher torques or expected cycle numbers. A similar (open-circuit) experimental rig was used by Kirupasankar et al. [70]; however, there are concerns regarding the presented work. To start, the authors have not detailed the experimental rig design; the torque transducer accuracy and capacity are not stated, and there are no bearings shown within the rig schema. Furthermore, the experimental gear pair is installed on a cantilever, possibly leading to the uneven load distribution along the gear pair face width.

6. CONCLUSION

In addition to the general conclusions, this section includes two sub-sections. In the first one, hypotheses are revisited to determine whether they are true or not. Based on the presented work, the second sub-section provides an outlook on the field and ideas for future studies.

This study aimed to provide a basis for future research on the optimisation of polymer gear pairs. Due to the identical geometry, the method was devised using the steel gear pairs. The number of variables was determined first (Paper I), providing the knowledge necessary to carry out the optimisation using the multi-objective procedure (Paper II). The same multi-objective procedure was used to find the solutions for polymer gear pairs (Paper III), granted that different constraints were used. The expression required for prediction of friction coefficient in polymer pairs was determined experimentally (Paper IV).

The detailed guidelines for optimisation of steel and polymer gear pairs are provided (Section 2 and Section 3) along with the rough design guidelines (Section 5). The benefits of using the large number of teeth and positive profile shift coefficients were recognised for both materials, while the trends were different regarding the face width. The power losses are a function of the normal load value and distribution, sliding velocity, and friction coefficient, meaning that the friction coefficient mostly causes differences in the outcomes. The normal load and sliding velocity properties were mostly the same due to the geometry, while the friction coefficient formulations were significantly different.

The polymer gear pair optimisation has proven to be a more complex task due to the additional constraints, most namely the wear and the tooth temperature (flank and root). The wear criterion severely reduces the design space, leading to a lower number of Pareto optimal solutions. Consequently, the gear designer has less freedom when selecting the most suitable configuration.

6.1. Hypotheses

The hypotheses set in Introduction section are revisited within this subsection to determine the validity of initial assumptions.

By using a multi-objective optimisation procedure it is possible to detect the influence of additional criteria, caused by the special design requirements, on the values of gear pair parameters.

The first hypothesis is proven to be valid. As shown in Section 5 and papers II and III, the influence of special design requirements such as low-volume or efficient design (low power losses) is noted. Based on the results, different design strategies can be utilised depending on the desired requirement (see Section 5.1 and Section 5.2).

Proposed procedure will enable the comparison of parameter influences on the final design for gear pairs made of polymer and steel.

The second hypothesis is proven to be valid. The statement is based on appended papers II and III, in which steel and polymer gears are submitted to identical design requirements (low volume, low power losses). Due to the changes in friction coefficient behaviour between steel gear pairs and polymer gear pairs, guidelines for selection of near-optimal values of geometric parameters depend on the material. For the detailed comparison, see Section 5.3.

6.2. Outlook and future work

The guidelines for the selection of the gear pair parameters such as the gear module, face width, and a number of teeth could enable faster and higher quality design. However, due to a sheer number of available optimisation methods, some of which can be found within the commercial software, a question remains if the extensive and robust research on the subject is justifiable; the results would mostly benefit smaller, non-specialised manufacturers. Expanding the applicability of optimisation processes to new materials, such as polymers, seems like a more attractive route.

The polymer materials are suitable for gear manufacture due to their ability to work without lubrication, low price, low density, and a high potential for mass production. Their most significant downside is a degradation of mechanical properties with the increase of the temperature, as the local surges are prominent due to low thermal conductivity. Thus, the need for optimisation is existent and increases along with their popularity. By using the power losses or sliding velocity as an objective function, in addition to the volume, limiting factors such as the temperature and wear could be mitigated.

7. REFERENCES

[1]   Türich A. Producing profile and lead modifications in threaded wheel and profile grinding. Gear Technology 2010:54–62.

[2]   Papalambros PY, Wilde DJ. Principles of Optimal Design. Second edi. Cambridge: Cambridge University Press; 2000. doi:10.1017/cbo9780511626418.

[3]   International Organization for Standardization. ISO 6336:2006 - Calculation of load capacity of spur and helical gears — Application for industrial gears. Geneva, Switzerland: ISO; 2006.

[4]   VDI Verein Deutscher Ingenieure. VDI 2736 Thermoplastic gear wheels 2014:73.

[5]   Petry-Johnson TT, Kahraman A, Anderson NE, Chase DR. An experimental investigation of spur gear efficiency. Journal of Mechanical Design 2008;130:62601. doi:10.1115/1.2898876.

[6]   Konak A, Coit DW, Smith AE. Multi-objective optimization using genetic algorithms: A tutorial. Reliability Engineering and System Safety 2006;91:992–1007. doi:10.1016/j.ress.2005.11.018.

[7]   Deb K, Pratap A, Agarwal S, Meyarivan T. A fast and elitist multiobjective genetic algorithm: NSGA-II. IEEE Transactions on Evolutionary Computation 2002;6:182–97. doi:10.1109/4235.996017.

[8]   Arora JS. Introduction to Optimum Design. 3rd editio. Oxford: Academic Press; 2004. doi:10.1016/B978-0-12-064155-0.X5000-9.

[9]   Litvin FL, Fuentes A. Gear geometry and applied Theory. Cambridge: Cambridge University Press; 2004.

[10]   Radzevich BSP. Dudley's Handbook of Practical Gear Design and Manufacture. 2nd editio. Boca Raton: CRC Press; 2012.

[11]   Linke H, Börner J, Heß R. Cylindrical gears Calculation – Materials – Manufacturing. Hanser Publications; 2016.

[12]   International Organization for Standardization. ISO 53:1998 - Cylindrical gears for general and heavy engineering — Standard basic rack tooth profile. 1998.

[13] International Organization for Standardization. ISO 4468:2009 - Gear hobs — Accuracy requirements. 2009.

[14] Oberšmit E. Ozubljenja i zupčanici. Zagreb: SNL; 1982.

[15] Höhn BR. Improvements on noise reduction and efficiency of gears. Meccanica 2010;45:425–37. doi:10.1007/s11012-009-9251-x.

[16] Pedrero JI, Rueda A, Fuentes A. Determination of the ISO tooth form factor for involute spur and helical gears. Mechanism and Machine Theory 1999;34:89–103. doi:10.1016/S0094-114X(98)00017-2.

[17] Erhard G. Designing with Plastics. Munich: Hanser Publishers; 2006. doi:10.3139/9783446412828.

[18] Michaelis K, Höhn B, Hinterstoißer M. Influence factors on gearbox power loss. Industrial Lubrication and Tribology 2011;63:46–55. doi:10.1108/00368791111101830.

[19] Höhn BR, Michaelis K, Wimmer A. Low loss gears. Gear Technology 2007:28–35.

[20] Diez-Ibarbia A, Fernandez-del-Rincon A, De-Juan A, Iglesias M, Garcia P, Viadero F. Frictional power losses on spur gears with tip reliefs. The friction coefficient role. Mechanism and Machine Theory 2017;112:240–54. doi:10.1016/j.mechmachtheory.2017.02.012.

[21] Diez-Ibarbia A, Fernandez-del-Rincon A, de-Juan A, Iglesias M, Garcia P, Viadero F. Frictional power losses on spur gears with tip reliefs. The load sharing role. Mechanism and Machine Theory 2017;112:240–54. doi:10.1016/j.mechmachtheory.2017.02.012.

[22] Li S, Kahraman A. Prediction of Spur Gear Mechanical Power Losses Using a Transient Elastohydrodynamic Lubrication Model. Tribology Transactions 2010;53:554–63. doi:10.1080/10402000903502279.

[23] Diez-Ibarbia A, del Rincon AF, Iglesias M, de-Juan A, Garcia P, Viadero F. Efficiency analysis of spur gears with a shifting profile. Meccanica 2016;51:707–23. doi:10.1007/s11012-015-0209-x.

[24] Diez-Ibarbia A, Fernández del Rincón A, Iglesias M, De Juan A, García P, Viadero F. Efficiency Analysis of Shifted Spur Gear Transmissions. In: Flores, P; Viadero F,

editor. New Trends in Mechanism and Machine Science. Mechanisms and Machine Science, Springer; 2015, p. 373–81. doi:10.1007/978-3-319-09411-3_40.

[25]   Baglioni S, Cianetti F, Landi L. Influence of the addendum modification on spur gear efficiency. Mechanism and Machine Theory 2012;49:216–33. doi:10.1016/j.mechmachtheory.2011.10.007.

[26]   Jurkschat T, Lohner T, Stahl K. Improved calculation of load-dependent gear losses by consideration of so far disregarded influences. Proceedings of the Institution of Mechanical Engineers, Part J: Journal of Engineering Tribology 2018;0:135065011876679. doi:10.1177/1350650118766794.

[27]   Magalhes L, Martins R, Locateli C, Seabra J. Influence of tooth profile and oil formulation on gear power loss. Tribology International 2010;43:1861–71. doi:10.1016/j.triboint.2009.10.001.

[28]   Li S, Kahraman A. A Transient Mixed Elastohydrodynamic Lubrication Model for Spur Gear Pairs. Journal of Tribology 2010;132:011501. doi:10.1115/1.4000270.

[29]   Sánchez MB, Pleguezuelos M, Pedrero JI. Approximate equations for the meshing stiffness and the load sharing ratio of spur gears including hertzian effects. Mechanism and Machine Theory 2017;109:231–49. doi:10.1016/j.mechmachtheory.2016.11.014.

[30]   Naruse C, Haizuka S, Nemoto R, Kurokawa K. Studies on Friction Loss, Temperature Rise and Limiting Load for Scoring of Spur Gear. Bulletin of JSMEB 1986;29:600–8. doi:10.1248/cpb.37.3229.

[31]   Sánchez MB, Pleguezuelos M, Pedrero JI. Enhanced model of load distribution along the line of contact for non-standard involute external gears. Meccanica 2013;48:527–43. doi:10.1007/s11012-012-9612-8.

[32]   Xu H, Kahraman A, Anderson NE, Maddock DG. Prediction of Mechanical Efficiency of Parallel-Axis Gear Pairs. Journal of Mechanical Design 2007;129:58. doi:10.1115/1.2359478.

[33]   Velex P, Ville F. An Analytical Approach to Tooth Friction Losses in Spur and Helical Gears—Influence of Profile Modifications. Journal of Mechanical Design 2009;131:101008. doi:10.1115/1.3179156.

[34]   Diez-Ibarbia A, Fernandez-Del-Rincon A, Garcia P, De-Juan A, Iglesias M, Viadero F.

Assessment of load dependent friction coefficients and their influence on spur gears efficiency. Meccanica 2018;53:425–45. doi:10.1007/s11012-017-0736-8.

[35] Schlenk L. Untersuchungen zur Freßtragfähigkeit von Großzahnrädern (PhD Thesis). Technical University Munich, 1995.

[36] Amarnath M, Sujatha CÃ, Swarnamani S. Experimental studies on the effects of reduction in gear tooth stiffness and lubricant film thickness in a spur geared system. Tribology International 2009;42:340–52. doi:10.1016/j.triboint.2008.07.008.

[37] Xu H. Development of a Generalized Mechanical Efficiency Prediction Methodology for Gear Pairs (PhD Thesis). The Ohio State University, 2005.

[38] Martin KF. A review of friciton predictions in gear teeth. Wear 1978;49:201–38.

[39] Marjanovic N, Ivkovic B, Blagojevic M, Stojanovic B. Experimental determination of friction coefficient at gear drives. Journal of the Balkan Tribological Association 2010;16:517–26.

[40] Höglund E. Influence of lubricant properties on elastohydrodynamic lubrication. Wear 1999;232:176–84. doi:10.1016/S0043-1648(99)00143-X.

[41] Britton RD, Elcoate CD, Alanou MP, Evans HP, Snidle RW. Effect of Surface Finish on Gear Tooth Friction. Journal of Tribology 2000;122:354–60. doi:10.1115/1.555367.

[42] Drozdov YN, Gavrikov YA. Friction and scoring under the conditions of Simultaneous rolling and sliding of bodies. Wear 1968;11:291–302. doi:10.1016/0043-1648(68)90177-4.

[43] O'Donoghue JP, Cameron A. Friction and temperature in rolling sliding contacts. ASLE Transactions 1966;9:186–94. doi:10.1080/05698196608972134.

[44] Benedict GH, Kelley BW. Instantaneous coefficients of gear tooth friction. ASLE Transactions 1961;4:59–70. doi:10.1080/05698196108972420.

[45] Larsson R. Transient non-Newtonian elastohydrodynamic lubrication analysis of an involute spur gear. Wear 1997;207:67–73. doi:10.1016/S0043-1648(96)07484-4.

[46] Li S, Kahraman A. A Method to Derive Friction and Rolling Power Loss Formulae for Mixed Elastohydrodynamic Lubrication. Journal of Advanced Mechanical Design, Systems, and Manufacturing 2011;5:252–63. doi:10.1299/jamdsm.5.252.

[47] Lyon RH. Product Sound Quality – from Perception to Design. Sound and Vibration 2003;37:18–22.

[48] Zhang J, Xia S, Ye S, Xu B, Zhu S, Xiang J, et al. Sound quality evaluation and prediction for the emitted noise of axial piston pumps. Applied Acoustics 2019;145:27–40. doi:10.1016/j.apacoust.2018.09.015.

[49] Fonseca DJ, Shishoo S, Lim TC, Chen DS. A genetic algorithm approach to minimize transmission error on automotive spur gear sets. Applied Artificial Intelligence 2005;19:153–79. doi:10.1080/08839510590901903.

[50] Velex P, Ajmi M. Dynamic tooth loads and quasi-static transmission errors in helical gears - Approximate dynamic factor formulae. Mechanism and Machine Theory 2007;42:1512–26. doi:10.1016/j.mechmachtheory.2006.12.009.

[51] Welbourn DB. Fundamental Knowledge of Gear Noise - a Survey. Institution of Mechanical Engineers, Conference Publications 1979:9–14.

[52] Åkerblom M. Gear Noise and Vibration: A Literature Survey. Machine Design 2009.

[53] Pedrero JI, Pleguezuelos M, Artés M, Antona JA. Load distribution model along the line of contact for involute external gears. Mechanism and Machine Theory 2010;45:780–94. doi:10.1016/j.mechmachtheory.2009.12.009.

[54] Yokota T, Taguchi T, Gen M. A solution method for optimal weight design problem of the gear using genetic algorithms. Computers & Industrial Engineering 1998;35:523–6. doi:10.1016/S0360-8352(98)00149-1.

[55] Marcelin J-L. Genetic optimisation of gears. International Journal of Advanced Manufacturing Technology 2001;17:910–5. doi:10.1007/s001700170101.

[56] Marcelin J-L. Using genetic algorithms for the optimization of mechanisms. Int J Adv Manuf Technol 2005;27:2–6. doi:10.1007/s00170-004-2162-z.

[57] Korta JA, Mundo D. Multi-objective micro-geometry optimization of gear tooth supported by response surface methodology. Mechanism and Machine Theory 2017;109:278–96. doi:10.1016/j.mechmachtheory.2016.11.015.

[58] Gologlu C, Zeyveli M. A genetic approach to automate preliminary design of gear drives. Computers and Industrial Engineering 2009;57:1043–51.

doi:10.1016/j.cie.2009.04.006.

[59] Tudose L, Buiga O, Ştefanache C, Sóbester A. Automated optimal design of a two-stage helical gear reducer. Structural and Multidisciplinary Optimization 2010;42:429–35. doi:10.1007/s00158-010-0504-z.

[60] Savsani V, Rao R V., Vakharia DP. Optimal weight design of a gear train using particle swarm optimization and simulated annealing algorithms. Mechanism and Machine Theory 2010;45:531–41. doi:10.1016/j.mechmachtheory.2009.10.010.

[61] Mendi F, Ba??kal T, Boran K, Boran FE. Optimization of module, shaft diameter and rolling bearing for spur gear through genetic algorithm. Expert Systems with Applications 2010;37:8058–64. doi:10.1016/j.eswa.2010.05.082.

[62] Marjanovic N, Isailovic B, Marjanovic V, Milojevic Z, Blagojevic M, Bojic M. A practical approach to the optimization of gear trains with spur gears. Mechanism and Machine Theory 2012;53:1–16. doi:10.1016/j.mechmachtheory.2012.02.004.

[63] Golabi S, Fesharaki JJ, Yazdipoor M. Gear train optimization based on minimum volume/weight design. Mechanism and Machine Theory 2014;73:197–217. doi:10.1016/j.mechmachtheory.2013.11.002.

[64] Bonori G, Barbieri M, Pellicano F. Optimum profile modifications of spur gears by means of genetic algorithms. Journal of Sound and Vibration 2008;313:603–16. doi:10.1016/j.jsv.2007.12.013.

[65] Bozca M. Transmission error model-based optimisation of the geometric design parameters of an automotive transmission gearbox to reduce gear-rattle noise. Applied Acoustics 2018;130:247–59. doi:10.1016/j.apacoust.2017.10.005.

[66] Dogan S, Ryborz J, Bertsche B. Design of low-noise manual automotive transmissions. Proceedings of the Institution of Mechanical Engineers, Part K: Journal of Multi-Body Dynamics 2006;220:79–95. doi:https://doi.org/10.1243/14644193JMBD10.

[67] Walton D, Cropper AB, Weale DJ, Meuleman PK. The efficiency and friction of plastic cylindrical gears Part 1: Influence of materials. Proceedings of the Institution of Mechanical Engineers, Part J: Journal of Engineering Tribology 2002;216:75–8. doi:10.1243/1350650021543915.

[68] Walton D, Cropper AB, Weale DJ, Meuleman PK. The efficiency and friction of

plastic cylindrical gears Part 2: Influence of tooth geometry. Proceedings of the Institution of Mechanical Engineers, Part J: Journal of Engineering Tribology 2002;216:93–104. doi:10.1243/1350650021543924.

[69]   Mao K. A new approach for polymer composite gear design. Wear 2007;262:432–41. doi:10.1016/j.wear.2006.06.005.

[70]   Kirupasankar S, Gurunathan C, Gnanamoorthy R. Transmission efficiency of polyamide nanocomposite spur gears. Materials and Design 2012;39:338–43. doi:10.1016/j.matdes.2012.02.045.

[71]   Singh PK, Siddhartha, Singh AK. An investigation on the thermal and wear behavior of polymer based spur gears. Tribology International 2018;118:264–72. doi:10.1016/j.triboint.2017.10.007.

[72]   Fernandes CMCG, Rocha DMP, Martins RC, Magalhães L, Seabra JHO. Finite element method model to predict bulk and flash temperatures on polymer gears. Tribology International 2018;120:255–68. doi:10.1016/j.triboint.2017.12.027.

[73]   Roda-casanova V, Sanchez-marin F. A 2D finite element based approach to predict the temperature field in polymer spur gear transmissions. Mechanism and Machine Theory 2019;133:195–210. doi:10.1016/j.mechmachtheory.2018.11.019.

[74]   Kalin M, Kupec A. The dominant effect of temperature on the fatigue behaviour of polymer gears. Wear 2017;376–377:1339–46. doi:10.1016/j.wear.2017.02.003.

[75]   Bravo A, Koffi D, Toubal L, Erchiqui F. Life and damage mode modeling applied to plastic gears. Engineering Failure Analysis 2015;58:113–33. doi:10.1016/j.engfailanal.2015.08.040.

[76]   Artoni A. A methodology for simulation-based, multiobjective gear design optimization. Mechanism and Machine Theory 2019;133:95–111. doi:10.1016/j.mechmachtheory.2018.11.013.

[77]   Deb K. Introduction to Genetic Algorithms for Engineering Optimization. In: Onwubolu GC, Babu B., editors. New Optimization Techniques in Engineering, Berlin: Springer; 2004, p. 13–51.

[78]   Golub M. An implementation of binary and floating point chromosome representation in genetic algorithm. Proceedings of the 18th International Conference on … 1996:1–6.

[79] Jonikow CZ, Michalewicz Z. An experimental comparison of binary and floating point representations in genetic algorithms. Proceedings of the 4th International Conference on Genetic Algorithms, San Diego, CA, USA, July 1991 1991:31–6.

[80] Gotshall S, Rylander B. Optimal population size and the genetic algorithm. Proceedings On Genetic And Evolutionary Computation Conference 2000:1–5.

[81] Maaranen H, Miettinen K, Mäkelä MM. Quasi-random initial population for genetic algorithms. Computers and Mathematics with Applications 2004;47:1885–95. doi:10.1016/j.cainwa.2003.07.011.

[82] Maaranen H, Miettinen K, Penttinen A. On initial populations of a genetic algorithm for continuous optimization problems. vol. 37. 2007. doi:10.1007/s10898-006-9056-6.

[83] Eberhart, Yuhui Shi. Particle swarm optimization: developments, applications and resources 2002:81–6. doi:10.1109/cec.2001.934374.

[84] Gelatt CD, Vecchi MP, Kirkpatrick S. Optimization by Simulated Annealing. Science 1983;220:671–80. doi:10.1126/science.220.4598.671.

[85] van Laarhoven P. JM, Aarts EHL. Simulated annealing. Simulated Annealing: Theory and Application, Dordrecht: Springer; 1987, p. 7.

[86] Kapelevich AL. Direct Gear Design for Asymmetric Tooth Gears. Theory and Practice of Gearing and Transmissions, vol. 34, 2016, p. 381–92. doi:10.1007/978-3-319-19740-1.

[87] Brown BFW, Davidson SR, Hanes DB, Weires DJ, Brown FW, Davidson SR, et al. Analysis and Testing of Gears with Asymmetric Involute Tooth Form and Optimized Fillet Form for Potential Application in Helicopter Main Drives Analysis and Testing of Gears with Asymmetric Involute Tooth Form and Optimized Fillet Form for Potential Appli. AGMA Technical Paper 2010.

[88] Miettinen K. Introduction to Multiobjective Optimization. In: Branke J, Deb K, Miettinen K, Slowinski R, editors. Multiobjective Optimization: Interactive and Evolutionary Approaches, Berlin: Springer-Verlag; 2008, p. 1–26.

[89] Marler RT, Arora JS. The weighted sum method for multi-objective optimization: New insights. Structural and Multidisciplinary Optimization 2010;41:853–62. doi:10.1007/s00158-009-0460-7.

[90] Pogačnik A, Tavčar J. An accelerated multilevel test and design procedure for polymer gears. Materials and Design 2015;65:961–73. doi:10.1016/j.matdes.2014.10.016.

[91] International Organization for Standardization. ISO 54:1996 - Cylindrical gears for general engineering and for heavy engineering — Modules. 1996.

[92] Mao K, Li W, Hooke CJ, Walton D. Friction and wear behaviour of acetal and nylon gears. Wear 2009;267:639–45. doi:10.1016/j.wear.2008.10.005.

[93] Nutakor C, Talbot D, Kahraman A. An experimental characterization of the friction coefficient of a wind turbine gearbox lubricant. Wind Energy 2019:1–14. doi:10.1002/we.2303.

[94] Tavčar J, Grkman G, Duhovnik J. Accelerated lifetime testing of reinforced polymer gears. Journal of Advanced Mechanical Design, Systems, and Manufacturing 2018;12:JAMDSM0006-JAMDSM0006. doi:10.1299/jamdsm.2018jamdsm0006.

[95] Abderazek H, Ferhat D, Atanasovska I, Boualem K. A differential evolution algorithm for tooth profile optimization with respect to balancing specific sliding coefficients of involute cylindrical spur and helical gears. Advances in Mechanical Engineering 2015;7:1–11. doi:10.1177/1687814015605008.

Curriculum vitae

Daniel Miler was born on 19th of May 1991 in Zagreb, Croatia. He has finished both the elementary and high school in Đakovo, Croatia. He enrolled in the study of mechanical engineering at Faculty of Mechanical Engineering and Naval Architecture, University of Zagreb in 2010. He finished studies in 2015, earning Faculty Medals at both the undergraduate and graduate level. He has been employed at the same institution since 2016 as a research assistant. His research interests include mechanical design optimisation, with a focus on geared transmissions. He is a member of Croatian Society for Mechanics (CSM) and Croatian Society for the Theory of Machines and Mechanisms (CroFToMM). He is an author of 11 scientific articles, 4 of which were published in scientific journals (WoS CC). He is awarded an "Outstanding contribution in reviewing" by journal Mechanism and Machine Theory (Elsevier).

List of publications:

1. Miler D, Hoić M, Domitran Z, Žeželj D. *Prediction of friction coefficient in dry-lubricated polyoxymethylene spur gear pairs*. Mechanism and Machine Theory, 2019;138:205-222. doi:10.1016/j.mechmachtheory.2019.03.040

2. Miler D, Žeželj D, Lončar A, Vučković K. *Multi-objective spur gear pair optimization focused on volume and efficiency*. Mechanism and machine theory, 2018;125:185-195. doi:10.1016/j.mechmachtheory.2018.03.012

3. Miler D, Lončar A, Žeželj D, Domitran Z. *Influence of profile shift on the spur gear pair optimization*. Mechanism and machine theory, 2017;117:189-197. doi:10.1016/j.mechmachtheory.2017.07.001

4. Miler D, Škec S, Katana B, Žeželj D. *An experimental study of composite plain bearings: Influence of clearance on friction coefficient and temperature*. Strojniški vestnik, 2019;65(19):547-556. doi:10.5545/sv-jme.2019.6108

5. Miler D, Perišić MM, Mašović R, Žeželj D. Predicting student academic performance in Machine elements course. In: Tadeusz U (editor). Advances in Mechanism and Machine Science, 2019:825-834. In: Tadeusz U (editor). Advances in Mechanism and Machine Science, 2019:1111-1120. doi:10.1007/978-3-030-20131-9_110

6. Mašović R, Jagarčec V, Miler D, Domitran Z, Bojčetić N, Žeželj D. *Analysis of printing direction impact on dimensional accuracy of spur gears*. In: Tadeusz U (editor). Advances in Mechanism and Machine Science, 2019:1111-1120. doi:10.1007/978-3-030-20131-9_110

7. Miler D, Lončar A, Žeželj D. Impact of design constraints on the spur gear pair parameters. In: Herák D (editor). Proceedings of 58th International Conference of Machine Design Departments - ICMD 2017, Prague, Czech Republic, 2017.

8. Čular I., Vučković K., Miler D., Žeželj D. *Numerical Bending Fatigue Analysis of a Surface Hardened Spur Gears*. In: Reis L, Freitas M, Anes V (editors). Proceedings of the 18th International Conference on New Trends in Fatigue and Fracture; Lisabon, Portugal, 2018.

9. Žeželj D, Miler D. *Manufacturing Technology-based Approach to Teaching Engineering Drawing*. In: Marjanović D, Štorga M, Škec S, Bojčetić N, Pavković N (editors). Proceedings of the 15th International Design Conference (DESIGN 2018), Dubrovnik, Croatia, 2018.doi:10.21278/idc.2018.0530

10. Žeželj D, Mađer M, Miler D. Analiza posipanja kolnika česticama metodom diskretnih elemenata. In: Penava D, Guljaš I, Bošnjak K (editors). Zbornik radova osmog susreta hrvatskog društva za mehaniku, Osijek, Croatia, 2017.

11. Miler D, Žeželj D, Lončarek I. Case Study on CAE Tools: Optimization of a 6-axis Robotic Arm for MAG Welding. In: Marković B, Antunović R (editors). Proceedings COMETa 2016, Sarajevo, Bosnia and Herzegovina, 2016.

<u>Appendix</u>

Paper I

Paper I

Influence of profile shift on the spur gear pair optimization

Daniel Miler[1*], Antonio Lončar[2], Dragan Žeželj[1] and Zoran Domitran[1]

[1] *Faculty of Mechanical Engineering and Naval Architecture, University of Zagreb, 10002 Zagreb, Ivana Lučića 5, Croatia*
[2] *SedamIT Ltd, 10000 Zagreb, Koledovcina 2, Croatia*

Abstract

Due to the established load capacity calculations and extensive literature, gearbox design process is rather simple. In order to gain a competitive edge, transmission designers and manufacturers are forced to constantly improve the design process and the product quality. The gearbox design process can be improved by using genetic algorithm to determine the optimal values of gear pair parameters. In this paper, besides the frequently used gear optimization variables, i.e. the module, the face width, and the number of teeth, profile shift coefficients of both gears are included to create a five-variable process. Since the profile shift influences the form, zone and stress factors, as well as the transversal and face load factors, it affects the optimization results significantly. The gear pair volume served as a fitness function, while the tooth root bending strength and the contact pressure calculations were used as constraints. Optimization results of the pair without profile shift and the arbitrary profile shifted pair were compared. The genetic algorithm solution is found for three data sets; the solution is verified using commercial gear optimization software.

Keywords: Gear; Profile shift; Optimization; Design; Genetic algorithm; Initial parameters.

1. Introduction

At the first sight, a gearbox design process is straightforward; the element is often seen and strength calculations [1, 2] are well known and can be easily found in the technical literature. Analytic, numeric or experimental methods can be used [3]. However, the problem arises when the starting parameter values are being determined. In order to satisfy the strict economic, safety and effectiveness requirements, a designer has to use the optimal design methodology [4, 5]; using the conventional methods, it is hard to decide whether they are the best possible ones.

A genetic algorithm (GA) is a nature-inspired stochastic optimization method suitable for solving complex technical problems, mostly due to its assured convergence [6]. Since the gear design objectives are often conflicting, Marcelin [7] examined the performance of genetic algorithm in solving the gear optimization problem. Doing independent research, Yokota et al. also examined the method efficiency, but they included the shaft torsional strength calculation [8]. Their work resulted in a significant weight improvement, confirming the method applicability.

In order to minimize the gear train volume, Gologlu and Zeyveli [9] used the GA to automate the preliminary design of two-stage gear drive. Savsani et al. [4] used the particle swarm (PS) and simulated annealing (SA) optimization algorithms to minimize the spur gear train weight; they compared the results with the ones obtained using the GA. However, even though they found that the PS and SA optimization algorithms outperformed the GA in some aspects, the GA optimization remains the most frequently used method in the field of gear

optimization. Mendi et al. [10] broadened the optimization process and studied the use of the GA for gearbox design. In addition to gears, shafts and bearings were also observed. Marjanović et al. presented a solution to the optimization problem of spur gear trains [11]. Using the approach based on the selection matrix, the authors described the process of selecting the optimal concept and material. Tudose et al. [12] attempted to solve the same optimization problem of helical gears instead of spur gears. The authors used a two-phase evolutionary algorithm to automate the design of a complete two-stage helical gear transmission, including the shafts, the bearings and the housing. The next step in solving the optimization problem by using the GA can be made by taking the micro-geometric modifications into account, as suggested by Bonori et al. [13].

When it comes to the profile shift coefficients, Diez-Ibarbia et al. studied their influence on the spur gear efficiency [14]. The group concluded that an increase in the profile shift influences the load sharing properties of a pair of gears, thus lowering the transmission efficiency. Abderazek et al. included the profile shift coefficients in their optimization process; a differential evolution algorithm was used to determine the optimal profile shift values for an arbitrary pair [15]. The pinion and wheel number of teeth and the sum of profile shifts were used as input data. Furthermore, the same authors investigated the use of adaptive mixed differential method for balancing specific sliding coefficients and maximum bending stresses [16]. The influence of profile shift on the internal spur gear pair mesh

---
[*]Corresponding author. Tel.: +385 1 6168 175
E-mail address: daniel.miler@fsb.hr

stiffness was studied by Chen et al. [17]. It was found that with an increase in the value of profile shift coefficient, the single-tooth mesh stiffness also increases, while the multi-tooth stiffness decreases, influencing dynamic responses. Research on the asymmetric spur gears was conducted by Senthil Kumar et al. [18]. They determined the optimal values of rack cutter shifts to increase the bending load capacity of a specific case. An iterative procedure was established using the finite element method and the Direct gear design® method [19].

However, a literature review revealed a gap. Some of the earlier studies were conducted either without taking the profile shift influence into account [3, 7-9] or with the profile shift included, but with pre-setting the module, the number of teeth (pinion), and the sum of profile shift coefficients [15, 16]. The exclusion of gear profile shifts shows that the values of the form factor Y_F, the stress factor Y_S, the zone factor Z_H, the transverse load factors $K_{F\alpha}$ and $K_{H\alpha}$, and the face load factors $K_{F\beta}$ and $K_{H\beta}$ are simplified. On the other hand, the pre-setting of the gear module, the teeth number, and the profile shift coefficient sum will not yield optimal gearbox parameters.

In this paper, the authors determined the influence of profile shift coefficients on the gear pair optimization. The pinion and wheel profile shifts x_1 and x_2 are included as additional variables. The outcome was an automated five-variable optimization process. Results obtained for pairs without profile shift ($x_1 = x_2 = 0$) and for pairs with arbitrary profile shifts were compared, which is a main novelty of the conducted study. For the gear load calculation, the method B of the ISO 6336:2006 [1] standard was used. Since the profile shift coefficients influence a lot of calculation factors, all calculation factors are also included in the optimization process.

Finally, limitations of the study should be noted. Optimization was carried out using the tooth root strength and surface durability as limiting conditions. Gearing efficiency and dynamic properties were not considered, but provide a basis for the future work.

2. Method

The research method was based on the ISO 6336:2006 standard for the gear load capacity calculation and on the genetic algorithm. The application uses input parameters for formulating boundary conditions, which restrict the optimization space. Five factors were selected as variables – gear module m, pinion tooth number z_1, face width b, pinion profile shift x_1, and profile shift x_2. Optimization results obtained for the pair without profile shift and that with arbitrary profile shift were compared. The optimization process flowchart is shown in *Fig. 1*.

The described process was carried out using three different sets of input data *(Table 1)*. Sets 1-3 represent the medium-duty, high-quality, and low-quality steel gear pairs.

Each set consists of the desired input torque T_1, the rotational speed n_1, the transmission ratio i, the application factor K_A, the IT quality grade, the starting time t_{st}, and the material strength properties. Gears were assumed to be full steel discs; the steel density was $\rho = 7830$ kg/m³. Gear dimensions influence the calculation of the torque T, which is a sum of the operational and the starting torque caused by the gear pair moment of
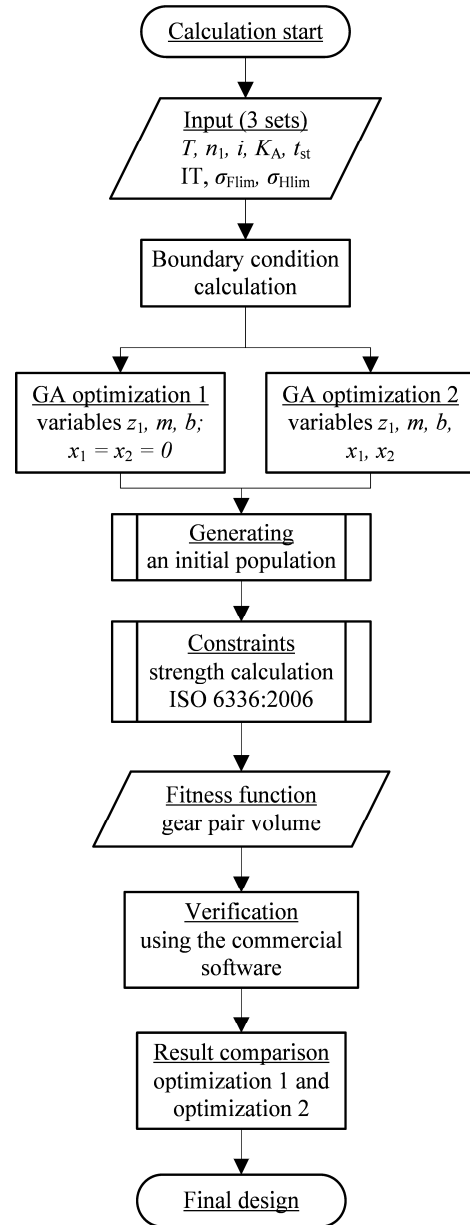
Fig. 1 Optimization process

inertia at the start of operation (1):

$$T = T_1 + \frac{\pi^2 n_1 \rho}{16 t_{st}} m^4 z_1^2 b (z_1^2 + z_2^2). \tag{1}$$

Next, variables of the module, the face width, and the number of teeth on the pinion were limited to provide

Table 1 Example sets of input data

	Set 1	Set 2	Set 3
T_{input}	100 Nm	30 Nm	250 Nm
n_1	960 min⁻¹	2850 min⁻¹	720 min⁻¹
i	3.55	4.5	2.8
K_A	1.6	1.25	1.2
IT grade	7	6	9
Material	Cf 53 (2)	14 Ni 6	51 CrMoV 4 (1)
t_{st}	1 s	0.5 s	2 s
σ_{Flim}	275 N/mm²	430 N/mm²	275 N/mm²
σ_{Hlim}	1080 N/mm²	1500 N/mm²	650 N/mm²

Table 2 Boundary conditions

Factor		Set 1	Set 2	Set 3
Face width	b	6…25 m		
Gear module	m	2…8 mm	1…5 mm	6…20 mm
Number of teeth (pinion)	z_1	14…24		
Profile shift (pinion)	x_1	0… x_{1max}		
Profile shift (wheel)	x_2	-0.7…0.7		

practically feasible solutions. The module values were chosen from the ISO standard [20], while the number of teeth on the pinion and the face width were limited to discrete values. The maximal pinion profile shift coefficient was limited by the tooth thickness at the tip diameter $(x_{1max} = 0.4 \ m)$. Additionally, the centre distance is assumed to be a non-standard floating number to avoid an unnecessary increase in the gear dimensions. Boundary conditions are shown in *Table 2*.

2.1 Genetic algorithm

The genetic algorithm optimization was then carried out. The exhaustive search of the design space was not feasible due to a large number of combinations. The tooth root stress and the contact surface durability were used as design constraints. Floating point representation was used instead of the binary one because of its precision and consistency [21].

The wheel and pinion pair volume was calculated as a function of the addendum diameter d_a, the gear width b, and the transmission ratio i. Since the pair volume was used as a fitness function (2), the addendum diameter was chosen for its calculation instead of the pitch diameter to include the influence of profile shift on the pair fitness. The number of teeth z_2 was found by multiplying z_1 with the transmission ratio and by rounding the obtained value to the closest integer. The data set with the lowest volume was declared to be the fittest.

$$V = f(b, m, z_1) = \frac{\pi b}{4}(d_{a1}^2 + d_{a2}^2). \tag{2}$$

The population size influences both the solution accuracy and the computation time. An increase in the initial population size also increases the number of generations needed for the solution to converge [22]. Uniform representation of the initial population across the solution space is often more important than the randomness of its units [23]. The chosen population size was 300 individuals and the initial population variables were generated as random vectors. The process was conducted using the mutation rate of 0.55 in the generation with two elite chromosomes. To ensure precision, the optimization of each set was replicated 10 times on the three sets of input data.

2.2 Strength calculation

Satisfactory gear strength was achieved by setting the tooth root stress and surface durability as constraints (3), (4). Conditions are formulated as follows:

$$\sigma_{FP} - \frac{2T}{z_1 b m^2} K_A K_{F\alpha} K_{F\beta} K_V Y_F Y_S \geq 0 \tag{3}$$

$$\sigma_{HP} - Z_B Z_H Z_E Z_\varepsilon \sqrt{\frac{2T(i+1)}{m^2 z_1^2 bi} K_A K_v K_{H\alpha} K_{H\beta}} \geq 0 \tag{4}$$

The form factor Y_F and the stress factor Y_S were determined separately for all the units in each generation. The zone factor Z_H, defined as a function of the working transverse pressure angle and the pressure angle at the pitch circle, and the contact ratio factor Z_ε were also included. Additionally, the single pair tooth contact was accounted for by calculating the values of the single pair tooth contact factors Z_B and Z_D. If both factors were greater than 1, the one with the greater value was included.

The transversal load factors $K_{H\alpha}$ and $K_{F\alpha}$, and the dynamic factor K_v were calculated according to the method B of the standard [1]. The influence of the face load factors $K_{H\beta}$ and $K_{F\beta}$ was also considered, but due to the complexity of their determination [24], simplified relations described in the method C of [1] were used. It was assumed that the gearing is supported symmetrically.

Using equations (5) and (6), the permissible stresses σ_{HP} and σ_{FP} were found for both the genetic algorithm and the commercial software optimization process. Their values were adjusted according to the operating conditions, such as surface roughness, pitch error, and oil viscosity (*Table 3*).

$$\sigma_{FP} = \frac{\sigma_{Flim}}{S_{Fmin}} Y_{ST} Y_{NT} Y_{\delta relT} Y_{RrelT} Y_X \tag{5}$$

$$\sigma_{HP} = \frac{\sigma_{Hlim}}{S_{Hmin}} Z_{NT} Z_L Z_v Z_R Z_W Z_X \tag{6}$$

Since the velocity factor Z_V, the roughness factor Z_R, the relative notch sensitivity factor $Y_{\delta relT}$, and the relative surface factor Y_{RrelT} are functions of the optimization variables, they were included in the optimization. The size factors Y_X and Z_X and the work hardening factor Z_W were not considered and are thus equal to 1.

However, in the optimization process, there were factors with constant values *(Table 3)*. The contact pressure safety factor S_{Hmin} and the tooth root stress safety ratios S_{Fmin} were used in both the optimization and evaluation phases. The life factors Y_{NT} and Z_{NT} were calculated for a required service life of 20,000 h. In addition, the oil viscosity parameter Z_L was calculated for the oil of ISO viscosity grade VG 220.

Table 3 Permissible stress calculation parameters

Factor		Set 1	Set 2	Set 3
Stress correction factor	Y_{ST}	2		
Life factor (root)	Y_{NT}	0.888	0.868	0.893
Life factor (contact)	Z_{NT}	0.908	0.878	0.916
Lubricant factor	Z_L	1.026	1.02	1.038
Safety factor (flank)	S_{Hmin}	1	1.175	1.2
Safety factor (root)	S_{Fmin}	1.5		

2.3 Result validation

GA results were compared with those provided by the commercial software *KISSsoft* (KS) which offers *rough* and

fine sizing calculations. The data from *Table 1* and *Table 2* were used for the *rough sizing*, which provided 100 sets of parameters. The set with the lowest weight was selected and used for the *fine sizing*, with weight as the main criterion. The best rated solutions were found after setting the module values to the standardized ones. The results *(Table 4)* were used to validate the results of the GA. Finally, all the final solutions generated using the GA were checked by means of the KS commercial software to verify whether the strength requirements are met.

3. Results

The results obtained after running each data set through the described optimization process are shown in *Table 4*. Solutions of each set were found for both the pairs with arbitrary profile shift and those without profile shift. The algorithm was run a total of 60 times since all the cases were replicated 10 times. The volume discrepancy of replications is shown in *Table 5*. The pairs without profile shift converged quickly: therefore, there was no deviation.

An i5-6500 quad-core processor with 8 GB of RAM was used for calculations. The average calculation time for running 500 generations of sets with no profile shifts was 0.81s. The calculation of an arbitrary profile shift set using 30,000 generations took 36.9s, on average. The calculation time could be further reduced by introducing simplifications and by reducing the number of generations or by lowering the initial population size at the cost of result precision. Further discretization of intervals from which the profile shift

coefficients were chosen would result in a faster convergence; lowering the computational cost accordingly. However, faster convergence without the loss of precision can also be achieved by a quasi-random generation of initial population, i.e. by Sobol sequences, as suggested by Maaranen et al. [25, 26].

The pairs without profile shift converge quickly. To ensure the validity of results, 500 generations were used. For the pairs with arbitrary profile shift coefficients, the change in the highest fitness solution obtained using the GA from generation to generation is shown in *Figure 2*. It shows the ratio between the n generation and the 30000th generation fitness values. The number of generations required to provide a satisfactory solution is 500. A further increase in the generation number does not contribute to the solution quality and it increases the computation time. The mean fitness difference between 500 and 30,000 generations is 0.066%, 1.84% and 0.0048% for sets 1, 2 and 3, respectively.

Since the solutions for all three sets exhibited a tendency towards the lower face width boundary, the process was repeated to enable further observation. The lower boundary condition was set to $b = 2m$. Results are shown in *Table 6*.

Table 4 Optimization results

	GA		KISSsoft
SET 1	$x_1 = x_2 = 0$	x_1, x_2	
Volume, mm³	2 901 072	1 896 336	2 302 937
Weight, kg	22.715	14.848	18.032
Face width, mm	28	22.5	23.5
Gear module, mm	4	3.75	3.875
Number of teeth (pinion)	24	23	24
Profile shift (pinion)	-	0.699	0.496
Profile shift (wheel)	-	0.136	0.657
SET 2			
Volume, mm³	481 644	326 083	357 344
Weight, kg	3.771	2.553	2.798
Face width, mm	12	12.25	11
Gear module, mm	2	1.75	1.75
Number of teeth (pinion)	24	22	24
Profile shift (pinion)	-	0.638	0.463
Profile shift (wheel)	-	0.559	0.595
SET 3			
Volume, mm³	37 009 972	24 170 985	27 726 692
Weight, kg	289.8	189.3	217.1
Face width, mm	72	60	62
Gear module, mm	12	10	10
Number of teeth (pinion)	22	23	24
Profile shift (pinion)	-	0.691	0.417
Profile shift (wheel)	-	0.291	0.310

Table 5 Optimization results with adjusted face width boundaries

	GA		KISSsoft
SET 1	$x_1 = x_2 = 0$	x_1, x_2	
Volume, mm³	2 139 236	1 488 870	1 620 690
Weight, kg	16.75	11.66	12.69
Face width, mm	12	10	10
Gear module, mm	6	5	5
Number of teeth (pinion)	21	23	24
Profile shift (pinion)	-	0.492	0.449
Profile shift (wheel)	-	0.056	0.454
SET 2			
Volume, mm³	379 498	292 507	319 157
Weight, kg	2.971	2.290	2.499
Face width, mm	6	5	5
Gear module, mm	3	2.5	2.5
Number of teeth (pinion)	20	23	24
Profile shift (pinion)	-	0.596	0.441
Profile shift (wheel)	-	0.490	0.465
SET 3			
Volume, mm³	28 435 384	18 440 962	20 613 027
Weight, kg	222.6	144.4	161.4
Face width, mm	36	32	27
Gear module, mm	18	16	13.5
Number of teeth (pinion)	18	17	24
Profile shift (pinion)	-	0.560	0.346
Profile shift (wheel)	-	0.306	0.454
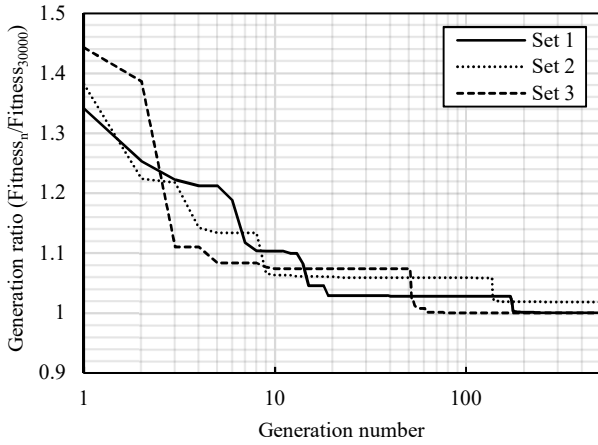
Fig. 2 Solution fitness change depending on the generation

4. Discussion

Results of the GA optimization for each of the sets show that lower volume was achieved by increasing the module m and the profile shift coefficient x_1, rather than by finding a balance between the module and the face width. During the optimization process, the main problem was the tendency of the results towards the lower face width boundary. For this reason, before discussing the influence of profile shift on the spur gear optimization, the results were further analysed. The additional examination was conducted by lowering the face width boundary *(Table 6)*: it showed that the algorithm continued choosing the lowest possible width.

The same behaviour was displayed while validating the results using the *KISSsoft* sizing algorithms. The authors suppose that the main cause of that behaviour was the lower tangential force. Since the transmitted operating torque T was constant due to negligible differences caused by the gear pair inertia, the same number of pinion teeth with an increase in the module m value reduces the magnitude of the normal force F_n on the tooth flank. The lower magnitude of the normal force causes the values of its radial and tangential components to fall. By simplifying the stress calculation formulae on the assumption that both the factors Z, Y, and K and the input parameters T_1 and i are constant, it can be written:

$$\sigma_F = \frac{2T}{z_1 bm^2} K_i Y_i = C_F \cdot \frac{1}{z_1 bm^2}, \tag{7}$$

$$\sigma_H = Z_i \sqrt{K_i} \sqrt{\frac{2T_1}{(mz_1)^2 b} \frac{i+1}{i}} = C_H \cdot \frac{1}{mz_1 \sqrt{b}} \tag{8}$$

Equations (7) and (8) show that the resulting contact pressure is inversely proportional to the pitch diameter and to the square root of the face width. C_F and C_H represent the results of all the constants for a given case. Equation (7) shows that, an increase in m causes a more rapid reduction in the tooth root bending stress than an increase in z_1 and b. Similarly, an increase in the pitch diameter also reduces the contact pressure more sharply than the face width (8). To conclude, both equations confirm that the module m has the biggest influence on the calculation, which is in agreement with the results.

The contact pressure was a limiting factor in all the cases, despite the lower safety factor required. The following considerations are thus focused on the factors that influence the surface durability.

Optimization results *(Table 4)* show that the influence of the profile shift is significant. According to the results, using pairs with profile shifts yields 34.6%, 32.3%, and 34.7% smaller volume, compared with the volume of pair without profile shift.

Values of the differing calculation factors are shown in *Table 7*. When comparing the dynamic factors K_v, the face load factors $K_{H\beta}$ and the transverse load factors $K_{H\alpha}$, all the sets exhibited lower $K_{H\beta}$ and $K_{H\alpha}$ values when the profile shift was present. The $K_{H\beta}$ values were reduced by 8.1%, 3.4%, and 10% and those of $K_{H\alpha}$ by 17.1%, 8.8%, and 10.1%. Even though the positive profile shift coefficient increases the meshing stiffness of the pair, the lower module and face width values caused lower mesh stiffness in the profile shifted gears, enabling a more favourable face load distribution. The difference in $K_{H\alpha}$ was caused by the transverse contact ratio ε_α which was reduced by 15%-17% in the pairs with profile shift. K_v was mostly unaffected by profile shifts.

Due to the greater working transverse pressure angle caused by positive profile shifts, the zone factor Z_H values of the pairs with profile shift were smaller, 2.355, 2.327, and 2.31 compared to 2.495 of the gears without profile shift. The contact ratio factor Z_ε was reduced by 5.6% - 6.2% in the pairs without profile shift. The remaining differences in the contact pressure calculation factor value were less than 1%.

Even though the optimization process that includes varying profile shifts is more complex and requires a larger initial population size and more generations, the authors believe that the influence of profile shift should be included. In cases where it is not possible, fixing the profile shift values x_1 and x_2 to 0.5 will yield lower pair weights. As seen from the commercial software results, the resulting volume will be much smaller. The GA volumes do not exhibit the same level of symmetry when allocating the profile shift coefficients to the pinion and the wheel, as seen in the set 1 and 3 results *(Tables 4 and 6)*.

Table 6 Fitness discrepancy across replications

Factor	Set 1	Set 2	Set 3
Lowest volume	1 896 336	326 083	24 170 985
Highest volume	1 918 950	327 360	24 396 635
Difference	22614	1277	225650
Difference (%)	1.19 %	0.392 %	0.934 %
Mean volume	1 901 409	326 360	24 319 960
Standard deviation	8744	497	96580

Table 7 Stress calculation factor values

Data set		K_v	$K_{H\alpha}$	$K_{H\beta}$	Z_H	Z_ε	$c_{\gamma\alpha}$
1	$x_1 = x_2 = 0$	1.124	1.314	1.400	2.495	0.872	21.15
	x_1, x_2	1.100	1.088	1.286	2.355	0.921	20.50
2	$x_1 = x_2 = 0$	1.097	1.096	1.218	2.495	0.870	21.53
	x_1, x_2	1.076	1	1.176	2.327	0.924	20.81
3	$x_1 = x_2 = 0$	2	1.296	1.854	2.495	0.878	15.14
	x_1, x_2	2	1.165	1.669	2.310	0.926	16.34

Pairs without profile shift converge quickly. It took 3 generations for sets 1 and 3 and 23 generations for set 2 to converge. The fast convergence was caused mainly by lower optimization space – only 3 discrete variables were needed, while the initial population size remained the same.

Lastly, in this paper the profile shift influence was observed exclusively on the spur gears. Presented study can be conducted on the helical gears with two possible directions; by using the constant helix angle or by introducing a helix angle as new optimization variable. Former would have a minor influence on the computational cost, while the latter, to retain the same solution accuracy, would increase the cost.

5. Conclusions

A design process of a spur gear pair was conducted using the GA: the obtained results were compared with the specialized commercial software results. After analysing three sets of data with both methods, the inclusion of profile shifts as variables resulted in 32.3% to 34.7% lower gear pair weight. The authors concluded that the profile shift coefficients should be included as optimization variables when the aim is to achieve the minimal weight of a pair. In case that the profile shift variation is not possible, we suggest setting the profile shift coefficient values to $x_1 = x_2 = 0.5$.

Additionally, using a higher value of the gear module at the expense of the face width has a smaller volume as a result since the best results are found at the lower face width boundary. The GA also tends to maximize the pinion profile shift, resulting in larger tooth radii of curvature, which is beneficial for both the contact and the tooth root bending stress. Lastly, the flank safety was a limiting factor for all the observed data sets despite using the lower safety factor.

Besides the observed calculation parameters, the gear disc design should also be considered. In this paper it was assumed that gears were full discs, without any mass reduction. A low width pair, such as the highest fitness pairs in this paper, would eliminate a possibility of mass reduction.

Following the recent trends, for a future work the authors plan on addressing both the gearing efficiency and the dynamic transmission error as factors that influence the fitness function. Another possibility for a future work is using a specific sliding as an additional constraint. Due to high profile shift values, it will influence the gearing longevity. Achieving the balance between the specific sliding velocities will result in a more uniform pinion and wheel wear.

Nomenclature

b	: face width
C_F	: product of all the calculation constants (bending)
C_H	: product of all the calculation constants (contact)
d_{a1}	: tip diameter (pinion)
d_{a2}	: tip diameter (wheel)
i	: transmission ratio
K_A	: application factor
$K_{F\alpha}$	: transverse load factor (root stress)
$K_{F\beta}$	: face load factor (root stress)
$K_{H\alpha}$	: transverse load factor (contact stress)
$K_{H\beta}$	: face load factor (contact stress)
K_v	: dynamic factor
K_i	: product of all the dynamic factors
m	: gear module
n_1	: rotational speed (pinion)
ρ	: density (steel)
σ_{Flim}	: nominal stress number (bending)
σ_{FP}	: nominal permissible stress (bending)
σ_{Hlim}	: allowable stress number (contact)
σ_{HP}	: allowable permissible stress (contact)
T	: calculation torque
T_1	: input torque
t_{st}	: starting time
V	: volume
x_1	: profile shift coefficient (pinion)
x_{1max}	: maximal allowable profile shift coefficient (pinion)
x_2	: profile shift coefficient (wheel)
Y_F	: tooth form factor
Y_i	: product of all the tooth root bending factors
Y_S	: stress correction factor
Z_B	: single pair tooth contact factor (pinion)
Z_D	: single pair tooth contact factor (wheel)
Z_E	: elasticity factor
Z_H	: zone factor
Z_i	: product of all the contact factors
Z_ε	: contact ratio factor
z_1	: number of teeth (pinion)
z_2	: number of teeth (wheel)

Acknowledgements

References

[1] ISO Standard 6336:2006, Calculation of load capacity of spur and helical gears, International Organization for Standardization, Geneva, Switzerland, 2006.

[2] AGMA Standard 2001--D04, Fundamental Rating Factors and Calculation Methods for Involute Spur and Helical Gear Teeth, American Gear Manufacturers Association Alexandria, VA, 2004.

[3] T.J. Lisle, B.A. Shaw, R.C. Frazer, External spur gear root bending stress: A comparison of ISO 6336:2006, AGMA 2101-D04, ANSYS finite element analysis and strain gauge techniques, Mech. Mach. Theory. 111 (2017) 1-9. doi: 10.1016/j.mechmachtheory.2017.01.006

[4] V. Savsani, R. V. Rao, D.P. Vakharia, Optimal weight design of a gear train using particle swarm optimization and simulated annealing algorithms, Mech. Mach. Theory. 45 (2010) 531–541. doi:10.1016/j.mechmachtheory.2009.10.010.

[5] A. Almasi, Latest technologies and modern guidelines on gear units, Aust. J. Mech. Eng. 12 (2014). doi:10.7158/M12-085.2014.12.3.

[6] J.-L. Marcelin, Using genetic algorithms for the optimization of mechanisms, Int J Adv Manuf Technol. 27 (2005) 2–6. doi:10.1007/s00170-004-2162-z.

[7] J.-L. Marcelin, Genetic optimisation of gears, Int. J. Adv. Manuf. Technol. 17 (2001) 910–915. doi:10.1007/s001700170101.

[8] T. Yokota, T. Taguchi, M. Gen, A solution method for optimal weight design problem of the gear using genetic algorithms, Comput. Ind. Eng. 35 (1998) 523–526. doi:10.1016/S0360-8352(98)00149-1.

[9] C. Gologlu, M. Zeyveli, A genetic approach to automate preliminary design of gear drives, Comput. Ind. Eng. 57 (2009) 1043–1051. doi:10.1016/j.cie.2009.04.006.

[10] F. Mendi, T. Baskal, K. Boran, F.E. Boran, Optimization of module, shaft diameter and rolling bearing for spur gear through genetic algorithm, Expert Syst. Appl. 37 (2010) 8058–8064. doi:10.1016/j.eswa.2010.05.082.

[11] N. Marjanovic, B. Isailovic, V. Marjanovic, Z. Milojevic, M. Blagojevic, M. Bojic, A practical approach to the optimization of gear trains with spur gears, Mech. Mach. Theory. 53 (2012) 1–16. doi:10.1016/j.mechmachtheory.2012.02.004.

[12] L. Tudose, O. Buiga, C. Ştefanache, A. Sóbester, Automated optimal design of a two-stage helical gear reducer, Struct. Multidiscip. Optim. 42 (2010) 429–435. doi:10.1007/s00158-010-0504-z.

[13] G. Bonori, M. Barbieri, F. Pellicano, Optimum profile modifications of spur gears by means of genetic algorithms, J. Sound Vib. 313 (2008) 603–616. doi:10.1016/j.jsv.2007.12.013.

[14] A. Diez-Ibarbia, A.F. del Rincon, M. Iglesias, A. de-Juan, P. Garcia, F. Viadero, Efficiency analysis of spur gears with a shifting profile, Meccanica. 51 (2016) 707–723. doi:10.1007/s11012-015-0209-x.

[15] H. Abderazek, D. Ferhat, I. Atanasovska, K. Boualem, A differential evolution algorithm for tooth profile optimization with respect to balancing specific sliding coefficients of involute cylindrical spur and helical gears, Adv. Mech. Eng. 7 (2015) 1–11. doi:10.1177/1687814015605008.

[16] H. Abderazek, D. Ferhat, I. Atanasovska, Adaptive mixed differential evolution algorithm for bi-objective tooth profile spur gear optimization, Int. J. Adv. Manuf. Technol. (2016) 1–11. doi:10.1007/s00170-016-9523-2.

[17] Z.G. Chen, W.M. Zhai, Y.M. Shao, K.Y. Wang, Mesh stiffness evaluation of an internal spur gear pair with tooth profile shift, Sci. China Technol. Sci. 59 (2016) 1328–1339. doi:10.1007/s11431-016-6090-6.

[18] V. Senthil Kumar, D. V. Muni, G. Muthuveerappan, Optimization of asymmetric spur gear drives to improve the bending load capacity, Mech. Mach. Theory. 43 (2008) 829–858. doi:10.1016/j.mechmachtheory.2007.06.006.

[19] A. L. Kapelevich, Direct gear design, CRC Press, Taylor & Francis Group, Boca Raton, 2013.

[20] ISO Standard 54:1996, Cylindrical gears for general and heavy engineering, International Organization for Standardization, Geneva, Switzerland, 1996.

[21] C.Z. Jonikow, Z. Michalewicz, An experimental comparison of binary and floating point representations in genetic algorithms, Proc. 4th Int. Conf. Genet. Algorithms, San Diego, CA, USA, July 1991. (1991) 31–36.

[22] S. Gotshall, B. Rylander, Optimal population size and the genetic algorithm, Proc. Genet. Evol. Comput. Conf. (2000) 1–5.

[23] H. Maaranen, K. Miettinen, M.M. Mäkelä, Quasi-random initial population for genetic algorithms, Comput. Math. with Appl. 47 (2004) 1885–1895. doi:10.1016/j.cainwa.2003.07.011.

[24] V. Roda-Casanova, F.T. Sanchez-Marin, I. Gonzalez-Perez, J.L. Iserte, A. Fuentes, Determination of the ISO face load factor in spur gear drives by the finite element modeling of gears and shafts, Mech. Mach. Theory. 65 (2013) 1–13. doi:10.1016/j.mechmachtheory.2013.02.006.

[25] H. Maaranen, K. Miettinen, A. Penttinen, On initial populations of a genetic algorithm for continuous optimization problems, 2007. doi:10.1007/s10898-006-9056-6.

[26] P. Bratley, B. Fox, Algorithm 659: implementing Sobol's quasirandom sequence generator, ACM Transactions on Mathematical Software, 14 (1988) 88-100.

Paper II

Multi-objective spur gear pair optimization focused on volume and efficiency

Daniel Miler[1], Dragan Žeželj[1*], Antonio Lončar[2] and Krešimir Vučković[1]

[1] *Faculty of Mechanical Engineering and Naval Architecture, University of Zagreb, 10002 Zagreb, Ivana Lučića 5, Croatia*

[2] *SedamIT Ltd, 10000 Zagreb, Koledovcina 2, Croatia*

Abstract

Besides satisfying the essential strength requirements, gearbox design should ensure additional desirable properties in order to be competitive. For example, a gearbox should be efficient, durable, quiet, compact, and light. Nowadays, as a consequence of rising environmental concerns, high efficiency is a rather desirable feature. In this article, a genetic algorithm was used for conducting a multi-objective optimization of gear pair parameters with a goal of reducing the transmission volume and power losses. Gearing efficiency primarily depends on the normal load, sliding velocities, and the friction coefficient. Gearing efficiency was calculated analytically, using the approximate load distribution formulae and efficiency formulation developed by Schlenk. The resulting formula was included in the genetic algorithm as an objective. To verify it, results were compared to the ones obtained by other authors. Optimization variables consisted of the gear module, the face width, the pinion and wheel profile shift coefficients and the number of teeth of the pinion. Solutions have shown that the trade-off between volume and efficiency is obligatory and a combination of the lower gear module, the lower face width, the higher profile shift coefficients and the higher number of teeth of the pinion yield good results regarding both objectives.

Keywords: Spur gear; Efficiency calculation; Volume minimization; Multi-objective optimization; Genetic algorithm.

---

1. Introduction

During the gearbox design phase, gear pair parameters, and consequently gear pair properties, are defined by the calculation standards such as ISO and AGMA [1, 2]. Nonetheless, the resulting design is often not competitive on the market even though it satisfies all the necessary strength requirements. For this reason, additional desirable properties are included to improve it, either in terms of higher durability, higher efficiency, or a lighter and more compact design.

Optimization methods provide a fast way of solving the above-mentioned problems by finding the optimal set of parameters for each observed case. In the field of gear optimization, genetic algorithms (GA) have been widely used since they were proposed by Marcelin and Yokota [3, 4, 5]. GA is a bio-inspired optimization algorithm that replicates the theory of evolution. By combining the best performing specimens in a generation, all of which satisfy both the obligatory and additional criteria, a solution with the highest fitness value is found. GA has been used for solving a substantial number of tasks in the field, such as the gear train volume minimization, gearbox design, and the optimization of micro-geometric modifications [6, 7, 8, 9, 10]. If multiple conflicting objectives exist, searching for the optimal results separately for each objective is not recommended. Konak et al. provide a brief description of GAs used for multi-objective optimization in [11]. They state that the optimal solution with respect to one objective will often result in an unacceptable result with respect to other objectives. The final solution will always be a trade-off between objectives; therefore, Pareto optimal solution sets are preferred. Other optimization algorithms successfully used in the field include particle swarm optimization and simulated annealing [12].

Environmental concerns coupled with constant demands to increase the green energy market share make high efficiency a rather desirable product property. Gearbox losses consist of bearing, seal and gear losses [13], which can be further divided into churning and frictional losses. Gearing efficiency is considered to be a function of the load normal to the gear tooth, sliding velocity, and friction coefficient [14]. Extensive theoretical research has been conducted on gear pair efficiency. Baglioni et al. analysed the differences in spur gear efficiency caused by different friction coefficient formulations [15]. The same authors also assessed variations in efficiency resulting from the changes in addendum modifications. Four often used methods of profile shift distribution have been assessed: design for balanced sliding, design for decreased noise, DIN 3992 method (balanced gears), and Maag guidelines (a compromise between strength and efficiency). The analysed guidelines can be found in the technical literature [16, 17]. Marques et al. [18] assessed the effects of using either a local or a constant friction coefficient value on the spur and the helical gear power losses. Two different load distribution models were presented. Power losses of spur gears with tip reliefs were studied by Diez-Ibarbia et al., who assessed the role of friction coefficient formulation [19] and load

sharing model [20] by using the method presented in [14]. Velex and Ville proposed using the displacements instead of the forces to formulate the problem, eliminating the requirement of a load distribution model [21]. Considering the friction coefficient, most of conducted studies utilize either the Niemann equation [17] or a formulation suggested by Hai Xu, based on a non-Newtonian thermal elastohydrodynamic lubrication model [22]. Li and Kahraman [23] proposed the transient, non-Newtonian, EHL model which accounted for the changes in contact parameters such as the normal force, the curvature radii, the surface velocities, and the slide-to-roll ratio. The influence of module and coefficient of addendum modification on power losses was experimentally evaluated by Naruse et al. [24]. They found that a higher gear module results in greater power losses due to friction at both the lower and higher loads. The surface quality effect was evaluated by Britton et al. who experimentally proved that superfinishing of gears will result in 30% lower temperatures [25]. Petry-Johnson et al. studied the spur gear spin and mechanical losses [26] by varying the gear module, lubricant properties, operating torque, rotational speed, and the number of teeth. The reported results were in agreement with [24].

Meshing stiffness, which affects both the gearing strength and efficiency, can be determined using both the analytical and the numerical approach. An analytical solution is often found by modelling the tooth as a cantilever beam. A low length-to-depth ratio implies that the Timoshenko beam theory will offer a smaller error compared to the Euler-Bernoulli theory [27]. When gears are concerned, differences between deflections calculated using these two theories differ by up to 40%. After finding the deflection, local deformations are included. A numerical approach using the finite element method (FEM) is frequently applied. Pedersen and Jørgensen used FEM to determine the stiffness of the individual gear teeth throughout the mesh [28]. However, even though FEM results are accurate, it is hard to draw general conclusions [29]. Simple approximate equations suitable for optimization purposes were proposed by Sanchez et al. [30]. The authors report a maximal error of 6% in the studied case. Lastly, an interesting approach was suggested by Raghuwanshi and Parey [31], who measured the spur gear mesh stiffness using a digital correlation technique.

In this article, as an extension of our previous study [32], the influence of spur gear pair parameters on the gearing efficiency and volume was researched. There are a large number of guidelines on how to distribute the addendum modifications across the pair [16, 17]. Since variations in the addendum modification cause changes in the sliding velocity, mesh stiffness, normal load, and the line of action length, the resulting efficiency values were assessed. The aim of the authors was to provide a basis for automated optimization, which will account for both the efficiency and volume. Since a multi-objective optimization was required, a non-dominated sorting genetic algorithm II (NSGA-II) was used [33]. The existing tooth root strength and surface durability calculations, load distribution expressions, and efficiency formulae are incorporated in the algorithm, which was then used to find the Pareto optimal solutions. As suggested by Konak et al. [11], a set of Pareto optimal solutions is better suited to practical problems then single solutions because it enables the designer to choose an objective trade-off. The number of teeth z_1 of the pinion, the gear face width b, the gear module m, and the pinion and wheel profile shift coefficients (x_1 and x_2) were also included as variables.

To finish off, the authors would like to point out that the dynamic transmission error (DTE) was not considered in this study. The main reason was the lack of applicable analytical solutions. To the best of our knowledge, most of the research is still conducted using the finite element method, which significantly increases the computational cost due to a sizeable initial population and the number of generations.

2. Method

The spur gear pair under consideration has to satisfy both the tooth root strength and surface durability conditions before being further investigated. The required expressions were found in the ISO 6336:2006 standard [1]. The genetic

Table 1
Datasets used in the optimization process

	Sets of input data		
	Set 1	Set 2	Set 3
T_1	100 Nm	30 Nm	250 Nm
n_1	960 min⁻¹	2850 min⁻¹	720 min⁻¹
i	3.55	4.5	2.8
K_A	1.6	1.25	1.2
IT grade	7	6	9
Material	Cf 53 (2)	14 Ni 6	51 CrMoV (1)
t_{st}	1 s	0.5 s	2 s
σ_{Flim}	275 N/mm²	430 N/mm²	275 N/mm²
σ_{Hlim}	1080 N/mm²	1500 N/mm²	650 N/mm²

Table 2
Boundary conditions and stress calculation factors

	Boundary conditions		
	Set 1	Set 2	Set 3
b		2…25 m	
m	2…8 mm	1…5 mm	6…20 mm
z_1		14…24	
x_1		0…x_{1max}	
x_2		-0.7…0.7	
	Values of stress calculation factors		
Y_{NT}	0.888	0.868	0.893
Z_{NT}	0.908	0.878	0.916
Z_L	1.026	1.02	1.038

algorithm with the variables z_1, b, m, x_1, and x_2 was then used to find the specimen with the highest fitness. A decrease in the number of digits will reduce the specimen redundancy in the initial population. Boundary conditions were set for each of the variables to avoid solutions that are non-feasible. In-depth explanations of the strength calculations and their integration in the genetic algorithm can be found in the previous study [32]. The optimization process was carried out on three sets of input data including the input torque T_1, the rotational speed n_1, the transmission ratio i, the application factor K_A, the IT quality grade, the starting time t_{st}, and the material strength properties. It should be noted that the parameters corresponding to the pinion have no index, while their wheel counterparts were indexed by 2. The boundary conditions and the datasets can be seen in *Table 1* and *Table 2*.

In a hypothetic case, transverse contact ratio of a spur gear pair must be greater than one. However, for the industrial applications, practical limit of 1.2 is recommended by AGMA. To ensure the necessary continuity of action, additional constraint (1) was included:

$$\varepsilon_\alpha - 1.2 \geq 0 \tag{1}$$

Lastly, this study is limited to the gears modelled as full steel discs. The centre distance has a non-standard value to enable more flexibility to the algorithm. Only profile alterations are due to addendum modifications; the tip relief and the profile modifications were not considered.

2.1. Efficiency calculation

Efficiency is defined as a degree to which a system is successful in producing a desired result, and can be calculated as a ratio between the useful and the invested energy. The total gearing losses can be load-dependent, such as losses due to friction, or load-independent (spin) losses caused by windage, oil churning, rotary seals, and bearings [26]. Since the load-independent losses are more prominent at high speeds, and were not considered in similar studies [14, 15, 34], their influence was not considered in order for the data to be comparable. For geared transmissions, load-dependent power losses are considered to be a function of the sliding velocity, the friction coefficient, and the normal load. The calculation was carried out according to (2), also used in [14, 35, 34], defining losses as:

$$P_{loss} = \frac{F_{bn}}{p_{et}} \int_{\psi_A}^{\psi_E} \frac{F_N(\psi)\mu(\psi)v_S(\psi)}{F_{bn}} \, d\psi \tag{2}$$

Both the load and sliding conditions change throughout the mesh. In this article, the coordinate ψ was used *(Figure 1)* in order to simplify the calculation and make it suitable for use in GA. Its value equals the pinion curvature radius at a given point. Instead of coordinate θ used for representing a position on the pitch line in [35], ψ was used to make the integration of (2) simpler. By using the linear coordinate ψ instead of the angular θ, the integral will contain polynomial instead of trigonometrical functions. The linear coordinate ψ extends along the pitch line, starting at point A and ending at point E. F_{Nmax} and F_{tmax} are the maximum contact force and the maximum tangential force, respectively. The normal force $F_N(\psi)$, the friction coefficient μ, and the sliding velocity $v_S(\psi)$ change along the line of action, influencing the losses. The tracking of power losses along the mesh is possible; Diez-Ibarbia et al. [14] used the instantaneous power loss factor H_{vinst} equal to the expression in the integral in (2).
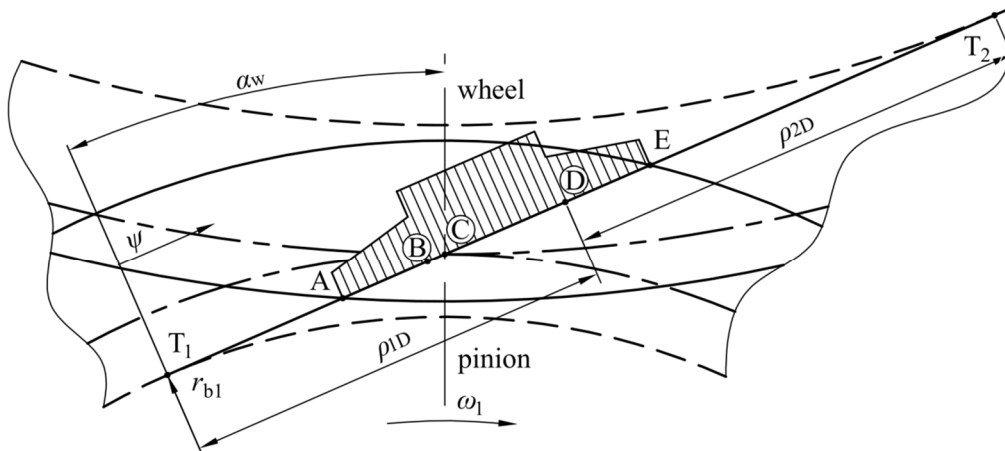
Figure 1
Position of coordinate ψ along the line of contact AE

Oil of ISO viscosity class VG 220, with density of $\rho_{oil} = 895$ kg/m³ and nominal viscosities of $v_{40} = 220$ mm²/s and $v_{100} = 17.5$ mm²/s [1]. Dynamic viscosity at 100 C° was $v_{d100} = 15.575$ mPa·s. The power constant b_1 was equal to 0.0651 since the lubricant base is mineral [36]. The mean surface roughness Ra was chosen according to the quality grade specified for each of the sets *(Table 1)*. The friction coefficient μ was assumed to be constant along the pitch line; it was calculated using the approximation done by Schlenk [34, 37]:

$$\mu_{\mathrm{m}} = 0.048 \cdot \left(\frac{F_{\mathrm{tb}}}{b \cdot v_{\Sigma C} \cdot \rho_{\mathrm{redC}}} \right)^{0.2} \cdot v_{\mathrm{d}}^{-0.05} \cdot R_{\mathrm{a}}^{0.25} \cdot \left(\frac{F_{\mathrm{tb}}}{b} \right)^{b_1}. \tag{3}$$

Sliding velocities along the line of contact were determined next. The sliding velocity at an arbitrary point was expressed as $v_s(\psi)$ and was calculated using the instructions from technical literature [38]:

$$v_{\mathrm{S}}(\psi) = (\omega_1 + \omega_2)\overline{MC} = 2\pi n_1 \left(1 + \frac{1}{i} \right)(\psi - r_{\mathrm{b1}} \tan \alpha_{\mathrm{w}}) \tag{4}$$

2.2. Load distribution

The finite element method used earlier [14] was replaced by approximate mesh stiffness equations (7) proposed by Sánchez et al. in [30]. The authors report a maximum error of 6%. The application of the same load distribution calculation for efficiency calculation was presented in [39]. The main reason for that was simplicity of the expression and its compatibility with the genetic algorithm. FEM was not suitable because of its computational cost since the running of all the combinations would significantly increase the optimization time. The load sharing ratio along the line of action R_{M} *(Figure 1)* is defined as:

$$R_{\mathrm{M}}(\xi) = \frac{F_{\mathrm{N}}(\xi)}{F_{\mathrm{Nmax}}}. \tag{5}$$

Profile parameter ξ is the ratio of the curvature radius at a given point to the circular base pitch [40]. To include the load sharing ratio in (7), it was written as $\xi = f(\psi)$. The ξ value for an arbitrary point M at the line of action is:

$$\xi = \frac{z_1 \psi}{\pi d_{\mathrm{b}}} = \frac{z_1 \tan(\alpha_{\mathrm{w}} + \theta)}{2\pi}. \tag{6}$$

Approximate load sharing equations from [30] written as $R_{\mathrm{M}} = f(\psi)$ using (6) were written as:

$$R_{\mathrm{M-AB}}(\psi) = 0.36 + \frac{0.28}{\varepsilon_\alpha - 1} \cdot \frac{z_1}{\pi d_{\mathrm{b}}}(\psi - \psi_{\mathrm{A}}); \qquad \psi_{\mathrm{A}} \leq \psi \leq \psi_{\mathrm{A}} + \frac{\pi d_{\mathrm{b}}(\varepsilon_\alpha - 1)}{z_1}$$

$$R_{\mathrm{M-BD}}(\psi) = 1; \qquad \psi_{\mathrm{A}} + \frac{\pi d_{\mathrm{b}}(\varepsilon_\alpha - 1)}{z_1} \leq \psi \leq \psi_{\mathrm{A}} + \frac{\pi d_{\mathrm{b}}}{z_1}, \tag{7}$$

$$R_{\mathrm{M-DE}}(\psi) = 0.36 - \frac{0.28}{\varepsilon_\alpha - 1} \cdot \left[\frac{z_1}{\pi d_{\mathrm{b}}}(\psi - \psi_{\mathrm{A}}) - \varepsilon_\alpha \right]. \quad \psi_{\mathrm{A}} + \frac{\pi d_{\mathrm{b}}}{z_1} \leq \psi \leq \psi_{\mathrm{A}} + \frac{\varepsilon_\alpha \pi d_{\mathrm{b}}}{z_1}.$$

ψ_{A} is the pinion curvature radius at the inner point of contact A:

$$\psi_{\mathrm{A}} = a_{\mathrm{w}} \sin \alpha_{\mathrm{w}} - \sqrt{r_{\mathrm{a2}}^2 - r_{\mathrm{b2}}^2}. \tag{8}$$

2.3. Final efficiency expressions

Combining the equations (2), (3), (7), and (8), one obtains the final formula for calculating the gearing efficiency. Once the pair geometry is known, losses depend on the parameter ψ, meaning that (2) can be easily integrated into the existing optimization process. If the lowest point of the single tooth contact (LPSC) B is positioned between the pitch point C and the highest point of single tooth contact (HPSC) D ($\psi_{\mathrm{B}} > \psi_{\mathrm{C}}$), a different formula is required. In such cases, due to the change in the sliding velocity direction at the pitch point C, losses will be calculated using (10). Integration intervals for $\psi_{\mathrm{C}} > \psi_{\mathrm{B}}$ (9) and $\psi_{\mathrm{B}} > \psi_{\mathrm{C}}$ (10) are written as:

$$P_{\text{loss}} = \frac{\mu_{\text{m}} F_{\text{Nmax}}}{m\pi \cos \alpha_{\text{w}}} \left[\int_{\psi_{\text{A}}}^{\psi_{\text{B}}} v_{\text{s}}(\psi) R_{\text{M-AB}}(\psi) d\psi + \int_{\psi_{\text{B}}}^{\psi_{\text{C}}} v_{\text{s}}(\psi) R_{\text{M-BD}}(\psi) d\psi + \atop + \int_{\psi_{\text{C}}}^{\psi_{\text{D}}} |v_{\text{s}}(\psi)| R_{\text{M-BD}}(\psi) d\psi + \int_{\psi_{\text{D}}}^{\psi_{\text{E}}} |v_{\text{s}}(\psi)| R_{\text{M-DE}}(\psi) d\psi \right]. \tag{9}$$

$$P_{\text{loss}} = \frac{\mu_{\text{m}} F_{\text{Nmax}}}{m\pi \cos \alpha_{\text{w}}} \left[\int_{\psi_{\text{A}}}^{\psi_{\text{C}}} v_{\text{s}}(\psi) R_{\text{M-AB}}(\psi) d\psi + \int_{\psi_{\text{C}}}^{\psi_{\text{B}}} |v_{\text{s}}(\psi)| R_{\text{M-AB}}(\psi) d\psi + \atop + \int_{\psi_{\text{B}}}^{\psi_{\text{D}}} |v_{\text{s}}(\psi)| R_{\text{M-BD}}(\psi) d\psi \int_{\psi_{\text{D}}}^{\psi_{\text{E}}} |v_{\text{s}}(\psi)| R_{\text{M-DE}}(\psi) d\psi \right]. \tag{10}$$

During the integration, the direction of the sliding speed $v_{\text{s}}(\psi)$ was always taken as positive to avoid negative losses:

$$|v_{\text{s}}(\psi)| = \begin{cases} 2\pi n_1 \left(1 + \dfrac{1}{i}\right)(\psi - r_{\text{b1}} \tan \alpha_{\text{w}}); & \psi = [\psi_{\text{A}}, \psi_{\text{C}}] \\ 2\pi n_1 \left(1 + \dfrac{1}{i}\right)(r_{\text{b1}} \tan \alpha_{\text{w}} - \psi); & \psi = [\psi_{\text{C}}, \psi_{\text{E}}] \end{cases} \tag{11}$$

Lastly, to verify the efficiency calculation presented in (9) and (10), the results obtained using these expressions were compared with the ones from the studies [14, 15, 26, 34] and also with expression (12) from [34]:

$$P_{\text{loss[29]}} = T_1 \cdot \omega_1 \cdot \mu_{\text{m}} \cdot \frac{\pi \cdot (i+1)}{z_1 \cdot i} \cdot (1 - \varepsilon_\alpha + \varepsilon_1^2 + \varepsilon_2^2) \tag{12}$$

Efficiency values from the studies [14, 15, 26, 34] were read from diagrams since numerical data were unavailable. From the data shown in *Table 3* one can see that (9) and (10) exhibit a lower relative difference when compared with (12) from [34], except in the comparison with Baglioni et al [14]. Hence, expressions (9) and (10) are suitable for further use.

2.4. Genetic algorithm

Genetic algorithm properties were identical to the ones used in the previous study [32] for the sake of easier comparison. An initial population of 500 individuals was used, with a mutation rate of 0.55. Each subsequent generation had two elite chromosomes. In that study, the largest result discrepancy in the fitness function value between the 30,000th and the 500th generation was 1.86%. In order to keep the computation time low and to provide quality results, in this study, 1,000 generations were calculated. To find the relation between the gear pair volume and its efficiency, both volume and efficiency were used as objective functions. The volume objective function f_1 is shown in [32] and it reads as follows:

Table 3
Comparison of efficiency values obtained using different calculation methods

		Petry-Johnson et al. [26]	Baglioni et al. [15]	Diez-Ibarbia et al. [14]	
Gear pair parameters	$z1, z2$	40, 40	18, 27	18. 36	18, 36
	$x1, x2$, mm	0, 0	0, 0	0, 0	0.5, -0.5
	m, mm	2.32	3	3	3
	b, mm	26.7	26.7	26.7	26.7
	α	28°	20°	20°	20°
	Ra, μm	0.05	0.8	0.8	0.8
Operating conditions	T, Nm	684	159	159	40
	n_1, min⁻¹	10000	3000	1500	6000
	v_{d}, mPa·s	34.7	50	10.6	10.6
Efficiency in a referenced study		0.9979	0.985 (method I) 0.981 (method II)	0.9941	0.994
Efficiency according to (9, 10)		0.9983	0.9922	0.9938	0.9938
Efficiency according to [34]		0.9985	0.9918	0.9935	0.9936

$$f_1 = V = \frac{\pi b}{4}(d_{a1}^2 + d_{a2}^2) \qquad\qquad (13)$$

The second objective function was found by calculating the gearing efficiency. Its calculation is modelled on [14, 35]. Load distribution calculation was adapted for the application in GA; thus, instead of the finite element method, approximate expressions developed by Sanchez et al. were used [30]. The final form of the efficiency objective function f_2 is equal to equations (9) or (10), depending on the position of LPSC.

Multi-objective optimization was conducted, resulting in a set of Pareto optimal (non-dominated) solutions. An overview and a comparison between different multi-objective genetic algorithms (MOGA) are shown in [11]. In this article we used the non-dominated search genetic algorithm II (NSGA-II), presented by Deb et al. [33]. NSGA-II is a well-tested and efficient algorithm, having a computational complexity of $O(MN^2)$, where M is the number of objectives and N the population size.

3. Results

Optimization using the NSGA-II was carried out for each of the sets. Number of fitness function evaluations was limited to 100,000. When compared to the single-objective optimization presented in the previous study [32], the computational cost has increased. Even though the computational time could be further reduced, it was not the aim of this study. Results are presented graphically in *Figures 2-4*. With the increase in the population size, a smaller number of Pareto optimal solutions were found, mostly due to their higher quality. It should be noted that the torque required to achieve the nominal working speed n_1 in time t_{st} was included in the calculations.

For the set 1 *(Figure 2)*, 389 sets of solutions were found. Results were spread out, with the lowest volume being $17.12 \cdot 10^5$ mm^3. The corresponding power losses of 54.43 W ($\eta = 0.9946$) were the highest, meaning that the minimum volume yields a significant increase in losses. Solutions at the other end of the spectrum were evaluated next; if results with the highest efficiency were used, the volume would increase significantly. For this reason, solutions with the extreme volumes were discarded, with the limit set on the volume of $50 \cdot 10^5$ mm^3. The highest volume observed, i.e. $50 \cdot 10^5$ mm^3, was associated with the lowest losses, i.e. 37.39 W ($\eta = 0.9963$).

Set 2 results *(Figure 3)* follow the same rule, showing a trade-off between the power losses and volume reduction. Two hundred and eighty-six Pareto optimal solutions were found. Achieving the minimum volume will increase the transmission power losses. A volume of $32.26 \cdot 10^4$ mm^3 results in a loss of 50.83 W ($\eta = 0.9944$). At the other end of the spectrum, in a similar way as in set 1, the volume was limited to 10^6 mm^3 *(Figure 3)*, resulting in a power loss of 34.59 W ($\eta = 0.9961$). This means that a 3.1 times bigger increase in volume yields only a 31.9% decrease in power losses.

Results obtained for the set 3 are limited to the volume of $50 \cdot 10^6$ mm^3. Four hundred and thirteen solutions were found, with the lowest achieved volume of $20.41 \cdot 10^6$ mm^3 and an accompanying loss of 100.8 W ($\eta = 0.9946$). By increasing the volume to the upper observed limit, losses fall to 67.23 W ($\eta = 0.9964$), meaning that a 33.3% decrease in power losses will increase the volume 2.45 times.
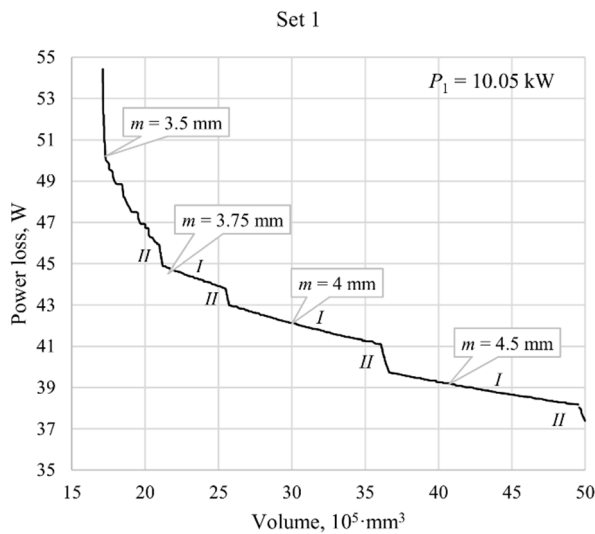
Figure 2
Optimization results (Pareto optimal solutions) for set 1
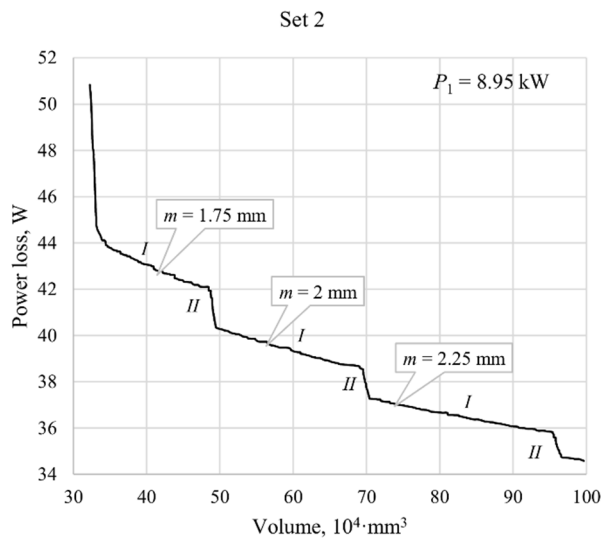
Figure 3
Optimization results (Pareto optimal solutions) for set 2
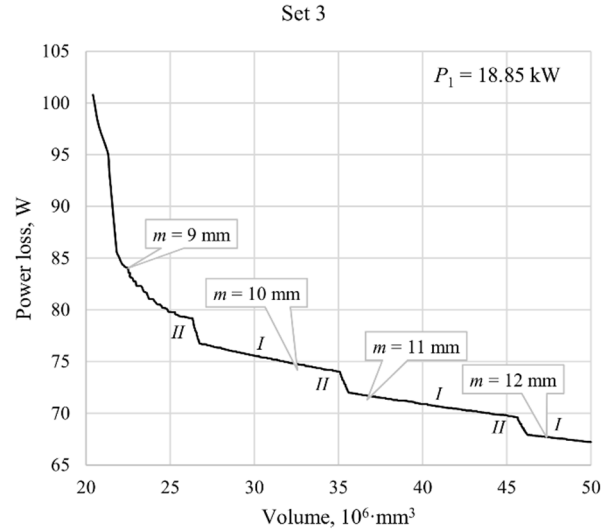
Figure 4
Optimization results (Pareto optimal solutions) for set 3

Such results for all the three sets confirm that the trade-off between the volume and efficiency is necessary in the design of spur gear pairs.

4. Discussion

All the datasets exhibited similar behaviour. With an increase in volume, occasional sharp declines in power losses were found. Two repeating intervals were identified; the first ones having the low inclination with respect to the horizontal axis (labelled *I* in *Figures 2-4*) and the second, steeper ones, connecting two neighbouring lower inclination areas (labelled *II*). Exceptions were solutions with the lowest volumes.

Low inclination intervals *(I)* were caused by the gear module changes. Since the modules are standardized, discrete changes in the module result in discrete changes in power losses. The gear module changes are shown in *Figures 2-4*. Even though both Naruse et al. [24] and Petry-Johnson et al. [26] reported that losses due to friction increase with the module size, in the observed cases, lower modules resulted in bigger losses. The main cause of that was the operating torque T_1, which caused an increase in the normal load F_N as the values of the module m and the working diameter d_{w1} fell. A slower, gradual decrease in power losses along the horizontal axis was caused by variations in the face width *(Figure 5a)*. When analysing the face width values b, solutions followed a rule found in our previous study [32]. All the solutions gravitated towards the lower width boundary ($b_{min} = 6 \cdot m$). An increase in the face width decreases power losses, which is in agreement with the statements presented by Michaelis et al. in [13]. Also, it should be added that pairs with higher volumes will have higher durability due to increases in the values of module and width, but such pairs can be considered oversized.

Steeper intervals *(II)* display a substantial power loss reduction combined with a small increase in volume. The main cause is an increase in the value of the wheel profile shift coefficient x_2 *(Figure 5b)*. As x_2 increases, the wheel addendum diameter d_{a2} and, consequently, the volume increase. On the other hand, an increase in x_2 results in an increase in the pressure angle α_w, leading to a fall in the transverse contact ratio ε_α. Even though a decrease in the value of ε_α has a detrimental effect on load distribution, it also shortens the line of action AE and friction coefficient value (as shown in [41]), thus reducing the losses in the process. Negative influence of ε_α on the transmission efficiency was also found in [20]. Furthermore, our results are in agreement with other studies; both Baglioni et al. [15] and Diez-Ibarbia et al. [14] observed the influence of addendum modification on the gearing efficiency. The low positive x_1 value was initially beneficial, but after approximately 0.1, it started to adversely affect the efficiency. Since the efficiencies were observed only for the case of $x_1 = - x_2$, we estimated the influence of x_1 and x_2 on the efficiency using the formulae (9) and (10). For the observed case (similar to set 2 solutions), results have shown that increasing the wheel profile shift coefficient x_2, combined with a positive x_1 result in higher efficiency *(Figure 6)*. Negative x_1 significantly decreases the efficiency. Lastly, x_1 is always chosen from the upper end of the spectrum ($x_{1max} = 0.7$), confirming the results of the previous study conducted by by Magalhes et al. [42]. Magalhes et al. found that a significant increase in addendum modification coefficient, when coupled with a higher number of teeth and lower gear module, results in a reduction of power losses. Same results were reported by Pleguezuelos et al. [43] after studying the influence of design parameters on the spur gear pair efficiency.
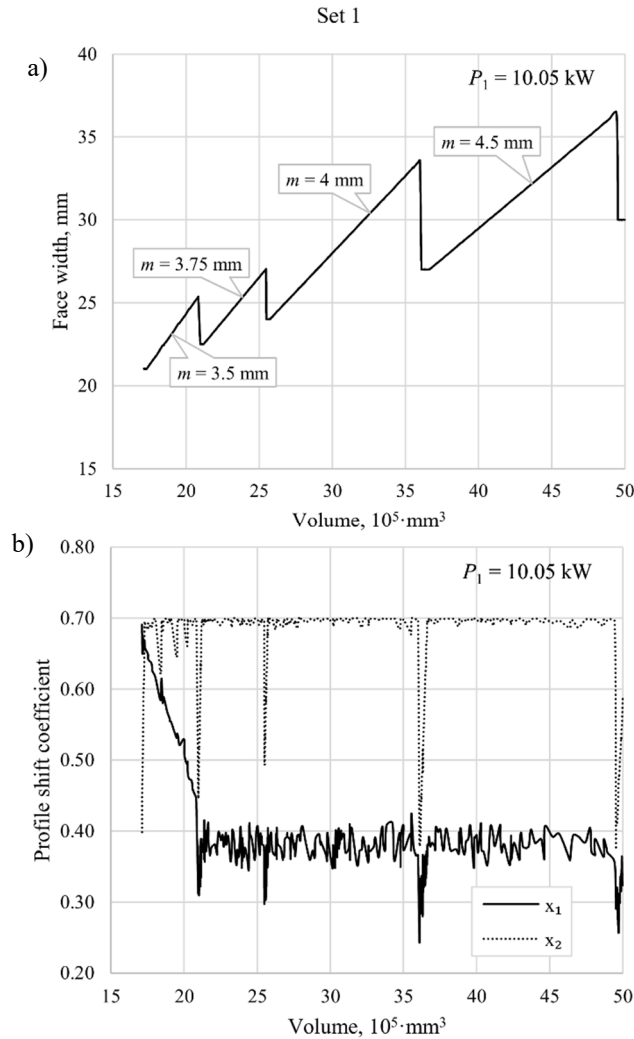
Figure 5
Relation between a) the face width *b* and the volume; b) the profile shift coefficients and the volume

To conclude, *Figure 5a* and *Figure 5b* prove that the wheel addendum modification was responsible for the steeper intervals, while the lower inclination intervals were caused by the face width. Lower x_2 values causing steeper intervals are in agreement with the dependence of losses on the addendum modification shown in *Figure 6*; they caused a sharp increase in losses while providing a small volume decrease.

Considering the number of teeth of the pinion and the wheel in set 1, the algorithm tended to choose the highest value for all the Pareto optimal cases, 24 for the pinion and 85 for the wheel. A similar thing happened with sets 2 (pinion 24, wheel 108) and 3 (pinion 24, wheel 67). Few set 3 solutions chose 22 for the pinion and 63 for the wheel number of teeth. Those are the solutions causing the deviations in the set 3 leftmost area *(Figure 4)*. Deviations in the lowest volumes occurred for all the three sets. Those deviations were caused by an increase in the pinion profile shift coefficient, whose value increased to 0.7 from 0.35-0.4 used for the other solutions *(Figure 5b)*. Thicker teeth enabled the use of a smaller module, thus further increasing the volume at the price of higher power losses. It should be noted that, besides the gear profile geometry modifications, the use of larger number of teeth, and smaller modules is characteristic for low-loss gears proposed by Höhn et al. in [44].

As for power losses and volume reduction, most viable solutions are the ones at the right end of intervals *II*. For set 1, three such solutions are known: with modules of 3.75, 4, and 4.5 mm. The final solution can be chosen based on the desired volume-power loss ratio.
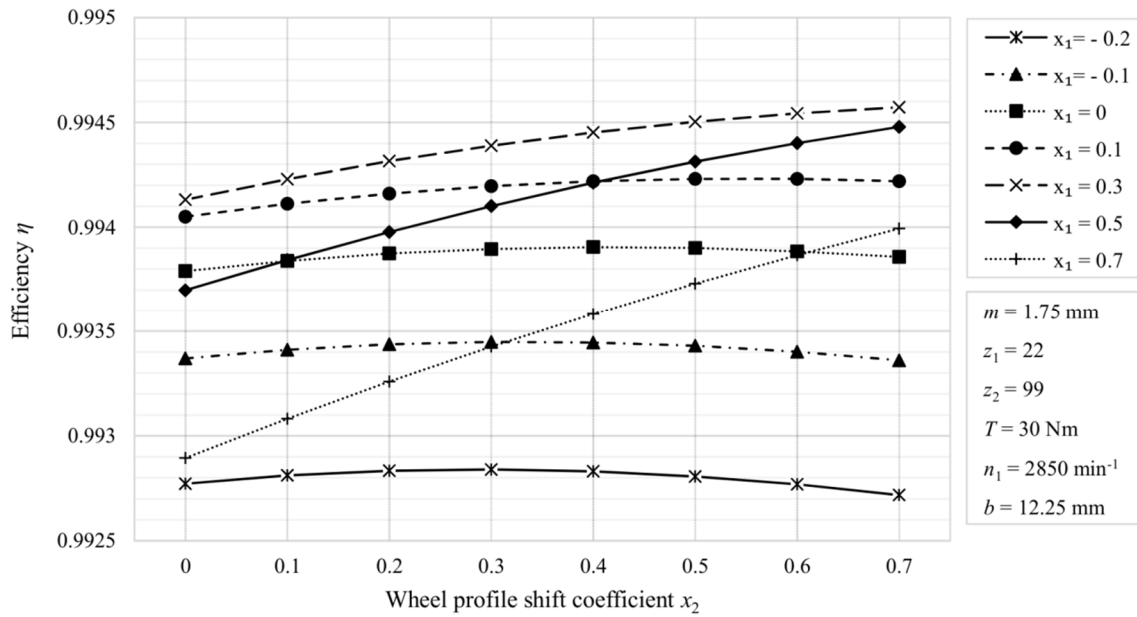
Figure 6
Influence of the addendum modifications x_1 and x_2 on the gearing efficiency η obtained by using (9) and (10)

5. Conclusion

Multi-objective spur gear pair optimization was conducted, with high efficiency and a reduction in volume as objectives. Optimization variables included the gear module, face width, number of teeth (pinion), and the profile shift coefficients of both gears. Efficiency was calculated using the analytical calculation method which accounted for the load distribution along the line of action. The said method was presented in detail, and its results were compared to the ones obtained by other authors. To calculate the pair volume, addendum diameters were used to account for the addendum modifications.

Based on the optimization results of three datasets, the authors observed the following:
- increase in the gear module m size results in a lower power loss.
- increase in the wheel profile shift coefficient x_2 significantly decreases power losses when combined with the positive pinion profile shift coefficient x_1.
- solutions with the lowest volumes tend to have the highest pinion profile shift coefficient x_1,
- increase in the pair width causes limited decreases in power losses, while significantly increasing the volume,
- all the sets converged towards a larger number of teeth of the pinion z_1, which was limited ($z_{1max} = 24$).

As a broad guideline, choosing the low width, a large number of teeth of the pinion, and positive profile shift coefficients to decrease the line of action length will yield good results with respect to the volume and efficiency.

Lastly, simplifications have been made. Dynamic transmission error (DTE) was not considered, since its calculation requires the use of FEM, which was not compatible with the selected optimization algorithm. FEM would drastically increase the complexity and computational cost due to a large initial population and number of generations. Suitable analytical solutions have not been found in literature. Furthermore, DTE would surely influence the load distribution along the line of action. In the future, inclusion of manufacturing errors in the optimization process would result in an optimization process with three objectives, volume, efficiency, and noise; this would enable finding solutions that offer a good balance of the three.

Nomenclature

b : face width, mm
b_1 : power constant
d_{a1} : addendum diameter (pinion), mm
d_{a2} : addendum diameter (wheel), mm
F_{tb} : normal load, N
F_N : circumferential force at base circle, N

i	: transmission ratio
K_A	: application factor
m	: gear module, mm
n_1	: rotational speed (pinion), s^{-1}
P	: transmitted power, W
P_{loss}	: power loss, W
p_{et}	: transverse base pitch, mm
Ra	: arithmetic mean roughness, μm
R_m	: load sharing ratio along the line of action
T_1	: input torque, Nm
t_{st}	: starting time, s
v	: pitch line velocity, m/s
v_d	: dynamic oil viscosity, mPa·s
v_s	: sliding velocity, m/s
$V_{\Sigma C}$	: sum velocity, m/s
x_1	: profile shift coefficient (pinion)
x_{1max}	: maximal allowable profile shift coefficient (pinion)
x_2	: profile shift coefficient (wheel)
Y_{NT}	: life factor for tooth root stress for reference test conditions
Z_L	: lubricant factor
Z_{NT}	: life factor for contact stress for reference test conditions
z_1	: number of teeth (pinion)
z_2	: number of teeth (wheel)
α_w	: operating pressure angle, rad
ε_1	: tip contact ratio of the pinion
ε_2	: tip contact ratio of the pinion
ε_α	: transverse contact ratio
η	: efficiency
μ_m	: friction coefficient
ζ	: involute profile parameter [30, 40]
ρ_{redC}	: reduced radius of curvature (point C), mm
σ_{Flim}	: nominal stress number (bending), N/mm^2
σ_{Hlim}	: nominal stress number (contact), N/mm^2
θ	: rotation angle, rad
ψ_i	: curvature radius at point i on the line of action, mm

Acknowledgement

References

[1] ISO Standard 6336:2006, *Calculation of load capacity of spur and helical gears,* Geneva, Switzerland: International Organization for Standardization, 2006.

[2] A. 2001--D04, *Fundamental Rating Factors and Calculation Methods for Involute Spur and Helical Gear Teeth,* Alexandria: American Gear Manufacturers Association, 2004.

[3] J.-L. Marcelin, "Genetic optimisation of gears," *International Journal of Advanced Manufacturing Technology,* vol. 17, no. 12, pp. 910-915, 2001.

[4] J.-L. Marcelin, "Using genetic algorithms for the optimization of mechanisms," *Int J Adv Manuf Technol,* vol. 27, pp. 2-6, 2005.

[5] T. Yakota, T. Taguchi and M. Gen, "A solution method for optimal weight design problem of the gear using genetic algorithms," *Computers & Industrial Engineering,* vol. 35, no. 3-4, pp. 523-526, 1998.

[6] G. Bonori, M. Barbieri and F. Pellicano, "Optimum profile modifications of spur gears by means of genetic algorithms," *Journal of Sound and Vibration,* vol. 313, no. 3-5, pp. 603-616, 2008.

[7] C. Gologlu and M. Zeyveli, "A genetic approach to automate preliminary design of gear drives," *Computers and Industrial Engineering,* vol. 57, no. 3, pp. 1043-1051, 2009.

[8] N. Marjanovic, B. Isailovic, V. Marjanovic, Z. Milivojevic, M. Blagojevic and M. Bojic, "A practical approach to the optimization of gear trains with spur gears," *Mechanism and Machine Theory,* vol. 53, pp. 1-16, 2012.

[9] F. Mendi, T. Baskal, K. Boran and F. E. Boran, "Optimization of module, shaft diameter and rolling bearing for spur gear through genetic algorithm," *Expert Systems with Applications,* vol. 37, no. 12, pp. 8058-8064, 2010.

[10] L. Tudose, O. Buiga, C. Ştefanache and A. Sóbester, "Automated optimal design of a two-stage helical gear reducer," *Structural and Multidisciplinary Optimization,* vol. 42, no. 3, pp. 429-435, 2010.

[11] A. Konak, D. W. Coit and A. E. Smith, "Multi-objective optimization using genetic algorithms: A tutorial," *Reliability Engineering and System Safety,* vol. 91, pp. 992-1007, 2006.

[12] V. Savsani, R. V. Rao and D. P. Vakharia, "Optimal weight design of a gear train using particle swarm optimization and simulated annealing algorithms," *Mechanism and Machine Theory,* vol. 45, no. 3, pp. 531-541, 2010.

[13] K. Michaelis, B. Höhn and M. Hinterstoißer, "Influence factors on gearbox power loss," *Industrial Lubrication and Tribology,* vol. 63, no. 1, pp. 46-55, 2011.

[14] A. Diez-Ibarbia, A. Fernandez del Rincon, M. Iglesias, A. de-Juan, P. Garcia and F. Viadero, "Efficiency analysis of spur gears with a shifting profile," *Meccanica,* vol. 51, no. 3, pp. 707-723, 2016.

[15] S. Baglioni, F. Cianetti and L. Landi, "Influence of the addendum modification on spur gear efficiency," *Mechanism and Machine Theory,* vol. 49, pp. 216-233, 2012.

[16] Maag Gear Company Ltd., Maag gear book: calculation and practice of gear, gear drives, toothed couplings and synchronous clutch couplings, Zurich, Switzerland: Maag Ltd., 1990.

[17] G. Niemann and H. Winter, Maschinenelemente - Band 2, Berlin, Germany: Springer-Verlag, 2003.

[18] P. M. T. Marques, R. C. Martins and J. H. O. Seabra, "Power loss and load distribution models including frictional effects for spur and helical gears," *Mechanism and Machine Theory,* vol. 96, pp. 1-25, 2016.

[19] A. Diez-Ibarbia, A. del Rincon, M. Iglesias, A. de Juan, P. Garcia and F. Viadero, "Frictional power losses on spur gears with tip reliefs: The friction coefficient role," *Mechanism and Machine Theory,* vol. 121, pp. 15-27, 2018.

[20] A. Diez-Ibarbia, A. Fernandez-del-Rincon, A. de-Juan, M. Iglesias, P. Garcia and F. Viadero, "Frictional power losses on spur gears with tip reliefs. The load sharing role," *Mechanism and Machine Theory,* vol. 112, pp. 240-254, 2017.

[21] P. Velex and F. Ville, "An Analytical Approach to Tooth Friction Losses in Spur and Helical Gears - Influence of Profile Modifications," *Journal of Mechanical Design,* vol. 131, no. 10, p. 101008, 2009.

[22] H. Xu, Development of a generalized mechanical efficiency prediction methodology for gear pairs. PhD thesis, Columbus: The Ohio State University, 2005.

[23] S. Li and A. Kahraman, "A Transient Mixed Elastohydrodynamic Lubrication Model for Spur Gear Pairs," *Journal of Tribology,* vol. 132, no. 1, p. 011501, 2010.

[24] C. Naruse, S. Haizuka, R. Nemoto and K. Kurokawa, "Studies on Frictional Loss, Temperature Rise and Limiting Load for Scoring of Spur Gear," *Bulletin of JSME,* vol. 29, no. 248, pp. 600-608, 1986.

[25] R. D. Britton, C. D. Ecolate, M. P. Alanou, H. P. Evans and R. W. Snidle, "Effect of Surface Finish on Gear Tooth Friction," *Journal of Tribology,* vol. 122, no. 1, pp. 354-360, 2000.

[26] T. T. Petry-Johnson, A. Kahraman, N. E. Anderson and D. R. Chase, "An experimental investigation of spur gear efficiency," *Journal of Mechanical Design,* vol. 130, no. 6+, p. 62601, 2008.

[27] F. Romano, "Deflections of Timoshenko Beam with Varying Cross-Section," *International Journal of Mechanical Science,* vol. 38, no. 8-9, pp. 1017-1035, 1996.

[28] N. L. Pedersen and M. F. Jørgensen, "On gear tooth stiffness evaluation," *Computers and Structures,* vol. 135, pp. 109-117, 2014.

[29] M. B. Sánchez, M. Pleguezuelos and J. I. Pedrero, "Enhanced model of load distribution along the line of contact for non-standard involute external gears," *Meccanica,* vol. 48, no. 3, pp. 527-543, 2013.

[30] M. B. Sanchez, M. Pleguezuelos and J. I. Pedrero, "Approximate equations for the meshing stiffness and the load sharing ratio of spur gears including hertzian effects," *Mechanism and Machine Theory,* vol. 109, no. September 2016, pp. 231-249, 2017.

[31] N. K. Raghuwanshi and A. Parey, "Experimental measurement of spur gear mesh stiffness using digital image correlation technique," *Measurement,* vol. 111, pp. 93-104, 2017.

[32] D. Miler, A. Lončar, D. Žeželj and Z. Domitran, "Influence of profile shift on the spur gear pair optimization," *Mechanism and Machine Theory,* vol. 117, pp. 189-197, 2017.

[33] K. Deb, A. Pratap, S. Agarwal and T. Meyarivan, "A fast and elitist multiobjective genetic algorithm: NSGA-II," *IEEE Transactions on Evolutionary Computation,* vol. 6, no. 2, pp. 182-197, 2002.

[34] B. R. Höhn, "Improvements on noise reduction and efficiency of gears," *Meccanica,* vol. 45, no. 3, pp. 425-437, 2010.

[35] A. Diez-Ibarbia, A. Fernandez del Rincon, M. Iglesias, A. De Juan, P. Garcia and F. Viadero, "Efficiency analysis of shifted spur gear transmissions," *New Trends in Mechanism and Machine Science,* no. 24, pp. 373-381, 2015.

[36] R. Martins, J. Seabra, A. Brito, C. Seyfert, R. Luther and A. Igartua, "Friction coefficient in FZG gears lubricated with industrial gear oils: Biodegradable ester vs. mineral oil," *Tribology International,* vol. 39, pp. 512-521, 2006.

[37] L. Schleng, Untersuchungen zur Freßtragfähigkeit von Großzahnrädern. PhD thesis., Frankfurt/Main, Germany: TU München, 1995.

[38] S. P. Radzevich, Dudley's handbook of practical gear design and manufacture, Boca Raton: Taylor & Francis Group, 2012.

[39] J. I. Pedrero, M. Pleguezuelos and M. B. Sanchez, "Study of the influence of the design parameters on the efficiency of spur gears," in *International gear conference 2014 - Conference Proceedings*, Lyon Villeurbanne, France, 2014.

[40] J. I. Pedrero, P. Miguel, M. Artés and J. A. Antona, "Load distribution model along the line of contact for involute external gears," *Mechanism and Machine Theory,* vol. 45, no. 5, pp. 780-794, 2010.

[41] A. Diez-Ibarbia, A. Fernandez-Del-Rincon, P. Garcia, A. De-Juan, M. Iglesias and F. Viadero, "Assessment of load dependent friction coefficients and their influence on spur gears efficiency," *Meccanica,* vol. 53, no. 1-2, pp. 425-445, 2018.

[42] L. Magalhes, R. Martins, C. Locateli and J. Seabra, "Influence of tooth profile and oil formulation on gear power loss," *Tribology International,* vol. 43, no. 10, pp. 1861-1871, 2010.

[43] M. Pleguezuelos, J. I. Pedrero and M. B. Sánchez, "Analytical expression of the efficiency of involute spur gears," *Mathematical Problems in Engineering,* vol. 2013, 2013.

[44] B.-R. Hőhn, K. Michaelis and A. Wimmer, "Low Loss Gears," *Gear Technology,* vol. 24, no. June, pp. 28-35, 2007.

Paper III

Optimisation of polymer spur gear pairs
with experimental validation

Daniel Miler[1*], Matija Hoić[1], Stanko Škec[12] and Dragan Žeželj[1]

[1] *Faculty of Mechanical Engineering and Naval Architecture, University of Zagreb, 10002 Zagreb, Ivana Lučića 5, Croatia*
[2] *Technical University of Denmark, Anker Engelunds Vej 1, 2800 Kongens Lyngby, Denmark*

Abstract

This research study aims to present a procedure for optimisation of polymer gear pairs, along with the rough guidelines for their design. Multi-objective optimisation of polymer spur gear pairs was carried out using the gear pair module, face width, pinion number of teeth, and both the pinion and wheel profile shift coefficients as design variables. Two objective functions were used to rate the designs – overall volume and frictional power losses. Compared to well-researched steel gear pair optimisation, additional boundary conditions were necessary: tooth flank and root temperatures, abrasion wear, and tooth addendum displacement. Two arbitrary datasets were used as examples, each made of polyoxymethylene. For each of the sets, a Pareto optimal solution was manufactured, enabling the experimental validation using an open-circuit experimental rig. As no literature was found on the polymer gear pair optimisation, results were compared to ones for steel gear pairs. The results have shown that there are distinct differences when determining the values of geometric parameters; lower volume pairs made of polymer had greater face widths, while the opposite was observed in steel gears. The differences between the analytical and experimental results were up to 21%, suggesting that the results are in agreement.

Keywords: Polymer gears; POM; Design guidelines; Gear pair optimisation; Power losses; Experimental study.

---

1. Introduction

The literature on gear pair calculation and design is plentiful, however, most of the studies are focused on steel gears due to their wide range of applicability. The steel gears are robust and able to transmit large torques while retaining high efficiency and compact design. For these reasons, they are one of the indispensable components in industrial transmissions, more specifically automotive and aerospace industry, and energy generation, among others [1]. Additionally, use of steel gears in food processing and pharmaceutical industries is possible, but additional care is advised due to extensive regulation; toxic greases or oils are most frequently used lubricants.

Besides the steel gears, their polymer counterparts are rapidly rising in popularity. Their ability to work without lubrication, low manufacturing price, low weight, and a high potential for serial production make them an suitable choice for the design of various products, for example, household appliances [2]. The downside of polymer gears is the inherent degradation of their mechanical properties as the temperature increases [3]. The local increase in the temperature is more prominent due to the low thermal conductivity (i.e. are thermal insulators) of polymer materials. To predict the bulk and flash temperature in polymer gears, Fernandes et al. [4] have developed a thermal model, validated using the available experimental results. Roda-Casanova and Sanchez-Marin [5] proposed a universal approach to determine the temperature field of polymer spur gears, meaning that the proposed approach is applicable to spur gears regardless of material or geometry. The proposed approach should, however, be carefully applied to gear pairs of a larger face width, since the 2D finite element method was used to develop it. As the vast majority of the heat in the point of contact is generated by friction [5], a reduction in frictional power losses would reduce the degradation of the material properties of polymer gears.

Various studies on applicability of polymers as gear materials have been conducted, mostly focused on the failure modes. Singh et al. [6] assessed the potential of three different polymers as gearing materials. Polyoxymethylene (POM) was found to be more durable then acrylonitrile butadiene styrene (ABS) and high-density polyethylene (HDPE). After investigating the thermal and wear behaviour, the authors have found that, when compared to rotational speed, operational torque has seven to eight times greater influence on the surface temperature. Duhovnik et al. [2] carried out an experimental study on the effect of profile shape on polymer gear pair properties, revealing the different gear failure modes. The gears failed due to fatigue at lower loads, and due to the temperature at higher loads. Additionally, polymer gears are highly sensitive to the number of load cycles. Differences between the temperatures calculated according to the VDI 2736 [7] guidelines and experimentally recorded ones were found. Kalin and Kupec [8] formulated the S-N curves at different temperatures and loading, confirming the adverse effect of temperature on

---

fatigue life.

When discussing the efficiency of polymer gear pairs, Walton et al. [9,10] assessed the influences of material and tooth geometry on the efficiency of cylindrical plastic gears. An experimental rig was developed, aiming to evaluate efficiencies and determine the friction coefficients depending on the geometry and material. The authors concluded that coefficients of friction are higher in the low-module gears and at higher sliding velocities. Kirupasankar et al. [11] evaluated the transmission efficiency of polyamide nanocomposite spur gears by using the numerical methods supplemented by experimental verification. The detrimental effect of torque on the gear pair efficiency was detected. Such finding implies that friction coefficient in polymer gear pairs is dependent on the normal load, which is in agreement with the previous study by the authors [12]. It must be noted that Kirupasankar et al. [11] used the friction coefficient formulation proposed by Schlenk [13], which is developed using the steel gear pairs, while the frictional power losses were evaluated using the expressions for frictional heat generation proposed by Koffi et al. [14],

No specific guidelines relating the desired transmission criteria, such as low volume or low power losses, and required geometry of polymer gear pairs have been found during the literature review. At the same time, many studies on optimisation of steel gears were carried out. For this reason, studies on steel gear pair optimisation were used as a basis in the development of polymer gear pair optimisation process. In steel gear optimisation, the volume (or weight) is the most frequently used objective function [15–20], with efficiency being in the second place [21]. Yokota et al. [15] and Marcelin [16] assessed the performance of a genetic algorithm when solving an optimal gear weight design problem. Savsani et al. [19] have compared the performances of the genetic algorithm, simulated annealing, and particle swarm optimisation when optimising gear pairs. Even though the particle swarm optimisation had performed better, the genetic algorithm remains the most frequently used within the field. Gologlu and Zeyveli [17] have attempted to automate the preliminary design of two-stage helical gearbox. The work was continued by Tudose et al. [18], who extended the objective function to include the shaft, bearings, and housings. Finally, Miler et al. [21] have conducted a multi-objective optimisation of steel spur gear pairs using the pair volume and power losses as optimisation criteria.

Building on the previously published work, in this article, we carried out the optimisation of polymer gear pairs, aiming to discern trends which could be a stepping stone in formulating the design guidelines. Additionally, the optimisation process was outlined in detail, as its formalisation could increase the quality of polymer gear transmissions. To the best of our knowledge, no similar research studies have been conducted. Similarly to [21], the multi-objective optimisation process was conducted using volume and power losses as objective functions. The most significant differences were found in friction coefficient formulation and additional, polymer-specific, constraints. In preparation for the study at hand, the experimental study [12] has been carried out to find an expression for the prediction of friction coefficient in polyoxymethylene gears lubricated using a solid lubricant (PTFE). The analytical results presented within this study are also verified experimentally, and the detected trends are compared to ones found in gear pairs made of steel.

2. Method

The study of the relationship between the transmission features and geometric parameters of polymer gear pair, such as the gear module, the face width, the number of teeth, and the addendum modifications was carried out using the multi-objective optimisation. This research study consists of two segments – analytical and experimental. The task of the former is to determine the optimal (or near-optimal) solutions, while the latter is used to validate them. The research method is presented on Figure 1.
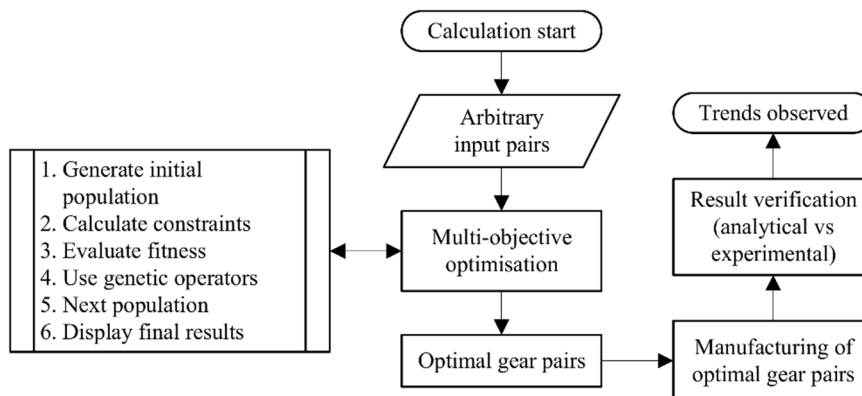
Figure 1 – Research flowchart

The optimisation problem (analytical segment) is formulated using the five-step procedure proposed by Arora [22]. The first two steps, problem description and data/information collection, are covered within the literature review

presented in the introduction section. The design variables are defined in the third step and shown in Section 2.1, while the optimisation criteria (fourth step), expressed as objective (fitness) functions, are derived in Section 2.2. The constraints necessary to ensure a functional and industrially viable solution (fifth step) are outlined in Section 2.3. Once the problem was formalised, an algorithm suitable for solving it was selected (see Section 2.4).

An experiment was then carried out to validate the analytical results. For detailed rig description, see Section 2.5, and for additional photographs and videos, see supplemental data. The gear pairs found using the optimisation process were manufactured to enable a comparison of calculated and measured objective function values. Lastly, the assessment of bearing power losses was required to isolate the gear pair power losses from the overall measured values (see Section 2.6).

Two sets of input parameters were used to carry out the optimisation process (Table 1). The gears were made of polyoxymethylene (POM), a polymer often used in gear manufacturing [7]. As operational torque T [Nm] and rotational speed n_1 [min^{-1}] were shown to have a significant influence on the surface temperature [2] and efficiency [11], their values were varied. Application factor K_A was chosen according to the ISO 6336:2006 [23] standard. Lastly, the standard values of transmission ratios were used.

The load calculation constants were selected from VDI 2736 guidelines [7]. The gears were lubricated with solid lubricant; polytetrafluorethylene (PTFE). Gear flank and root heat transfer coefficients $k_{9,Flank}$ and $k_{9,Root}$ were also taken as advised in the VDI 2736. Housing heat transfer resistance $R_{\lambda,G}$ value was 0, since housing was open. Poisson coefficient was assumed to be constant, $\nu = 0.4$.

Table 1 – Example gear pairs (input data chosen arbitrary)

	Parameter		Set 1	Set 2
Input data	Material	-	POM	
	Operational torque (input)	T / Nm	14	12
	Rotational speed (pinion)	n_1 / min^{-1}	750	1000
	Transmission ratio	i	2	3.18
	Application factor	K_A	1.2	1.25
Constants	Lubrication	-	Solid lubricant (PTFE)	
	Heat transfer coefficient (flank)	$k_{9,Flank}$	9000 K·(m/s)$^{0.75}$mm$^{1.75}$/W	
	Heat transfer coefficient (root)	$k_{9,Root}$	2100 K·(m/s)$^{0.75}$mm$^{1.75}$/W	
	Heat transfer resistance (housing)	$R_{\lambda,G}$	0	
	Ambient temperature	ϑ_0	20 °C	
	Relative duty cycle (over 10 min period)	ED	100%	
	Wear coefficient (POM/POM)	k_w	60.4 · 10^{-8}mm^3/(Nm)	
	Safety factor (flank)	S_F	1.1	
	Safety factor (root)	S_H	1.3	

2.1. Definition of design variables

As the aim is to increase the quality of polymer spur gear pairs without the need for additional machining operations, the design variables were selected accordingly. Only variables required to describe the basic ("macro") geometry were considered. Thus, micro-geometry modifications such as tooth tip relief or crowning were not considered.

The studies on optimisation of steel gears by other authors were analysed, and an overview is presented in Table 2. Based on the literature review, gear module m [mm], pair face width b [mm], pinion number of teeth z_1 [-], and pinion and wheel profile shift coefficients x_1 [-] and x_2 [-] were selected as design variables. The important task was to determine whether the profile shift coefficients should be used as there was no consensus. Some authors included the profile shift coefficients [18,24], whereas others disregarded them [15,17,19,25]. Since the authors previously confirmed [20] that x_1 and x_2 indeed have a major influence on results, they were included as design variables. The helix angle β was not considered as the study at hand is focused on spur gears ($\beta = 0°$). The design variable vector is written as:

$$x = (m, b, z_1, x_1, x_2). \tag{1}$$

Table 2 – The aims, algorithm types and properties of studies on gear pair optimisation (steel gears)

Authors	Algorithm	Aim	Objective	Design variables
Yokota et al. [15], 1998.	GA	To determine whether the GA is suitable for solving the optimal gear weight design problem (one-stage).	$f(x) = G$	$x = [m, z_i, b]$
Marcelin [16], 2001.	GA	To examine the possibility of using the genetic algorithm for solving the one-stage gear design problem.	$f(x) = V$	$x = [m, z_i, x_i, \beta]$
Gologlu and Zeyveli [17], 2009.	GA	To automate the preliminary design of a two-stage helical gear train.	$f(x) = V$	$x = [m^{(i)}, z^{(i)}, b^{(i)}]$
Tudose et al. [18], 2010.	GA	To optimize the two-stage helical gear transmission design problem, including shafts, bearings, and housing.	$f(x) = G$	$x = [m^{(i)}, z^{(i)}, x^{(i)}, \beta^{(i)}]$
Savsani et al. [19], 2010.	GA, PSO, SA	To compare the performance of different algorithms when solving the minimum weight design problem.	$f(x) = G$	$x = [m, z_i, b]$
Mendi et al. [25], 2010.	GA	To obtain the optimal dimensions of the gearbox shafts, gears, and the rolling bearing.	$f(x) = V$	$x = [m, z_i, b]$
Miler et al. [20], 2017	GA	To determine the influence of including the profile shift coefficients as design variables when solving the optimal gear weight design problem.	$f(x_i) = V$	$x_1 = [m, z_i, b]$ $x_2 = [m, z_i, b, x_1, x_2]$
Miler et al. [21], 2018	NSGA-II	To conduct the multi-objective optimization of spur gear pairs focused on volume and efficiency.	$f_1(x) = V$ $f_2(x) = P_{loss}$	$x = [m, z_i, b, x_1, x_2]$

The design variable boundaries (shown in Table 3) were introduced for two reasons: first, to exclude unfeasible solutions and second, to reduce the number of possible combinations. The reduction in the size of the design variable intervals ensures faster solution convergence, lowering the computational cost.

The gear module m values are selected from the interval $m \in [1.75, 4]$ since the expression for the prediction of friction coefficient [12] is found by fitting the function to the experimental values of specimens with radii of relative curvature up to 21 mm. As the friction coefficient behaviour outside of the interval was not studied, extrapolation is not advisable. The gear face width was also limited. The lower boundary prevents the design of gears with near-zero widths, which are unrealistic as resulting tooth geometry lacks stability in the lateral direction. The upper boundary ensures that face width is used effectively; the even load distribution along the face width is harder to achieve at higher widths due to shaft and housing tolerances. The pinion number of teeth was limited to prevent tooth undercutting. Lastly, profile shift coefficients of the pinion are restricted to prevent undercutting on one side (lower boundary), and excessive wear and sliding velocities on the other side (upper boundary).

Table 3 – Design variable boundaries

Design variable		Boundaries
Gear module	m	1.75…4 mm
Face width	b	$(6…30) \cdot m$
Number of teeth (pinion)	z_1	14…24
Addendum modification (pinion)	x_1	$x_{1min}…x_{1max}$
Addendum modification (wheel)	x_2	-0.7…0.7

2.2. Objective functions – gear pair volume and power loss

The gear pair volume and power losses were perceived as desirable additional features and used as objective functions. Most of the gear pair optimisation studies [15–20,25,26] are focused on pair volume/weight as rating criterion (more details in Table 2). On the other side, increased efficiency in polymer gear pair ensures its longevity [8,27], urging researchers to carry out several studies on the subject [9–11].

When calculating the gear pair volume, it is essential to include the influence of addendum modification (i.e. profile shift coefficients x_1 and x_2). The objective function $f_1(x)$ is calculated as a sum of two solid discs:

$$f_1(\boldsymbol{x}) = \frac{\pi b}{4}(d_{a1}^2 + d_{a2}^2). \tag{2}$$

Generally, gear pair power losses consist of a frictional, churning, and windage losses [28]. The churning power losses are caused by gear flanks being submerged in the oil, while the windage losses are prominent at higher rotational velocities, most notably above 6000 rpm [29]. As we aimed to investigate the gear pairs lubricated using the solid lubricant at rotational velocities of up to 1500 rpm, both the churning and windage losses were not considered. The

frictional power losses are calculated as a function of normal load, sliding velocity, and friction coefficient [30].

Friction coefficient, as a function of movement type, load, velocity, temperature, loading time, and surface roughness [31], has a significant impact on power loss and wear. Schlenk's friction coefficient formulation [13] is often unjustifiably used in such applications, since it was developed for steel gears. In a previous study [12], an expression for prediction of friction coefficient in dry-lubricated polyoxymethylene (POM) gears was experimentally derived:

$$\mu(\rho_{rel}, w, v_S) = 0.054912 + 0.39837\rho_{rel}^{0.030658} \cdot w^{-1.0272} \cdot v_S^{0.17843}. \tag{3}$$

where ρ_{rel} [mm] is the radius of relative curvature, w [N/mm] is specific load, and v_s [m/s] is sliding velocity. The objective function representing the power losses $f_2(x) = P_{loss}$ is found by combining equation (3) and approximate load distribution expression by Sanchéz et al. [32] into the power loss expression proposed by Diez-Ibarbia et al. [30]:

$$f_2(\boldsymbol{x}) = \frac{F_{Nmax}}{m\pi \cos \alpha_w} \left[\begin{array}{l} \int_{\psi_A}^{\psi_B} \mu(\psi)v_s(\psi)R_{M-AB}(\psi)d\psi + \int_{\psi_B}^{\psi_C} \mu(\psi)v_s(\psi)R_{M-BD}(\psi)d\psi + \\ + \int_{\psi_C}^{\psi_D} \mu(\psi)|v_s(\psi)|R_{M-BD}(\psi)d\psi + \int_{\psi_D}^{\psi_E} \mu(\psi)|v_s(\psi)|R_{M-DE}(\psi)d\psi \end{array} \right]. \tag{4}$$

We used a similar expression in a previous work [21], with the difference of friction coefficient formulation. In the referenced study, friction coefficient was assumed to be constant along the line of action. Also, oil-lubricated steel gears were studied instead of the polymer gears lubricated using solid lubricant. It should be noted that, when including (4) into the algorithm, the position of point B must be verified and integration intervals altered accordingly.

2.3. Formulation of constraints – ensuring the load capacity

The design constraints are necessary to ensure that gear pairs found using the optimisation process are viable. Regardless of the material, gear pairs must be able to withstand the nominal load, have adequate durability, and geometry (to prevent jamming and ensure continuity of action). When comparing the thermoplastic spur gear pairs and their steel counterparts, design space is more constrained in the former. While the design of steel gears is constrained by the tooth root strength and flank durability (calculated according to [7,23]) and the transverse contact ratio (see Equation 10), additional constraints exist when designing the thermoplastic spur gear pairs. The additional constraints include tooth root and flank temperatures (see Equation 7), flank wear (8), and tooth addendum displacement (9).

Load capacity calculation was conducted according to the VDI 2736 [7] guidelines based on the ISO 6336:2006 standard [23]. Notable differences include simplifications of dynamic calculation factors and more load capacity criteria. Since polymers display good vibration damping properties when compared to metals, dynamic calculation factors $K_{H\alpha}$, $K_{F\alpha}$, $K_{H\beta}$, $K_{F\beta}$, and K_V are not considered (as recommended by technical guidelines [7]). Simplified dynamic factors K_H and K_F were used instead:

$$K_H = K_A \cdot K_{H\alpha} \cdot K_{H\beta} \cdot K_V \approx K_A$$

$$K_F = K_A \cdot K_{F\alpha} \cdot K_{F\beta} \cdot K_V \approx K_A \tag{5}$$

Tooth root and flank load capacity constraints are covered in [20] and are identical for thermoplastic and steel gears. It should be noted that Hasl et al. [33] used a modified method for calculation of polymer tooth root stresses. Experimental results have shown that VDI 2736 offers adequate fatigue strength data when observed in subcritical range ($N < 0.8$) and with temperatures under 80°C.

Polymers are good thermal insulators, meaning that heat resulting from friction at the gear flanks remains near the contact points, forming the regions with the increased temperature. Since an increase in temperature has an adverse influence on the mechanical properties of polymers, additional care is required when designing polymer gears. With the increase in temperature, thermoplastics used for gear design exhibit a decrease in Young's modulus E, shear modulus G, and nominal stress numbers σ_{Hlim} (contact) and σ_{Flim} (bending). Consequently, the value of elasticity factor Z_E is influenced by the variations in E and G. Expressions describing the temperature-caused changes of Young modulus were found using the polynomial interpolation [31].

For this reason, the practically viable range must be determined for polyoxymethylene. In [31], Erhard suggested temperature limits for long-term applications of polymer materials. Maximum long-term temperature of 80 °C was selected as highest permissible temperature. An additional constraint was included to prevent the algorithm from choosing the solutions resulting in higher temperatures:

$$\vartheta_{\text{Long-term}} - \max(\vartheta_{\text{Flank}}, \vartheta_{\text{Root}}) \geq 0, \tag{6}$$

with ϑ_{Flank} and ϑ_{Root} calculated using VDI 2736:

$$\vartheta_i = \vartheta_0 + P \cdot \mu \cdot H_v \cdot \left(\frac{k_{\vartheta,i}}{b \cdot z \cdot (v \cdot m)^{0.75}} + \frac{R_{\lambda,G}}{A_G} \right) \cdot ED^{0.64}, \tag{7}$$

Abrasion wear and tooth deformations must also be taken into account [34]. To avoid excessive abrasive wear due to dry running, mean linear wear W_m must be lower than the permissible wear $W_P = 0.1\ m$:

$$W_P - \frac{T \cdot 2 \cdot \pi \cdot N_L \cdot H_v \cdot k_w}{b \cdot z \cdot l_{Fl}} \geq 0, \tag{8}$$

with T operational torque [Nm], N_L number of load cycles [-], H_v gear loss factor [-], k_w wear coefficient [10^{-6}mm^3/(Nm)], and l_{Fl} length of the active tooth flank [mm]. Lower Young modulus results in larger deformations and consequently, displacements. Tooth addendum displacement λ_{add} must not exceed the permissible value of $\lambda_P = 0.07\ m$:

$$0.07 \cdot m - \frac{7.5 \cdot F_t}{b} \cdot \left(\frac{1}{E_1} + \frac{1}{E_2} \right) \geq 0. \tag{9}$$

Lastly, the transverse contact ratio is included as a necessary boundary condition to ensure continuity of action and to reduce vibrations originating from the meshing teeth pairs. Minimal value of 1.2 is recommended by AGMA [35]:

$$\varepsilon_\alpha - 1.2 \geq 0. \tag{10}$$

The gear pair that satisfies all the load capacity criteria is deemed valid. When compared to the steel gears, a larger number of criteria is required to determine the polymer gear load capacity. Thus, larger initial population should be used for optimisation. More details on algorithm settings are shown in the section 2.4.

2.4. Algorithm settings

The algorithm was chosen based on the problem definition; a non-dominated sorting genetic algorithm - NSGA-II [36] was used to carry out the optimisation. The maximum number of function evaluations was 500 000, with an initial population of 1000 units. NSGA-II is a widely used multi-objective evolutionary algorithm. It was suitable due to ensured convergence and no need for specifying a sharing parameter. Following characteristics of design variables and objective functions were considered:

- Variable types are mixed – both discrete and continuous variables exist. The numbers of teeth and modules are discrete, while the dynamic calculation factors and profile shift coefficients are continuous.
- Non-discrete variables are not allowed instead of discrete variables – by converting discrete to continuous variables using relaxation techniques, the quality of the solution will decrease during the subsequent rounding.
- Functions are not differentiable – besides the discrete variables, there are calculation factors such as R_M (load sharing ratio) which are not smooth.
- Multiple objectives exist – there are two objective functions, requiring the algorithm to be suitable for multi-objective optimisation.

2.5. Experimental rig

The experiment was necessary to validate the analytical results. The open-circuit experimental rig was designed in order to measure the frictional power losses in gear pairs (see Figure 2). The rig consists of two AC motors, first having the nominal power of 4 kW while operating at 2800 min^{-1}, and second of 12 kW while operating at 3000 min^{-1}. The former is providing the operational torque, working as driving machine, while the latter is providing the reactive torque (driven machine). Two torque transducers were mounted between the shafts and motors to determine the gear pair power losses. The 20 Nm transducer was mounted onto the input shaft, while the larger, 50 Nm transducer is mounted onto the output shaft. Both had accuracy grades of 0.1. The overall power loss between the transducers is calculated as:

$$P_{\text{loss}\Sigma} = 2\pi(n_{t1} \cdot T_{tt1} - n_{t2} \cdot T_{tt2})$$ (11)

where T_{tt1} [Nm] is torque measured by 20 Nm transducer (input), T_{tt2} [Nm] torque measured by 50 Nm transducer (output), n_{t1} [s^{-1}] number of rotations per second measured at the input shaft, and n_{t2} [s^{-1}] number of rotations per second at the output shaft.
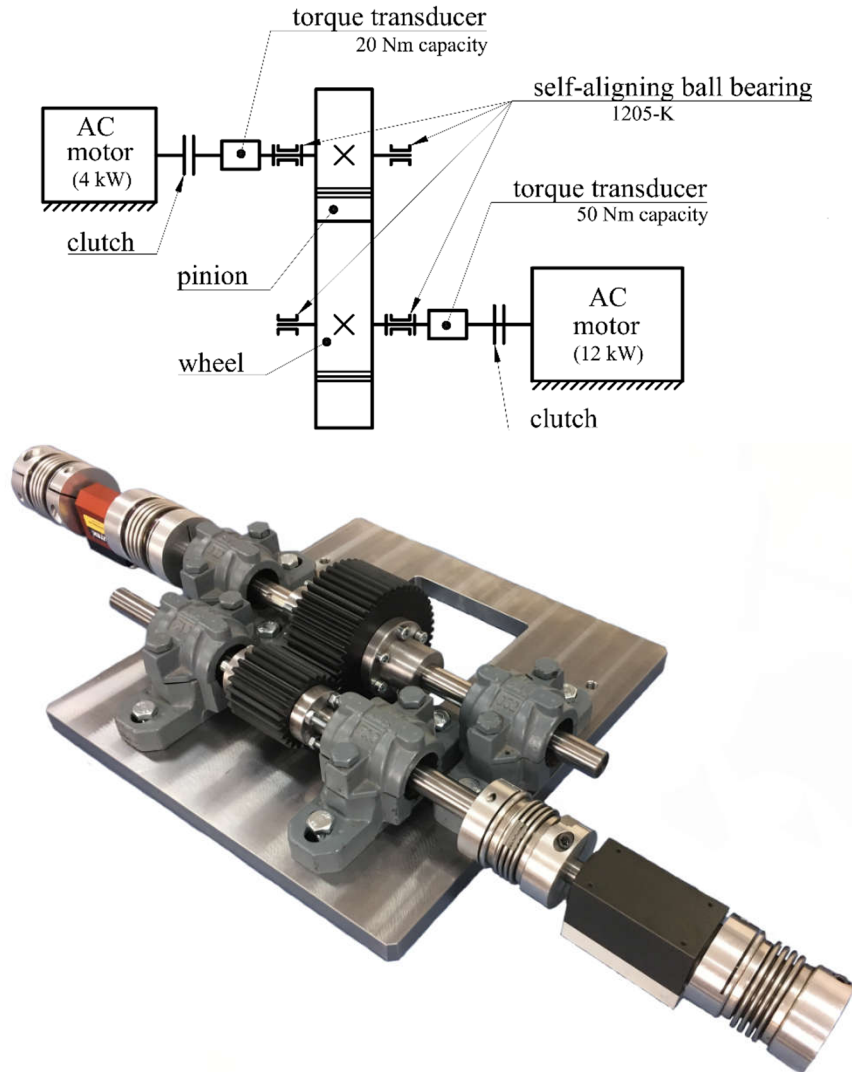
Figure 2 – Experimental rig schema (top), experimental rig (bottom)

The rig was designed to examine gear pairs with various centre distances, since it was necessary to ensure that pairs found in the optimisation process could be examined. Variations in centre distance were achieved by moving the bearing housings. Since centre distance tolerances in gear reducers are narrow, thus requiring the high precision machining, etalons for their adjustment (see Figure 3, technical drawings shown in supplementary data) were designed and manufactured to ensure the necessary shaft positions. These etalons ensured the correct relative positions of axes, providing both the dimensional and geometric accuracy. The manufacturing tolerance of etalon bore spacing was +0.02 mm, with bore tolerances of H6.

Figure 3 – Etalons for sets 1 (two pairs were manufactured for each of the sets)

2.6. Bearing power losses

Torques required to rotate the bearings must be determined before comparing the measured and calculated power loss values. The manufacturer provided model for calculation of torques [37]:

$$P_{\text{lossB}} = \frac{2\pi n_1}{60}(M_{\text{rr}-\text{shaft1}} + M_{\text{sl}-\text{shaft1}}) + \frac{2\pi n_2}{60}(M_{\text{rr}-\text{shaft2}} + M_{\text{sl}-\text{shaft2}}) \tag{11}$$

Two pairs of self-aligning ball bearings 1205-K were used (bearing series 12). The bearings were grease lubricated and; high-quality lithium soap grease with a mineral oil base was used (GA14, base oil class ISO-VG 150. Grease viscosity was 150 mm^2/s. Since seals were removed to decrease bearing power losses and grease was used to avoid emerging the bearings within the lubricant, only rolling M_{rr} and sliding M_{sl} frictional moments were calculated. Resulting bearing power losses P_{lossB} were subtracted from overall experimental values ($P_{\text{loss}\Sigma}$) to enable the comparison of analytical and experimental results.

3. Results

3.1. Optimisation results

The multi-objective optimisation was carried out as described in Section 2. The results are displayed as Pareto optimal fronts, one for each example set (Figure 4). One of the solutions was selected from each front for further experimental validation with two main aims: to further decrease the pair volume, and to increase the power losses. Lower gear pair volume reduces the manufacturing costs, while the higher power losses, even though such aim in unconventional, were easier to measure during the experiment.

The gear modules in set 1 solutions ranged between the 2.25 mm and 4 mm, with lower modules being found in solutions with higher power losses and lower volume. The face widths ranged between the 57.18 mm and 24.43 mm, while the power losses increased with the increase in face width. All the Pareto optimal solutions converged towards 24 teeth, the upper boundary of z_1. The variations in pinion profile shift coefficient between the different solutions were rather low, ranging between 0.527 and 0.568. Same was found for wheel profile shift coefficients which were close to the upper boundary of the profile shift coefficient (0.7), where x_2 values ranged between 0.619 and 0.7.

The Pareto optimal solutions operating under the set 2 conditions had modules between 2.25 mm and 3.75 mm, following trends identical to set 1. The face width also followed similar trends, increasing as the gear pair volume decreases, ranging between 22.9 mm and 49.4 mm. All the solutions had pinions with 24 teeth. The pinion profile shift coefficients were tightly clustered, similarly to the results found in set 2, ranging between 0.528 and 0.546. The profile shift coefficients of wheels x_2 [0.645, 0.696] were found near the upper profile shift coefficient boundary (0.7).

The active boundary conditions were further examined for both sets. The straightforward way to determine whether the condition was active is by excluding a boundary and subsequently repeating the optimisation process. Changes in the Pareto optimal front indicate whether the boundary was active or not. The wear condition (Equation 8) was active for both sets, implying that failure due to wear is expected. Such a conclusion is in agreement with the studies by other authors [38].

112
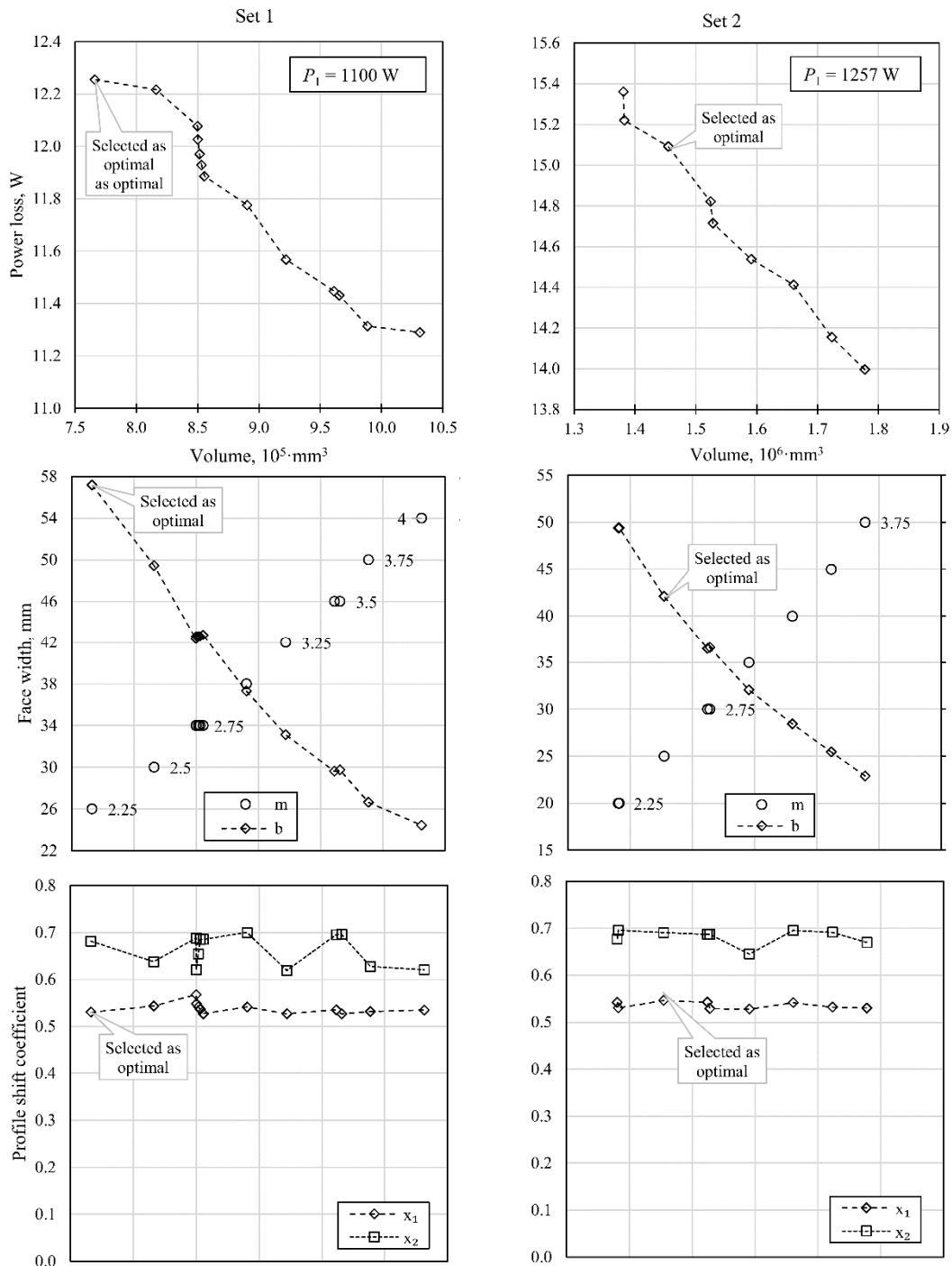
Figure 4 – Optimisation results

3.2. Experimental results

The measurements have been carried out using the open-circuit experimental rig, as described in Section 2.5. Gear pairs were selected for experimental validation following the aims presented in Section 3.1., and are shown in Table 4. The aimed run length was 600 s, under working conditions as defined in Table 1. However, it was not possible to achieve the necessary torque levels (28 Nm for set 1 and 38 Nm for set 2) using the 12 kW motor as a driven machine. The rotational velocity was regulated using the frequency converter.

Even though the nominal power is ten times the power transmitted through the gear pair, a combination of low rotational velocity (375 min^{-1} for set 1 and 317 min^{-1} for set 2) and high torque required a high electric current. In turn, high electric current led to a safety fuse overload or motor overheating, depending on the case. Thus, lower values of operational torques had to be used in the experiment. The corresponding expected values were calculated

113

using the analytical method outlined in Equation (4). The results are shown in Table 5, while diagrams showing the power losses during the experimental run can be found in Appendix A.

Table 4 – Pareto optimal solutions chosen for experimental validation

		Set 1	Set 2
Gear module	m /mm	2.25	2.5
Face width	b / mm	57 (57.29)	42 (42.39)
Number of teeth (pinion)	z_1	24	24
Number of teeth (wheel)	z_2	48	76
Profile shift coefficient (pinion)	x_1	0.528	0.528
Profile shift coefficient (wheel)	x_2	0.664	0.696
Expected power loss	P_{loss} / W	12.26	15.09
Efficiency	η	0.9889	0.988

Three runs were carried out using different gear sets and operational parameters (Table 5). The most significant power losses were found in run 1, where gear set 1 was used. Generally, the efficiency of gears and bearings was slightly above 0.98. The differences between the analytical and experimental results ranged between -21.5% and 20.8%. Regarding the gear pair temperature, it was concluded that it remained constant throughosut the run (thermal camera was used). After operating for 500 seconds, temperature of 24 °C was measured (compared to 16 °C surroundings). Since the relative duty cycle ED is defined over the course of 10 minutes, which was completed, it can be concluded that there was no notable thermal influence.

Table 5 – Pareto optimal solutions chosen for experimental validation

		Run 1	Run 2	Run 3
Gear pair used	-	Set 1	Set 2	Set 2
Rotational speed - pinion (mean)	n_1 / min^{-1}	756	992	998
Measured torque - pinion (mean)	T_1 / Nm	9.68	5.42	6.94
Measured torque - wheel (mean)	T_2 / Nm	19.04	16.97	21.73
Run length	t / s	382	431	185.5
Data points acquired	N / -	22887	25850	11131
Input power	P_1 / W	773.5	563.1	725.8
Output power	P_2 / W	758.4	552.3	711.8
Overall power losses	$P_{loss\Sigma}$ / W	15.16	10.78	13.78
Overall	η_m / -	0.9804	0.9809	0.9810
Bearing power losses (found using [37])	P_{lossB} / W	1.63	1.42	1.63
Gear pair power losses	$P_{loss\text{-}m}$ / W	13.53	9.36	12.15
Gear pair efficiency	$\eta_{g\text{-}m}$ / -	0.9825	0.9831	0.9831
Expected power loss (analytical)	P_{loss} / W	10.71	11.37	12.22
Expected gear efficiency (analytical)	η_g / -	0.9862	0.9798	0.9832
Difference	Δ_s / %	20.8	-21.5	-0.58

4. Discussion

The efficiencies calculated for selected Pareto optimal solutions (Table 4 and Table 5) are in agreement with values found during experimental testing. When compared to studies on polymer gear efficiency by Walton et al. [9,10], both the analytical and experimental efficiency values are higher. It should be, however, noted that Walton et al. [9,10] studied dry running POM-POM gear pairs; the friction coefficients were ranging from 0.2 to 0.5, compared to values up to 0.2 using the expression presented in [12]. Generally, based on the optimisation results (Figure 4) and the literature review, the following can be concluded:

- The gear pairs with higher power losses and lower volume generally had higher face width and lower gear module. The probable explanation is the friction coefficient formulation; it was shown that the friction coefficient drops as the specific normal load increases and sliding velocity decreases. By selecting a lower gear module, normal load increases, while the sliding velocity decreases. Such behaviour is caused by a decrease in gear diameter coupled with the constant rotational velocity and operational torque at the input. Additionally, sliding velocity also directly affects the power losses (Equation 4).
- The profile shift coefficients were positive, with higher values selected in sets 2 and 3. The values of profile

shifts in sets 2 and 3 were generally the same for all the pairs located on the Pareto front. Large positive profile shift coefficients increase the tooth flank curvature radii.

- The largest allowable numbers of teeth were selected for all the solutions on the Pareto front. Increase in a number of teeth also increases the tooth flank curvature, reducing the contact stress. The increase in number of teeth also goes in hand with the decrease of gear module, which is in agreement with conclusions by Walton et al. [10].
- Generally speaking, resulting design solutions are in agreement with the guidelines by Höhn et al. [39] for steel gear pairs, who advocate lowering the gear module, increasing the face width, increasing the pressure angle, and reducing the transverse contact ratio. However, the study presented by Walton et al. [10] is not in agreement regarding the pressure angle; they found that the gears with a pressure angle of 13.7° had higher efficiency when compared to the benchmark gear pair ($\alpha = 20°$).

Several simplifications were needed to carry out the study at hand. The differences between the experimental and analytical values were up to 21.5%. Even though such a difference implies good fit, possible causes should be examined further. The friction coefficient formulation used within the article [12] does not account for the slide-to-roll ratio, even though Nutakor et al. [40] have found that it affects the friction coefficient. However, the study by Nutakor et al. was carried out using the heavily loaded steel gear pairs. In addition to the omission of the slide-to-roll ratio, the bearing power loss calculation should be considered. Both the manufacturer-provided expressions for prediction of bearing power losses and tolerances of measuring equipment could partially account for the differences in the results.

Lastly, concerning the gear pair load capacity, the optimisation study was carried out conservatively. Since VDI 2736 guidelines are widely accepted as a means for the determination of load capacity of thermoplastic gear pairs, friction coefficient suggested within ($\mu = 0.28$) was used while determining boundary conditions. The results are thus more conservative, as the formulation suggested by the authors in [12] provided lower friction coefficient values.

4.1. Comparison with steel gear pairs

The results for steel gear pairs from [21] were also compared to the results from the study at hand (see Figure 5). Both groups of solutions are normalised by dividing each of the values on each axis with the lowest value on the corresponding axis. The differences were found while comparing steel and polymer gear pairs, implying the need for separate design guidelines. A key difference is in the face width influence. The lower face widths were generally selected in low-volume steel gear pairs, while in polyoxymethylene gear pairs large face width corresponded with the pairs of same characteristics (for details see [21] for steel gears and Figure 4 for polyoxymethylene gears).

The calculated values are of the same order of magnitude as those reported by other researchers for spur gear pairs made of steel. Petry-Johnson et al. [29] reported the efficiency of 0.9979, Baglioni et al. [41] of 0.985 (Method I) and 0.981 (Method 2), while Diez-Ibarbia et al. [30] reported 0.994. The gear pair parameters and operating conditions of referenced studies can be found in [21]. The predicted values are generally lower than those in steel gear pairs, which was expected due to changes in lubrication regime. Dry lubricant (PTFE) resulting in boundary lubrication was used instead of the oil or grease (mixed or EHD lubrication regime).
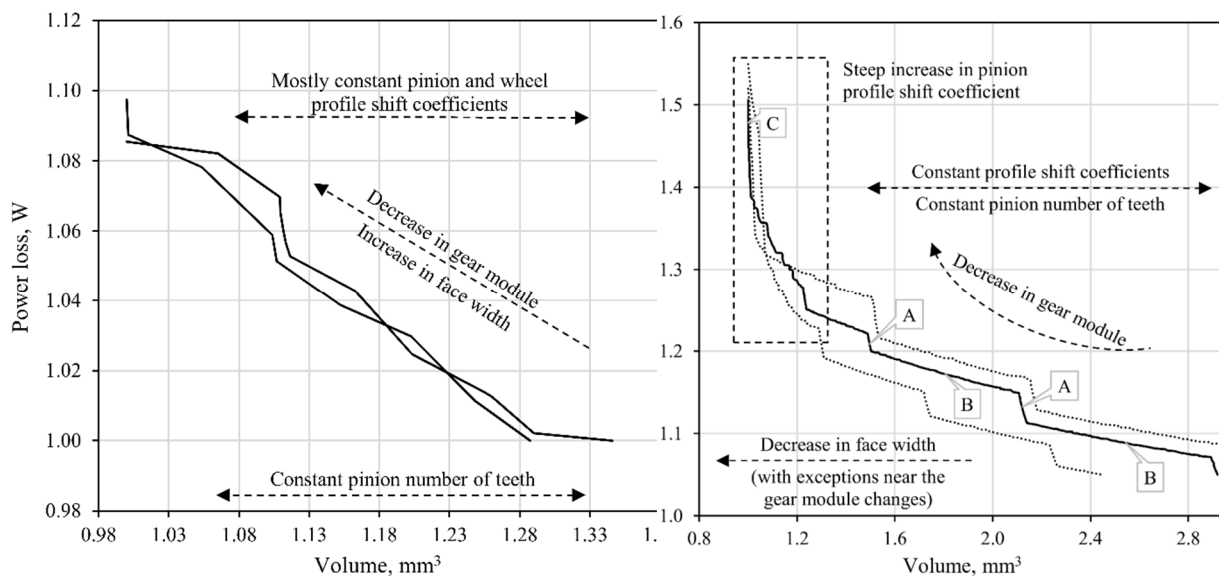
Figure 5 – Comparison of results from for steel (left [21]) and polymer gear pair (right) optimisation

For both materials, decrease in gear module increases power losses and decrease in volume. Additionally, no notable differences were found in profile shift coefficients and numbers of teeth.

Besides the design variable values, possible over-constraining in polymer gear pairs should be discussed. In addition to the constraints used in steel gear pairs – tooth root strength, Hertzian (contact) stress, and transmission ratio, four additional constraints are bestowed upon their polymer counterparts. Those include tooth root and flank temperatures, flank wear, and tooth tip deformation. A total of 7 constraints severely limits the design space, as seen in Figure 5 – much larger variations of designs are possible for steel gears. The ratio between the lowest values of objective functions for steel gears is up to 2.9 (volume) and 1.55 (power losses). In polymer gears, values of the same ratio are up to 1.34 (volume) and 1.1, consequently leaving fewer possibilities to the designers.

Another difference was the active constraints. In steel gears, gear pair load capacity was mainly limited by Hertzian pressure, regardless of whether the steel was heat treated or not. In polymer gears, load capacity was limited by wear criterion, which was an active constraint in both sets. Such results were expected, as wear is one of the most common failure types in polymer gears (other being the tooth root failure). The wear failure is most often encountered in dry running gear pairs [42]. Another example is a study by Bravo et al. [38], in which the authors suggested that in POM/POM pairs working at lower load levels will fail due to wear.

5. Conclusion

The research study on polymer gear pair optimisation was carried out. The main finding is that differences between optimal results of polymer and steel gears exist, requiring different design guidelines. When compared to steel gear pair optimisation, the design space in polymer gears is significantly more constrained; gear pair flank wear seems to be the active constraint (i.e. most likely type of failure) in the observed sets. Based on the results obtained for selected sets of input data, the following conclusions were made:

- The critical difference is in face width. In steel gear pairs, low-volume pairs generally had low face width while the opposite is correct in polymer gear pairs.
- The combination of lower gear module and long face width results in higher power losses and lower volume.
- The pinion number of teeth is generally selected on the upper allowable boundary – each pinion located within the optimal solutions had 24 teeth.
- The pinion and wheel profile shift coefficients are positive and remain the same for all the solutions on Pareto optimal front. Generally, the value of 0.53 was selected for the pinion, and 0.7 for the wheel.

The experimental results were found using the open-circuit experimental rig. The analytical and experimental results are in agreement, with differences ranging from -21.5% to 20.8%. The deviations could be partially attributed to the friction coefficient formulation, bearing power loss prediction model, and measuring accuracy. It should also be added that gear pair power losses measured using the open-circuit device are greatly affected by the accuracy grade of the torque transducers. Subsequent separation of the bearing power losses could further reduce the measurement accuracy.

Future studies on the subject could be carried out using different types of thermoplastic materials, leading to more comprehensive guidelines. Additionally, the authors used VDI 2736 to carry out the calculation of gear pair load capacity, including the constant value of the friction coefficient, resulting in a more conservative solution. Thus, the effect of friction coefficient prediction expression [12] in combination with the VDI 2736 formulae could be subject worthy of further investigation, leading to more precise gear pair load estimation.

Nomenclature

b	: face width
d_{a1}	: tip diameter (pinion)
d_{a2}	: tip diameter (wheel)
ED	: relative duty ratio
f_1	: first objective function (volume)
f_2	: second objective function (frictional power losses)
i	: transmission ratio
F_t	: tangential load
K_A	: application factor
K_F	: dynamic factor (root)
K_H	: dynamic factor (flank)
λ	: tooth addendum displacement
m	: gear module
n_1	: rotational speed (pinion)

P_{loss} : frictional power losses
P_{lossB} : bearing power losses
$P_{loss\Sigma}$: overall power losses (measured value)
R_M : load sharing ratio
ρ : density (steel)
ρ_{rel} : radius of relative curvature
T_1 : input torque
ϑ_{Flank} : tooth flank temperature
ϑ_{Root} : tooth root temperature
v_s : sliding velocity
$\boldsymbol{x}$: design variable vector
x_1 : profile shift coefficient (pinion)
x_{1max} : maximal allowable profile shift coefficient (pinion)
x_2 : profile shift coefficient (wheel)
w : specific load
W_m : mean linear wear
W_P : permissible wear
z_1 : number of teeth (pinion)
z_2 : number of teeth (wheel)

Acknowledgement

117

Appendix A. $P_{loss\Sigma} - t$ **diagrams**

Run 1
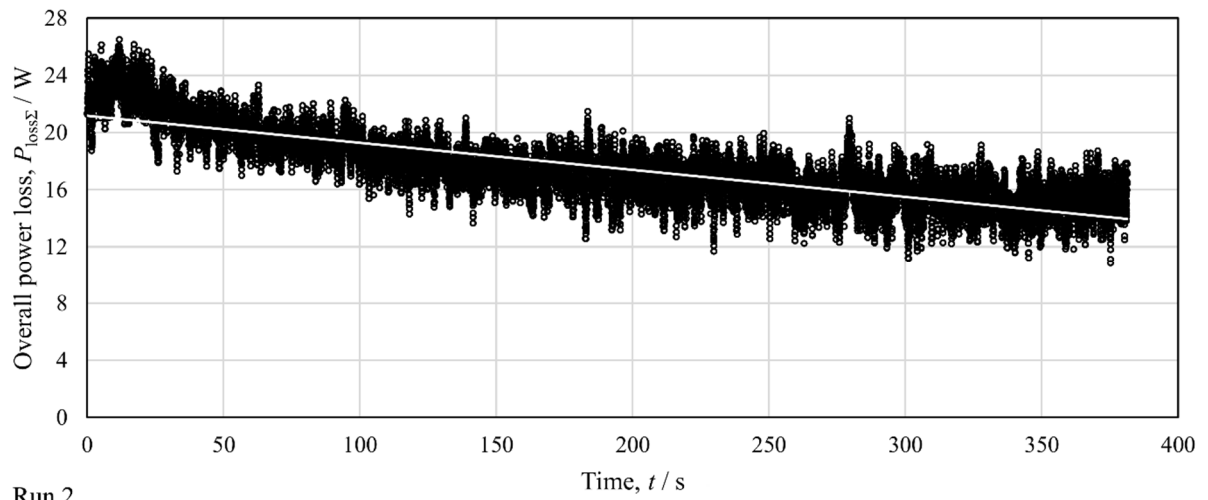
Run 2
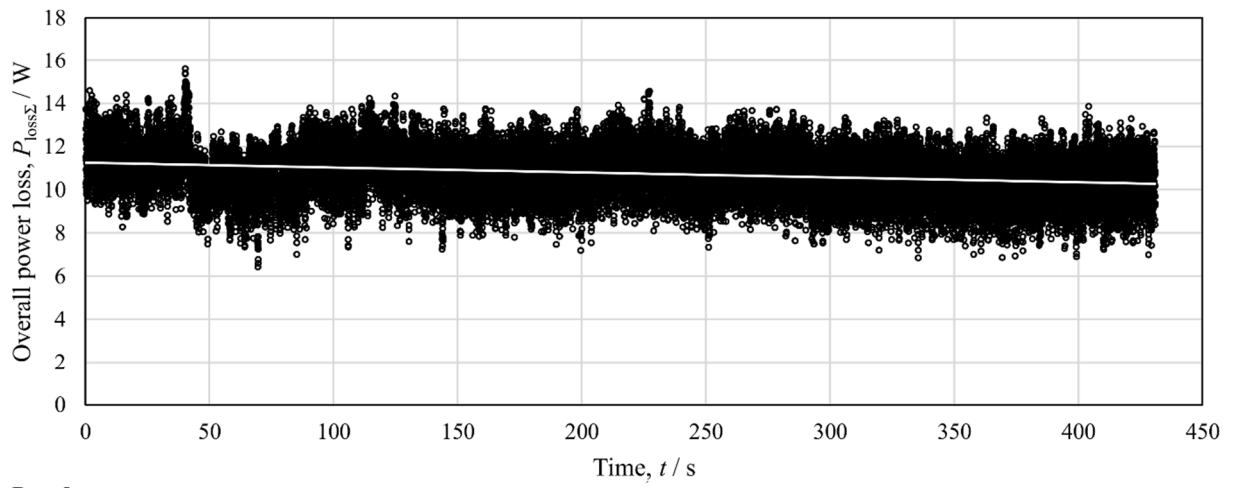
Run 3
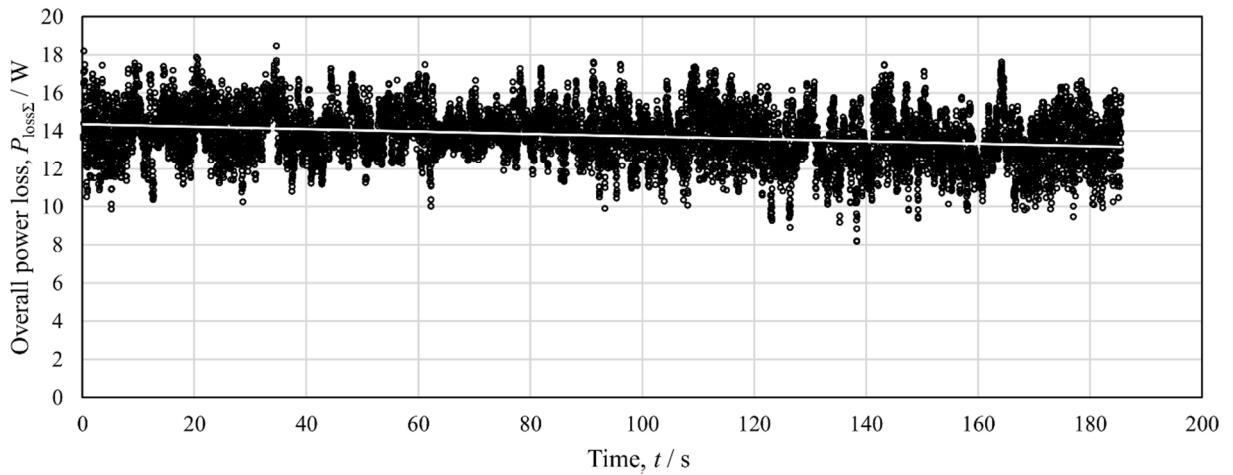
Figure 6 – Experimental data

References

[1]   A. Almasi, Latest technologies and modern guidelines on gear units, Australian Journal of Mechanical Engineering. 12 (2014). doi:10.7158/M12-085.2014.12.3.

[2]   J. Duhovnik, D. Zorko, L. Sedej, The effect of the teeth profile shape on polymer gear pair properties, Tehnicki Vjesnik - Technical Gazette. 23 (2016) 199–207. doi:10.17559/TV-20151028072528.

[3]   K. Terashima, N. Tsukamoto, N. Nishida, J. Shi, Development of Plastic Gear for Power Transmission: Abnormal Wear on the Tooth Root and Tooth Fracture near Pitch Point, Bulletin of JSME. 29 (1986) 1598–1604. doi:10.1299/jsme1958.29.1598.

[4]   C.M.C.G. Fernandes, D.M.P. Rocha, R.C. Martins, L. Magalhães, J.H.O. Seabra, Finite element method model to predict bulk and flash temperatures on polymer gears, Tribology International. 120 (2018) 255–268. doi:10.1016/j.triboint.2017.12.027.

[5]   V. Roda-Casanova, F. Sanchez-Marin, A 2D finite element based approach to predict the temperature field in polymer spur gear transmissions, Mechanism and Machine Theory. 133 (2019) 195–210. doi:10.1016/j.mechmachtheory.2018.11.019.

[6]   P.K. Singh, Siddhartha, A.K. Singh, An investigation on the thermal and wear behavior of polymer based spur gears, Tribology International. 118 (2018) 264–272. doi:10.1016/j.triboint.2017.10.007.

[7]   VDI Verein Deutscher Ingenieure, VDI 2736 Thermoplastic gear wheels, (2014) 73.

[8]   M. Kalin, A. Kupec, The dominant effect of temperature on the fatigue behaviour of polymer gears, Wear. 376–377 (2017) 1339–1346. doi:10.1016/j.wear.2017.02.003.

[9]   D. Walton, A.B. Cropper, D.J. Weale, P.K. Meuleman, The efficiency and friction of plastic cylindrical gears Part 1: Influence of materials, Proceedings of the Institution of Mechanical Engineers, Part J: Journal of Engineering Tribology. 216 (2002) 75–78. doi:10.1243/1350650021543915.

[10] D. Walton, A.B. Cropper, D.J. Weale, P.K. Meuleman, The efficiency and friction of plastic cylindrical gears Part 2: Influence of tooth geometry, Proceedings of the Institution of Mechanical Engineers, Part J: Journal of Engineering Tribology. 216 (2002) 93–104. doi:10.1243/1350650021543924.

[11] S. Kirupasankar, C. Gurunathan, R. Gnanamoorthy, Transmission efficiency of polyamide nanocomposite spur gears, Materials and Design. 39 (2012) 338–343. doi:10.1016/j.matdes.2012.02.045.

[12] D. Miler, M. Hoić, Z. Domitran, D. Žeželj, Prediction of friction coefficient in dry-lubricated polyoxymethylene spur gear pairs, Mechanism and Machine Theory. 138 (2019) 205–222. doi:10.1016/j.mechmachtheory.2019.03.040.

[13] L. Schlenk, Untersuchungen zur Freßtragfähigkeit von Großzahnrädern (PhD Thesis), Technical University Munich, 1995.

[14] D. Koffi, R. Gauvin, H. Yelle, Heat generation in thermoplastic spur gears, Journal of Mechanisms Transmissions and Automation in Design. 107 (1985) 31–36. doi:10.1115/1.3258688.

[15] T. Yokota, T. Taguchi, M. Gen, A solution method for optimal weight design problem of the gear using genetic algorithms, Computers & Industrial Engineering. 35 (1998) 523–526. doi:10.1016/S0360-8352(98)00149-1.

[16] J.-L. Marcelin, Genetic optimisation of gears, International Journal of Advanced Manufacturing Technology. 17 (2001) 910–915. doi:10.1007/s001700170101.

[17] C. Gologlu, M. Zeyveli, A genetic approach to automate preliminary design of gear drives, Computers and Industrial Engineering. 57 (2009) 1043–1051. doi:10.1016/j.cie.2009.04.006.

[18] L. Tudose, O. Buiga, C. Ştefanache, A. Sóbester, Automated optimal design of a two-stage helical gear reducer, Structural and Multidisciplinary Optimization. 42 (2010) 429–435. doi:10.1007/s00158-010-0504-z.

[19] V. Savsani, R. V. Rao, D.P. Vakharia, Optimal weight design of a gear train using particle swarm optimization and simulated annealing algorithms, Mechanism and Machine Theory. 45 (2010) 531–541. doi:10.1016/j.mechmachtheory.2009.10.010.

[20] D. Miler, A. Lončar, D. Žeželj, Z. Domitran, Influence of profile shift on the spur gear pair optimization, Mechanism and Machine Theory. 117 (2017) 189–197. doi:10.1016/j.mechmachtheory.2017.07.001.

[21] D. Miler, D. Žeželj, A. Lončar, K. Vučković, Multi-objective spur gear pair optimization focused on volume and efficiency, Mechanism and Machine Theory. 125 (2018) 185–195. doi:10.1016/j.mechmachtheory.2018.03.012.

[22] J.S. Arora, Introduction to Optimum Design, 3rd edition, Academic Press, Oxford, 2004. doi:10.1016/B978-0-12-064155-0.X5000-9.

[23] International Organization for Standardization, ISO 6336:2006 - Calculation of load capacity of spur and helical gears — Application for industrial gears, ISO, Geneva, Switzerland, 2006.

[24] J.-L. Marcelin, Using genetic algorithms for the optimization of mechanisms, Int J Adv Manuf Technol.

27 (2005) 2–6. doi:10.1007/s00170-004-2162-z.

[25] F. Mendi, T. Baskal, K. Boran, F.E. Boran, Optimization of module, shaft diameter and rolling bearing for spur gear through genetic algorithm, Expert Systems with Applications. 37 (2010) 8058–8064. doi:10.1016/j.eswa.2010.05.082.

[26] S. Golabi, J.J. Fesharaki, M. Yazdipoor, Gear train optimization based on minimum volume/weight design, Mechanism and Machine Theory. 73 (2014) 197–217. doi:10.1016/j.mechmachtheory.2013.11.002.

[27] K. Mao, W. Li, C.J. Hooke, D. Walton, Friction and wear behaviour of acetal and nylon gears, Wear. 267 (2009) 639–645. doi:10.1016/j.wear.2008.10.005.

[28] K. Michaelis, B. Höhn, M. Hinterstoißer, Influence factors on gearbox power loss, Industrial Lubrication and Tribology. 63 (2011) 46–55. doi:10.1108/00368791111101830.

[29] T.T. Petry-Johnson, A. Kahraman, N.E. Anderson, D.R. Chase, An experimental investigation of spur gear efficiency, Journal of Mechanical Design. 130 (2008) 62601. doi:10.1115/1.2898876.

[30] A. Diez-Ibarbia, A.F. del Rincon, M. Iglesias, A. de-Juan, P. Garcia, F. Viadero, Efficiency analysis of spur gears with a shifting profile, Meccanica. 51 (2016) 707–723. doi:10.1007/s11012-015-0209-x.

[31] G. Erhard, Designing with Plastics, Hanser Publishers, Munich, 2006. doi:10.3139/9783446412828.

[32] M.B. Sánchez, M. Pleguezuelos, J.I. Pedrero, Approximate equations for the meshing stiffness and the load sharing ratio of spur gears including hertzian effects, Mechanism and Machine Theory. 109 (2017) 231–249. doi:10.1016/j.mechmachtheory.2016.11.014.

[33] C. Hasl, P. Oster, T. Tobie, K. Stahl, Bending strength of oil-lubricated cylindrical plastic gears: Modified bending strength calculation based on VDI 2736, Forschung Ingenieurwesen. 81 (2017) 349–355. doi:10.1007/s10010-017-0224-2.

[34] A.R. Breeds, S.N. Kukureka, K. Mao, D. Walton, C.J. Hooke, Wear behaviour of acetal gear pairs, Wear. 166 (1993) 85–91. doi:10.1016/0043-1648(93)90282-Q.

[35] B.S.P. Radzevich, Dudley's Handbook of Practical Gear Design and Manufacture, 2nd editio, CRC Press, Boca Raton, 2012.

[36] K. Deb, A. Pratap, S. Agarwal, T. Meyarivan, A fast and elitist multiobjective genetic algorithm: NSGA-II, IEEE Transactions on Evolutionary Computation. 6 (2002) 182–197. doi:10.1109/4235.996017.

[37] H. Linke, J. Börner, R. Heiß, Cylindrical gears: Calculation, materials, manufacturing, Hanser Publications, Cincinnati, Ohio, 2016.

[38] A. Bravo, D. Koffi, L. Toubal, F. Erchiqui, Life and damage mode modeling applied to plastic gears, Engineering Failure Analysis. 58 (2015) 113–133. doi:10.1016/j.engfailanal.2015.08.040.

[39] B.R. Höhn, K. Michaelis, A. Wimmer, Low loss gears, Gear Technology. (2007) 28–35.

[40] C. Nutakor, D. Talbot, A. Kahraman, An experimental characterization of the friction coefficient of a wind turbine gearbox lubricant, Wind Energy. (2019) 1–14. doi:10.1002/we.2303.

[41] S. Baglioni, F. Cianetti, L. Landi, Influence of the addendum modification on spur gear efficiency, Mechanism and Machine Theory. 49 (2012) 216–233. doi:10.1016/j.mechmachtheory.2011.10.007.

[42] A.K. Singh, Siddhartha, P.K. Singh, Polymer spur gears behaviors under different loading conditions: A review, Proceedings of the Institution of Mechanical Engineers, Part J: Journal of Engineering Tribology. 0 (2017) 135065011771159. doi:10.1177/1350650117711595.

Paper IV

Prediction of friction coefficient in dry-lubricated polyoxymethylene spur gear pairs

Daniel Miler[1*], Matija Hoić[1], Zoran Domitran[1] and Dragan Žeželj[1]

[1] *Faculty of Mechanical Engineering and Naval Architecture, University of Zagreb, 10002 Zagreb, Ivana Lučića 5, Croatia*

Abstract

In this article, the authors have experimentally determined the friction coefficient in the polyoxymethylene gear pairs lubricated by a dry film lubricant. The obtained expression increases the precision of the frictional power loss calculation, which is essential when the frictional power loss is used as the optimization criterion. The friction coefficient was characterized for three influencing parameters: radius of relative curvature, sliding velocity, and normal load. The full factorial organization was used for the experiment design; five curvature radii levels, four sliding velocity levels, and three load levels were used. Each of the runs was recorded three times, which resulted in a total of 180 experimental runs. The resulting expression for the friction coefficient is valid for the gear modules between 1 and 4.5 mm and sliding speeds of up to 2.7 m/s. The normal load was found to have the greatest influence on the friction coefficient, while the sliding velocity influenced only the specimens running under lower load levels. A further increase in the values of radii of relative curvature above 5 mm had no effect on the friction coefficient. The experimental data is provided in full.

Keywords: polyoxymethylene (POM); friction coefficient; prediction; spur gear; experimental study

---

1. Introduction

The use of polymer materials in gear manufacturing is on the rise; today, they are even more widely used than steel. Despite their limited load capacity, these materials are a good choice when designing household appliances [1]. The advantages of polymer materials, such as no need for lubrication, low manufacturing price, low weight, and the potential for serial production, make them a good choice when designing mechanical transmissions. A disadvantage of polymer gears is the rapid degradation of mechanical properties as the temperature increases [2]. This means that by reducing the power losses, which are responsible for heat generation, the mechanical properties will be indirectly improved. Thus, since most of the polymer materials are thermal insulators, higher efficiency will be an important criterion when evaluating the design efficacy.

The gear pair power losses are generally divided into two groups [3]: load-independent losses and load-dependent losses. The load-independent losses are always present and are caused by air windage, oil churning, and inertial power loss, among other things [4]. However, these losses are noticeable only at higher rotational speeds. The load-dependent gear pair losses are a function of load, sliding velocity, and friction coefficient [5]. If the elastohydrodynamic lubrication (EHL) theory is used, lubricant properties and surface roughness should also be included [6]. When determining power losses, the load and the sliding velocity are found by using theoretical expressions, while the friction coefficient is determined experimentally.

The friction coefficient between the meshing gear pairs has a major influence on the power losses. Thus, many studies have been conducted, almost exclusively on steel gear pairs, in an attempt to predict its value. Marjanović et al. [7] attempted to determine the most suitable form of friction coefficient formulation. The combination of Hertzian pressure and sliding velocity was suggested. Schlenk [8] assumed a constant friction coefficient along the line of action and proposed a formula for its calculation. The mean friction coefficient is expressed as a function of specific load, sliding velocity at the operating pitch circle, relative curvature radii (reduced), surface roughness, and lubricant viscosity and type. Xu [9] used the non-Newtonian thermal elastohydrodynamic lubrication (EHL) model to determine the friction coefficient in discrete points along the line of action. Li and Kahraman [10] also used EHL to derive the friction coefficient and power loss formulae suitable for gear design. The friction coefficient was determined as a function of normal load, sliding velocity, and relative curvature radius. Fernandes et al. [11] searched the literature to give a review on the friction coefficient prediction equations for gear pairs. Additionally, the authors suggested an additional formulation based on a modified Hersey parameter.

As for polymer gear pairs, the literature is less extensive. Studies are mostly conducted using pin-on-disc or twin-disc tests [12–15], thus offering no possibilities for integration into the gear pair model where the

---

* Corresponding author.
 E-mail: daniel.miler@fsb.hr
 Tel.: +385 1 6168 221

curvature, sliding velocity, and load vary along the pitch line. Kukureka et al. [16] also conducted a study using the twin-disc test to examine the wear mechanisms in two unlubricated polyoxymethylene specimens. The load, rolling speed, and slip ratio levels were varied; it was found that temperature has a dominant influence on the wear rate. Unfortunately, no friction coefficient formulation was offered based on the findings. Chaudri et al. [17] also studied the non-lubricated friction in engineering polymers; a test in which a polybutylene terephthalate (PBT) pin was sliding along a polyoxymethylene surface was done. The authors found that the normal load had strongly influenced the friction coefficient. Myshkin et al. [18] did a review of the studies on friction and wear in polymers. However, no consensus on type of relationship between the variables was found. Some of the covered research studies reported no dependence between the friction coefficient and the load or the sliding velocity, while some others reported that dependence. When gear pairs are concerned, a review of the polymer spur gear pair behaviour was conducted by Singh et al. [19]. The review presents the main research trends and points out polyoxymethylene (POM) and polyamide (PA) as the most often used polymer materials in gear manufacturing.

The accelerated testing procedure for the verification of polymer gear design was proposed by Pogačnik and Tavčar [20] and later updated by Tavčar et al. [21]. The proposed experimental procedure provides a number of tribological parameters, including the friction coefficient, while requiring only $2 \cdot 10^5$ load cycles. However, one cannot find any studies predicting the friction coefficient for thermoplastic gear pairs. Even though there are some experimental studies on the friction coefficient between two polymer specimens [12–17,19], no results applicable for its prediction have been found. The main reason is a disregard for variations in the curvature radius and the sliding velocity along the pitch line, i.e. the variables that change as the gears rotate. Changes in the Hertzian pressure are caused by the curvature radius variations stemming from involute geometry; as the gear flanks are elastic, the curvature radius has a major impact on the contact surface. The sliding velocity variations are a result of differences in tangential components of the pinion and the wheel velocities.

For this reason, an experimental study on the friction coefficient between the POM specimens has been conducted, accounting for variations in the curvature, the sliding velocity, and the normal load. The aim of this research is to provide a function for predicting the friction coefficient. Such expression would enable the optimization of POM gear pairs to be conducted using the power losses as the objective function. By using a precise friction coefficient approximation, the optimization of polymer gear pairs by means of the methods applied to steel gears [22,23] would be possible. Also, a more precise power loss calculation would contribute to the precision in the calculation of the flank and root temperature, which has a major influence on the wear and longevity of the gear pair.

2. Experimental characterization

An experimental study was conducted to determine the friction coefficient values along the mesh of polyoxymethylene (POM) spur gear pairs. Since the involute gear geometry is complex, the tooth flanks were replaced with models having the equivalent relative curvature radius. The influence of slide-to-roll ratio was not considered in this study. It should be noted that specimens were lubricated by a dry film lubricant (PTFE) since the contact surfaces of unlubricated specimens were damaged almost instantly.

The experimental rig enables variations in the specific load, the sliding velocity, and the radius of relative curvature. A detailed description of the rig is given in Section 2.1. The process of variable selection is shown in Section 2.2. The number of variables was limited to a sufficient number of levels for each variable to increase the result accuracy. The relative curvature radius, the specific load, and the sliding velocity were chosen.

The design of the experiment is shown in Section 2.3. The full factorial design was used, resulting in a 180 experimental runs.

2.1. Experimental rig

The experimental rig consists of an electric motor, a shaft, a housing, two load cells, and a load application mechanism. Two different specimens are used to conduct the experiment, a rotating one, which is mounted onto a shaft, and a static one, which is able to move along the z axis. Thus, the rig has two main axes, the axis of rotation and vertical axis z (see Figure 1). The former consists of an electric motor, a torque transducer, bearings, and a shaft, while the latter consists of a compressive load cell and weights. Additionally, to achieve a line contact and ensure uniform distribution of the normal load along the tooth flank, static specimens freely adjust their position around auxiliary axes z (vertical axis) and y (the horizontal axis), as shown in Figure 1b. The rotating specimen is circular, while the static specimen has a rounded face. This configuration emulates the line contact found in spur gear pairs. The torque is provided by a 0.55 kW asynchronous electric motor. The rotational velocity is adjusted using a frequency regulator. The weights are attached to a lever mechanism to provide the normal load which is directly applied to the compressive load cell holding the static specimen. The

compressive load cell of a maximum capacity of 500 N and an accuracy grade of 0.2 was used. The 20 Nm (accuracy grade 0.2) torque transducer was used to measure the torque. The normal load was regulated by varying the total weight at the lever.

The friction coefficient is calculated as a ratio of the frictional and the normal force (1):

$$\mu = \frac{F_{fr}}{F_n} = \frac{T_m}{\rho_{rot}F_n} \tag{1}$$

where T_m [Nmm] is the torque measured by the torque transducer, ρ_{rot} [mm] is the radius of the rotating specimen, and F_n [N] is the normal load.
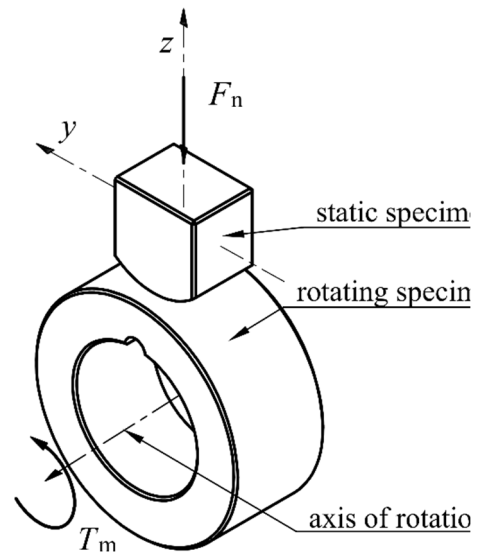
Figure 1 – Experimental rig (left) and the load schema (right)

2.2. Variable selection

As shown in the literature overview, the friction coefficient between the gear pairs in mesh depends on various factors. Schlenk [24] devised an expression for the prediction of friction coefficient in steel gears, in which it is approximated as a function of relative curvature radius, sliding velocity, specific load, mean surface roughness, oil viscosity, and oil type.

Due to a limited number of experimental runs, only the values regarded as the most substantial were experimentally investigated. The relative curvature radius, the sliding velocity, and the specific load were selected as these variables were perceived as essential by other researchers, Schlenk [8,24], Li and Kahraman [6], and Marjanović et al. [7]. Due to a large number of variables and the test rig limitations, the slide-to-roll ratio and temperature of specimens were not considered in our study.

As the number of simultaneously meshing gear tooth pairs varies along the path of contact, each of the intervals was regarded separately. To define the intervals, specific points along the mesh must be explained (Figure 2): mesh start A, lowest point of single tooth contact (LPSTC) B, pitch point C, highest point of single tooth contact (HPSTC) D, and mesh end E. Between the point A and the LPSTC, two pairs of teeth are meshing simultaneously. Between the LPSTC and the HPSTC, a single pair of teeth transmits the load. Lastly, between the HPSTC and the end of contact E, two pairs of teeth are in mesh simultaneously. The first interval was between the first two specific points, A and B (two pairs in contact), the second between B and D (one pair in contact), and the third between points D and E (two pairs in contact). The load distribution was calculated using

the approximate expressions provided in [25]. It should be stressed that previous studies [5,26] have shown that the intervals AB and DE account for the largest share of power losses, thus increasing the importance of accurate friction coefficient prediction.

The explanations of the variable selection and the subsequent level selection processes are given in Sections 2.2.2 to 2.2.4. The rest of the variables were chosen as control variables, and are presented in Section 2.2.4.
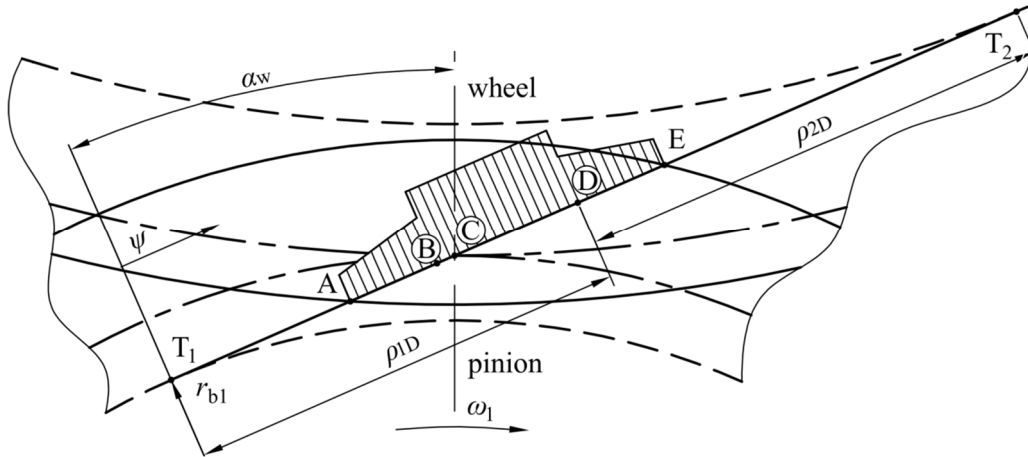
Figure 2 – Pitch line AE and load distribution across the gear tooth pairs (from [23]*, with the authors' permission)*

2.2.1. Sample gear pair population

A sample gear pair population was generated with the goal selecting more representative variable levels. After creating the sample population, the variable level range was adapted to cover only the technically viable cases. Additionally, the measuring grid density can be increased in more populous areas to increase prediction precision. The geometric gear pair parameters were varied within the applicability range of the equation resulting from the experiment. The variable ranges used to create the sample population are:

- Standard gear modules (m) ranging from 1.5 mm to 4.5 mm,
- Pinion tooth numbers (z_1) of 14, 19 and 24,
- Transmission ratios (i) of 1, 2, 3, and 4, which determined the number of the driven gear teeth,
- Profile shift coefficients of both the pinion (x_1) and the wheel (x_2); values of 0, 0.35, and 0.7 were used. In some of the pairs, a profile shift coefficient of 0.7 would result in a sharp (pointed) tip. In such pairs, values of 0, 0.5 x_{maxT}, and x_{maxT} were used, with x_{maxT} being the highest permissible profile shift coefficient regarding the tip sharpness. Negative values were not considered since the previously conducted studies on gear pair optimization [22,23] had shown that optimal values were always positive.

By combining the above-listed values, 1404 spur gear pairs were obtained. After including the points A, B, D, and E, the total number of points increased fourfold. Point C was only considered when choosing the levels for radii of relative curvature since the normal load is equal to that in points B and D and there is no sliding.

2.2.2. Radius of relative curvature

The test specimen shape is varied to mimic the gear flank geometry. In spur gear pairs, the geometry at the point of contact between the meshing teeth can be represented using the radius of relative curvature; for example, ρ_{redC} was used in Schlenk's friction coefficient formulation for steel gears [8,24]. The radius of relative curvature in a gear pair can be calculated for each point along the pitch line. It is a function of position on the pitch line, gear module, number of pinion and wheel teeth, profile shift coefficients, and tip relief [27]. Since the values of the radius of relative curvature vary along the pitch line, they were discretized at specific mesh points; the relative curvature radii of sample population were calculated for mesh points A, B, C, D, and E. Results are shown in Figure 3. Gears with the tip relief were not considered in this study.
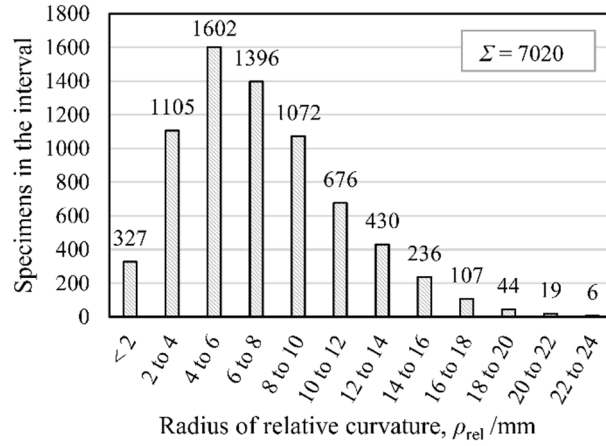
Figure 3 – Distribution of radii of relative curvature

Figure 4 – Test specimens

Five levels (measuring points) were then selected. To provide more precise results, the interval span was reduced after the initial analysis, resulting in a maximum relative curvature radius ρ_{relmax} of 21 mm. The internal levels were chosen as quartiles to increase the measurement grid density in the intervals of the highest specimen concentration. Load levels of $\rho_{\text{relQ1}} = 4.424$ mm (1755th value), $\rho_{\text{relQ2}} = 6.616$ mm (3510th value), and $\rho_{\text{relQ3}} = 9.494$ mm (5265th value) were chosen. The chosen radius of relative curvature values are:

$$\rho_{\text{rel}} = [1, 4.4, 6.6, 9.5, 21] \text{ mm} \tag{2}$$

Due to limited outer dimensions of the rotating specimen, its dimension was kept constant, meaning that the variations in the relative curvature were obtained by altering the tip radius of static specimens. The radius of all rotating specimens was selected as $\rho_{\text{rot}} = 25$ mm, and the dimensions of the tip radius of the static specimens were subsequently calculated using [28]:

$$\rho_{\text{stat}} = \frac{\rho_{\text{rot}} \cdot \rho_{\text{rel}}}{\rho_{\text{rot}} - \rho_{\text{rel}}}, \tag{3}$$

resulting in $\rho_{\text{stat}} = [1, 5.4, 9, 15.3, 131]$ mm.

2.2.3. Normal load

In thermoplastic gears, the gear pair load capacity is limited by tooth root bending strength, flank durability, tooth temperature, and tip deformation [29]. Since the flank temperature and Hertzian stress were shown to be limiting factors [22], the normal load levels were chosen accordingly. The highest normal loads according to the flank temperature and Hertzian stress were calculated according to the VDI guidelines [29] for each of the sample population specimens. The selection process is shown in Figure 5, while the values of constant parameters are discussed in Section 2.2.5.
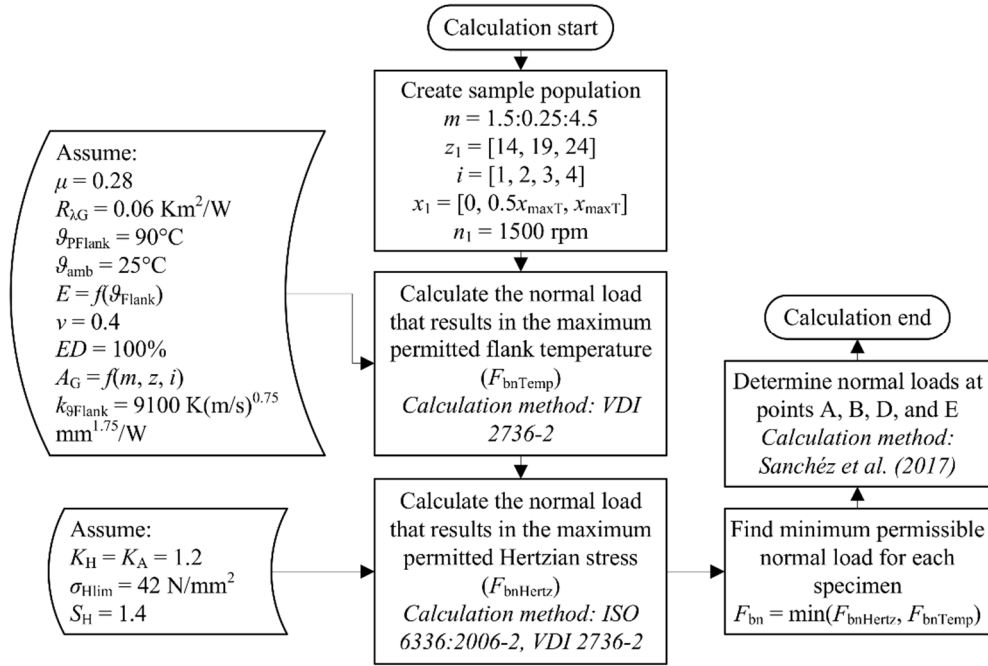
Figure 5 – Calculation of highest permitted normal load

The load acting on the flanks of gears in mesh varies along the pitch line. In standard gear profiles (as defined in ISO 53:1998 [30]), the transverse contact ratio ε_α is between 1.2 (the advised value) and 1.98 [28,31]. The mesh stiffness varies along the line of action, causing the unequal load distribution between the simultaneously meshing teeth. To determine the exact load distribution, approximate expressions provided by Sanchez et al. in [25] are used. The gear face width $b = 15$ mm was used for all specimens.
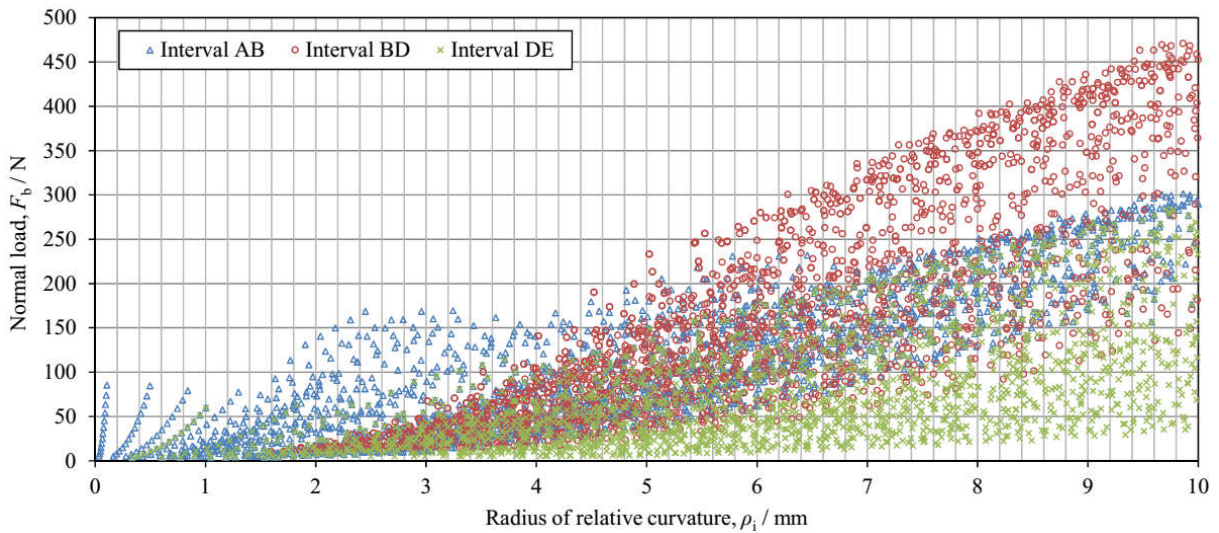
Figure 6 – Load levels determined using the sample population

The resulting normal loads are shown in Figure 6. Three load levels were chosen for each radius of relative curvature selected in Section 2.2.2: the highest value found in Figure 6, the lowest value, and the mid-point (see Table 1). For the radius of relative curvature of 21 mm, the normal load identical to that used for 9.5 mm specimens was used. It should be noted that the load levels for specimens with radii of relative curvature of 9.5 mm and 21 mm were planned as 15 N, 240 N, and 450 N, according to the data shown in Figure 6. However, such loads resulted in excessive damage in both cases (shown in Figure 10). A detailed explanation is given in Section 4, i.e. Discussion.

127

Table 1 – The normal load values used in the experiment

		Normal load [N]		
		I	II	III
Radius of relative curvature [mm]	1	15	35	55
	4.4	15	82.5	150
	6.6	15	165	310
	9.5	15	170	325
	21	15	170	325

2.2.4. Sliding velocity

The influence of sliding velocity on the friction coefficient was also observed. The highest sliding velocities along the path of contact are found either in point A or in point E, depending on the profile shift coefficients of the pinion and the wheel. The sliding velocity is equal to 0 at the pitch point C, after which its direction changes. At an arbitrary point, however, the sliding velocity is a function of the rotational velocity, the transmission ratio, the radius of curvature, and the working pressure angle α_w, as shown in [23]:

$$|v_s(\rho)| = \begin{cases} 2\pi n_1 \left(1 + \dfrac{1}{i}\right)(\rho_i - r_{b1} \tan \alpha_w); & \rho_i = [\rho_A, \rho_C] \\ 2\pi n_1 \left(1 + \dfrac{1}{i}\right)(r_{b1} \tan \alpha_w - \rho_i); & \rho_i = [\rho_C, \rho_E] \end{cases} \tag{4}$$

To simplify expression (4), the working pressure angle α_w was calculated for non-standard centre distances a_w resulting from the existing profile shift coefficients; subsequently, the sliding velocities were calculated for points A, B, D, and E. A rotational velocity of 1500 rpm was used. The results are shown in Figure 7.

Four sliding velocity levels, uniformly distributed across the interval, levels were chosen based on the results. The sliding velocity of $v_{Smin} = 0.05$ m/s was chosen as the lowest, as the low sliding velocities are present in the proximity of pitch point. The highest sliding velocity to be measured is $v_{Smax} = 2.7$ m/s (i.e. the highest velocity that can be measured). The sliding velocities higher than v_{Smax}, which could be found in rare cases were not considered for two reasons: the intensive wear and limitations of the experimental rig. Generally, high sliding velocities are avoided through the selection of profile shift coefficients. Finally, two mid-points were chosen: $v_{S2} = 0.9$ m/s and $v_{S3} = 1.9$ m/s, resulting in a sliding velocity vector expressed as follows:

$$v_s = [0.05, 0.9, 1.9, 2.7] \text{ m/s} \tag{5}$$
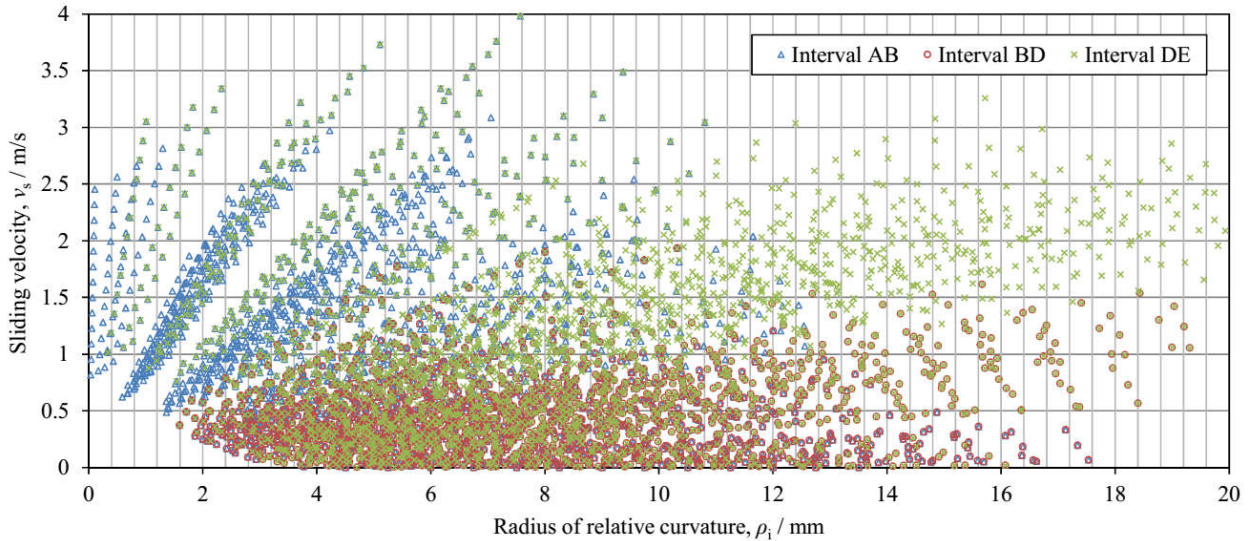
Figure 7 – Sliding velocity distribution

128

2.2.5. Control variables

A number of constants and assumptions were required to design the experiment. The constant Poisson coefficient $v = 0.4$ [29] was used for all the calculations. The Young modulus E [N/mm^2] is affected by temperature; its value was found in [32]. The cubic interpolation results in the following expression:

$$E_{\text{POM}} = 0.0008 \cdot \vartheta^3 - 0.1188 \cdot \vartheta^2 - 20.855 \cdot \vartheta + 3856.5 \qquad (6)$$

To determine the permissible normal loads regarding the flank temperature, the VDI 2736 [29] data was used. The friction coefficient was $\mu = 0.28$. The housing was assumed to be closed, resulting in $R_{\lambda G} = 0.06$ Km^2/W. A full load spectre was assumed ($ED = 100\%$), along with the effective gear flank heat conductivity $k_{9\text{Flank}} = 9100$ K(m/s)$^{0.75}$mm$^{1.75}$/W. The permissible flank pressure for POM/POM gear pairs was not found in [29] and was thus selected from [32] for the operating temperature of 90 °C and $2\cdot10^6$ load cycles. The outer housing surface A_G [mm^2] was simplified and calculated as a function of gear module m, gear face width b, centre distance a_w, and kinematic diameter of the wheel d_{w2}:

$$A_G = (2a_w + 4m) \cdot (d_{w2} + 2m) \cdot (b + 2m) \qquad (7)$$

2.3. Design of experiment

The experiment was designed as a full factorial with three variables: radius of relative curvature, specific load, and sliding velocity. Five levels of the relative curvature radii (thus, five static specimens), four sliding velocity levels, and three normal load levels were used, resulting in 60 experimental runs. The measurements were carried out three times, resulting in a total of 180 experimental runs. Order in which the measurements were carried out was randomized for each pair. The sliding velocity and the load were constant during each run, which lasted 10 s with a 60 s pause between two consecutive runs.

3. Experimental results and modelling

A total of 180 experimental runs were completed. The results are presented in Figure 8, while the friction coefficients measured for each of the replications can be found in Appendix A. The measured friction coefficient values varied greatly; $\mu = [0.032, 0.709]$. The lowest value was measured in a specimen of 21 mm radius of relative curvature running under a load of 353 N at a sliding velocity of 0.9 m/s, while the highest value was measured in a specimen of 6.6 mm radius of relative curvature running under a load of 15 N load at a sliding velocity of 2.7 m/s.

The normal load has the most significant influence on the friction coefficient (Figure 8; see also Appendix D for more details). With an increase in the normal load, the friction coefficient decreases. Higher values of friction coefficient were generally measured for lower load levels. The values of friction coefficient gradually decreased as the normal load increased, with a steeper decrease in the lower load levels. The exception were specimens with the smallest radius of relative curvature ($\rho_{\text{rel}} = 1$ mm), running at the lowest sliding velocity ($v_s = 0.05$ m/s). In such specimens, the lowest friction coefficient values were measured for the medium load level (35 N). Finally, it should be added that the relation between the normal load and friction coefficient is complex and is further discussed in Section 4.
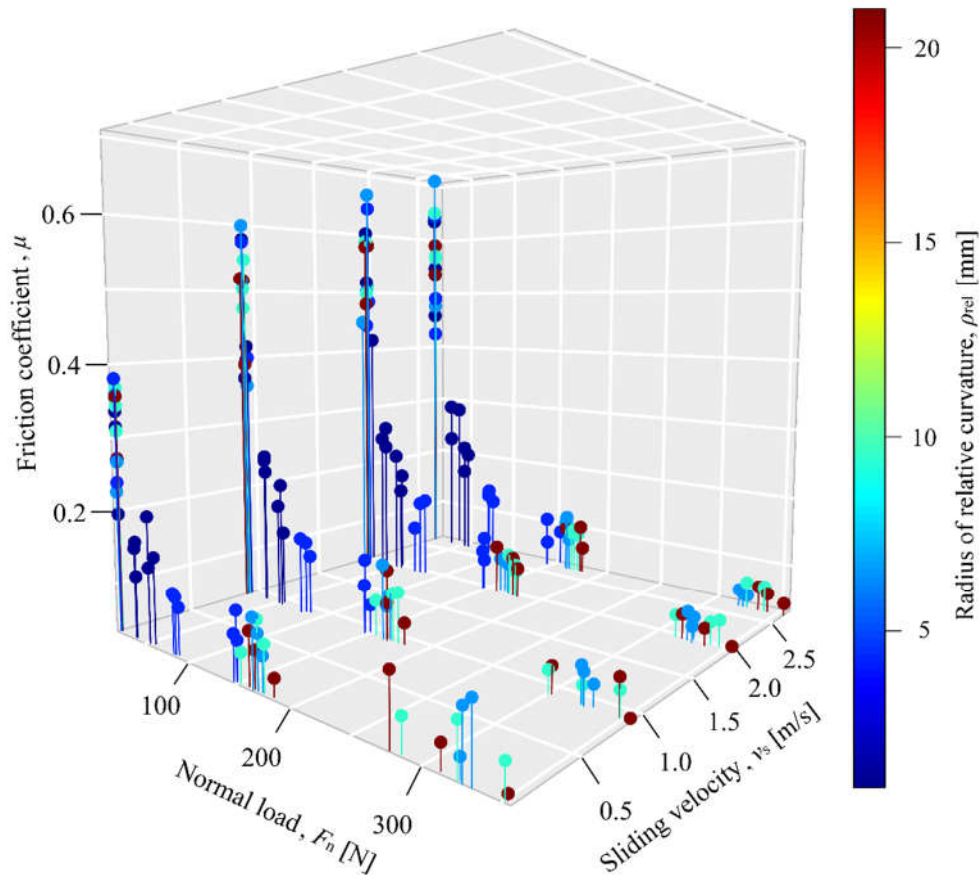
Figure 8 – Experimental results (for greyscale version see Appendix B)

The radius of relative curvature was shown to have a rather modest influence, as seen in Figure 8; the radii of relative curvature of 6.6 mm, 9.5 mm, and 21 mm are scattered at both the medium (165 N) and heavy (325 N) load levels. For a detailed display, see Appendix C. It must be stressed that load levels were chosen for each of the radii separately, which means that a direct comparison is not possible for all the radii. Only the specimens running under the "low load" can be compared directly, as the low load is 15 N for all the pairs. In specimens working under the 15 N load, small variations in the friction coefficient were found with an increase in the radius of relative curvature for all three replications. A slight increase was found in pairs working at a sliding velocity of 2.7 m/s. For medium and heavy loads, a direct comparison is possible only for specimens with 6.6, 9.5, and 21 mm radius of curvature due to the similar load levels. In those specimens, the radius of relative curvature was found to have no influence on the friction coefficient, regardless of the sliding velocity. At medium and heavy loads, similar trends and values were found among the replications. The scatter occurring at a radius of relative curvature of 1 mm should also be noted. As seen in Appendix A 1 mm radius in combination with a low normal load (15 N) resulted in the highest dissipation of measured values. The most likely reason is an increase in the influence of frictional force between the load cell and the experimental rig housing due to the low normal load, in combination with measured values being on the lower end of the load cell spectrum.

The sliding velocity had the greatest impact on the friction coefficient at lower load levels, where the friction coefficient rose with the increase in velocity, as shown in Figure 8. For more details, see Appendix E. At low loads, the friction coefficient increased with the increase in the sliding velocity, regardless of the radius of relative curvature. The increase was steeper at lower velocities. In medium and heavy loads, the influence of sliding velocity on the friction coefficient was not found, with the exception of specimens with 1 mm radius of curvature, in which the friction coefficient slightly increased with the sliding velocity. The result scatter was higher in the specimens with the radius of relative curvature of 1, 4.4, and 6.6 mm operating at low loads. The sliding velocity did not affect the scattering.

3.1. Friction coefficient prediction

After carrying out the experiment, results were used to find a function that could reliably predict the friction coefficient for PTFE-lubricated POM spur gears. To account for the changes in face width, the specific load w was used instead of the normal load F_n. The suggested model (8) was based on the formulation proposed by Schlenk [8,24]:

$$\mu = c_0 + c_1 \cdot \rho_{rel}^{c_2} \cdot w^{c_3} \cdot v_s^{c_4} \tag{8}$$

The non-linear least squares (*nls*) function within the *R* software was used to fit the equation:

$$\mu(\rho_{rel}, w, v_S) = 0.054912 + 0.39837\rho_{rel}^{0.030658} \cdot w^{-1.0272} \cdot v_S^{0.17843}. \tag{9}$$

The goodness of the fit was evaluated by observing the residuals and by comparing the fitted function with the observed data. The residual plot is shown in Figure 9; no trends were observed as the index changes. The residuals also have no drift and the error is independent of the index. Lastly, no distinct pattern structures or curves were spotted. The residual standard error of 0.043 was calculated on 175 degrees of freedom. Therefore, it can be concluded that the fitted function properly describes the observed data.
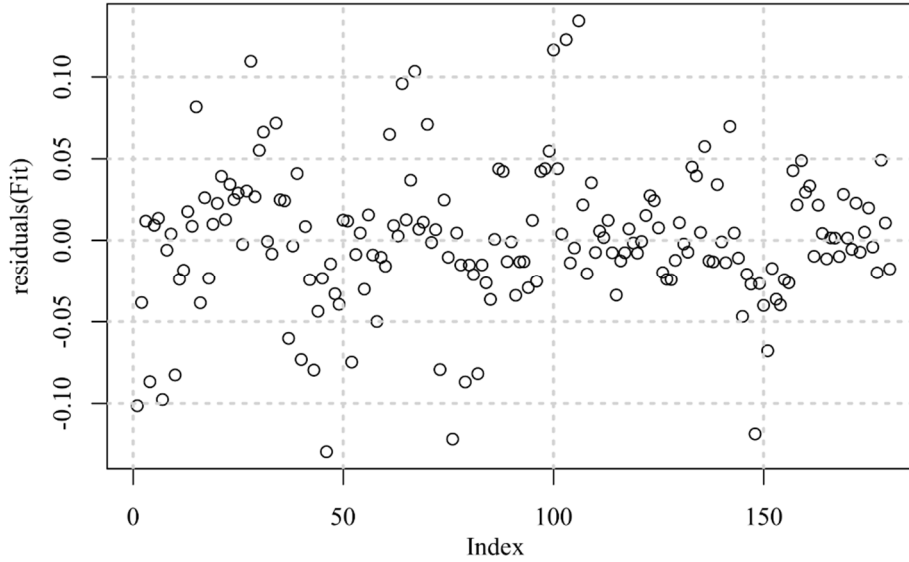
Figure 9 – Residuals between the observed and the fitted values

The resulting expression (9) is applicable within the experiment boundaries (10):

$$\begin{aligned} \rho_{rel} &\in [1, 21] \text{ mm} \\ v_S &\in [0.05, 2.7] \text{ m/s} \\ F_n &\leq f(\rho_{rel}) \end{aligned} \tag{10}$$

The upper normal load F_n is limited by the Hertzian stress and the flank temperature. The simplified function (11) is included to make the finding of the maximum F_n for which the prediction is reliable. The simplified function is obtained by fitting a polynomial to the experimental and the sample population (Figure 4) data. The face width b of 15 mm was used to derive it.

$$\frac{F_n}{b}(\rho_{rel}) = \begin{cases} 3.66 \text{ N/mm} & \rho_{rel} < 1 \text{ mm} \\ (0.1542\rho_{rel}^3 - 1.3704\rho_{rel}^2 + 5.6297\rho_{rel} - 0.5736) \text{ N/mm}; & 1 \text{ mm} \leq \rho_{rel} \leq 6.6 \text{ mm} \\ 21.66 \text{ N/mm} & \rho_{rel} > 6.6 \text{ mm} \end{cases} \tag{11}$$

Using the experimental rig described in Section 2.1, it was not possible to measure the friction coefficient at sliding velocities below 0.05 m/s. If expression (9) is to be used for power loss prediction, the friction coefficient could be predicted for $v_s < 0.05$ m/s as $\mu(v_s < 0.05 \text{ m/s}) = \mu(v_s = 0.05 \text{ m/s})$. The error would be smaller as the

sliding velocity is directly responsible for the power losses, which means that lower velocities decrease power losses.

4. Discussion

The experiment was organised as full factorial as the influence of individual parameters was not known. Also, it was hard to anticipate all the interactions between parameters, and whether there are saddle points within the observed interval. Thus, it was decided to cover the entire range. The normal load, sliding velocity, and radius of relative curvature were selected as experimental variables as they were included in the vast majority of models for prediction of friction coefficient in gear pairs [6–8,24]. Carrying out a full factorial experiment requires a large number of experimental runs, which were possible due to a short time interval of each run.

Expression (9) is meant to be used in the optimization of spur gear pairs made of POM. When the prediction of the friction coefficient is made possible, it is possible to calculate the efficiency using the expression provided by Diez-Ibarbia et al. [33]. The efficiency could be used as the objective function.

The normal load was found to have a dominant influence on the friction coefficient which decreases with an increase in load. Initially, experimental runs for specimens with radii of relative curvature of 9.5 and 21 mm were conducted under the 450 N load as the highest load (as obtained by calculation). However, when specimens were exposed to a combination of high load (450 N) and high sliding velocity (2.7 m/s), intensive wear occurred (Figure 10). After 5 to 7 seconds, the specimens melted (2nd and 3rd static specimen in Figure 10). Thus, the normal load levels were adjusted to enable the experiment. Similar behaviour was reported by Mao et al. [34] and Breeds et al. [35], who stated that when the torque is below the critical value, the wear rate of POM gears is very low. A further increase in torque dramatically increased the wear rate and caused the softening and the subsequent failure of gears. When compared to the static specimens used in the experiment, the gear flanks last longer as each flank is in contact for only a fraction of a load cycle. Furthermore, it is not possible to determine whether the increase in friction coefficient is caused solely by the normal load. An increase in normal load also causes an increase in temperature, which was known to affect the friction coefficient [18]. The necessary data could be obtained by including the temperature as a variable [34]. However, it would significantly increase the complexity of the experimental, as each test specimen should be heated to a specific temperature prior to the measurement. In this study, the temperature was not considered since the measurement times were low (10 s) and no significant variations in the measured friction coefficient during each experimental run were observed.

The sliding velocity caused an increase in the values of friction coefficient in specimens running under lighter loads. The influence diminished as the load increased. Walton et al. [36] also found that the friction coefficient in POM gear pairs increased with the increase in sliding velocity up to a rotational speed of 1000 rpm. Specimens operating under heavier loads were also found to be less affected by the sliding velocity.

The radius of relative curvature has a minor influence on the friction coefficient. With the exceptions of radii of relative curvature between 1 and 6.6 mm, no effect was found. Such observation is fortunate as severe gear tooth deformations, in combination with wear, impact the gear geometry by changing the curvature radii of both the pinion and the wheel teeth. Further investigations are needed to determine whether the influence of curvature may be neglected.

Figure 10 – Damaged static (left) and rotating (right) specimens

The intensive wear occurred while testing 9 mm and 15.3 mm radii specimens, corresponding to $\rho_{rel} = \{6.6, 9.5\}$. Unsuccessful runs were discarded and repeated; one run for 9 mm specimen, and two for 15.3 mm. In leftmost static specimen (Figure 10) the wear is most probably a result of a broken-of particle entering the contact while in the 2nd and 3rd specimen, the damage was caused by temperature overload. Such processes resulted in non-uniform frictional forces across the contact width, resulting in rotation of the specimen around the y-axis (Figure 1b) and subsequently, asymmetric wear. For this reason, it is advised to include wear as a criterion when selecting the measuring points (Figure 5).

The results are in agreement with studies conducted by other researchers who used both gears and simplified models. The most notable examples include the studies done by Mao et al. [34] and Walton et al. [36]. Lastly, the accuracy of the suggested expression could be further improved by including influences of the slide-to-roll ratio and temperature.

4.1. Example of the friction coefficient along the pitch line

To better illustrate the application of expression (9), the friction coefficient was calculated for five arbitrary sets (Table 2) of input parameters. The load distribution on gear teeth pairs is calculated using the approximate equations created by Sanchez et al. [25]. The coordinate ψ [mm] corresponds to the pinion flank curvature radius. Sets are chosen to display how the variations in one of the parameters affect the results; the effects of the operational torque, the pinion and wheel profile shift coefficients, and the rotational velocity were considered.

Table 2 – Arbitrary datasets

		Set 1	Set 2	Set 3	Set 4	Set 5	Set 6
Gear module	m, / mm	4					
Face width	b, / mm	15					
Pinion number of teeth	z_1	20					
Wheel number of teeth	z_2	20					40
Operational torque	T, / Nm	12	12	12	12	14	12
Pinion profile shift coefficient	x_1	0	0.2	0.2	0	0	0
Wheel profile shift coefficient	x_2	0	0.2	0	0	0	0
Rotational speed (pinion)	n_1, / rpm	1000	1000	1000	1200	1000	1000

The resulting friction coefficient distribution along the pitch line is shown in Figure 11. The influence of load level is considerable because the friction coefficient decreases between the points B and D, where only one pair of teeth is in mesh. When considering intervals AB and DE, the results are different from those in the existing literature [9,11] since most of the studies were conducted using a liquid lubricant. In the cases with liquid lubricants, increased sliding velocity has a beneficial effect on the oil film formation. Thus, at higher sliding velocities found in the proximity of points A and E friction is reduced. In the presented study, an increase in sliding velocity resulted in an increase in the value of friction coefficient, causing an exponential increase in friction coefficients when approaching the points A and E.
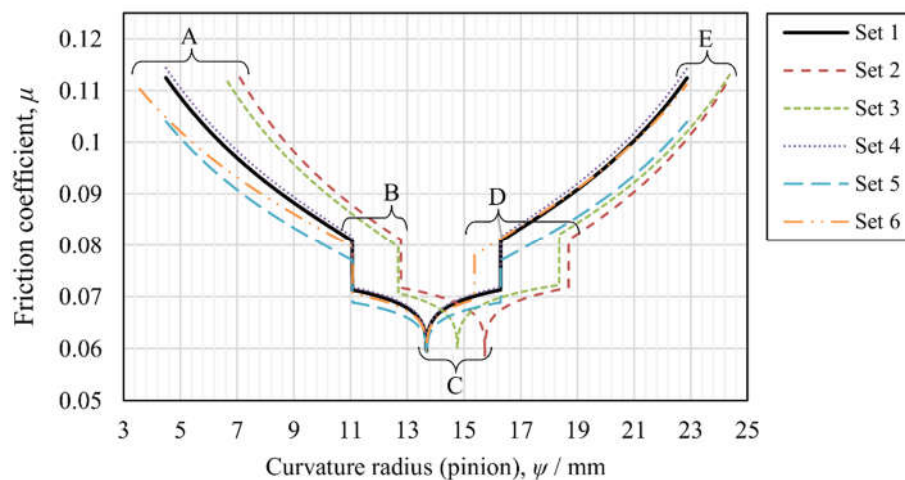
Figure 11 – Predicted friction coefficient along the pitch line

Furthermore, the effects of an increased load (Set 5) and increased sliding velocity (Set 4) are apparent, as can be seen from Figure 8. Variations in the profile shift coefficients x_1 and x_2 have minor influence, as expected. The increase in the profile shift coefficient mainly affects the radius of curvature, which was found to have a near-negligible impact. The diagram is shifted to the right hand side due to the increases in the overall curvature.

5. Conclusion

An experimental study using simplified models was conducted with the aim of providing an expression for the prediction of friction coefficient in polyoxymethylene spur gear pairs. The motive was to increase the precision of flank prediction expressions found in technical guidelines [29] and to enable the optimization of gear pairs made of POM. The friction coefficient function was found by fitting a function to experimental dataset consisting of 60 points, tested three times. The effects of radius of relative curvature, normal load, and sliding velocity were assessed. The following conclusions can be made for the examined pair of materials:

1. The function fitted to experimental data was assessed; by observing the residuals, it was determined that the fitted function properly describes the observed data.
2. When compared to other gear pair friction coefficient models, a difference in trends along the intervals with higher sliding velocities notably the AB and DE intervals, is found. The most likely reason is a combination of lower normal load and higher sliding velocity found at the mesh start since both were found to result in an increase of friction coefficient. The second likely reason is the lack of an oil film; most of the studies on friction in gear pairs were conducted using lubricated steel gears, where an increase in the sliding velocity has a beneficial effect on the hydrodynamic lubrication. In the presented study, the lubricant film is dry (dry PTFE was used as a lubricant), meaning that there is no oil wedge.
3. The normal load has dominant influence on the friction coefficient between the specimens of POM pairs. With the increase in load, the friction coefficient decreases; the change is more marked at lower load levels.
4. The sliding velocity also affected the friction coefficient; its value increased as the sliding velocity increased. Variations were more prominent in specimens running under lighter loads.
5. The radius of relative curvature had a rather small amount of influence on the results.

Limitations of the presented study should be addressed. The number of variables was limited to ensure a reasonable number of experimental runs, as the experiment was designed as full factorial aiming to increase robustness. Thus, influences of temperature and slide-to-roll ratio were not examined. The former was not considered as experimental runs were short (10 s), implying a small change in temperature. By including the temperature, it would be possible to gain more insight into the tribological properties, such as the influence of normal load on the friction coefficient. The slide-to-roll ratio was also not considered, even though there is evidence showing that it affects the friction coefficient. Finally, it should be noted that including temperature and the slide-to-roll ratio would drastically increase the complexity of the experiment.

Verification of the results on gear pairs will be conducted in a future study. The power losses calculated using the predicted friction coefficient will be compared with those measured by means of an open-circuit device.

Nomenclature

A_G	: outer housing surface, mm^2
b	: face width, mm
ED	: load spectre, %
F_n	: normal load, N
$F_{bnHertz}$	: largest normal load allowed (in relation to the Hertzian stress), N
F_{bnTemp}	: largest normal load allowed (in relation to the tooth temperature), N
i	: transmission ratio
k_{9Flank}	: effective gear flank heat conductivity, K(m/s)$^{0.75}$mm$^{1.75}$/W
m	: gear module, mm
n_1	: rotational speed (pinion), rpm
$R_{\lambda G}$	: calculation factor accounting for the housing design (open or closed), Km^2/W
T_m	: measured torque, Nm
v_S	: sliding velocity, m/s
w	: specific load (F_n/b), N/mm
x_1	: profile shift coefficient (pinion)
x_2	: profile shift coefficient (wheel)
x_{maxT}	: maximum allowable profile shift coefficient (in relation to the tooth tip thickness)

z_1 : number of teeth (pinion)
z_2 : number of teeth (wheel)
μ : friction coefficient
ρ : curvature radius, mm
ρ_{rel} : radius of relative curvature, mm
ρ_{rot} : radius of a rotating specimen, mm
ρ_{stat} : radius of a static specimen, mm
σ_{Hlim} : allowable stress number (contact)
ϑ : larger of the tooth root and flank temperatures, °C

Acknowledgement

Appendix A: Experimental data

Table 3 – Experimental data

No.	Radius of relative curvature [mm]	Sliding velocity [m/s]	Normal load [N]	Measurement order			Static specimen No.			Rotating specimen No.			Friction coefficient		
Replication number:				1	2	3	1	2	3	1	2	3	1	2	3
1	1	0.05	15	3	8	9	1.11	1.12	1.13	2.11	2.12	2.13	0.195	0.315	0.336
2	1	0.05	35	2	3	2	1.11	1.12	1.13	2.11	2.12	2.13	0.116	0.163	0.154
3	1	0.05	55	8	12	7	1.11	1.12	1.13	2.11	2.12	2.13	0.134	0.203	0.149
4	1	1	15	7	2	12	1.11	1.12	1.13	2.11	2.12	2.13	0.368	0.416	0.578
5	1	1	35	9	5	5	1.11	1.12	1.13	2.11	2.12	2.13	0.227	0.245	0.250
6	1	1	55	10	1	11	1.11	1.12	1.13	2.11	2.12	2.13	0.180	0.139	0.213
7	1	2	15	4	7	6	1.11	1.12	1.13	2.11	2.12	2.13	0.417	0.518	0.602
8	1	2	35	11	9	3	1.11	1.12	1.13	2.11	2.12	2.13	0.235	0.267	0.249
9	1	2	55	12	11	4	1.11	1.12	1.13	2.11	2.12	2.13	0.187	0.223	0.164
10	1	3	15	6	4	10	1.11	1.12	1.13	2.11	2.12	2.13	0.458	0.548	0.635
11	1	3	35	1	6	1	1.11	1.12	1.13	2.11	2.12	2.13	0.229	0.289	0.281
12	1	3	55	5	10	8	1.11	1.12	1.13	2.11	2.12	2.13	0.171	0.215	0.203
13	4.4	0.05	15	5	4	8	1.21	1.22	1.23	2.21	2.22	2.23	0.239	0.268	0.381
14	4.4	0.05	82.5	6	9	1	1.21	1.22	1.23	2.21	2.22	2.23	0.094	0.111	0.107
15	4.4	0.05	150	10	3	2	1.21	1.22	1.23	2.21	2.22	2.23	0.119	0.090	0.081
16	4.4	1	15	12	12	11	1.21	1.22	1.23	2.21	2.22	2.23	0.399	0.395	0.575
17	4.4	1	82.5	8	2	4	1.21	1.22	1.23	2.21	2.22	2.23	0.135	0.115	0.141
18	4.4	1	150	4	7	10	1.21	1.22	1.23	2.21	2.22	2.23	0.070	0.099	0.132
19	4.4	2	15	9	6	12	1.21	1.22	1.23	2.21	2.22	2.23	0.443	0.484	0.645
20	4.4	2	82.5	1	11	5	1.21	1.22	1.23	2.21	2.22	2.23	0.105	0.153	0.148
21	4.4	2	150	7	8	9	1.21	1.22	1.23	2.21	2.22	2.23	0.077	0.091	0.111
22	4.4	3	15	2	5	6	1.21	1.22	1.23	2.21	2.22	2.23	0.424	0.491	0.644
23	4.4	3	82.5	11	10	3	1.21	1.22	1.23	2.21	2.22	2.23	0.124	0.133	0.142
24	4.4	3	150	3	1	7	1.21	1.22	1.23	2.21	2.22	2.23	0.070	0.085	0.110
25	6.6	0.05	15	3	4	2	1.31	1.32	1.33	2.31	2.32	2.33	0.226	0.267	0.359
26	6.6	0.05	165	10	1	6	1.31	1.32	1.33	2.31	2.32	2.33	0.100	0.076	0.119
27	6.6	0.05	310	4	8	12	1.31	1.32	1.33	2.31	2.32	2.33	0.055	0.108	0.119
28	6.6	1	15	2	10	10	1.31	1.32	1.33	2.31	2.32	2.33	0.356	0.517	0.599
29	6.6	1	165	7	2	8	1.31	1.32	1.33	2.31	2.32	2.33	0.094	0.077	0.134
30	6.6	1	310	5	6	5	1.31	1.32	1.33	2.31	2.32	2.33	0.057	0.072	0.077

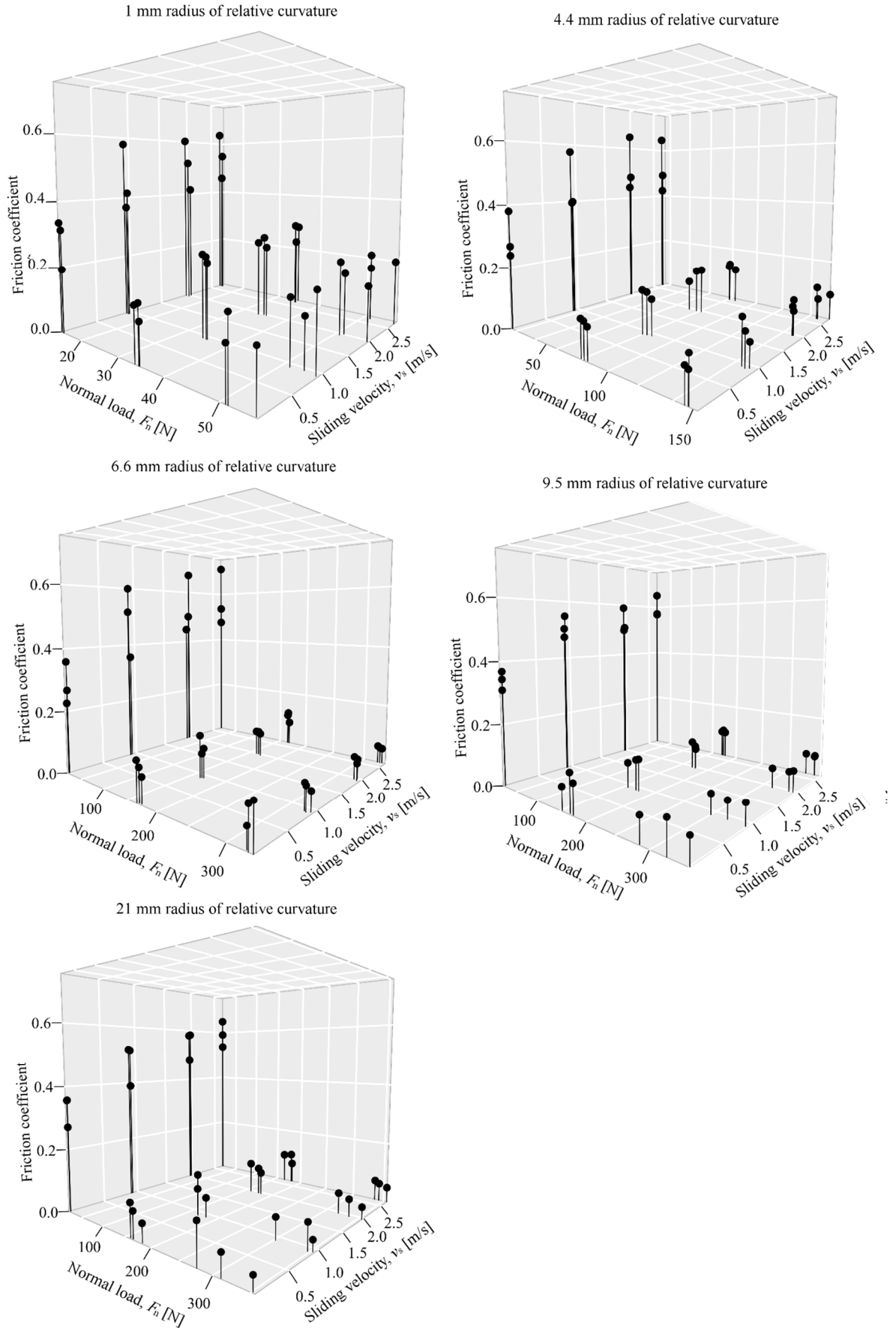| 31	6.6	2	15	11	5	11	1.31	1.32	1.33	2.31	2.32	2.33	0.449	0.502	0.668
32	6.6	2	165	1	12	1	1.31	1.32	1.33	2.31	2.32	2.33	0.079	0.082	0.083
33	6.6	2	310	12	7	7	1.31	1.32	1.33	2.31	2.32	2.33	0.054	0.062	0.071
34	6.6	3	15	9	9	4	1.31	1.32	1.33	2.31	2.32	2.33	0.477	0.537	0.709
35	6.6	3	165	8	11	9	1.31	1.32	1.33	2.31	2.32	2.33	0.082	0.110	0.119
36	6.6	3	310	6	3	3	1.31	1.32	1.33	2.31	2.32	2.33	0.050	0.051	0.056
37	9.5	0.05	15	10	2	6	1.41	1.42	1.43	2.41	2.42	2.43	0.344	0.309	0.368
38	9.5	0.05	170	1	4	8	1.41	1.42	1.43	2.41	2.42	2.43	0.070	0.090	0.116
39	9.5	0.05	325	2	7	3	1.41	1.42	1.43	2.41	2.42	2.43	0.070	0.092	0.072
40	9.5	1	15	6	5	5	1.41	1.42	1.43	2.41	2.42	2.43	0.474	0.504	0.548
41	9.5	1	170	8	3	11	1.41	1.42	1.43	2.41	2.42	2.43	0.100	0.097	0.080
42	9.5	1	325	7	1	2	1.41	1.42	1.43	2.41	2.42	2.43	0.064	0.053	0.061
43	9.5	2	15	4	11	10	1.41	1.42	1.43	2.41	2.42	2.43	0.499	0.510	0.588
44	9.5	2	170	3	10	1	1.41	1.42	1.43	2.41	2.42	2.43	0.080	0.069	0.093
45	9.5	2	325	12	8	4	1.41	1.42	1.43	2.41	2.42	2.43	0.067	0.062	0.062
46	9.5	3	15	5	12	7	1.41	1.42	1.43	2.41	2.42	2.43	0.568	0.571	0.651
47	9.5	3	170	9	6	12	1.41	1.42	1.43	2.41	2.42	2.43	0.094	0.094	0.101
48	9.5	3	325	11	9	9	1.41	1.42	1.43	2.41	2.42	2.43	0.068	0.069	0.065
49	21	0.05	15	9	5	6	1.51	1.52	1.53	2.51	2.52	2.53	0.272	0.357	0.356
50	21	0.05	170	6	4	2	1.51	1.52	1.53	2.51	2.52	2.53	0.054	0.099	0.078
51	21	0.05	325	4	9	1	1.51	1.52	1.53	2.51	2.52	2.53	0.038	0.116	0.061
52	21	1	15	1	11	4	1.51	1.52	1.53	2.51	2.52	2.53	0.389	0.520	0.517
53	21	1	170	7	12	3	1.51	1.52	1.53	2.51	2.52	2.53	0.061	0.125	0.083
54	21	1	325	2	3	10	1.51	1.52	1.53	2.51	2.52	2.53	0.032	0.065	0.077
55	21	2	15	8	2	7	1.51	1.52	1.53	2.51	2.52	2.53	0.481	0.582	0.580
56	21	2	170	12	6	9	1.51	1.52	1.53	2.51	2.52	2.53	0.076	0.103	0.090
57	21	2	325	3	7	5	1.51	1.52	1.53	2.51	2.52	2.53	0.038	0.065	0.055
58	21	3	15	10	1	12	1.51	1.52	1.53	2.51	2.52	2.53	0.537	0.590	0.648
59	21	3	170	5	8	11	1.51	1.52	1.53	2.51	2.52	2.53	0.071	0.100	0.106
60	21	3	325	11	10	8	1.51	1.52	1.53	2.51	2.52	2.53	0.049	0.066	0.058

Appendix B: Black and white version

1 mm radius of relative curvature

4.4 mm radius of relative curvature

6.6 mm radius of relative curvature

9.5 mm radius of relative curvature

21 mm radius of relative curvature

Figure 12 – Greyscale version of the overall data

137

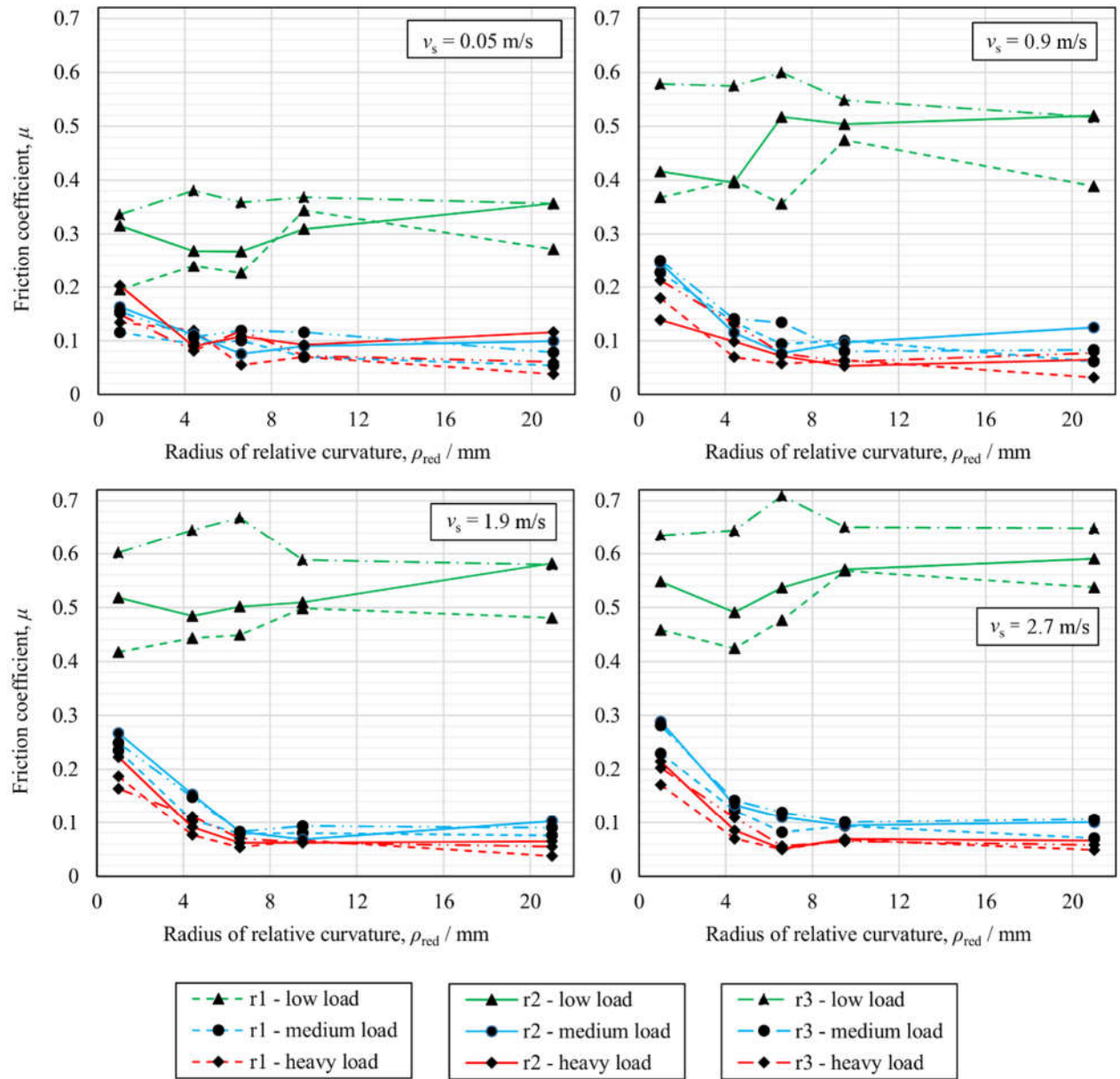## Appendix C: The radius of relative curvature

Figure 13 - Influence of the radius of relative curvature on the friction coefficient
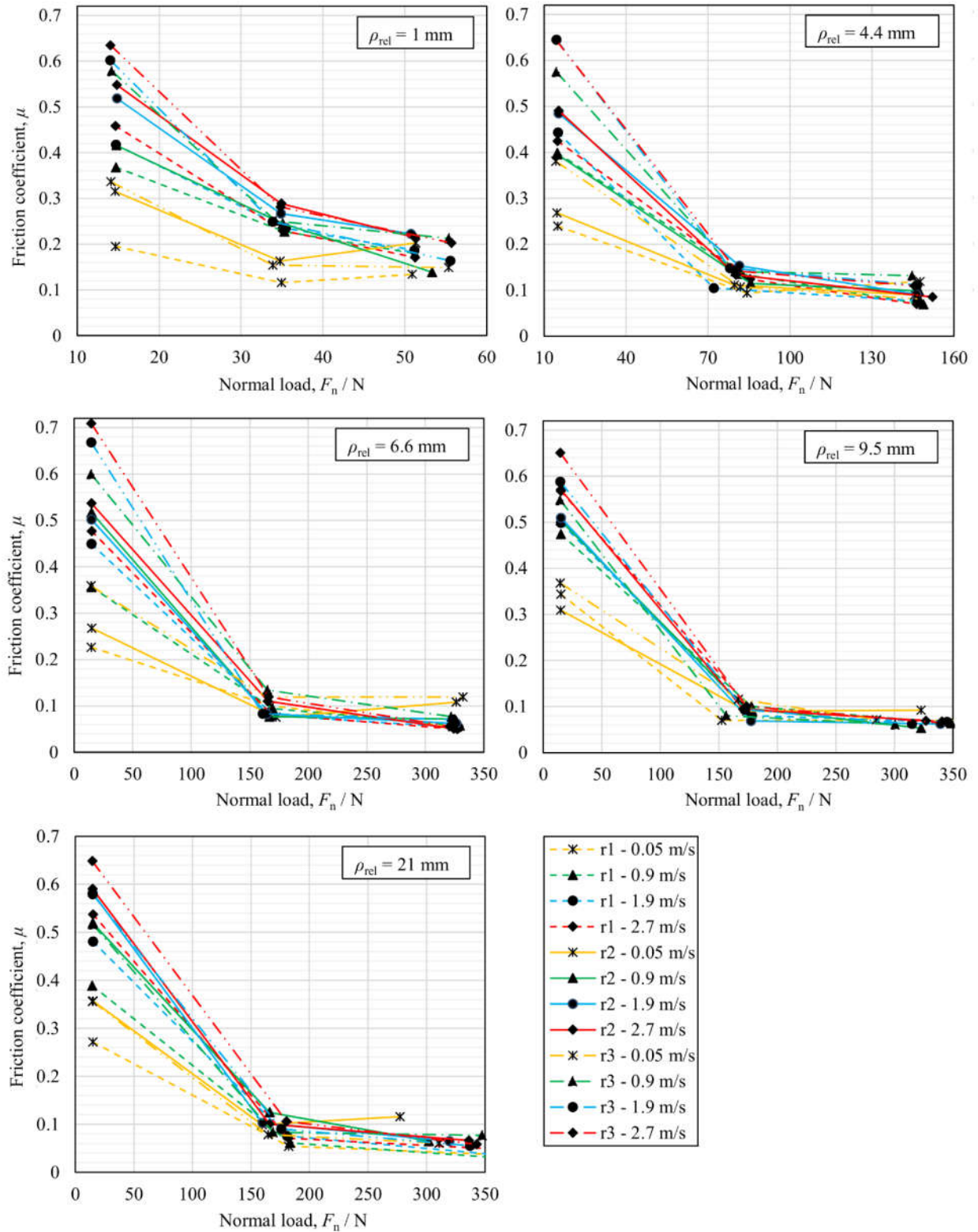
Appendix D: The normal load

Figure 14 - Influence of normal load on the friction coefficient
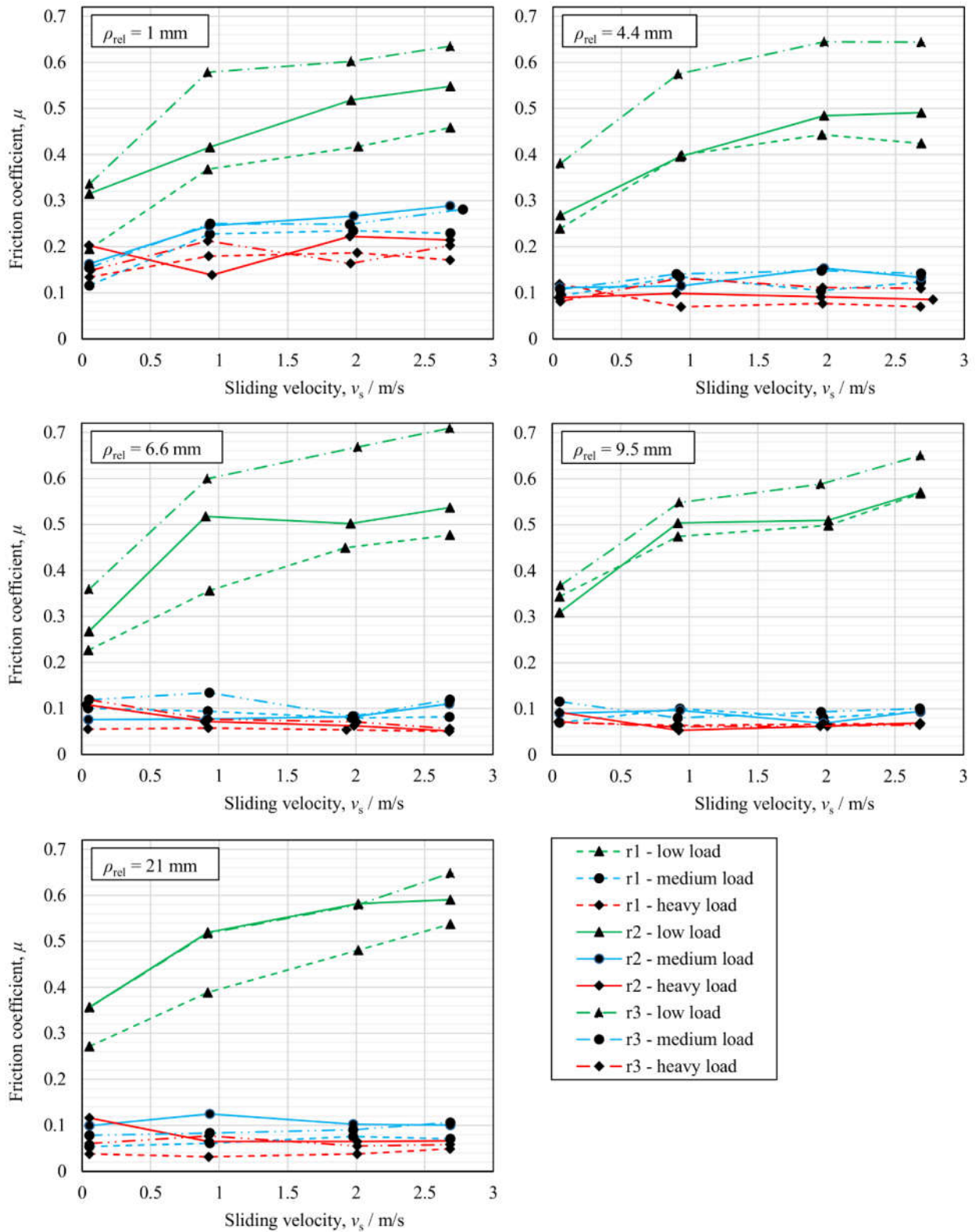
Appendix E: The sliding velocity

Figure 15- Influence of sliding velocity on the friction coefficient

References

[1] J. Duhovnik, D. Zorko, L. Sedej, The effect of the teeth profile shape on polymer gear pair properties, Tehnicki Vjesnik - Technical Gazette. 23 (2016) 199–207. doi:10.17559/TV-20151028072528.

[2] K. Terashima, N. Tsukamoto, N. Nishida, J. Shi, Development of Plastic Gear for Power Transmission: Abnormal Wear on the Tooth Root and Tooth Fracture near Pitch Point, Bulletin of JSME. 29 (1986) 1598–1604. doi:10.1299/jsme1958.29.1598.

[3] K. Michaelis, B. Höhn, M. Hinterstoißer, Influence factors on gearbox power loss, Industrial Lubrication and Tribology. 63 (2011) 46–55. doi:10.1108/00368791111101830.

[4] T.T. Petry-Johnson, A. Kahraman, N.E. Anderson, D.R. Chase, An experimental investigation of spur gear efficiency, Journal of Mechanical Design. 130 (2008) 62601. doi:10.1115/1.2898876.

[5] A. Diez-Ibarbia, A. Fernandez-del-Rincon, A. de-Juan, M. Iglesias, P. Garcia, F. Viadero, Frictional power losses on spur gears with tip reliefs. The load sharing role, Mechanism and Machine Theory. 112 (2017) 240–254. doi:10.1016/j.mechmachtheory.2017.02.012.

[6] S. Li, A. Kahraman, A Transient Mixed Elastohydrodynamic Lubrication Model for Spur Gear Pairs, Journal of Tribology. 132 (2010) 011501. doi:10.1115/1.4000270.

[7] N. Marjanovic, B. Ivkovic, M. Blagojevic, B. Stojanovic, Experimental determination of friction coefficient at gear drives, Journal of the Balkan Tribological Association. 16 (2010) 517–526.

[8] L. Schlenk, Untersuchungen zur Freßtragfähigkeit von Großzahnrädern (PhD Thesis), Technical University Munich, 1995.

[9] H. Xu, Development of a Generalized Mechanical Efficiency Prediction Methodology for Gear Pairs (PhD Thesis), The Ohio State University, 2005.

[10] S. Li, A. Kahraman, A Method to Derive Friction and Rolling Power Loss Formulae for Mixed Elastohydrodynamic Lubrication, Journal of Advanced Mechanical Design, Systems, and Manufacturing. 5 (2011) 252–263. doi:10.1299/jamdsm.5.252.

[11] C.M.C.G. Fernandes, R.C. Martins, J.H.O. Seabra, Coefficient of friction equation for gears based on a modified Hersey parameter, Tribology International. 101 (2016) 204–217. doi:10.1016/j.triboint.2016.03.028.

[12] K.D. Dearn, S.N. Kukureka, D. Walton, Engineering polymers and composites for machine elements, Polymer Tribology. (2009) 1–37. doi:doi:10.1142/9781848162044_0014.

[13] Y.K. Chen, S.N. Kukureka, C.J. Hooke, M. Rao, Surface topography and wear mechanisms in polyamide 66 and its composites, Journal of Materials Science. 35 (2000) 1269–1281. doi:10.1023/A:1004709125092.

[14] J.K. Lancaster, Estimation of the limiting PV relationships for thermoplastic bearing materials, Tribology. 4 (1971) 82–86. doi:10.1016/0041-2678(71)90136-9.

[15] B. Bin Jia, T.S. Li, X.J. Liu, P.H. Cong, Tribological behaviors of several polymer-polymer sliding combinations under dry friction and oil-lubricated conditions, Wear. 262 (2007) 1353–1359. doi:10.1016/j.wear.2007.01.011.

[16] S.N. Kukureka, Y.K. Chen, C.J. Hooke, P. Liao, The wear mechanisms of acetal in unlubricated rolling-sliding contact, Wear. 185 (1995) 1–8. doi:10.1016/0043-1648(94)06575-6.

[17] A.M. Chaudri, M. Suvanto, T.T. Pakkanen, Non-lubricated friction of polybutylene terephthalate (PBT) sliding against polyoxymethylene (POM), Wear. 342–343 (2015) 189–197. doi:10.1016/j.wear.2015.08.023.

[18] N.K. Myshkin, M.I. Petrokovets, A. V. Kovalev, Tribology of polymers: Adhesion, friction, wear, and mass-transfer, Tribology International. 38 (2005) 910–921. doi:10.1016/j.triboint.2005.07.016.

[19] A.K. Singh, Siddhartha, P.K. Singh, Polymer spur gears behaviors under different loading conditions: A review, Proceedings of the Institution of Mechanical Engineers, Part J: Journal of Engineering Tribology. 0 (2017) 135065011771159. doi:10.1177/1350650117711595.

[20] A. Pogačnik, J. Tavčar, An accelerated multilevel test and design procedure for polymer gears, Materials and Design. 65 (2015) 961–973. doi:10.1016/j.matdes.2014.10.016.

[21] J. Tavčar, G. Grkman, J. Duhovnik, Accelerated lifetime testing of reinforced polymer gears, Journal of Advanced Mechanical Design, Systems, and Manufacturing. 12 (2018) JAMDSM0006-JAMDSM0006. doi:10.1299/jamdsm.2018jamdsm0006.

[22] D. Miler, A. Lončar, D. Žeželj, Z. Domitran, Influence of profile shift on the spur gear pair optimization, Mechanism and Machine Theory. 117 (2017) 189–197. doi:10.1016/j.mechmachtheory.2017.07.001.

[23] D. Miler, D. Žeželj, A. Lončar, K. Vučković, Multi-objective spur gear pair optimization focused on volume and efficiency, Mechanism and Machine Theory. 125 (2018) 185–195. doi:10.1016/j.mechmachtheory.2018.03.012.

[24] B.R. Höhn, Improvements on noise reduction and efficiency of gears, Meccanica. 45 (2010) 425–437. doi:10.1007/s11012-009-9251-x.

[25] M.B. Sánchez, M. Pleguezuelos, J.I. Pedrero, Approximate equations for the meshing stiffness and the

load sharing ratio of spur gears including hertzian effects, Mechanism and Machine Theory. 109 (2017) 231–249. doi:10.1016/j.mechmachtheory.2016.11.014.

[26] A. Diez-Ibarbia, A.F. del Rincon, M. Iglesias, A. de-Juan, P. Garcia, F. Viadero, Efficiency analysis of spur gears with a shifting profile, Meccanica. 51 (2016) 707–723. doi:10.1007/s11012-015-0209-x.

[27] International Organization for Standardization, ISO 6336:2006 - Calculation of load capacity of spur and helical gears — Application for industrial gears, ISO, Geneva, Switzerland, 2006.

[28] H. Linke, J. Börner, R. Heß, Cylindrical gears Calculation – Materials – Manufacturing, Hanser Publications, 2016.

[29] VDI Verein Deutscher Ingenieure, VDI 2736 Thermoplastic gear wheels, (2014) 73.

[30] International Organization for Standardization, ISO 53:1998 - Cylindrical gears for general and heavy engineering — Standard basic rack tooth profile, 1998.

[31] B.S.P. Radzevich, Dudley's Handbook of Practical Gear Design and Manufacture, 2nd editio, CRC Press, Boca Raton, 2012.

[32] G. Erhard, Designing with Plastics, Hanser Publishers, Munich, 2006. doi:10.3139/9783446412828.

[33] A. Diez-Ibarbia, A. Fernández del Rincón, M. Iglesias, A. De Juan, P. García, F. Viadero, Efficiency Analysis of Shifted Spur Gear Transmissions, in: F. Flores, P; Viadero (Ed.), New Trends in Mechanism and Machine Science. Mechanisms and Machine Science, Springer, 2015: pp. 373–381. doi:10.1007/978-3-319-09411-3_40.

[34] K. Mao, W. Li, C.J. Hooke, D. Walton, Friction and wear behaviour of acetal and nylon gears, Wear. 267 (2009) 639–645. doi:10.1016/j.wear.2008.10.005.

[35] A.R. Breeds, S.N. Kukureka, K. Mao, D. Walton, C.J. Hooke, Wear behaviour of acetal gear pairs, Wear. 166 (1993) 85–91. doi:10.1016/0043-1648(93)90282-Q.

[36] D. Walton, A.B. Cropper, D.J. Weale, P.K. Meuleman, The efficiency and friction of plastic cylindrical gears Part 1: Influence of materials, Proceedings of the Institution of Mechanical Engineers, Part J: Journal of Engineering Tribology. 216 (2002) 75–78. doi:10.1243/1350650021543915.